Imperial College London

Developing the Transcription & Translation Machinery of *Plasmodium falciparum* as a Target for Next Generation Interventions Against Malaria

Author: Fabio Fisher
Supervisor: Prof. Jake Baum

Department of Life Sciences
Imperial College London

May 2021

This thesis is submitted in fulfilment of the requirements for the degree of Doctor of Philosophy

Declaration of Originality

I, **Fabio Fisher** confirm that the work presented here in this thesis is of my own creation and that any information used from other sources or found in conjunction with collaborators on projects associated with this thesis is clearly cited.

Copyright Declaration

Acknowledgements

I want to thank the following people for their continued support and inspiration throughout this PhD.

My friends and loving family. My mother and dear grandmother for always being there, giving their time and believing in me. My father, three siblings, grandparents, uncles, aunties and cousins for all their advice and support. My sister-in-law and baby niece for bringing so much joy and fun in challenging times.

Over the past year particularly, during the ongoing global health crisis, I remember and give thanks to my uncle for his strength, among many others, fighting a brave battle against COVID-19. Also my father who faced his own adversity in health with a fierce determination.

A special thanks to Professor Jake Baum for his enduring guidance, direction and unwavering patience as my supervisor in delivering this thesis. I am thankful to our Imperial colleagues in the Baum lab, past and present, who have been a continual source of inspiration and knowledge.

Finally, thank you to my partner who has been by my side over the past four years, through all the highs and lows, offering her wisdom and own brand of humour to help keep me sane.

Last, but certainly not least, my neighbour's cat Bob.

Abstract

Malaria remains a serious global threat but exploiting the essential processes of transcription and translation within the malaria parasite may enable the development of next generation interventions. Until recently these two processes have not been extensively pursued for the purposes of drug development, parasite growth inhibition and malaria antigen production. Whilst antimalarial compounds have helped millions of individuals exposed to malaria, they lack the ability to truly eradicate malaria. Vaccines offer real potential for disease eradication however, there is currently no licensed malaria vaccine. As such the following strategies were pursued that exploit the transcription and translation machinery of the most virulent malaria parasite, *P. falciparum*.

Firstly, to facilitate the discovery of translation inhibitors with novel modes of action (MoA), a dual in vitro translation (Dual-IVT) assay was developed. Translationally active lysates from human and *P. falciparum* were used to screen a library of 400 bioactive compounds revealing four with parasite specific activity. The human element of the Dual-IVT assay, during the initial stages of the COVID-19 was then shifted towards COVID-19 antigen production.

Next, with a view to develop transcription as a target for next-generation antimalarials selection-linked integration was used to facilitate the characterisation of the three nuclear DNA directed RNA polymerase (RNAP) complexes from *P. falciparum*. Introducing affinity tags enabled their purification from parasite lysate. Exploits are underway to take advantage of recent advances in cryo-EM technology. Purifying each of the three complexes and solving

their structures to atomic resolution will increase our understanding of them.

Finally, although most malaria vaccine candidates have focused on the circumsporozoite protein (CSP). This strategy has resulted in short-lasting, low efficacy protection based on small sections of CSP that are used due to difficulty in its expression. To advance CSP beyond its current limitations, attempts were made to construct a *P. falciparum* derived cell-free protein synthesis system. This allowed the production of the ectodomain of CSP which, may have resulted in its translocation into endogenous microsomes.

Through exploitation of the parasite translation machinery and the use of genetic tools, this work aims to establish technologies that will contribute to the discovery of new parasite specific translation inhibitors, further our understanding of transcription and enable the production of difficult to express *Plasmodium* proteins.

Contents

List of Figures

List of Tables

Abbreviations

aaRS Aminoacyl-tRNA Synthetase

ACT Artemisinin-based Combination Therapy

CFPS Cell-Free Protein Synthesis

CHO Chinese Hamster Ovary

CBR Click-Beetle Red

CDS Coding Sequence

CECF Continuous-Exchange Cell-Free

CoV Coronavirus

COVID Coronavirus Disease

CSP Circumsporozoite Protein

DHA Dihydroartemisinin

DMSO Dimethyl Sulfoxide

EC_{50} Half maximal effective Concentration

GPI Glycosylphosphatidylinositol

hDHFR Human Dihydrofolate Reductase

HEK Human Embryonic Kidney

Hrp3 Histidine-Rich-Protein 3

HTP High-Throughput

IGR Intergenic Region

IVT *in vitro* Translation

MoA Mode of Action

MSP Merozoite Surface Protein

Pf *Plasmodium falciparum*

Poly(A) Polyadenylate

RBC Red Blood Cell

RBD Receptor Binding Domain

RNAP RNA Polymerase

rRNA Ribosomal RNA

SARS Severe Acute Respiratory Syndrome

SLI Selection-Linked Integration

TBV Transmission Blocking Vaccine

TX-TL Transcription-Translation

UPR Unfolded Protein Response

UTR Untranslated Region

WGCF Wheat-Germ Cell-Free

WGS Whole Genome Sequencing

WT Wild-Type

Chapter 1

Introduction

1.1 Malaria, a Global Burden

In 2019 there were an estimated 229 million cases of malaria that resulted in 409,000 deaths, the majority of which occurred in Africa. Greater prevention and control measures introduced since 2010 have been successful in reducing the overall mortality rate of malaria infection by 29% but this progress has now stalled (see Figure 1.1). According to the World Health Organization (WHO) half of the world's population are currently at risk from malaria infection(World Health Organization, 2019). Unfortunately, infants are particularly susceptible to complicated malaria infection accounting for 15% of all childhood deaths recorded in Africa(World Health Organization, 2015). Infants' symptoms can include cerebral malaria, metabolic acidosis and severe anaemia; this is in contrast to adults living in malaria endemic areas (Murphy & Breman, 2001). Adults' symptoms vary widely resulting in the occurrence of peaks of parasitaemia that cause asymptomatic febrile symptoms which are usually controlled by an infected individual's immune system (Njama-Meya et al., 2004). Humans are known to be infected by five *spp* of *Plasmodium* that cause malaria but of these *spp* the one that is by far the most virulent is *Plasmodium falciparum*, responsible for the majority of malaria associated deaths in sub-Saharan Africa and Southeast Asia (Haynes D. J. et al., 1976). Malaria is now confined to the tropical, sub-tropical regions of the world relying on a mosquito vector from the *Anopheles* genus for its transmission. However, its confinement to this region of the globe was not always the case, only disappearing from the United Kingdom by the beginning of the 20th century. This decline can be attributed to the drainage of swamps, an increase in the standard of living and the distribution of quinine (Chin & Welsby, 2004). This highlights malaria's preventability and the possibility of eradication from endemic areas if there are sufficient resources, capital and the will to do so.

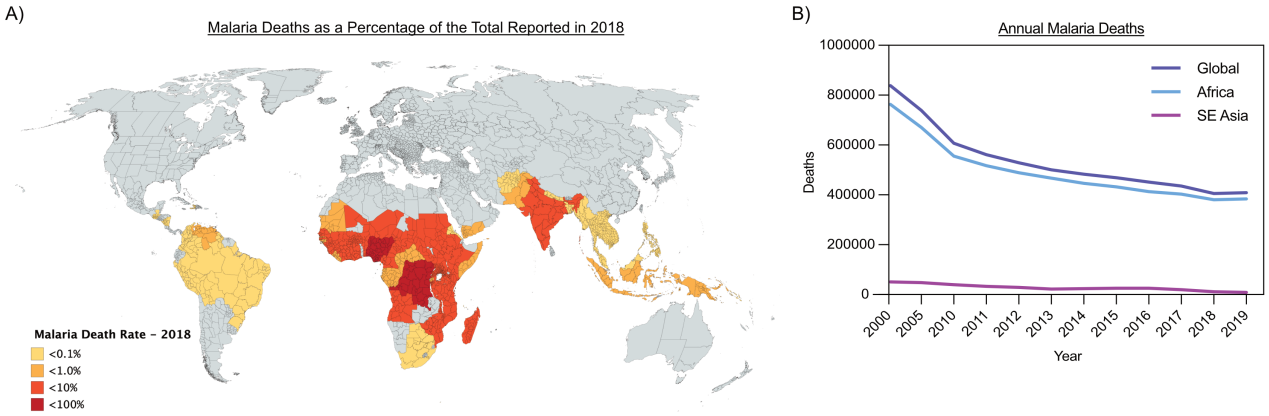

Figure 1.1: Malaria - Deaths in Perspective
A) The world map highlights the burden of deaths attributed to malaria concentrated in Sub-Saharan Africa and Southeast Asia. The countries shaded in the darker red have had the highest percentage of deaths attributed to *P. falciparum* in 2018 (map created using mapchart.net and modified with data obtained from the World Health Organization). **B**) The progress in malaria control from 2000-2018, as indicated by malaria deaths for that year. While the amount of deaths from 2000-2010 was on a steep decline, this trajectory has now levelled off. Sub-Saharan Africa accounts for the highest malaria deaths each year compared with any other region. This highlights the burden malaria creates in this area of the globe(World Health Organization, 2019).

1.2 Life Cycle of *Plasmodium falciparum*

The life cycle of *P. falciparum* is complex requiring both a human and mosquito host within which the parasite goes through distinct phenotypic changes that adapt it for its particular environment. Infection of a human host begins when a female *Anopheles* mosquito takes a blood meal, injecting thousands of motile sporozoites from her salivary glands into the peripheral blood of the host (see Figure 1.2). Sporozoites then migrate to the liver where they traverse and invade primary hepatocytes. After approximately one week these intrahepatic schizonts will eventually burst releasing merozoites into the blood stream to start the intraerythrocytic stage of infection. During this stage, the parasite goes through a 48-hr life cycle of invasion and replication within red blood cells (RBC). The rupture of RBCs at the end of the 48-hr life cycle results in the clinical symptoms that are attributed to malaria. On successful invasion by a merozoite into an RBC the parasite forms a juvenile ring which progresses into a feeding trophozoite form. During the trophozoite stage, RBC sequestration occurs due to

the secretion and export of receptors onto the RBC surface which promote binding to the endothillium. The parasite then continues to develop into a blood stage schizont occupying the majority of the RBC space, eventually segmenting into merozoites that burst out of the infected RBC to infect others (Bray & Garnham, 1982). As this process continues <10% of the total circulating parasites commit to the sexual stage of the parasite's life cycle forming male and female gametocytes (Josling et al., 2018). These will circulate in the peripheral blood and are transmitted to a mosquito during a blood meal. Within the mosquito midgut the parasites form male and female gametes and the process of exflagellation occurs, with male gametes fertilising female gametes, producing a zygote. The zygote, called an ookinate, traverses the mosquito midgut wall forming oocysts that then undergo endomitosis (Tuteja, 2007). Oocysts rupture releasing thousands of sporozoites that will migrate to the salivary gland to start the life cycle once more by being injected into another human host on taking a blood meal(Q. Wang et al., 2005).

The life cycle of *P. falciparum* has a number of points that present themselves as useful targets for therapeutic development and targeting. This includes the point at which sporozoites are injected from an infected mosquito to a human host during a blood meal. As parasite numbers here are reported to be <100, this represents a bottleneck in parasite numhers within the host. Blocking this point and halting parasite development in the liver would prevent the release of merozoites into the blood stream from a hepatic schizont. Secondly therapeutics that target the asexual blood stage are appealing since they reduce the clinical symptoms associated with infection as they prevent parasite replication and invasion of RBCs (Rosenberg et al., 1990; White, 2017). Finally, blocking the transmission from human host to mosquito, although this has no impact on symptoms associated with infection, it would over time cut the person to person transmission, reducing the spread of disease.

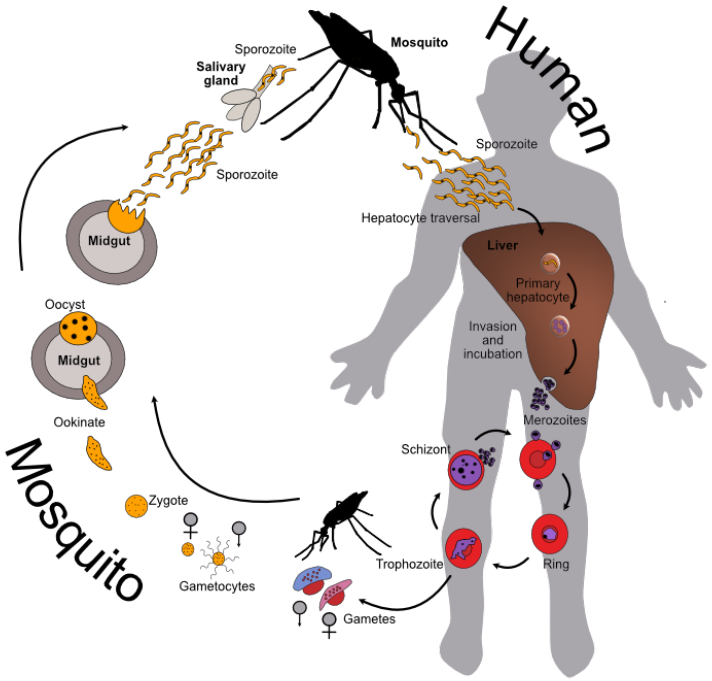

Figure 1.2: The Life Cycle of *P. falciparum*
The cycle begins when a female mosquito from the *Anopheles spp* takes a blood meal injecting sporozoites from her salivary gland into the peripheral blood of a human host.

1.3 Antimalarial Drug Discovery

In 2015 the WHO announced the 'Global Malaria Action Plan', an initiative that called for the reduction of malaria incidences and deaths ten-fold by 2030, therefore bringing us closer to global eradication. Antimalarial drugs have been at the frontline of global malaria control for centuries (see Figure 1.3 (A)), initially with the use of quinine from 1820 but within the last century drugs such as chloroquine, mefloquine and artemisinin have transformed malaria treatment (Schlitzer, 2007).

1.3.1 Chloroquine

Chloroquine was the first synthetic antimalarial synthesised in 1934 and introduced towards the end of World War II. The drug was incredibly effective at killing parasites in an infected individual; boosted by its ease of manufacture and cost effectiveness, the drug was soon put into widespread use (Krafts et al., 2012). Chloroquine is a diprotic base that on activation becomes

protonated, accumulates in the food vacuole of the parasite and interferes with intraerythrocytic parasite development by disrupting the seizure of toxic heme produced from the normal digestion of haemoglobin. Ordinarily during the trophozoite stage of parasite development, haemoglobin is digested producing heme which the parasite converts into hemozoin within the digestive food vacuole, thus preventing parasite death. Chloroquine's ability to disrupt this process made it an incredibly effective drug at eliminating the clinical symptoms associated with malaria infection (Frosch et al., 2007). However, chloroquine's introduction and widespread use placed *P. falciparum* under intense selective pressure with resistant parasites being detected in the Mekong and Southeast Asia areas by 1957 (see Figure 1.3 (B)). Resistance eventually spread so that by 1990 it had been detected in nearly every malaria endemic area on Earth (D. Payne, 1987). Chloroquine resistance is attributed to single nucleotide polymorphisms (SNPs) emerging within the transmembrane domain of the *P. falciparum* chloroquine resistance transporter gene *(crt)*. *Pf*CRT is a 46kDa transmembrane protein localised to the food vacuole of *P. falciparum* and has been shown to be essential in chloroquine sensitive parasites. Efforts to gain *Pf*CRT inactive parasite lines have not been possible, highlighting its physiological relevance that is not yet fully understood (Coppée et al., 2020). Resistant parasites containing the K76T and A220S mutations are 40-50 times more effective at expelling chloroquine compared to chloroquine sensitive parasites (Durrand et al., 2004).

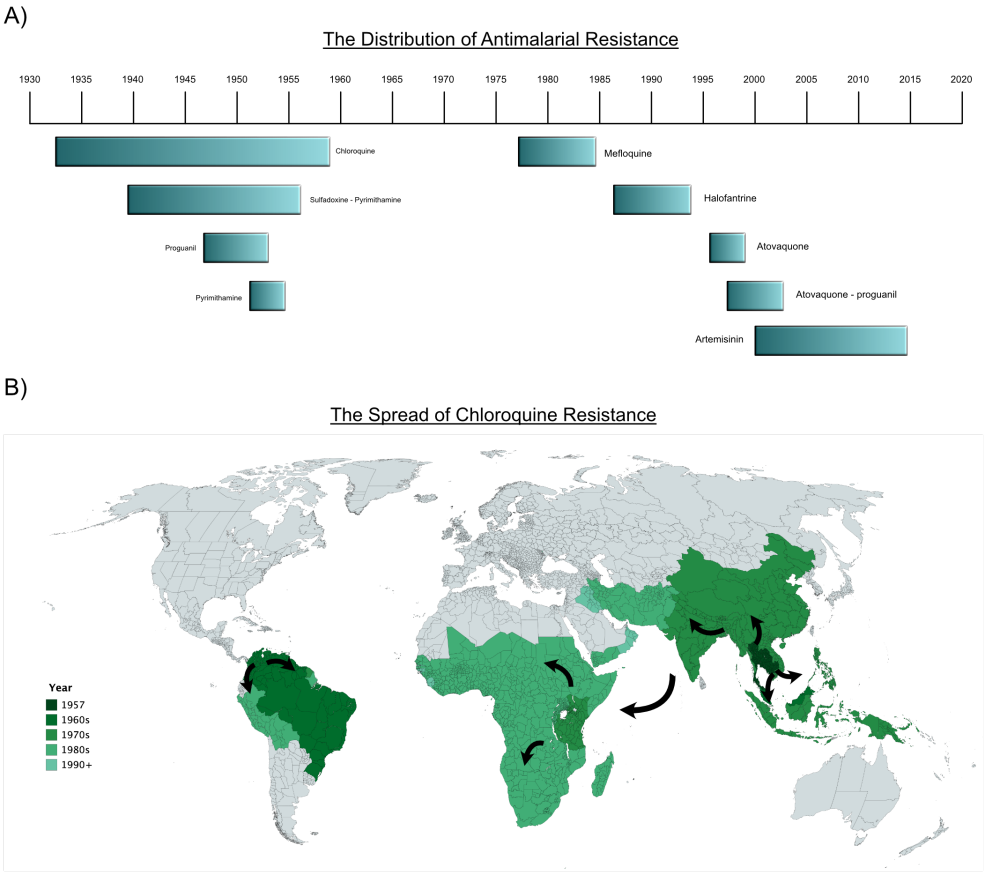

Figure 1.3: Antimalarial Drug Resistance Through the Ages
A) The reported spread of drug resistance in widely used antimalarials over the last 100 years. The beginning of the cyan bars dennotes the first instance of resistance in the field whilst the end shows the year in which the first case of resistance was reported (Mishra et al., 2017). **B**) The spread of chloroquine resistance from 1957-1990. The world map highlights the spread of chloroquine resistance emerging in malaria in the late 1950s in Southeast Asia and South America. Resistance then continued to spread outwards, eventually reaching Africa in the 1970s. Chloroquine resistance, by the 1990s had reached all malaria endemic areas in the world. The arrows on the map show the direction of spread whilst the intensity of the green shading shows the year in which resistance was reported (adapted from D. Payne, 1987).

1.3.2 Mefloquine

In an effort to combat chloroquine resistance new synthetic drugs were developed and distributed for malaria treatment and prevention, mefloquine was one of them. Between 1963 and 1976 the Walter Reed Army Hospital screened over 250K compounds for their ability to kill *P. falciparum* parasites (Rothe, 1975). Mefloquine was discovered, which because of its long half-life within the blood, could be used prophylactic and as a treatment for uncomplicated malaria infection (Pennie et al., 1993).

By 1982 resistance to mefloquine was emerging in Thailand (Boudreau et al., 1982)and by 1990 treatment failures of 40% were being reported (Na-Bangchang et al., 2010); mefloquine resistance is now confined to areas where it has been in widespread use. The mechanism of resistance to mefloquine as well as its exact mode of action (MoA) still remains unclear. Many resistance studies focus on mutations within the *P. falciparum* P-glycoprotein homologue gene *Pf*mdr1, a homologue of the human P-glycoprotein adenosine triphosphate (ATP) binding cassette (ABC) transporter family member (Hospital, 2004). The use of nonylphenol ethoxylate a potential inhibitor of *Pf*mdr1 on mefloquine resistant *P. falciparum* isolates sensitised 80% of them to mefloquine (Ciach et al., 2003).To ascertain the relationship between polymorphisms within *Pf*mdr1 and *in vivo* sensitivity to mefloquine Price et al analysed the genomic data from 618 patients infected with *P. falciparum* over a twelve-year period. By using real-time PCR an increase in the copy number of *Pf*mdr1 was found(Hospital, 2004). Further evidence using gel-enhanced liquid chromatography/tandem mass spectrometry (GeLC-MS/MS) based proteomics highlighted *Pf*mdr1 as having a two-fold increase in protein expression in *P. falciparum* induced mefloquine resistant lines compared to *P. falciparum* mefloquine sensitive lines. However, the authors found another 68 proteins that showed significant differences between mefloquine resistant and sensitive lines suggesting the picture is not so clear (Reamtong et al., 2015). Indeed, other studies by Phompradit et al revealed 58% of *in vitro* and 63% of *in vivo P. falciparum* mefloquine resistant lines as having an increase in the copy number of *Pf*mdr1 (Phompradit et al., 2014). Although this demonstrates a weight of evidence pointing towards a mefloquine efflux transporter protein, discerning the exact mechanism of resistance to mefloquine may be further confounded by not knowing its exact MoA or cellular target.

The MoA of mefloquine is not fully understood and the subject of contention based on conflicting biochemical and structural data. In 2014, Wong et al used cryo-EM to visualise the atomic structure of the +RS mefloquine enantiomer bound to the GTPase associated centre

of the 60S large ribosomal subunit of *P. falciparum* (see Figure 1.4). Biochemical studies revealed a decrease in parasite protein synthesis on exposure to mefloquine as detected by S-35 methionine incorporation *in vitro*. Taken together the authors concluded the inhibition of translation they observed was attributed to the interaction of mefloquine with the ribosome as indicated in their structural studies (Wong et al., 2017). However, in 2018 Sheridan et al highlighted the incidence of error in these types of translation-based assay by developing an *in vitro* translation (IVT) assay using isolated active translation machinery from *P. falciparum* and luciferase as a reporter. The authors validated their IVT assay against a panel of known inhibitors of translation in *P. falciparum*. They showed the inability of the S-35-radiolabelled methionine incorporation assay to pick up known inhibitors of protein translation that the IVT assay was able to detect. The authors assessed the capability of mefloquine at inhibiting translation. Mefloquine was found not to cause any inhibition of translation at 10µM, well above that which would ordinarily have a killing effect on *P. falciparum* parasites in a standard 72-hr growth inhibition assay (Sheridan et al., 2018). The structural and biochemical characterisation of mefloquine's MoA appears to complicate the drug's target and requires further study.

1.3.3 Artemisinin and ACTs

Artemisinin based combination therapy (ACT) has now become the frontline treatment for infected patients(Rodisch & Dudkin, 1983; Bhattarai et al., 2007). Artemisinin originally isolated from *Artemisia annua* (sweet wormwood) (Klayman et al., 1984) kills blood stage *P. falciparum* parasites, specifically affecting the trophozoite stage of parasite development. Its more potent semi-synthetic derivatives are now in widespread use such as dihydroartemisinin and artemether. These two derivatives have short half-lives and are therefore combined with drugs with longer half-lives, such as Lumefantrine (benflumetol) ensuring full elimination of circulating parasites(Tilley et al., 2016). This combination therapy is now licensed under the

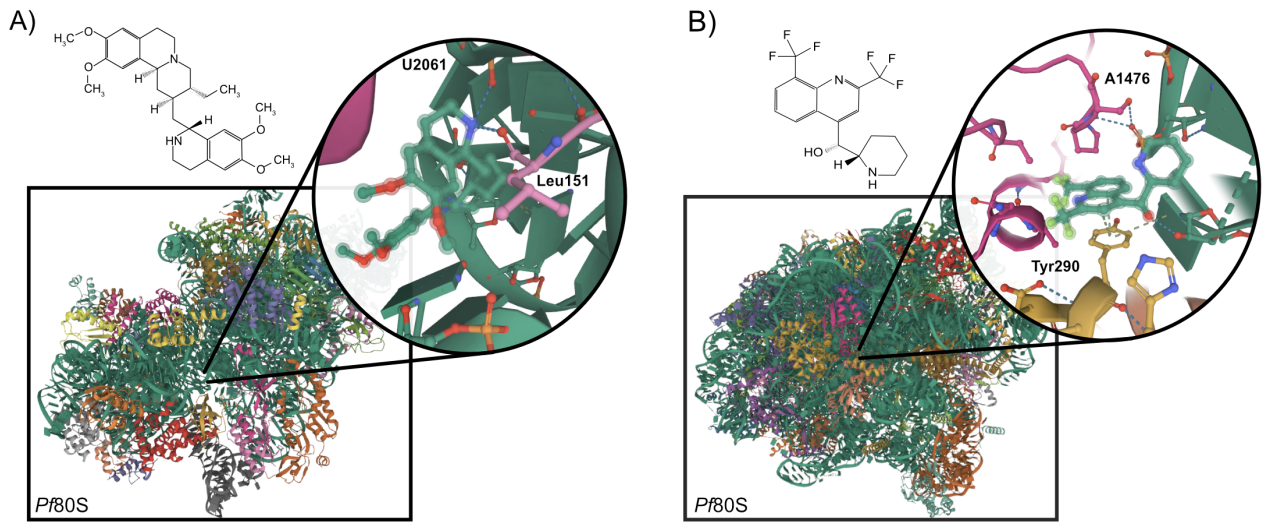

Figure 1.4: The *P. falciparum* 80S Ribosome Bound To Emetine & Mefloquine
Each ribosome is shown with a magnified section highlighting hydrogen bonds between drug and protein or nucleic acid. The chemical structure of each drug is also shown **A**) Here emetine is shown binding to the E-site of the small ribosomal subunit. Emetine benzo[a]quinolizine ring mimics a base stacking interaction with G973 and H23, furthermore its ethyl group forms a hydrophobic interaction C1075 and C1076 of H24. The isoquinoline ring is stacked against Leu151 and an oxygen atom on the backbone of U2061 of h45 forming a hydrogen bonds that stabilise the ring (PDB_3j7a - The PyMOL Molecular Graphics System, Version 2.0 Schrödinger, LLC.). **B**) The +RS enantiomer of mefloquine is shown in the magnified section binding to the ribosome GTPase associated centre that is critical for translocation of mRNA across the ribosome. The Tyr290 and His294 residues from a pocket that accommodates the mefloquine quinolone ring. Three stabilising hydrogen bonds are formed between the ribosome and mefloquine. Two from the piperidine that interact with Tyr290 and one from the hydroxyl group that forms the linker between the quinoline and piperidine ring, residue A1476 (PDB_5umd - The PyMOL Molecular Graphics System, Version 2.0 Schrödinger, LLC).

name of Coartem by Novartis, who in 1999 entered into partnership with the WHO to provide a cost-effective treatment in malaria endemic areas(Djimdé & Lefèvre, 2009).

Artemisinin and its combination drugs are the most effective antimalarial treatments available. However, reports of numerous treatment failures against *P. falciparum* reported in Cambodia after a 3-day course of ACTs in 2008 later spread through the Greater Mekong sub region (Imwong, Suwannasin, et al., 2017). Artemisinin resistance has been associated with mutations within the propeller region of the kelch-13 (K-13) gene located on chromosome-13 of *P. falciparum* parasites (Xie et al., 2020). In 2017 Imwong et al highlighted a single dominant artemisinin resistant (C580Y) *P. falciparum* strain which emerged from western Cambodia and has now spread to north eastern Thailand, southern Laos and south Vietnam (Imwong, Hien,

et al., 2017). This now threatens global malaria control and hopes for its elimination. Unlike antibiotics antimalarials are not rotated to reduce selection pressure due to limited drugs on the market which is in part due to difficulty in their regulation.

1.4 Factors Driving Antimalarial Resistance

The need for new antimalarial drugs is evident but understanding the factors that drive drug resistance in *P. falciparum* will serve as a guide in the race to find alternative antimalarial drugs with new MoAs. The human malaria *P. falciparum* 3D7 parasite contains a highly A/T rich 23-megabase nuclear genome consisting of 14 chromosomes, encoding approximately 14K genes (Gardner et al., 2002). Considering the size of a single parasite's genome, the quantity of parasites in an infected individual and the error rate of eukaryotic polymerases, there is a high degree of probability of randomly acquired mutations occurring within a population of parasites infecting a single individual. This is providing that the mutations which arise are not lethal or do not hamper with reproduction. Yet, spontaneous mutations that reduce parasite sensitivity to a particular drug are rare and dependent on the drug's MoA. For some drugs a single point mutation is sufficient to confer resistance, such is the case with atovaquone (Y268S of cytochrome b) (Fisher et al., 2012) and pyrimethamine (S/T108N of dihydrofolate reductase-thymidylate) (Basco et al., 1995). In contrast an event conferring resistance to the antimalarial chloroquine was rarer, taking approximately half a century to develop and requiring multiple independent mutations. Understanding the molecular factors that give a drug like chloroquine almost a 40-year resistance free rein compared to drugs such as atovaquone would greatly aid the malaria control and eradication agenda (Plowe, 2009).

1.4.1 Drug Properties, Drivers of Resistance

The pharmacokinetic and pharmacodynamics properties of a drug that a population of parasites are exposed to over time has a significant effect on the emergence of events that can cause resistance (White, 2013). A human host infected with malaria is likely to have a heterogenous population of parasites that will give varying responses to a single drug pressure. The population of circulating parasites within the infected individual that are resistant to an applied drug pressure are able to reproduce at a faster rate than those sensitive to the drug (Gerardin et al., 2016). This effect can be observed by the generation of mefloquine resistant strains of *P. berghei*. By passaging parasites through rodents exposed to suboptimal concentrations of mefloquine, resistant lines to the drug can be induced (Mackinnon & Read, 2004). This highlights the importance of circulating drug concentration within an infected individual and the consideration of those with short or longer half-lives. The transmission of genes that give resistance from parasite to parasite requires a pool of circulating gametocytes that infect a mosquito host during a blood meal. Different drug treatments affect the viability of the pool of circulating gametocytes in different ways (Diakité et al., 2019). The unintended consequence of the drug combination pyrimethamine-sulfadoxine or chloroquine causes an increase in the pool of circulating gametocytes thereby increasing the probability of transmission to a mosquito (Villa et al., 2021). Therefore, an ideal drug therapy would combine a drug that is highly effective at eliminating circulating asexual parasites but also reduce the quantity of circulating gametocytes, blocking transmission. However, with the scarcity of new compounds being validated for front-line antimalarial treatment and widespread drug resistance new compounds with novel modes of action are in need now more than ever.

1.4.2 High-Throughput Drug Screening is Needed to Accelerate Drug Discovery

Traditional methods of screening have centred on phenotypic based assays such as the *in vitro* 72-hr-growth inhibition assay (GIA). Here asexual blood stage parasites, responsible for the clinical symptoms of malaria are exposed to a drug *in vitro* and monitored for growth (Baldwin et al., 2005; Baniecki et al., 2007; Izumiyama et al., 2009; D. W. Wilson et al., 2010). These kinds of assays, also termed phenotypic based screens, offer the best data resolution when testing a compound. This is because culture adapted parasite strains can go through the entire blood-stage life cycle within a 96-well plate pre-printed with a compound of interest (Cranmer et al., 1997). Once 72-hrs has expired, the number of parasites within the wells of the plate can be determined, usually by lysing the parasite material and staining DNA which allows detection of parasite material by fluorescence measurements. This methodology allows researchers to slowly assess libraries of compounds searching for compounds with potent killing activity.

Once a compound is found to be a potential antimalarial candidate, its toxicology profile can be assessed using human cell lines e.g. HepG2 cells (Hovlid & Winzeler, 2016) (Dennis et al., 2018). Upon completion the compound's MoA can be determined, parasite lines resistant to the compound of interest may be generated. The resistant parasite is then isolated and next generation sequencing (NGS) performed to scan and detect mutations within the genome to pinpoint the exact resistance mutation(s). If contained within a single gene it may be recombinantly expressed and co-crystallized for the purposes of structure determination (Nzila & Mwai, 2009; Ross & Fidock, 2019). The interactions of the compound within a binding pocket can be subject to refinements to increase the potency of the compound. This compound discovery process can be a bottleneck to compound progression through a drug pipeline. This is highlighted by the time in which it takes to go from discovery to therapeutic delivery of a compound to the field.

However, a targeted based approach to drug discovery allows researchers to dismantle cellular processes into a single enzymatic step or reconstitute a subset of processes (Terstappen et al., 2007; Swinney, 2013). Thus, allowing the search for compounds that may inhibit one or a subset of processes. This however, like a phenotypic based screen, has its own disadvantages. Data resolution drops potentially resulting in false negatives due to the dynamics of a compound within an actively growing cell; though the speed of screening is drastically increased and toxic compounds can be eliminated through direct screening against the homologous processes in humans.

1.5 Translation Inhibitors

To avoid infection with *P. falciparum* becoming untreatable, further research into mechanisms of drug resistance and MoA are required. The current major antimalarial drug classes are; quinines, antifolates, artemisinin derivatives and hydroxynaphthoquinones (Mishra et al., 2017). Large chemical libraries have been screened in an effort to find new or repurpose old compounds as effective antimalarials. The first ultra-high throughput phenotypic based screen identifying inhibitors of asexual *P. falciparum* parasites was conducted in 2008. Here, 1.7M compounds were screened, 6000 of which were shown to have activity against *P. falciparum* parasites (Plouffe et al., 2008). In 2010, Gamo et al screened two million compounds from the GlaxoSmithKline (GSK) library finding 13,533 that showed 80% efficacy at 2µM (Gamo et al., 2010). Following from this a number of approaches have sought to address the lack of chemical diversity in antimalarial compounds. The use of phenotypic-based assays to screen 20,000 compounds from the MEDINA library (the world's largest library of natural and microbial derived compounds) by Perez-Moreno et al (2016) identified a number of compounds with antimalarial activity. An alternative to the phenotypic assay-based approach to drug discovery involves a targeted based approach, here an identified essential cellular pathway or small subset of path-

ways is probed for inhibition by reconstituting it *in vitro*. This type of assay is more suited to high-throughput (HTP) drug discovery pipelines, eliminating the need for cell maintenance and increasing the speed at which the MoA for compounds can be elucidated (Moffat et al., 2017). However, this type of assay is not without its drawbacks. The lack of an intact cell and its dynamic intracellular compartments often means there can be a disconnect between the efficacy of a compound found to be active. Therefore, a targeted based drug screen can be used to screen a large library of compounds quickly identifying those with inhibitory activity. This small subset of compounds can then be more easily assayed using a phenotypic or whole cell-based screen to give the maximum information resolution when moving forward with an active set of compounds.

1.5.1 Protein Synthesis, a New Target in The War Against Antimalarial Resistance?

Translation, the conversion of genetic message (mRNA) into protein is a highly orchestrated energy intensive process within a cell. In all eukaryotes it requires the coordination and interaction of many factors including tRNAs, accessory factors and mRNA all centred around the central ribosome (Moldavel, 1985). The proteins and macromolecular complexes that are core to this process present multiple targets as an avenue to disrupt translation in *Plasmodium spp.* The identification of inhibitors of protein synthesis has a well-established methodology, with curated libraries containing 1000s of compounds researchers can use. However, the rapid identification of parasite specific inhibitors is far more challenging, due to the conservation of the eukaryotic translation apparatus between human and parasite. Antibiotics that target protein translation have proved very successful in treating bacterial infections (Hauser et al., 2016), so much so that some have been repurposed as antimalarials. These include azithromycin, doxycycline and clindamycin whose target is the bacterial-like ribosome of the mitochondria or

apicoplast (Yadav et al., 2021).

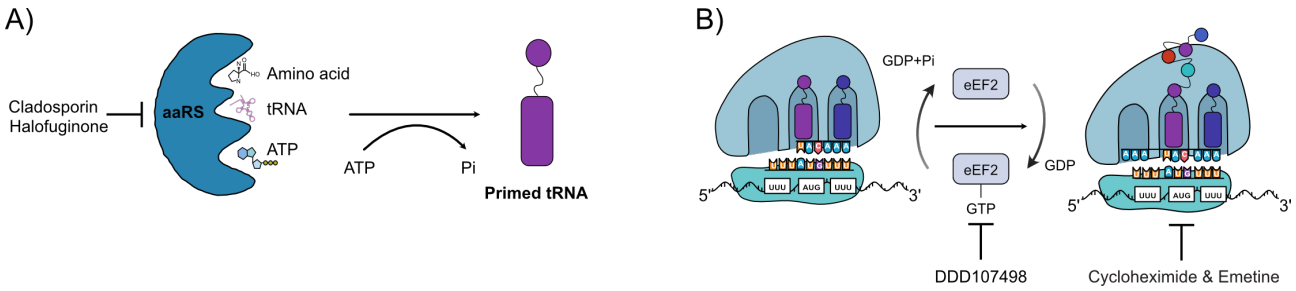

Figure 1.5: An Overview of Well Characterised *P. falciparum* Translation Inhibitors
A) A generalised aaRS reaction involving the binding of amino acid, conjugate tRNA and ATP. This enzyme catalyses the formation of a primed tRNA entity in an energy driven reaction. The aaRS inhibitor cladosporin inhibits the lysyl-aaRS whilst halofuginone targets the prolyl-aaRS. **B**) A snapshot of the 80S *P. falciparum* ribosome during mRNA translocation, a GTP dependent process requiring eEF2. As eEF2 drives translocation it allows the binding of tRNA to mRNA and in turn enables the continued growth of the polypeptide chain. The DDD107498 binds to *P. falciparum* eEF2 inhibiting protein synthesis, whilst emetine and cycloheximide bind directly to the E-site of the ribosome in both *P. falciparum* and human cells inhibiting translation.

1.5.2 Sites of Protein Translation in *P. falciparum*

Plasmodium parasites have three distinct areas where protein synthesis occurs; the apicoplast, cytoplasm and the mitochondria (Vembar et al., 2016). The cytoplasm is the focal point for the majority of protein synthesis within the parasite containing the 80S ribosome, formed from a large 60S and small 40S subunit. Interestingly *Plasmodium* possess two types of cytoplasmic ribosomes that differ in their ribosomal RNA (rRNA) content present at different points within their complex life cycles. One when the parasite is within the mosquito vector and one when the parasite is in the human host (Thompson et al., 1999). Compounds targeting this cytoplasmic compartment of translation are fast acting compared to those targeting the apicoplast which show a 'delayed death' phenotype requiring a full 48hrs before showing activity (Kennedy et al., 2019). The structure of the 80S ribosome of *P. falciparum* bound to the +RS enantiomer of mefloquine has given us insights into the similarities but also differences from the structure of the human ribosome (Wong et al., 2017). The structure of the ribosome in combination with the recent discovery of compounds targeting amino acyl-tRNA synthetases (Nyamai &

Tastan Bishop, 2019)and translation elongation factor-2 (eEF2) in *P. falciparum* (Rottmann et al., 2020)gives hope for a new class of antimalarials, one targeting translation(see Figure 1.5). This new class of therapeutics will need to be effective at rapidly targeting parasite growth and development alleviating the suffering from severe malaria infection. This makes cytoplasmic translation inhibitors more attractive as antimalarial compounds than those targeting the apicoplast, prokaryotic-like translation machinery.

1.5.3 The *P. falciparum* Ribosome

The *P. falciparum* 80S ribosome shares homology with its human counterpart however, the structure of the *Plasmodium* ribosome highlights some key differences. The atomic structure of a macromolecular complex like the ribosome, allows drug developers to refine compounds to better exploit differences between parasite and human complexes. The *P. falciparum* ribosome structure lacks a class of protein used for translation repression in yeast (STM1) and humans (SERBP1). This usually interacts with the 40S subunit passing through the P and A tRNA binding sites, potentially facilitating mRNA decay (Heaton et al., 2001), indicating a more translationally active ribosome that is not subject to the same repression as other eukaryotes. Whilst the core of the *P. falciparum* cytoplasmic ribosome is conserved with that of the human ribosome there are some key structural differences. The authors note that the rRNA towards the edges has extended segments that differ in their sequence, length or are even absent compared to the equivalent human rRNA extended segments (Sun et al., 2015; Wong et al., 2017; Wong et al., 2014).

1.5.4 Translation Elongation Factor-2, a New Antimalarial Target

Translation elongation factor-2 (eEF2) is one of several essential enzymes encoded by *P. falciparum* and humans(see Figure 1.5). It allows translocation of the ribosome along mRNA

in a GTP dependent manner. Although translation is generally conserved among eukaryotic cells, there is evidence to suggest processes required for active translation can be selectively inhibited in human pathogens. For example, the antifungal agent sordarin targets the yeast eEF2, which shares 67.2% sequence homology with its human counterpart (Domínguez et al., 1998). However, the compound is selective against yeast *in vitro* and does not inhibit human translation.

A phenotypic screen by the Drug Discovery Unit (DDU) at the University of Dundee of their Kinase Scaffold Library of approximately 4731 compounds, revealed a potent multi-stage inhibitor of *P. falciparum*. The compound DDD107498, a quinolone-4-carboxamide has an MoA localised to its inhibition of eEF2 in *P. falciparum* 3D7 parasites. This was elucidated by the creation of a parasite DDD107498 resistant line and whole genome sequencing (WGS), revealing a number of single nucleotide polymorphisms (SNPs) within the eEF2 gene. Radioactive S-35 methionine/cysteine incorporation by parasites in the presence of DDD107498 against a known translation inhibitor, cycloheximide, further pointed to an inhibitor of protein synthesis (Baragaña et al., 2015). The ability of an antimalarial to act as a potent killer of blood stage parasites but also prevent transmission is a strategy being pushed by The Bill and Melinda Gates Foundation in cooperation with the Medicines for Malaria Venture (MMV) and the WHO (Yahiya et al., 2019).

1.5.5 Aminoacyl-tRNA Synthetases, Essential for Translation - A New Avenue to Drug Discovery

Aminoacyl-tRNA synthetases (aaRS) are ancient enzymes responsible for attaching an amino acid to its conjugate tRNA and broken into two classes with one encoded aaRS per amino acid within the genome of most organisms (see Figure 1.5). The attachment of an amino acid to its destined tRNA occurs in two distinct steps; first the amino acid is activated by

ATP producing an AMP-activated amino acid, this is then followed by the transfer of the activated amino acid to tRNA forming an anminoacyl-tRNA (Cusack, 1997). *P. falciparum* encodes 36 aaRS proteins distributed between the apicoplast, mitochondria and cytoplasmic compartments. Of these, 15 are present in the apicoplast, 16 in the cytoplasm and four in the mitochondria. Four of the 36 enzymes (alanyl-RS, glycyl-RS, tyrosyl-RS and cysteinyl-RS) are found in apicoplast and cytoplasm, encoded by a single gene then exported to both areas within the parasite. The mitochondrion only encodes a single aaRS gene and as such relies on the import of aaRS proteins for translation(Khan, 2016). Humans on the other hand encode 36 aaRS proteins distributed between the cytoplasm and mitochondria, 16 in the cytoplasm and 17 in the mitochondria whilst the proteins lysyl-RS, glycyl-RS and glutamyl-RS are able to move between both. Finally, the aminoacylation of glutamine and proline in humans' cells occurs using a single bifunctional aaRS within the cytoplasm (Nie et al., 2019). This setup in both *P. falciparum* and human cells ensures each of the 20 amino acids can be linked to its conjugate tRNA at protein synthesis points throughout the cell. There have also been numerous studies highlighting additional non-canonical functions of aaRSs such as angiogenesis, RNA splicing, transcription regulation and apoptosis (Mirando et al., 2014; Wakasugi & Schimmel, 1999; Wei et al., 2016). The *P. falciparum* lysyl-RS (KRS) has even been shown to be involved in cell signalling through its production of diadenosine polyphosphate, a signalling molecule used in DNA replication and ion channel regulation. There is now widespread interest in targeting malaria aaRSs. Compounds targeting parasite specific aaRS enzymes have shown activity against all parasite stages, due their necessity at all stages of the life cycle (Vinayak et al., 2020). A number of revealing studies have focused on the aaRS inhibitory compounds cladosporin and halofuginone.

1.5.6 Cladosporin

Malaria parasites encode two different copies of the KRS1 protein that enable translation in both the apicoplast and cytoplasm (Istvan et al., 2011), whereas human cells encode a single copy of the hKRS gene that has been shown to be present in both the cytoplasm and mitochondria (Tolkunova et al., 2000). Cladosporin is a naturally derived compound produced as a secondary metabolite of the fungus *Cladosporium cladosporioides* (X. Wang et al., 2013). Cladosporin has been shown to have potent antimalarial activity against *P. falciparum* blood and liver stage parasites in *in vitro* culture whilst showing negligible activity against human cells. In fact, it showed >100-fold inhibition of the *P. falciparum* KRS compared to that of the human KRS. Cladosporin inhibits the *Pf*KRS1 by mimicking the structure of ATP, enabling association with the ATP binding pocket of *Pf*KRS1, inhibiting its function(Hoe*Pf*ner et al., 2012). The cladosporin moiety can be broken down into two parts; first its isocoumarin group which occupies the same space as ATP within the ATP binding pocket of *Pf*KRS1, via the interaction of two hydroxy groups with E332 and N339 of *Pf*KRS1. Cladosporins' pyran group occupies the same position as the ribose of ATP, precluding amino acid charging of tRNA(Das et al., 2018). However, although cladosporin has been shown to be a potential potent antimalarial compound, its inherent metabolic instability and consequently its bioavailability precludes the natural compound from direct use (see Figure 1.6 (A)). Interest in *Pf*KRS1 has resulted in the screening of the GlaxoSmithKline (GSK) malaria actives library of roughly 13,000 compounds for potential inhibitors (Baragaña et al., 2019). Inhibitors of *Pf*KRS1 were detected using a luciferase-based ATP assay using recombinantly produced *Pf*KRS1 and hKRS1. Those that were more amenable to structural manipulation compared with cladosporin were then pursued. This targeted based screening approach identified a single compound (compound 2) that showed similar levels of inhibition of *P. falciparum* as cladosporin. Compound 2 was also shown to be unstable but more importantly was chemically tractable. The crystal structure of compound 2

bound to *Pf*KRS1 indicated a mode of binding similar to that of cladosporin bound to *Pf*KRS1. Both are shown to be interacting with the ATP binding pocket of *Pf*KRS1 however the core of compound 2 is rotated by 30°. With structural-based drug design and further modification of compound 2, Baragaña et al in 2019 were able to identify a number of compounds that had similar potencies to cladosporin but importantly were more metabolically stable.

1.5.7 Halofuginone

Another aminoacyl-tRNA synthetase receiving attention is the *P. falciparum* prolyl-tRNA synthetase (PRS). Febrifugine is the active compound in the herb *Dichora febrifuga* which has been used for centuries as an alternative medicine for the treatment of malaria infection. Febrifugine is a quinazolinone alkaloid but due to its gastrointestinal toxicity in humans was derivatised yielding a number of less toxic compounds (Pines & Nagler, 1998). One of these derivatives, halofuginone was shown by Ryley et al in 1973 to have less cellular toxicity than the original febrifuge (Ryley & Betts, 1973). Halofuginone would later be shown to interact with the human PRS(Keller et al., 2012). Like its human counterpart halofuginone binds to two major pockets within the PRS of *P. falciparum*. Halofuginones hydroxypiperidine ring mimics the amino acid L-proline and its quinazolinone ring that of adenine 76 (A76) of tRNA with ATP assistance (see Figure 1.6 (B)). Humans and *P. falciparum* parasites only share 34% amino acid sequence homology between their respective PRSs, opening up the possibility of structural-based drug design of PRS inhibitors to exploit inherent differences. Sharma et al in 2017 highlighted the use of a structure guided approach to derivatization of halofuginone and other quinazolinone compounds coupled with *in vitro* compound testing. The authors developed nine compounds centred around the quinazolinone ring to fine-tune the interaction between the derivative and the *Pf*PRS by stopping non-specific interactions. This was accomplished through the substitution or removal of the keto linker group joining the quinazolinone ring to the hydroxypiperidine

ring; or through the replacement of the hydroxyl group with a keto group on the piperidine ring. The parasite and human PRSs in combination with the nine compound derivatives could then be used in aminoacylation assays to test for an inhibitory effect. This was also combined with growth inhibition assays using asexual blood stage parasites to build up a better picture of compound potency. The nine compounds show high selectivity for *Pf*PRS having a half-maximal effective concentration (EC<50) of 30nM to 1.5µM, highlighting their potency. Many of the compounds also show a low selectivity to the human PRS with some, almost 1000-times more affinity for the parasite PRS than the human homologue. Encouragingly the use of structural-based drug derivatisation for a chosen compound(s) with a known target enables HTP compound screening of a single pathway (Jain et al., 2015).

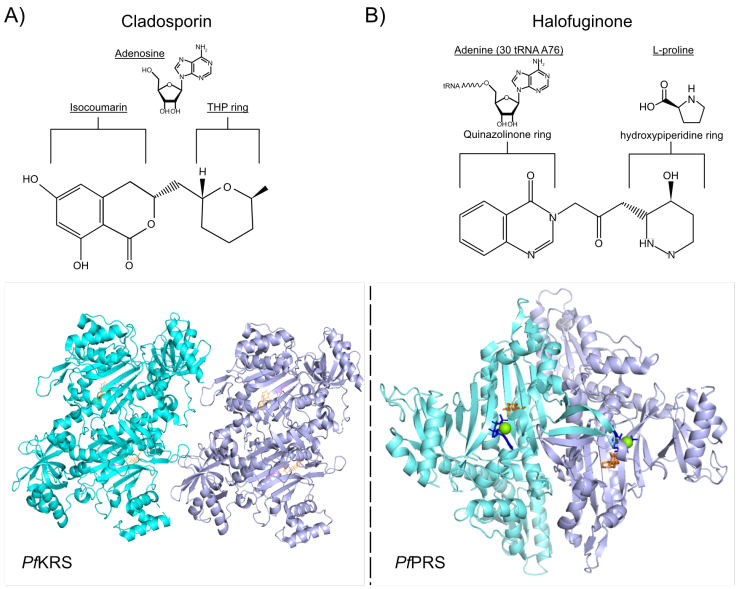

Figure 1.6: Targeting Protein Translation Opens up a Group of New Antimalarials.
The aaRS complexes are essential proteins within all eukaryotes responsible for priming tRNA with constituent amino acid, some of which in malaria can be inhibited over human homologues. The *P. falciparum* KRS (*Pf*KRS) and PRS (*Pf*PRS) are both class II aaRS fomed of two homodimers, each capable of binding an inhibitor moiety. **A**) Cladosporin is formed of an Isocoumarin group, made of dihydroxybenzene and lactone connected to a 2,6-disubstituted tetrahydropyran (THP) group. Here the structure of *Pf*KRS co-crystallised with cladosporin (orange) and L-lysine (pink) at 2.7Åare shown binding within the *Pf*KRS ATP binding pocket, consistent with the proposed theory that cladosporin inhibits through ATP mimicry (PDB_4ycv - The PyMOL Molecular Graphics System, Version 2.0 Schrödinger, LLC). **B**) Halofuginone is formed of a quinazolinone ring that fits inside the adenine binding pocket of the *Pf*PRS, linked to a piperidine ring that fits inside the L-proline binding pocket. The structure of the *Pf*PRS has been solved to 2.3 Å, co-crystallised with halofuginone (orange), magnesium (green) and adenosine 5'- β, γ-imido)triphosphate (blue) (PDB_4yqd - The PyMOL Molecular Graphics System, Version 2.0 Schrödinger, LLC).

1.6 Transcription - A Potential Target for Drug Development

Translation inhibitors such as DDD107498 have the potential to diversify the repertoire of effective antimalarials in circulation, reducing the risk of resistance, leading to improved malaria treatments. Inhibitors of parasite translation have also been shown to be stage transcending, allowing a single compound to be effective at reliving the clinical symptoms associated with infection but also stop transmission. DDD107498, also known as M5717 has successfully passed preclinical trials and has entered into clinical development (Rottmann et al., 2020). Such research and development highlights the need to look at pathways within *P. falciparum* that have been overlooked. One such fundamental process is the first step in gene expression, termed transcription.

1.6.1 Transcription – An Overview in *P. falciparum*

In eukaryotes transcription is made possible by three nuclear DNA-directed RNA polymerase (RNAP) complexes. These large multimeric complexes are classified based on their subunit structure, promotor, localisation within the cell and sensitivity to α-amanitin. In general, nuclear eukaryotic RNAPs contain two large molecular weight subunits and eight to twelve smaller subunits. The two larger subunits are essential for enzymatic function, possessing a variety of functionally active domains that have remained uncharacterised in *P. falciparum* (Kornberg, 2014). In contrast bacteria possess only a single RNAP complex that over the past two decades has been well characterised. Bacterial RNAP complexes are highly conserved and apart from the active site share little sequence similarity to their eukaryotic counterparts (Browning & Busby, 2016). However, only two clinically approved medications targeting bacterial RNAPs exist possibly as a result of the high rate of acquisition of resistance to newly developed compounds(Ma et al., 2016). Thanks to advancements in cryo-EM large macromolecular complexes

that would have remained hidden have now been elucidated. This makes structural-based drug design a real possibility when targeting large complexes in human pathogens(Bai et al., 2015; Renaud et al., 2018). While conservation of the three RNAPs across all eukaryotes is a factor, compounds found that target *P. falciparum* translation suggest targeting conserved processes is a possibility. Though malaria has been studied for over a century and its evolution spans millions of years little is known about the structure of its three nuclear RNAPs, three complexes that are essential for life (Carter & Mendis, 2002).

1.6.2 DNA-directed RNA Polymerase I

The critical function of RNAP I is to transcribe the genetic information encoding ribosomal RNA (rRNA) into precursors. These precursors then form both ribosomal subunits of the 80S ribosome. The 5.8S and 28S (large ribosomal subunit) and 18S (small ribosomal subunit) subunits are transcribed as a single polygenic transcript that is then processed (Sentenac, 1985). Whilst the majority of eukaryotes contain hundred to thousands of copies of rRNA genes per haploid genome, *Plasmodium* only contain between four to eight (Van Spaendonk et al., 2001). Interestingly *Plasmodium* was shown to possess two distinct types of 18S rRNAs, structurally distinct and expressed at different points within the parasite's life cycle (Escalante & Ayala, 1995). The switch between the two forms occurs after hepatocyte invasion and during gametocytogenesis and notably denoted as A or C-type (Van Spaendonk et al., 2001). The largest subunit of *P. falciparum* RNAPI (accession L11172) is predicted to have a conserved finger motif required for zinc binding and overall enzymatic activity. The large subunit has conserved regions that share 47% amino acid sequence homology with *S. cerevisiae* and 42% with Trypanosoma (Fox et al., 1993).

1.6.3 DNA-directed RNA Polymerase II

In eukaryotes RNAP II transcribes protein coding regions by producing mRNA, allowing gene expression (Myer & Young, 1998). A malaria parasite's intraerythrocytic development involves the tight transcript regulation of hundreds of genes. Within the 48-hr growth cycle of *P. falciparum* mRNA synthesis starts six hours post RBC invasion, rapidly increasing during the trophozoite stage and finally peaking during schizogony (Painter et al., 2018). The largest subunit of this complex (RPB1) is present as a single copy on chromosome three of the *P. falciparum* genome. The subunit has five eukaryotic conserved regions within its 2452 predicted amino acid sequence (W. B. Li et al., 1989). Transcription factors recruited to RNAPs allow eukaryotic organisms to regulate gene expression, the C-terminus of RPB1 facilitates this process through accumulation of post-translational modifications. The C-terminus of RPB1 is flexible, comprised of a handful of conserved amino acid heptad repeats. This C-terminal domain tends to be loosely associated with the size of an organism's genome with humans possessing 52 repeats but *Plasmodium* only possessing 12-17 repeats. As RNAP II transcribes a gene certain residues undergo sequential phosphorylation, that in turn can lead to initiation or termination of transcription. The association of nuclear factors that are involved in capping, splicing and mRNA processing to the RPB1 complex are also dependent on the phosphorylation of specific residues within the C-terminus as are those involved in gene regulation (Chapman et al., 2008).

1.6.4 DNA-directed RNA Polymerase III

Lastly, eukaryotic organisms use RNAP III the largest of the three polymerases for the transcription of 5s rRNA, tRNA and other small molecule RNA entities (Willis, 1994). During the parasite's phases of growth and development there is a critical requirement for large amounts of rRNA to meet its protein synthesis needs (Callebaut et al., 2005). In eukaryotes multi-gene

families encode rRNA that contains thousands of tandem repeats (Drouin & De Sa, 1995). The mechanisms by which *P. falciparum* and other *Plasmodium spp* increase their rRNA production are unclear as there has been no evidence showing the increase of rRNA gene transcription during these stages. The large subunit of *P. falciparum* RNAP III (RPC1) contains conserved regions that share up to 52% sequence homology with the large subunit of yeast RNAPIII and 45% with that from Trypanosoma. RPC1 contains a zinc-finger consensus sequence at positions 88-104 but compared to other eukaryotes the terminal histidine was replaced with tyrosine in *P. falciparum*. A conserved sequence Tyr-Asn-Ala-Asp-Phe- Asp-Gly-Asp-Glu-Met-Asn present in all of the eukaryotic largest subunits of RNAP was found indicating a high degree of sequence homology between *P. falciparum* and other eukaryotic organisms (W. B. Li et al., 1991).

1.6.5 A cryo-EM Revolution - Structural Aided Drug Design

Deciphering the atomic structures of large macromolecular complexes, such as the ribosome or RNAPs is key to fully understanding their precise molecular function and will aid future drug design or refinement. Without such a technique it would make attempting to solve the structure of the three RNAP of *P. falciparum* almost impossible, due to the sample requirements of x-ray crystallography. The use of cryo-EM, once referred to as 'blobology' has come into focus thanks to improved detectors with increased sensitivity (Smith & Rubinstein, 2014; Ceska et al., 2019). The requirement for small quantities of sample, the ability to image complexes that do not readily crystallise and the imaging of flexible molecules makes cryo-EM a powerful imaging technique. So much so that in 2017 Jacques Dubochet, Joachim Frank and Richard Henderson shared the Nobel prize in chemistry for the development of the cryo-EM technique. The technique has not fully replaced x-ray crystallography but resolutions of below 2Å are now possible, something inconceivable a decade ago(Cheng, 2015; Renaud et al., 2018).

1.7 Vaccines

The use of antimalarials to treat those suffering from severe malaria infection has dramatically altered the quality of life for those living in disease endemic areas (McCarthy & Coyle, 2010). In the last hundred years drug development and the push to find more effective antimalarial treatments combined with the use of insecticide-treated bed nets has brought us closer to malaria eradication (Diagana, 2015). Yet, this progress has now stalled demanding further innovation beyond the protection that current drugs can provide. Vaccines are crucial in providing a tool to disease control and eradication.

1.7.1 Vaccines Provide a Tool for Disease Eradication – Smallpox

Smallpox eradication through vaccination highlights our ability if there is the will to do so for large scale vaccine deployment programs. The causative agent of smallpox, the Variola virus is the only human specific disease eradicated from the planet according to the WHO (Rosengard et al., 2002). In 1980 the WHO concluded a worldwide vaccination programme that brought an end to a disease plaguing the world since the time of Ramses V, in ancient Egypt. Although smallpox eradication was only complete just over 40 years ago, the spark that would ignite its destruction was started centuries before mankind had even proven the existence of viruses(Y. Li et al., 2007). It was in the late 18th century that the surgeon and physician Edward Jenner made the key observation that milkmaids were generally immune to smallpox. In 1796, Jenner theorised the reason for this was that the maids had been continuously exposed to cowpox, a related illness but less severe than smallpox rendering the maids immune. Jenner, so sure of this theory inoculated James Phipps with cowpox, an eight-year-old boy and son of his gardener. Jenner scraped pus from a cowpox blister belonging to the cow Blossom, inoculating Phipps with the pus soon after. Phipps developed a fever after being infected with cowpox but soon recovered. Finally, Jenner infected Phipps with smallpox using the pus from a scabbed over

blister, a process termed variolation. Phipps never developed any symptoms associated with smallpox. Jenner repeated this process a number of times with the same outcome (Riedel, 2005). Jenner went on to publish his findings in a paper he called 'Vaccination', derived from the Latin *vacca* (Didgeon, 1963).

Vaccination, a word which is now synonymous with disease prevention and eradication was initially rejected by many scientists of the time before being brought into the mainstream. His seminal work led a journey that would bring an end to one of the deadliest human pathogens killing an estimated 300 million people. Jenner said, "I hope that someday the practice of producing cowpox in human beings will spread over the world - when that day comes, there will be no more smallpox." Not only was this the case for smallpox but vaccines have contributed to the fight against measles, mumps, rubella and polio as well as many others(Blume, 2000; Bankamp et al., 2019). Could vaccines therefore play a role in malaria eradication?

1.7.2 Introduction of The First Efficacious Malaria Vaccine

The WHO and its partners have set an ambitious target for the creation of a potent malaria vaccine by 2030, one that would provide at least >75% efficacy over two years and require only a single yearly booster (WHO, 2015). However, there are currently only a small number of vaccine candidates in advanced clinical trials. These all centre on the most virulent malaria parasite, *P. falciparum* but so far lack sustained protection (K. L. Wilson et al., 2019). The life cycle of *P. falciparum* is complex and comprised of distinct stages that expose different surface antigens to a host immune system. The current vaccine strategies can be broadly broken down into three types; those associated with blood-stage protection, preventing the the clinical symptoms associated with malaria (Wahlgren et al., 2017); transmission blocking vaccines (TBV), that prevent reinfection and reduce the spread of malaria; and thirdly, pre-erythrocytic vaccines that can halt the parasites' incubation within the liver of its host and progression to the blood stage

of infection. This final category of vaccines is therefore an attractive avenue to pursue as they have the ability to prevent the clinical symptoms associated with infection and have the added benefit of cutting transmission (Figure 1.7 (A)). Vaccine design usually starts with the selection of an antigen required by an invader for entry into cells or integral to the progression of its life cycle (Correia et al., 2014). In the case of malaria many of the advance vaccine candidates use surface antigens that were selected prior to the widespread use of advanced genomic and proteomics tools. Appreciation for the distribution, abundance and polymorphisms of surface antigens combined with a real understanding of their precise biological function will all aid malaria vaccine development.

1.7.3 Stopping Malaria Transmission – Transmission Blocking Vaccines

Whilst blood-stage vaccines attempt to give an individual protection from the clinical symptoms associated with malaria, TBV candidates attempt to stop the passaging and establishment of the sexual stages of *Plasmodium* within the mosquito vector. Blocking the transmission of malaria between individuals has historically centred on the use of insecticide-treated bed nets, DEET based sprays, chemoprophylaxis and more recently the use of genetic tools to induce mosquito sterility. This can be seen with the lack of transmission-based vaccines currently in clinical trials (Patel & Tolia, 2021). Regrettably the complexity of the malaria cycle makes finding a single stage-transcending antigen difficult. This is because the parasite will express many dominant surface antigens that are specifically optimised for the environment it finds itself in (Ferreira et al., 2004). Yet transmission reduction and elimination are a key step to disease eradication. To date one of the most appealing transmission blocking candidates is *Pf*s25, a 25kDa protein fixed to the ookinete surface via a GPI-anchor (Barr et al., 1991). *Pf*s25 is an important complex surface protein for ookinete survival against mosquito midgut proteases and

invasion of the mosquito midgut. It contains four epidermal growth factor (EGF)-like domains and eleven disulphide bonds. Importantly *Pf*s25 is only expressed whilst the parasite is within the mosquito and as such not subject to the same selection pressures as proteins interacting with the human immune system (Scally et al., 2017). Work is currently underway to tackle the challenges of eliciting high, long-lived antibodies that are effective at blocking transmission of *P. falciparum*. The expression of *Pf*s25 in traditional *E. coli*-based expression systems results in protein that is misfolded and aggregated (Lee et al., 2016). The importance of *Pf*s25 containing a GPI anchor in the context of eliciting an effective immune response has been studied through its production by an *E. coli*-based CFPS system. Through the use of an amber stop codon at its C-terminus and the incorporation of a non-natural amino acid, a GPI anchor could be added using click chemistry. Two versions, one with a GPI anchor and one without were generated. These were then used to elicit anti-*Pf*s25 antibodies within mice that were then evaluated by ELISA. The antibodies elicited from the *Pf*s25-GPI anchored protein were shown to be at higher levels when compared to antibodies produced in the absence of a GPI-anchor. By using the standard membrane feeding assay (SMFA) the authors were able to highlight the potency of the *Pf*s25-GPI induced antibodies. They showed a significant inhibition of transmission as measured by oocyst density in mosquito midguts over oocyst density using antibodies from *Pf*s25 lacking a GPI anchor (Kapoor et al., 2018).

1.7.4 An Intra-erythrocytic Vaccine

The current blood stage vaccine candidates have primarily focused on crucial ligands on the merozoite cell surface required for invasion of RBCs (Good, 2001). The most studied blood stage antigens centre on apical antigen 1 (AMA-1) and merozoite surface protein 1 (MSP-1) of *P. falciparum* (Ellis, Sagara, et al., 2010). Currently the only vaccine in this category that has shown some clinical efficacy has been FMP2.1/AS02A. The FMP2.1 vaccine is made of

recombinantly produced AMA-1 in *E. coli*. AMA-1 is an 83kDa protein that is pre-processed within the intra-erythrocytic parasite yielding a 66kDa protein before being exported to the parasite's cell surface. This occurs prior to the rupture and release of merozoites from an infected RBC. However, due to the protein's highly polymorphic nature, antibody-mediated inhibition is usually ineffectual as shown in the clinical data gathered from FMP2.1/AS02A vaccine trials in Malian and Kenyan children. Whilst the vaccine showed 64% efficacy in Malian children this was contingent on a controlled challenge by a single *P. falciparum* strain. In contrast Kenyan children, whilst having high AMA-1 antibody titres showed no inhibition of malaria parasites (Laurens et al., 2017).

The other heavily researched blood-stage candidate, MSP-1 is synthesised as a 196kDa precursor that is processed into four subunits which promote RBC rupture (Ferreira & Hartl, 2007). It is fixed to the cell surface of merozoites by a GPI anchor and may act as a scaffold for other proteins during subsequent RBC parasite attachment and invasion (Gerold et al., 1996). In animal trials immunisation with MSP-1 has shown some efficacy however, a number of human clinical trials have produced disappointing results yielding little protection from malaria infection (Ellis, Martin, et al., 2010). Historically clinical trials involving MSP-1 have used small sections of the protein rather than immunisation with the entirety of the protein. This is unfortunate as MSP-1 has been reported to potentially possess many T-cell and B-cell epitopes that could elicit a strong immune response (Parra et al., 2000). Therefore, the use of full-length MSP-1 in subsequent immunisation strategies could lead to better protection against malaria.

Due to the size and nature of MSP-1, like many other proteins of *P. falciparum* its production is hampered by heterologous protein expression systems. In 2013, it was reported that as many as 95% of full-length malaria proteins could not be expressed in traditional systems. This is due to a variety of reasons including; the high A/T content of coding regions in the *P.*

falciparum genome, frequent arginine and lysine repeats that cause premature termination of mRNA transcripts and the unique protein structures present in malaria. In 2020 an early phase I clinical trial involving malaria naïve adults immunised with full-length MSP-1 produced in *E. coli* together with a GLA-SE (Toll-like receptor 4) adjuvant induced memory T-cell and IgM and IgG MSP-1 specific antibodies. These were detected above the levels of semi-immune malaria individuals but were not strain transcending (Blank et al., 2020). However, when the antibodies were assessed by GIA or by an intraerythrocytic invasion they did not inhibit parasite growth *in vitro*. Therefore, although the trial produced antibodies capable of detecting both of the two dominant MSP-1 strains in Africa, the trial like so many other MSP-1 based vaccines lacked clinical efficacy. This is unsurprising considering many blood-stage vaccine candidates, based on dominant surface antigens are under intense immune pressure leading to a great deal of antigenic diversity thereby reducing their cross-strain protection (Servín-Blanco et al., 2016).

This raises the question in malaria vaccinology as to whether targeting the dominant surface antigen is the correct strategy. A change in approach may be needed to alter the historic direction of malaria effective vaccines. Parasites have evolved with humans to evade the immune system, additionally the length of time in which a merozoite is available for detection and elimination by the human immune system is small, especially when compared to transit times of sporozoites (Gomes et al., 2016). However, the *P. falciparum* Reticulocyte Binding Protein Homologue 5 (*Pf*Rh5) appears so far to be 'bucking' this trend. Rh5 is an essential merozoite invasion ligand binding to the RBC surface protein basigin. In its processed form Rh5 forms a kite-like structure of two, three-helical bundles of 45kDa with no transmembrane domain or GPI anchor (Wright et al., 2014). Whilst the precise manner in which Rh5 links to the surface of the merozoite still requires investigation, its potential as a blood stage antigen has gained much excitement. This is because antibodies raised against Rh5 not only have the ability to block merozoite binding to RBCs but also show cross strain *P. falciparum* inhibition. In fact,

when anti-Rh5 antibodies were tested *in vitro* they were shown to be effective against all known parasite Rh5 polymorphisms (Moore et al., 2021). However, in natural infections Rh5 is present at much lower levels compared to other blood-stage targets such as AMA-1 (Ord et al., 2015). Therefore, a number of vaccine strategies in phase I and II clinical trials are now attempting to induce higher levels of anti-Rh5 antibodies within human volunteers(Ragotte et al., 2020). In phase I clinical trials both a recombinant protein delivered with an adjuvant and a modified chimpanzee adeno virus (ChAd 63) carrying full-length Rh5 prevented malaria in heterologous challenges (R. O. Payne et al., 2017). Phase II trials using a Drosophila S2 cell-line expressing Rh5 are also currently underway.

1.7.5 Pre-erythrocytic Vaccines

Pre-erythrocytic vaccines focus on targeting the sporozoite stage of the *P. falciparum* life cycle. Sporozoites are injected from the mosquito during a blood meal (Bettencourt, 2020). This is the first interaction humans have with the malaria parasite, as little as one to 100 sporozoites flow from the mosquito to the host creating a bottleneck of malaria infection. The sporozoites then transit from the skin dermis to the liver, a journey purported to take approximately ten minutes (Yamauchi Lucy M. et al., 2007). This is in fact the longest period in the malaria life cycle where the parasite is extracellular and therefore susceptible to potential attack from the host's immune system. There are currently two well-established strategies for vaccine development that have been reported to elicit varying degrees of efficacy (see Figure 1.7 (B)).

1.7.6 Whole Sporozoite

The first whole, radiation attenuated sporozoite vaccine in controlled infections gave 80% protection in malaria naïve adults when challenged with a single parasite strain. However, a lower efficacy was reported when these individuals were challenged with heterologous strains

or malaria infections in the field (Epstein et al., 2011). Encouragingly though in mice the genetic attenuation of sporozoites has shown good efficacy but has not yet been trialled in humans (Kublin et al., 2017). Radiation attenuated sporozoites have now also been shown to induce protection against *P. falciparum* in a phase I/IIa clinical trial (Roestenberg et al., 2020). There are however, other logistical problems in delivering whole sporozoite vaccines, such as labour-intensive mosquito dissections and ultra-cold storage for the vaccine's transportation.

1.7.7 RTS,S – Why Hasn't it Delivered?

The second and most advanced malaria vaccine candidate named RTS,S/AS01 has only shown partial efficacy in phase III clinical trials since its initial development over three decades ago (Mahmoudi & Keshavarz, 2017). RTS,S is a fusion protein of the central tandem repeat region (NANP) and C-terminal regions of the circumsporozoite protein (CSP) from *P. falciparum*, fused to the hepatitis B surface antigen (HBsAg) (see Figure 3.1 (A)). Whilst many traditional vaccines in widespread use are live attenuated or dead pathogens, RTS,S forms virus-like particles (VLPs) that are delivered with the powerful AS01 adjuvant (Regules et al., 2011). CSP is the most abundant protein on the surface of sporozoites and plays a critical role in multiple aspects of the parasite's pre-erythrocytic life cycle (Julien & Wardemann, 2019). This includes the formation of sporozoites in the mosquito midgut, invasion of mosquito salivary glands and invasion of liver hepatocytes through its interaction with heparin sulphate proteoglycans (Malpede & Tolia, 2014). The N-terminal region of CSP is highly conserved amongst *Plasmodium spp*, usually containing between 25-42 copies of the NANP repeat region. The length of the NANP repeat region used in RTS,S has been related to vaccine efficacy through the measurement of IgG levels to the NANP region based on various lengths used in a variety of vaccine candidates (Oyen et al., 2018). The cysteine rich C-terminal region of CSP, the type I thrombospondin repeat region (TSR) is highly polymorphic and has been implicated

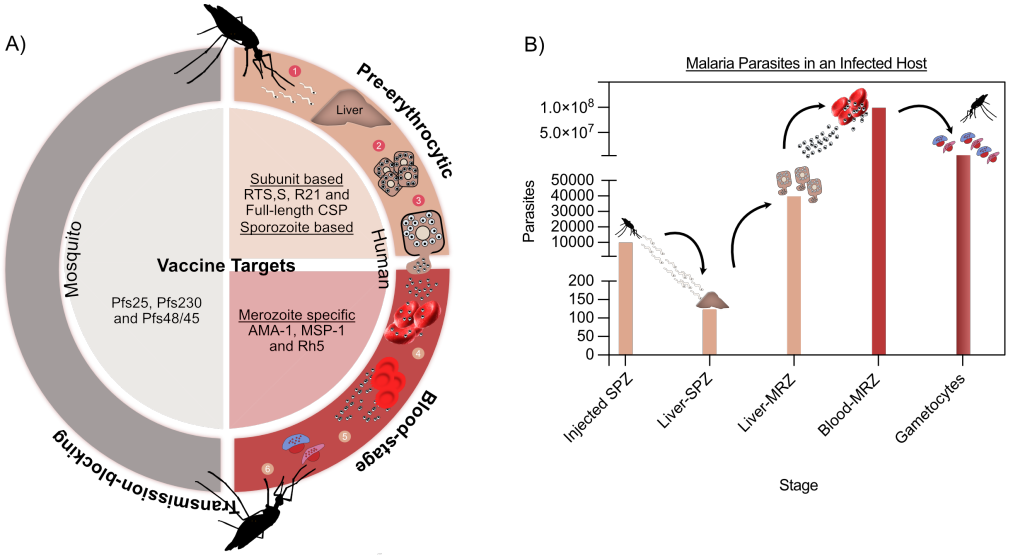

Figure 1.7: The Landscape of Malaria Vaccines
Malaria vaccines can be grouped into three main categories: pre-erythrocytic, blood-stage and transmission based. The infection landscape has a number of peaks and troughs of parasite numbers within the host, creating bottlenecks that may be beneficial for vaccine delivery. **A**) Highlighted here are some examples of vaccines undergoing trials and the stage of the parasite they prime the immune system to target. 1) Sporozoites are injected into a host. 2) Sporozoites invade liver cells and replicate. Pre-erythrocytic vaccines aim to prevent this, most notable RTS,S. This is a pinch-point in malaria infection as often only a few liver cells become infected by malaria parasites. 3) Merozoites burst from an infected cell entering the bloodstream. 4) Merozoites invade and replicate within RBCs. Notable vaccines surrounding the blood-stage centre on essential merozoite invasion ligands e.g. RH5 and MSP-1. 5) Some parasites will then commit to the sexual stage of development. TBVs aim to elicit an immune response to these parasites before they are transmitted. TBVs focus on dominant surface proteins present during the sexual stage of development such as *Pf*s25. **B**) Shown here are the reported *P. falciparum* parasite numbers per stage of infection. A mosquito injects roughly 1000 sporozoites (SPZ) into the peripheral blood of a human, 15-123 will successfully reach and invade primary hepatocytes. After approximately two weeks this will rupture releasing up to 40,000 merozoites (MRZ) into the blood stream of the infected host. Merozoites will then invade RBCs. Here parasite numbers have been reported to be as high as $1x10^8$ during subsequent rounds of invasion and replication within RBCs. Less than 5% of parasites will commit to the sexual stage of the malaria life cycle forming gametocytes. Targeting the pre-erythrocytic stage of malaria with vaccines means that the immune system has to deal with considerably less parasites than the blood stage. Yet if just a single parasite evades immune detection it can start the blood-stage of infection.

in vaccine efficacy through its regulation of phagocytic activity in hosts. Once sporozoites are injected from the mosquito to the human host, sporozoites must migrate to the liver, CSP has been shown to be involved in gliding motility and parasite invasion of liver cells, (Plassmeyer et al., 2009). CSP on the surface of sporozoites contain an N-terminal cleavage site that is protected from proteolytic activity during this motile stage. Proteolytic cleavage in the mam-

malian host exposes a CSP domain essential for liver cell attachment and invasion. Inhibiting this process significantly reduces the sporozoites from reaching the liver (Espinosa et al., 2015). The processing of *P. falciparum* CSP can be seen through western blot analysis of *P. falciparum* sporozoite lysates, showing two closely related bands at 60kDa(Herrera et al., 2015). Although *P. falciparum* CSP plays a crucial role in the invasion of human liver cells, clinical trials using CSP based vaccine delivery systems such as RTS,S have not delivered in terms of efficacy and long lived protection. To improve the efficacy of this CSP delivery system R21 was designed. This candidate reduces the quantity of the HBsAG and increases the density of CSP packed onto the VLP and is combined with the Matrix M adjuvant. In clinical trials this combination has outperformed RTS,S resulting in protection of 75% in African children. However, this vaccine is still based on the same NANP repeat region and C-terminal domain of CSP. This resulted in multiple booster shots being required over the year period the clinical trial was carried out in due to a loss of protection. Although this represents a key step forward, the practicality of requiring four doses of the vaccine spread just over a year remains highly impractical in the areas in which it needs to be deployed (Datoo et al., 2021).

1.7.8 Problems Associated With *P. falciparum* Antigen Production

Refinements of delivery systems and strategies surrounding *P. falciparum* CSP are currently being considered. The use of structural data from CSP binding antibodies could be used to improve monoclonal (mAb) neutralisation sites through protein engineering (Oyen et al., 2020). Second generation RTS,S vaccines based on full-length CSP and VLPs with a higher CSP density could elicit stronger immune responses (Dobanõ et al., 2019). The use of full-length CSP may therefore elicit a more effective immune response than an N-terminally truncated version through the exposure of more epitopes to the immune system. However, expression of suitable quantities of full-length *P. falciparum* CSP has been problematic (Noe et al., 2014).

Traditional *E. coli* based recombinant expression systems have struggled on many occasions to produce correctly folded soluble *P. falciparum* proteins of immunological interest (Mudeppa & Rathod, 2013). The Structural Genomics of Pathogenic Protozoa Group attempted to express 1000 *P. falciparum* open reading frames using *E. coli* but unfortunately were only able to successfully express 60 soluble proteins. They cited the unusually high A/T content of the *P. falciparum* genome, the presence of multiple disulphide bonds within candidate proteins, high molecular weights, multiple transmembrane domains and high amounts of low complexity regions leading to disordered proteins as markers for insoluble protein production (Mehlin et al., 2006). There are a number of factors that should therefore be considered when attempting to produce an antigen of interest, like CSP. Factors such as conformational stability and the ability for a protein to maintain proper folding can influence antigen processing in antigen presenting cells (APCs). Furthermore, a protein's stability and overall maintenance of its tertiary structure has an impact on the b-cell mediated immune response. To facilitate the best immune reponse an antigen needs to be synthesised such that it represents to the best possible degree the structure of the native protein (Joseph et al., 2015). That way unfavourable conformations that may not be seen in the WT protein are minimised, eliminating off target immune responses.

1.7.9 Glycosylation of Surface Proteins in *P. falciparum*

Protein post-translational modifications can be critical for a protein's stability, structure and biological function with N-linked glycosylation being one of the most important in nature (Müller, 2018). However, *Plasmodium spp* lack many of the conventional genes associated with N- and O-linked glycosylation. The type of glycosylation in malaria parasites can be segmented based on where the parasite is within its life cycle. Whilst replicating in the human host *P. falciparum* proteins present with N-linked glycosylation but on entering and replicating within the

mosquito vector this switches to O-linked glycosylation. The *Plasmodium* O-fucosyltransferase (POFUT2) enzyme is responsible for adding fucose sugars in O-linked glycosylation to serine or threonine within the TSR domains, more commonly referred to as fucosylation and is conserved amongst *Plasmodium spp.* This process yields O-linked β-D-glucosyl-1,3-α-L-fucose disaccharide fixed to TSR domains (see Figure 1.8 (C)). This is exemplified by sporozoite surface proteins, CSP and thrombospondin-related anonymous protein (TRAP). The essentiality of POFUT2 in *P. falciparum* can be seen when POFUT2 is excised by double crossover homologous recombination. Here, parasites deficient in POFUT2 mature into sporozoites but their gliding motility, cell traversal and invasion into hepatocytes are all impaired by approximately 80% when assessed in a humanised mouse liver. Deletion of POFUT2 does not affect growth in asexual blood stage parasites or up to stage V gametocytes providing further support for parasite glycosylation type segmentation based on its point of development (Lopaticki et al., 2017). Further support for the essentiality of POFUT2 in general comes from mammalian experiments where removal of POFUT2 was lethal in embryonic mice (Benz et al., 2016). Both CSP and TRAP proteins are essential for human infection by the sporozoite and are being used in a variety of vaccine delivery platforms (Lu et al., 2020). Glycans also play critical roles in protein function as glycosylation changes by an invading pathogen can have an impact on the host.

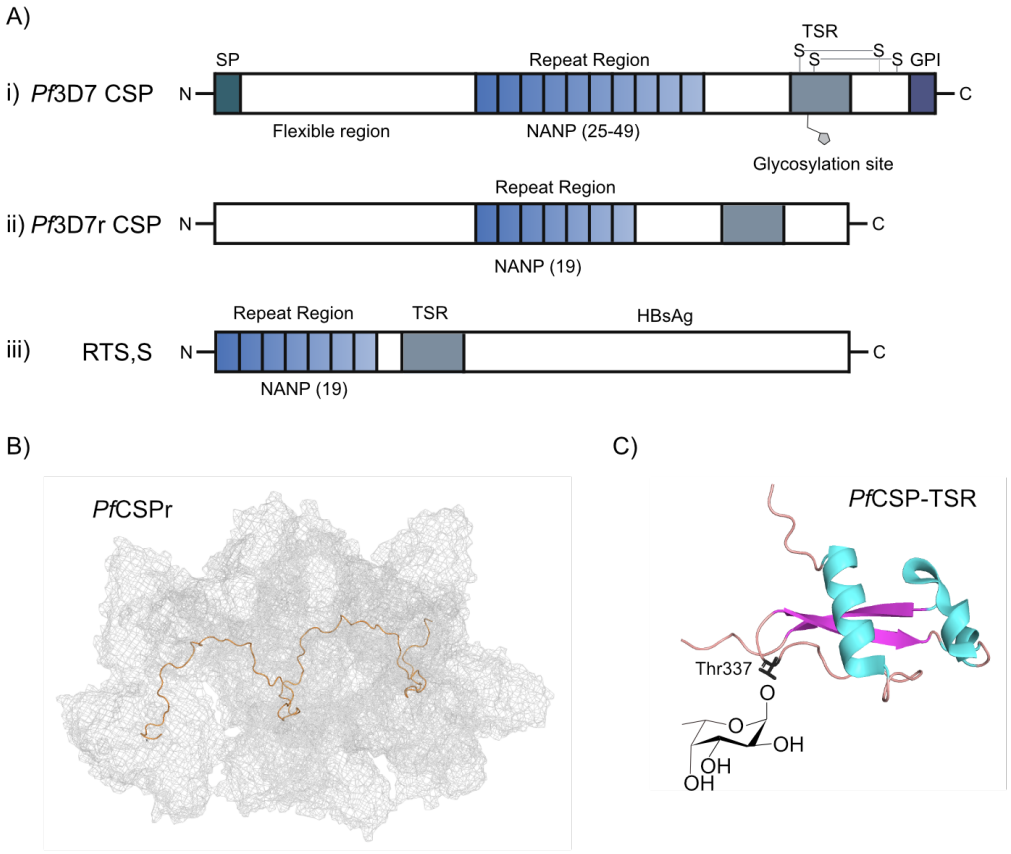

Figure 1.8: *P. falciparum* CSP, Sequence and Structure

Resolving the atomic structure of *P. falciparum* CSP has been hampered by the intrinsic disorder within the NANP repeat region. The use of cryo-EM in conjunction with variable domains of an anti-CSP monoclonal antibody (Fab311) were able to stabilise a recombinant *P. falciparum* CSP (*Pf*3D7 CSP) produced in *E. coli*. **A**) Three schematics compare the WT *Pf*3D7 CSP sequence and features to those of recombinant CSP (*Pf*3D7r CSP) used by Oyen et al to gain CSP antibody structural data and RTS,S used in various iterations for vaccine trials. WT CSP (i) has a N-terminal signal peptide (SP), followed by a flexible region responsible for binding heparin sulphate on hepatocytes and a structured TSR domain. The TSR domain contains a single glycosylation site with two disulphide bonds. The C-terminal contains a Gpi anchor that fixes CSP to the cell-surface. Recombinantly produced CSP (ii) contains shortened NANP and TSR domains. RTS,S (iii) contains the NANP repeat regions, the TSR domain fused to the hepatitis B surface antigen(Oyen et al., 2018). **B**) The cryo-EM structure of *Pf*CSPr bound to Fab311 fragments at 3.2Å. The Fab fragments bound are depicted as a mesh surface allowing CSP visualisation (PDB_6axk - The PyMOL Molecular Graphics System, Version 2.0 Schrödinger, LLC)). **C**) The crystal structure of the TSR domain of *P. falciparum* CSP solved to 1.70Å. The TSR domain is comprised of a four-layer stack containing a hydrophobic core and pocket. Although CSP is visualised as a flexible disordered structure (B), here the TSR domain shows a distinct structural fold. The TSR domain of *Pf*CSP contains a single fucosylation site at Thr337, fucose has been superimposed onto the structure as a representative example. The fucosylation site on the TSR domains of CSP and TRAP are conserved, POFUT2 catalyses the linkage of fucose to these proteins through the removal of GDP from the sugar moiety (adapted from PDB_6mhg - The PyMOL Molecular Graphics System, Version 2.0 Schrödinger, LLC).

1.8 Cell-Free Protein Synthesis

Cell-free protein synthesis systems are able to exploit the protein synthesis power of a cell while reducing or indeed eliminating many of the constraints associated with traditional cell-based recombinant technologies (Nirenberg, 1964). Proteins are the predominant target of drugs currently on the market today, with approximately 50% of these being membrane proteins (Lawson, 2015). Producing these proteins rapidly and properly folded especially in the context of diseases is paramount when investigating antibody recognition.

1.8.1 The Landscape of Cell-Free Systems

Traditionally recombinant protein production has centred on the use of *E. coli* of a variety of genetically modified strains due to its ease of use, ability to be rapidly upscaled and cost-effectiveness (Chen, 2012). Yet, many proteins such as antibodies or those involved in disease require a host of post-translational modifications or chaperones that *E. coli*-based systems simply cannot independently achieve. Eukaryotic based recombinant technologies using for example human embryonic kidney (HEK) 293 or Chinese hamster ovary (CHO) cells for the production of many complex membrane embedded or associated proteins have as a result been employed (J. Yin et al., 2007). However, the overexpression of membrane proteins can be cytotoxic to a cell resulting in the reduction of a target protein, protein misfolding or even cell death (Andréll & Tate, 2013). New expression technologies are required to alleviate this problem with an interesting solution coming from CFPS based systems. In essence the CFPS systems can be broken down into four constituent components. The cellular lysate, produced through the rupture and isolation of a selected cell type, chosen based on the complexity of the type of protein that the user desires to make; An energy regeneration system that supplements for the lack of functional mitochondria and is used to produce and regenerate ATP, essential for starting and maintaining active translation; Buffering components and salts that maintain the

stability of rRNA, mRNA and the surrounding protein complexes; finally, the template DNA containing not only the coding sequence (CDS) or the desired gene but also promotors enabling transcription of that gene and untranslated regions (UTRs) for efficient translation initiation within the ribosome (Khambhati et al., 2019) (see Figure 1.9).

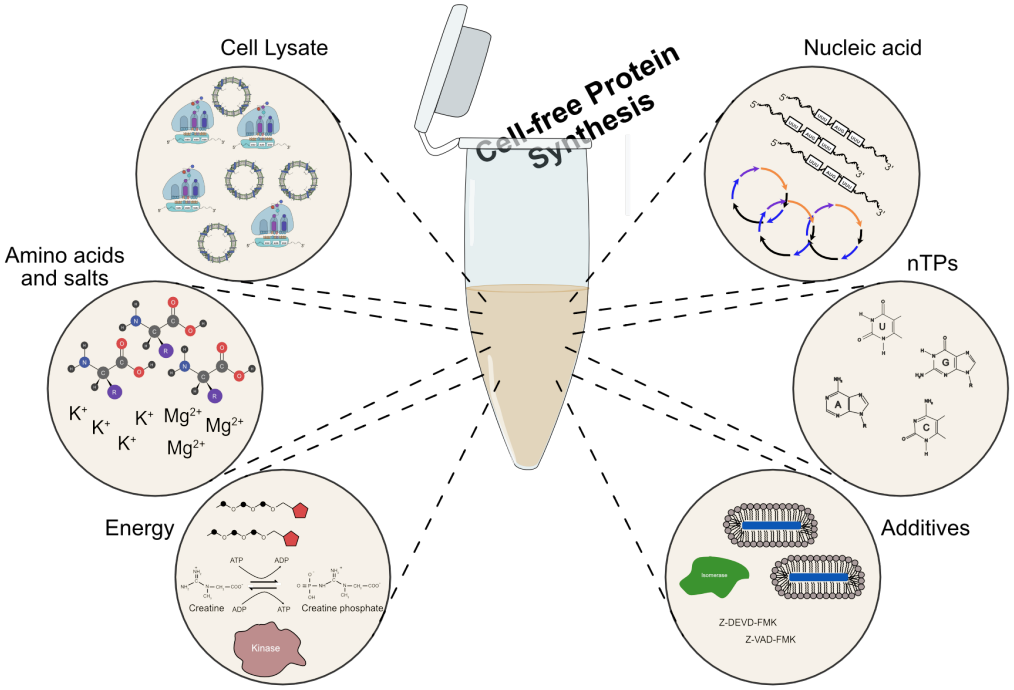

Figure 1.9: An Overview of Cell-Free Protein Synthesis
CFPS allows the rapid production of a protein of interest in substantially less time than equivalent cell-based technologies within a single reaction tube. A cell type is chosen for lysate production based on the user's needs. The salt composition can then be optimised through changing magnesium and potassium concentrations. This is important for ribosome and mRNA stabilisation, aaRS function as well as T7 RNAP function in TX-TL reactions. An energy regeneration system is critical for prolonged protein synthesis and aims to provide a continuous source of ATP. For the most part CFPS systems use the creatine phosphate/creatine phosphokinase setup to provide energy. Nucleic acids in the form of mRNA for a linked reaction or DNA in the form of a plasmid or PCR product for a TX-TL reaction. Additionally, an exhaustive list of additives can be added to a cell-free reaction including nanodisks and microsomes, disulphide isomerase and caspase inhibitors. The chosen additive is usually protein or system dependent.

1.8.2 *E. coli*-based Cell-Free Systems

The most widely used cell-free lysates are predominant derived from *E. coli* extracts as these systems have historically offered high-yield platforms for CFPS. Bacterial based CFPS have been used for decades, most notably since Matthaei and Nirenberg used an early incarnation of

the technology to aid in the deciphering of the genetic code (Nirenberg, 1964). Lysates derived from *E. coli* are relatively easy to grow and prepare so have become the chosen lysate for biopharmaceutical protein production (Casteleijn et al., 2013; J. Li et al., 2018). Advancement in prokaryotic systems has included the 'PURE' *E. coli* system, in which each of the components necessary for translation are recombinantly produced or individually purified (Shimizu & Ueda, 2010). This creates a highly controlled and 'pure' CFPS system where each of the factors involved in initiation, elongation and termination of a growing polypeptide chain can be modified and tuned. The 'PURE' system may even have the potential to enable the generation of a self-replicating *in vitro* translation system potentially creating the foundation of self-replicating artificial cells (Libicher et al., 2020). However, these *E. coli* derived CFPS systems are unable to 'naturally' produce post-translational modifications such as disulphide bond formation or complex levels of glycosylation (Matsuda et al., 2013). These types of modifications are required to produce many membrane or cell surface proteins that would in a eukaryotic cell usually occur in the endoplasmic reticulum (ER) (Oka & Bulleid, 2013), or in the periplasm within bacteria (Missiakas & Raina, 1997).

1.8.3 Disulphide Bond Formation

The extracellular eukaryotic environment contains many proteins that require disulphide bonds which are important for protein folding and overall stability(Bulaj, 2005). Antigens present on the surface of many disease-causing pathogens like CSP in *Plasmodum* (Rathore et al., 2001)or the Spike protein of SARS-CoV-2 (Xiong et al., 2020) all contain varying amounts of disulphide bonds. Laboratory strains of *E. coli* used for recombinant protein production use their periplasm as a compartment for disulphide bond formation however, this is inadequate for producing multi-disulphide bonded proteins at high-yields (Matos et al., 2014). The genetic modification of *E. coli* to create stains containing enzymes making disulphide bond formation

more favorable are now widely used. The use of these recombinant bacterial technologies enables the formation of simple disulphide bonds in overexpressed proteins within the cytoplasm. Partially modified *E. coli* strains can achieve this through the expression of DsbC isomerase enzymes, as is the case with the SHuffle T7 express lys^{Y} *E. coli* (New England Biolabs) strain (Lobstein et al., 2016). In the context of CFPS, the preparation of bacterial lysates results in the periplasm being compromised which removes the compartment necessary for simple disulphide formation (Swartz, 2001). The use of *E. coli* CFPS systems with lysates modified with disulphide bond isomerase C (DsbC) and the Skp chaperone have enabled the production of proteins with up to nine disulphide bonds (Matsuda et al., 2018). These include, the protease domain of a murine urokinase, a tissue type plasminogen activator and murine granulocyte-macrophage colony-stimulating factor (Yang et al., 2004). Whilst these types of lysates are commercially available they become more expensive based on the level of post-translational modification required in the expressed protein.

1.8.4 Glycosylation

The most common type of eukaryotic glycosylation is asparagine-linked (N-linked), which is required by certain proteins to enhance stability, aid protein folding and increase immunogenicity (Weerapana & Imperiali, 2006). Yet, currently there is little means in cell-based eukaryotic technologies to precisely control the levels and extent of glycosylation on a recombinant protein (Hossler et al., 2009). The open nature of CFPS systems allows for the direct control manipulation of the biochemical environment that is simply not possible in cell-based technologies. Therefore, to achieve N-linked glycosylation in an *E. coli* CFPS system, Jaroentomeechai et al used a modified CLM24 strain that possess two traits which allow for the modification of the bacterial lysate that make N-linked glycosylation more favourable. Firstly, the CLM24 strain lacks the ability to carry out O-linked glycosylation due to an inactivating insertion in

wbbL that encodes a rhamnosyl transferase. Secondly the CLM24 strain also lack the WaaL gene that encodes an O-linked ligase (Jaroentomeechai et al., 2018). Taken together these two features provided the authors with the ability to produce glycosylated proteins such as human erythropoietin through the introduction of *C. jejuni* PglB and glycosynthesis enzymes. The ability to glycosylate proteins using an *E. coli* based CFPS is an important step as, unlike mammalian derived lysates they are cheaper and easier to produce.

1.8.5 Membrane Proteins

Membrane proteins remain the target for many drugs currently on the market but many contrainsts exist in their manufacture using conventional expression systems. Traditionally membrane protein production using conventional cellular *E. coli*-based systems has involved the expression of an insoluble protein in inclusion bodies; the purification from inclusion bodies and subsequent solubilisation in membrane-mimicking agents such as detergents or liposomes. However, this is a laborious and time intensive process (Duquesne et al., 2016). The CFPS of membrane proteins using *E. coli* lysates has been increasing for well over ten years with techniques continuing to expand and evolve. The majority of membrane proteins produced by these systems are large, being >100kDa and containing multiple transmembrane domains(Rues et al., 2016). In addition, proteins that are membrane associated or anchored and contain large soluble domains such as CSP have proven challenging to produce (Paulick & Bertozzi, 2008). A number of strategies have been employed to obtain a variety of membrane proteins that ultimately depends on the nature of the protein's structure. Firstly, proteins can be produced in an insoluble manner, possibly retaining some structure which then require detergent based solubilisation (Schwarzer et al., 2017). Secondly, proteins produced in a CFPS system could be synthesised in the presence of detergents or lipids enabling their stabilisation and soluble production. However, the inclusion of such additives can negatively affect the translation kinetics

in a reaction reducing protein yield (Lyukmanova et al., 2012). The inclusion of detergents, lipids or nano disks can also produce a heterogenous mixture of protein in different orientations that need to be assessed for functionality.

1.8.6 Can *E. coli* CFPS Systems Deliver?

Whilst bacterial *E. coli* based CFPS have supercharged the cell-free landscape in terms of recombinant protein scalability, high-yield protein production and ease of use; they lack many naturally occurring macromolecular structures required for complex protein synthesis. Though elements, as detailed above can be supplemented into them, it is an exhausting process requiring precise knowledge of the exact pathways involved. In the context of *Plasmodium*, *E. coli*-based cell-free systems have been reported to have <10% success rate in the expression of soluble antigens for the purposes of vaccine development (Rui et al., 2011).

1.8.7 Wheatgerm CFPS – A Bridge Between Bacteria & Mammalian Cells

Wheat-germ CFPS (WGCF) systems have been extensively used in the context of malaria research for the production of antigens that can elicit an immune response (Fan et al., 2013; Richards et al., 2013). They represent a eukaryotic alternative to *E. coli*-based systems in the expression of difficult to express *Plasmodium* proteins. Like other CFPS systems, WGCF systems enable the rapid production of a protein of interest in hours to days without the need for laborious cell culturing techniques (Zhao et al., 2010). The WGCF system has a proven ability in expressing complex and soluble *Plasmodium* proteins over traditional *E. coli* systems (Miura et al., 2019; Tsuboi et al., 2010). The WGCF system has a proven, well-established ability in the expression of *P. falciparum* proteins such as the merozoite micronemal protein GAMA, a protein essential for parasite invasion of RBCs(Fan et al., 2013). The antibodies raised against

P. falciparum GAMA ectodomain in mice, produced in the WGCF system were able to detect the GAMA protein as well as block invasion *in vitro*. The expression of *P. vivax* potential vaccine candidates such as CSP (Longley et al., 2017) can be used to show key differences between wheatgerm and *E. coli* derived CFPS systems. A greater number of proteins were detected by ELISA when produced from the WGCF system and challenged by sera isolated from individuals in malaria endemic areas (Rui et al., 2011). This may be explained by an increase in soluble protein production in WGCF systems compared to *E. coli* CFPS systems, possibly due to native eukaryotic chaperones (Miura et al., 2013). The WGCF system has subsequently been used by Morita et al to screen a library of 1827 recombinant *P. falciparum* proteins (Morita et al., 2017). The serum isolated from individuals living in the malaria endemic area of Uganda was used to probe a panel of proteins for reactivity based on previous malaria infection. The study revealed that 54% of the 1827 proteins were immunoreactive, of these 128 induced antibody responses which could be correlated with malaria protection. Thus, highlighting the power over traditional recombinant cell-based technologies at HTP antigen screening for the detection of potential vaccine candidates.

1.8.8 WGCF Systems, The Pros and Cons

WGCF systems offer a eukaryotic approach to cell-free based technologies that are able to produce recombinant proteins in milligram quantities, far exceeding the efficiency of other mammalian or insect based eukaryotic systems (Novikova et al., 2018). Initially WGCF systems exhibited lysate instability as a result of a number of ribonucleases and proteases present in the endosperm of the wheat-germ (Cazenave et al., 1993). A concerted effort by K. Madin et al in 2000 led to a protocol that allowed for the removal of these from the endosperm making the lysate far more stable (Madin et al., 2000). Not only do WGCF systems offer high yields of protein production but they also show a greater success rate in the production of *P. falciparum*

and human proteins. WGCF systems have shown a greater success for the expression of complex human proteins compared to *E. coli*-based systems. In fact the for the production of 960 human open reading frames in both, resulted in a greater degree of success in the WGCF systems for the production of soluble protein (Langlais et al., 2007). WGCF systems unlike other CFPS systems can produce large complex proteins that only require minimal or no codon optimisation (Tsuboi et al., 2008). This is of particular advantage in the expression of *P. falciparum* proteins as the parasite's genome is unusually A/T rich compared to other organisms. However, like *E. coli*-based systems lysate prepared for WGCF reactions lack the ER compartment for the formation of disulphide bonds, membrane proteins and glycosylation due to the extraction process. However, for the production of more complex extracellular proteins, disulphide bond formation is usually required to enhance protein stability and reduce degradation. Like *E. coli* CFPS systems, WGCF systems can be supplemented with disulphide bond isomerases, reducing and oxidising agents to create a favourable environment for the formation of disulphide bonds. This has proved successful in the production of a single-chain antibody variable fragment (scFV) against the Salmonella O-antigen (Kawasaki et al., 2003). Although these examples highlight the power of WGCF systems, like all systems there are also some significant disadvantages. The preparation of lysate can be a laborious process taking up to five days, shifting many users to commercial kits and increasing the cost of protein production (Takai et al., 2010). The production of membrane and glycosylated proteins remains challenging and is not possible without lysate supplementation. Like bacterial systems WGCF systems can be supplemented with membrane like structures or ER remnants from other eukaryotic cells that have allowed the expression of with post-translational modifications such as N-linked glycosylation (Shields & Blobel, 1977).

1.8.9 Mammalian Based CFPS Systems – Systems for Complex Protein Production

Mammalian based CFPS systems have been increasing in interest due to the lysate's inherent ability to produce human-like glycosylation, without the need for supplementation (Quast et al., 2014). Mammalian systems are derived from a number of sources including Chinese hamster ovary cells (CHO) (Gupta & Siminovitch, 1977; Tran et al., 2018), human cells (HeLa) (Weber et al., 1975) and rabbit reticulocytes (Lockard & Lingrel, 1969). Having the ability to produce glycosylated proteins is extremely important for the engineering of protein-based therapeutics and vaccines (Cumming, 1991; Jefferis, 2009). Protein glycosylation has been shown to occur in approximately 50% of eukaryotic proteins in some form or another and shown to be critical for protein stability and immunogenicity (Apweiler, 1999). Apart from rabbit reticulocyte lysates CHO and human cell derived lysates harbour endogenous ER remnants in the form of microsomes. These are able to facilitate the post-translational modification of proteins with disulphide bonds, glycosylation and membrane attachment all being reported (Gurramkonda et al., 2018; Stech et al., 2017; Thoring et al., 2017). Like the ER in a cellular context, microsomes provide a discrete compartment where these types of modifications can occur, segregated from the main translation reaction (Stech et al., 2017). Mammalian cells share some evolutionary history with their *Plasmodium* counterparts due to their eukaryotic nature (Jeffares et al., 2007). These characteristics include N-linked and O-linked glycosylation, acylation and disulphide bond formation occurring within the ER (von Itzstein et al., 2008). Although WGCF systems have predominantly been used to express *P. falciparum* proteins, due to high protein yields their lysates lack the innate ability for disulphide bond formation and glycosylation. The use of commercially available CFPS kits derived from HeLa was successfully used to produce a number of *P. falciparum* rhoptry proteins, including Maurers cleft-2 transmembrane protein (Yadavalli & Sam-Yellowe, 2015). Natural codon usage allows for the production of high molecular weight

human proteins of interest for therapeutics or disease. A promising avenue for CFPS systems derived from human lysates is the expression of viral-like particles (VLPs) (Kobayashi et al., 2013) for the exploration of viral replication like the poliovirus or the production of artificial cells (Ho et al., 2015).

The expression of almost 70% of mammalian biopharmaceutical therapeutics on a large-scale involves the use of cell-based CHO technologies (Zhu et al., 2017). Like other recombinant cell-based technologies, CHO cells struggle to produce many large membrane proteins, multi-subunit proteins and other large complexes. However, the use of CHO derived CFPS technologies represents an alternative open strategy to the expression of many traditionally difficult to express proteins such as Toll-Like receptor-9 (TLR9) (Dondapati et al., 2019) and the human epidermal growth factor (EGFR) (Thoring et al., 2017). Like other mammalian-based systems they struggle to produce proteins with yields approaching those of *E. coli* and WGCF systems; though yields of mammalian-based systems have been increasing from the low microgram to almost milligram per millilitre yields (Thoring et al., 2017). Whilst bacterial-based systems have been shown to produce large amounts of protein in short spaces of time in a batch mode setup, mammalian-based systems require more complex setups. They also suffer from more costly and laborious cell culture techniques that increase expense.

1.8.10 Microsomes - A Power House of Eukaryotic Post-Translational Modifications.

The attractiveness of mammalian cell-free technologies over *E. coli*-based systems is due to the presence of endogenous microsomes in the lysate that are capable of performing a variety of post-translational modifications, including glycosylation. In ordinary circumstances a eukaryotic cell is compartmentalised into a variety of sub-cellular structures such as the nucleus, mitochondria, apicoplast (in the case of *Plasmodium*) and the ER (Gupta & Golding, 1996;

Foth et al., 2003).

The ER is the largest organelle in the cell and serves as a discrete environment that allows the formation of post-translational modifications not possible in the reducing environment of the cytoplasm. Translocation of a polypeptide into the ER is a highly conserved process amongst eukaryotes and can be divided into three steps; firstly targeting of a nascent or synthesised polypeptide to the ER. Secondly, introduction of the polypeptide into the translocation channel. Finally, release of the protein into the ER lumen or lateral release of the membrane protein into the lipid bilayer (Rapoport et al., 1996). During co-translational transport the ribosome is recruited to the ER membrane via the interaction of the emerging nascent polypeptide signal peptide (SP) and the signal recognition particle (SRP). The SRP slows translocation of mRNA along the ribosome until the mRNA-ribosome complex is directed to the ER surface. Translation can then continue once the SRP docks with the SRP receptor on the ER surface. SRP is then released from the ribosome after the hydrolysis of GTP and recycled for further use (Romisch et al., 1989). The nascent polypeptide chain then gets directed through the Sec61 translocon into the ER lumen (see Figure 1.10). Chaperones contained within the ER lumen e.g. immunoglobulin-heavy-chain-binding protein (BiP)/glucose-regulated protein 78 (Grp78) ensure directional travel into the ER lumen (Tyedmers et al., 2003). The signal peptide is then cleaved by a signal peptidase, removal of which completes the proteins entry into the lumen of the ER (Nguyen et al., 2018; Zimmermann et al., 2011). Proteins destined for membrane attachment may contain a hydrophobic amino acid sequence that will cause translation to pause or in the case of a GPI anchored protein contain a C-terminal signal sequence. The protein will then be directed laterally within the ER in a sequential process that binds or embeds the protein into membrane (Pierleoni et al., 2008).

For a protein inside the ER lumen there are a number of post-translational options available to it that may enable proper folding due the association with chaperones, the formation of

disulphide bonds using a host of isomerases and glycan attachment.

Many malaria vaccine candidates like *Pf*s25 (Kaslow et al., 1988), CSP(Peterson et al., 2002) and MSP-1 (Gilson et al., 2006) are anchored to the cell surface via GPI-anchors. *P. falciparum* GPIs reveals key differences compared to those of humans, specifically in the composition of palmitic and myristic acids fixed to inositol and the lack of phosphoethanolamine substitution around their core glycan. More specifically, mammalian cells contain amino-sugar or phosphoethanolamine modifications to the core glycan. These GPIs have been implicated in the induction of tumour necrosis factor and interleukin-1. The examination of semi-immune serum from individuals in malaria endemic areas has revealed the presence of antibodies directed towards the *P. falciparum* acylated phosphoinositol portion of GPIs. This is in contrast to malaria naïve adults where no such antibodies are found. Antibodies raised against chemically synthesised *P. bergheii* NH2-CH2-CH2-PO4-(Manα1-2)6Manα1-2Manα1-6Manα1-4GlcNH2α1-6myo-inositol-1,2-cyclic-phosphate can detect *P. falciparum* specific GPI in blood-stage trophozoites and schizonts but not GPIs from uninfected human RBCs. The pre-immunisation of mice with the chemically synthesised GPI resulted in substantially less tissue damage as a result of malaria infection and increased survival. Though interestingly increased survival was not coupled to the levels of parasitaemia with both glycan immunised and placebo groups having similar levels of circulating parasites (Naik et al., 2000; L. Schofield et al., 1993; Louis Schofield et al., 2002).

The lysis of many mammalian cell-types can be adapted to produce microsome containing lysate for use in CFPS. These include CHO cells (Fenz et al., 2014), HeLa cells (Gallwitz & Mueller, 1969) and HEK cells (Kaznacheyeva et al., 1998). These methods involve the gentle lysis of cells through the use of small gauge syringe needles. Endogenous microsomes have been used in CHO based CFPS platforms for the production of antibodies that require disulphide bond formation to be active. The presence of microsomes was shown to reduce the need for

supplementation of an oxidising environment like other cell-types not possessing endogenous microsomes (Thoring et al., 2017). Through supplementation of microsomes WGCF systems have also been shown to be able to synthesise proteins that require membrane association, for example the membrane glycoprotein of the vesicular stomatitis virus (Morrison & McQuain, 1977).

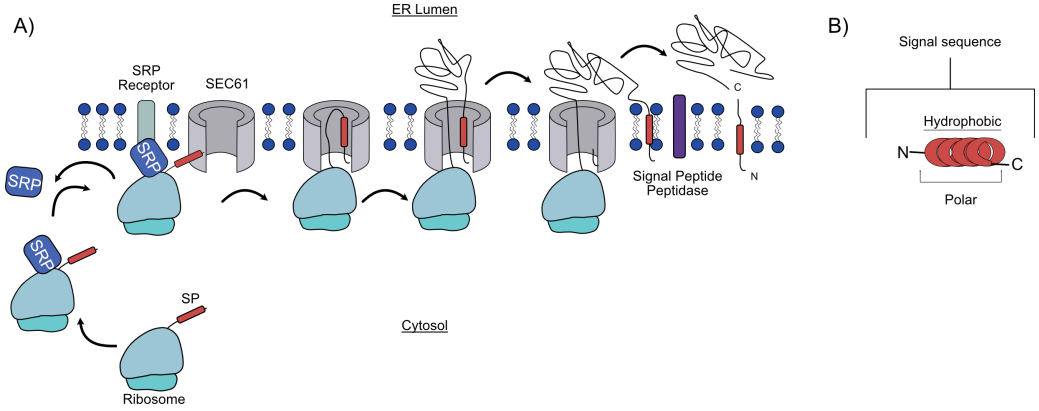

Figure 1.10: Translocation Into Microsomes
A) Microsomes are ER remnants that form spherical structures from the gentle lysis of certain cell types, acting as compartments for disulphide bond formation, glycosylation and lipidation. CFPS systems may contain endogenous microsomes or have exogenous microsomes supplemented in. A generalised depiction of translocation into the ER is shown. The signal recognition protein (SRP) binds to the signal peptide (SP) of a nascent polypeptide chain as it exits the ribosome, slowing translation. The ribosome-SRP complex moves to the ER membrane, making contact with the SRP receptor. This releases the signal peptide allowing docking of the ribosome and nascent polypeptide chain with the sec61 translocon. Translation is allowed to continue with the emerging polypeptide chain fed into the lumen of the ER. A signal peptide peptidase then cleaves the signal peptide from synthesised protein. **B**) A generalised schematic of a signal peptide (SP), located at the N-terminus of a protein sequence, generally made up of an α-helical hydrophobic region flanked by polar sequences.

1.8.11 Internal Ribosome Entry Site - Hot Wiring Translation

The mechanics for the initiation of translation within CFPS systems can vary widely between the organism in which the cellular lysate used for a translation reaction is isolated from (Hunt et al., 2020; Thoring et al., 2016). Bacteria have arguably the simplest form of translation initiation, requiring only a ribosome binding sequence, also known as a Shine-Dalgarno sequence. Here, recruitment of the ribosome and the rate in which that ribosome is able to initiate translation are predominantly the only rate limiting steps to begin the synthesis of a polypeptide.

Although bacteria do have other factors that can attenuate this process, such as heat shock proteins and ribosome binding proteins (Gualerzi & Pon, 2015). The regulatory elements of mammalian cells that are otherwise critical for normal cellular function can dramatically put the brakes on the ribosome's potential when present in the lysates used for CFPS. In eukaryotes translation initiation is a highly choreographed process that requires the association of two ribosomal subunits, tRNA and mRNA through the use of a variety of eukaryotic initiation factors (eIFs) (Sonenberg & Hinnebusch, 2009). The proper assembly and association of eIFs can however be a rate limiting step in protein synthesis especially in a cell-free context, often resulting in decreased protein yields (Sonenberg & Hinnebusch, 2009). Translation in eukaryotes can be broadly broken down into four main steps; initiation, elongation, termination and ribosome recycling. The initiation process is cap dependent, in that a m7G(5')ppp(5')N (cap) is bound to the 5' end of the mRNA strand. This cap structure is recognised by the multicomplex eIF-4a protein that also mediates the assembly of the 43S preinitiation complex that consists of the 40S ribosomal subunit bound to eIF-3, a complex composed of eIF-2-GTP and the Met-tRNAi initiator. The 43S pre-initiation complex scans the 5'UTR of the bound mRNA in a 5' to 3' direction until the start codon 'AUG' is detected. Once recognised Met-tRNAi is paired with the 'AUG' codon at the P site of the ribosome, which generates the 48S preinitiation complex. This is followed by the formation of the 80S elongation complex through the displacement of eIF-2-GDP by eIF-5B from Met-tRNAi promoting the 60S ribosomal subunit to interact with eIF-1A (Sonenberg & Hinnebusch, 2009).

IRES sequences are RNA regions that can recruit 40S ribosomal subunits in a cap-independent manner. Viruses that have uncapped positive sense RNA genomes require these IRES RNA structures to override the host's native translational apparatus. These IRES sequences are usually located within the 5' UTR of the genome or in some cases in the intergenic region (Lozano & Martínez-Salas, 2015). IRES elements are able subvert the host cell translational machinery

through the recruitment of the 40S ribosome and a subset of initiation factors (Martínez-Salas, 1999). It is the IRES RNA structure that determines its functionality making them extremely hard to predict based on sequence alone (Mokrejs et al., 2006). In fact, no IRES sequence homology could be found when comparing different *spp* of viruses such as hepatis C, dicistroviruses and picornaviruses. However, a direct comparison of IRES sequences from the same viral *spp* reveals a conservation of RNA structure (Koirala et al., 2019). In essence each *spp* of virus may have therefore evolved a particular IRES RNA structure suited to its own evolutionary pressures and needs.

1.8.12 IRES Structures and Classifications

Viral IRES elements can be broadly grouped into four overriding categories related to their RNA structure and the mechanism by which they are able to initiate translation. Group I includes members of the *Dicistroviridae* family such as that of the cricket paralysis virus (CrPV) and the palutia small stall intestine virus (PSIV). These require no interaction with initiation factors and instead bind directly to the 40S ribosomal subunit. Group II includes members of the *Flaviviridae* family including the hepatitis C virus and classical swine fever virus (CSFV). Group II IRES elements require the initiation factors eIF-2 and eIF3 but are still able to bind directly to the 40S ribosomal subunit. Group III includes members of the *Picornaviridae* family including encephalomyocarditis virus (EMCV) and the foot-and-mouth disease virus (FMDV). Group III IRES elements require the use of five translation initiation factors including eIF-2, eIF-3, eIF-4A, eIF-4B and eIF-4G as well as two IRES-transacting factors that are required for the recruitment of the 40S ribosomal subunit. Finally, group IV include some members of the *Picornaviridae* such as the rhinovirus and human papilloma virus (HPV). These require four translation initiation factors that include eIF-2, eIF-3, eIF-4A, eIF-4B and eIF-4G and the IRES-transacting factors polypyrimidine tract-binding protein (PTB),

poly rC-binding proteins (PCBP)-1 and PCBP-2 for 40S ribosomal binding. Once bound the AUG start codon is found through ribosomal scanning for translation to begin. The two most common IRES sequences for CFPS used today are the EMCV IRES and the IRES from the intergenic region of the CrPV.

1.8.13 The Cricket-Paralysis Virus (CrPV) IRES

The CrPV virus belongs to the Dicistroviridae family whose genome is translated in two distinct ORFs, each containing a specific IRES sequence (Tate et al., 1999). The IRES placed at the 5'UTR of ORF1 varies from virus to virus in the family showing little homology. However, the IRES located at the 5' intergenic region preceding ORF2 is conserved amongst the Dicistroviridae family (J. E. Wilson et al., 2000). Interestingly CrPV-IGR IRES has been shown to initiate translation in a way that is *spp* independent(Hertz & Thompson, 2011). Possibly due to the conservation of translation among eukaryotes, the CrPV-IGR IRES has been shown to initiate translation in mammalian, yeast, *Sf*29 and Leishmania cell lysates (Brödel et al., 2013). The CrPV intergenic region IRES is split into three distinct internal pseudoknots (PK1-3) of approximately 190 nucleotides (see Figure 1.11 (A)), with translation initiation beginning at GCU rather than the usual AUG. High-resolution models using cryo-EM of the CrPV IRES bound to the ribosome of yeast *Kluyveromyces lactis* reveal key features. A compact IRES structure allows it to interact directly with a specific cluster of ribosomal proteins, located between the head and the body of the 40S ribosomal subunit. This restricts the flexible head of the ribosomal 40S subunit, which in turn allows the binding of PK1. The PKI pseudoknot upon interaction with the ribosome establishes the correct reading frame by imitating the native initiator-mRNA interaction. This positions the viral RNA in the decoding centre of the 40S ribosomal subunit, anchoring the IRES to the P-site. This stabilisation is thought to facilitate the binding of the large 60S ribosomal subunit to form the 80S ribosome (see Figure 1.11 (B)).

The two remaining pseudoknots of the CrPV IRES are folded in such a way that expose two stem loops that are responsible for the majority of interactions with the 40S ribosomal subunit (Kerr et al., 2016).

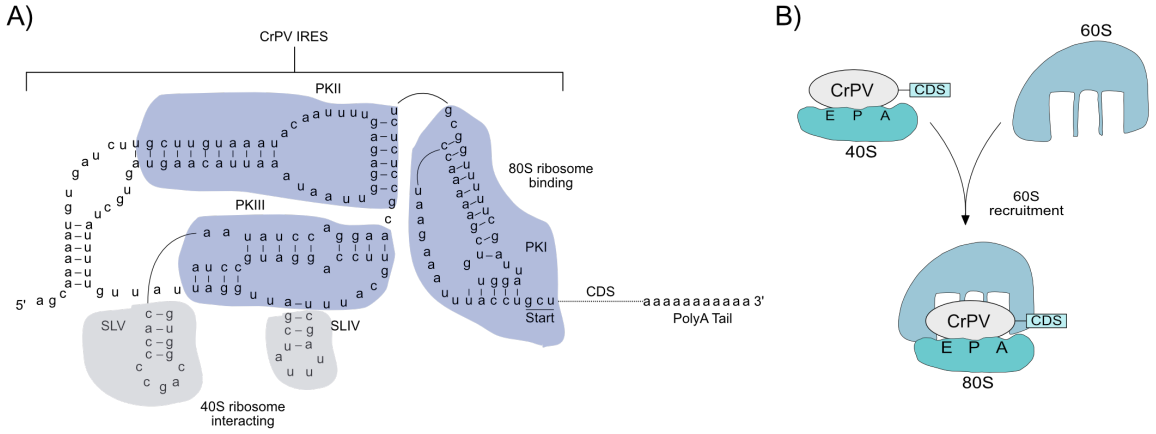

Figure 1.11: Internal Ribosome Entry Site
An IRES allows certain RNA viruses to 'short circuit' the usual cellular translation cap dependent initiation and scanning pathway by either recruiting a subset of initiation factors or none at all. **A**) The sequence structure of the CrPV-IRES forms a compact ordered structure of three pseudoknots (PKI-III) and two stem-loops. Together PKII and PKIII interact with the 40S ribosomal subunit and mediates the formation of the 80S subunit. Subsequent formation of the 80S ribosomal subunit allows PKI to facilitate binding to the ribosome A-site through mimicry of the anticodon stem of a tRNA. This is followed by a translocation step driven by eEF2 that moves PKI to the ribosome A-site, allowing delivery of the first aminoacyl-tRNA by eEF1A (adapted from Kerr et al., 2016). **B**) A simplified schematic showing the binding of the 40S ribosomal subunit by the CrPV IGR-IRES which leads to the recruitment of the 60S ribosomal subunit to form the 80S ribosome. This IRES has been shown to initiate translation in yeast, mammalian cells, leishmania and insect cells.

1.8.14 From Batch to Continuous Cell-Free Protein Production

Since the advent of cell-free translation, a number of different setups have evolved that have sought to increase protein yield by prolonging the length of time at which translation can be sustained. The transition from batch setups to continuous cell-free setups usually has the cost of a reduction of throughput that is purely based on the logistical challenges presented in the hardware of the setups (Spirin et al., 1988). A batch reaction is setup in a way that allows translation or transcription and translation (TX-TL) to occur in the same tube or in the case of HTP setups, the same well of a plate (Takahashi et al., 2015). A batch type of setup suffers

from the rapid depletion of ATP and the build-up of ADP and leads to the accumulation of free phosphate that can interact with magnesium ions which then destabilise the translation reaction (Pontes et al., 2015). However, this can be overcome through the continuous supply of translation components, including ATP and the removal of by-products. In its simplistic form this is achieved by segregating the reaction mixture containing the lysate, the buffering and energy components via semipermeable membrane. In an industrial setting this can be accomplished through large 'feeding' reservoirs and pumps or in a HTP context through the bilayer method. The bilayer method forms a partially permeable interphase between the lysate and mRNA/DNA mixture and a feeding component. This in principle allows the same process to occur, although the bilayer that is created will dissipate over time creating a homogenous mixture. The 'bilayer setup' whilst not able to achieve protein yields of the 'continuous' method, lends itself to a plate format and has been used successfully in WGCF protein synthesis (Sawasaki et al., 2002). Continuous CFPS has now been reported to achieve translation times of up to 48hrs, with mammalian CHO cell-free systems producing almost 1mg/ml protein yields (Ramm et al., 2020; Thoring et al., 2017).

1.8.15 Energy Regeneration – Powering up Protein Synthesis

Homeostasis in living cells provides a constant internal environment allowing a steady supply of energy to the cell providing the basic fuel requirements for growth and survival (Selye, 1975). However, in cell-free systems a reaction will eventually reach a biochemical equilibrium as the reaction proceeds resulting in a decrease of protein production (Rivas & Minton, 2018). Therefore, systems have been developed to try and delay this process by providing a constant supply or reservoir of energy components to a reaction mixture in the form of continuous-exchange or continuous-flow.

Energy regeneration in CFPS systems can be single or multi-step, involve the genetic modi-

fication of the organism from which lysate will be derived or, more recently involve the supplementation of functional mitochondria. Commonly CFPS systems use supplemented biochemical pathways that enable the phosphorylation of ADP to produce ATP through the linking of a high energy phosphate. This step can be achieved by using a phosphorylated compound coupled to a conjugate kinase (see Figure 1.12 (A)). For example, in mammalian based CFPS systems creatine phosphate can be converted to creatine using creatine phosphokinase, generating ATP in the process (Calhoun & Swartz, 2007). Other systems use phosphophenol pyruvate or acetyl phosphate coupled to a constituent kinase (Anderson et al., 2015; Kim & Swartz, 1999). However, although these energy regeneration systems will drive translation, they will eventually lead to the accumulation of inorganic phosphate ions (Kim & Swartz, 2001). These will go on to chelate magnesium ions that are essential for T7 RNAP, aaRS reactions and RNA stabilisation, precipitating them out of solution and causing early translation termination (Luttrell, 1994). Solutions to the problem of accumulating phosphates have included the recycling of free phosphate ions by pyruvate oxidase or switching to glucose as an energy source (Kim & Swartz, 1999). The use of glucose as energy presents its own challenges, such as the accumulation of protons in solution that lowers the pH in a cell-free reaction below an acceptable level. Solutions for this have included a change of buffers to counteract the pH change, or the addition of a modified glutamate decarboxylase modified to be active at low pH levels that can neutralise free hydrogen ions (Anderson et al., 2015). An innovative approach to a CFPS energy source used Tobacco plant BY-2 lysate supplanted with active exogenous mitochondria and glutamate. This allowed the production of NADH inside the mitochondria via the TCA reaction, in turn NADH fueling oxidative phosphorylation and the production of ATP (see Figure 1.12 (B)). This system marketed under the name ALiCE® has been reported to produce yields of up to 3mg/ml (LenioBio, n.d.).

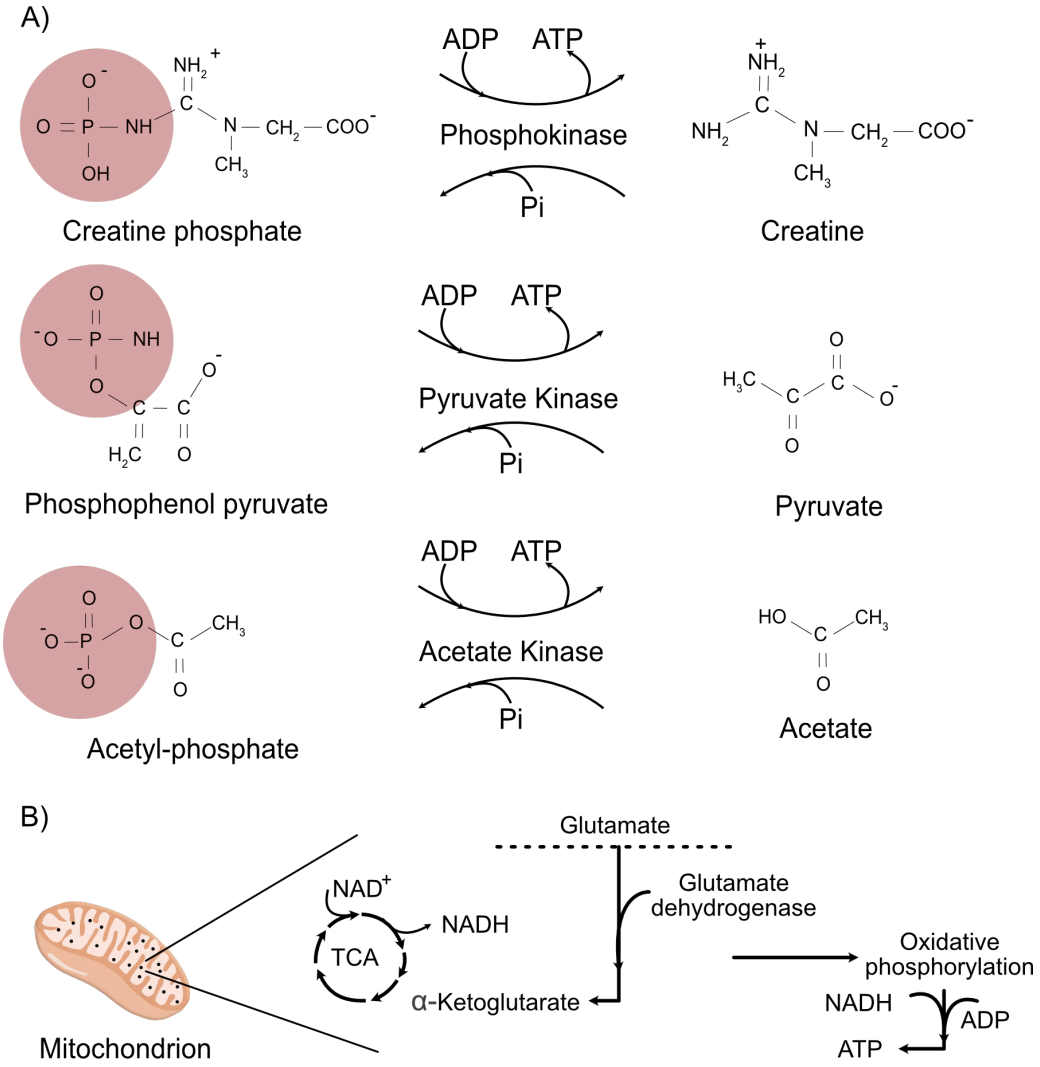

Figure 1.12: Energy Sources

Energy sources for CFPS come in a variety of forms that are supplemented into a reaction and are required for prolonged active translation. **A**) Three energy regeneration reactions are shown with the high-energy phosphate highlighted in red. A kinase facilitates the transfer of the phosphate group to ADP to form ATP, this occurs in equilibrium to the reverse reaction whereby free phosphate (Pi) is transferred back to the carrier compound. **B**) Recent CFPS systems based on plant cellular lysate have shown that the addition of exogenous mitochondria and the substrate glutamate can sustain a cell-free reaction beyond 48hrs. Here glutamate is converted to α-ketoglutarate by glutamate dehydrogenase and fed into the tricarboxylic acid cycle (TCA). This allows the conversion of NAD^+ to NADH, this is used in oxidative phosphorylation within the mitochondria facilitating the addition of phosphate to ADP forming ATP that can be used for CFPS.

1.9 Aims & Objectives

The development of antimalarial resistance to all front-line therapeutics represents a major problem for the treatment of infected patients in endemic areas. Although significant progress has been made towards malaria control and eradication using ACTs and insecticide-treated bed nets, this progress in recent years has stalled. Targeting infectious diseases often relies on both drug and vaccine-based strategies for control. Novel therapeutics that target pathways essential for parasite development could aid in malaria control and eradication. Translation inhibitors offer a new avenue for malaria control but the screening of these compounds for activity is slow and as such requires better screening technologies. Deciphering the precise MoA of these inhibitors has in part relied on recent advances in cryo-EM that have been able to provide atomic resolution structures with low sample preparation e.g. the 80S ribosome of *P. falciparum* bound to mefloquine. This has made structure guided drug design a distinct possibility for large complexes in *Plasmodium*.

Vaccine-based strategies represent an alternative route to drugs and offer better protection for those at risk from malaria in areas with poor healthcare than drugs can provide. Yet, current vaccines such as RTS,S or R21 have fallen short on their ability for mass rollout, requiring multiple booster doses with efficacy that wanes over time. The expression of *P. falciparum* extra-cellular proteins is challenging, often resulting in insoluble protein or the synthesis of smaller sections or subunits for vaccine delivery. These proteins or subunits often lack the specific post-translational modifications associated with an increased immune response. An efficacious vaccine is required, providing protection that is strain transcending, long-lasting and with at least 75% protection. The aims of this thesis can be broken down into three overriding core questions (and a single late question).

1. **Development of a Dual-IVT assay:** Historically methods for the detection of active translation inhibitors in *Plasmodium* have been slow and laborious. These have relied on

phenotypic based screens, elucidation of structures, WGS and biochemical characterisation via S35 methionine incorporation. A HTP assay incorporating translationally active lysates from the most virulent malaria parasite, *P. falciparum* and human cellular lysate could aid in the drug discovery process. Therefore, would it be possible to develop an *in vitro* translation assay for both *Plasmodium* and human cells (Dual-IVT) to drastically reduce the time from compound library to potent antimalarial discovery?

2. **Towards the structural resolution of *P. falciparum* RNAPI-III:** Structural aided drug design has been shown to be a useful tool in designing novel antimalarials or repurposing old ones through chemical modification. Transcription is an essential process for the malaria parasite but so far the structures of the three nuclear DNA-directed RNAPs in *P. falciparum* have remained elusive. Therefore, can solving the structures of these three polymerases from *P. falciparum* provide insights into the conservation of RNA polymerases between humans and malaria, whilst also enabling future drug development towards a *Plasmodium* specific transcription inhibitor?

3. **Development of a malaria CFPS system:** Expressing *P. falciparum* surface antigens often results in insoluble or improperly folded proteins using traditional heterologous systems. This usually results in the production of only small subsections of a protein of interest, lacking other potentially immunogenic domains and native glycosylation patterns. CFPS offers an alternative route to protein production unconstrained by the usual considerations of expression in a cellular-based system. There are currently no cellular-based *P. falciparum* systems that can be used to overexpress a protein of interest. Therefore, would it be possible to use *P. falciparum* cellular lysate in a cell-free setup that contains endogenous microsomes to produce a well-researched vaccine candidate such as CSP? In addition could this be immunised in a humanised mouse model and compared to the portion of CSP used in RTS,S expressed in yeast?

4. **Development & upscale of a human cell-free system** Over the last year COVID-19 has devastated world economies and at the time of writing has resulted in 2.72M deaths and 12M cases, caused by SARS-CoV-2. Pandemic preparedness strategies in response to the ongoing pandemic are required to monitor COVID-19 long-term and provide security for future pandemics. The rapid detection of new virus variants and the response of a population's pool of antibodies produced from infection or vaccination is necessary to monitor continual vaccine efficacy and herd immunity. CFPS allows a user to rapidly produce a protein of interest without the need for large culturing facilities and expensive equipment, cutting the time to produce an antigen from an isolated viral sequence. Therefore, could we repurpose the human derived lysate from the Dual-IVT system to produce the nucleocapsid and receptor binding domain (RBD) of the spike protein from SARS-CoV-2? Could these proteins be detected by patients who have previously been infected with SARS-CoV-2 and can this be adapted to HTP protein production?

Chapter 2

Materials & Methods

2.1 Cloning

2.1.1 Agarose Gel Electrophoresis

To separate and/or purify DNA samples from either a restriction digest or PCR reaction, a 1% agarose gel was made by combining agarose powder (Merck) and 1X Tris-acetic acid EDTA (TAE) buffer (Invitrogen). This was then heated until boiling, allowed to cool and supplemented with Sybr Safe (Invitrogen) at 1:50,000. The gel was then set in a cast and allowed to solidify. Once solid it was transferred into a mini sub-cell electrophoresis chamber (Bio-Rad) containing 1X TAE. DNA sample(s) in loading dye (NEB) were transferred into wells in the gel. After which 6 µl of a 1Kb Plus DNA ladder (ThermoFisher) was added into a well for size analysis. The gel was run at 120V for 30min. The DNA bands were visualised using either the Gel Doc XR+ (Bio-Rad) with UV light or a blue light transilluminator (Imgen).

2.1.2 Agarose Gel DNA Extractions

On completion of an agarose gel electrophoresis run the agarose gel was transferred to a blue light transilluminator (Imgen). The desired DNA band was then excised from the gel material using a scalpel and placed into a 1.5ml polypropylene tube. Extraction of the DNA was performed using the QIAquick gel extraction kit (Qiagen) as per the manufacturer's instructions. The resulting DNA was eluted into ultra-pure water in the final step of the extraction process for further analysis and/or cloning reactions.

2.1.3 Gibson Assembly®

Gibson Assembly was used in a single isothermal reaction. For this a 2X Gibson Assembly master mix was made from a 5X Isothermal buffer (0.5M Tris-HCl pH7.5 (Merck), 50mM MgCl2 (Merck), 1mM of dATP, dCTP, dGTP, dTTP (Invitrogen), 50mM DTT (Merck), 31.3mM

PEG8000 (Merk) and 5mM NAD (Merck) and 6.4U T5 exonuclease (NEB), 40U Phusion DNA polymerase (NEB) and 6,400U Taq DNA ligase (NEB). A single reaction was composed of 15µl of the Gibson Assembly master mix and 5µl containing the plasmid backbone, DNA elements to be inserted and water. Where DNA to be inserted into the plasmid was <150bp a 1:5 plasmid to insert ratio was used. Where DNA to be inserted into the plasmid was >150bp, a 1:1 plasmid to insert ratio was used. For each reaction a total of 25ng of purified plasmid was used. The molarity of DNA was calculated using the following formula.

$$m = \left(\frac{DI}{VMR}\right) VMxRIV$$

- m - mass (g)
- DI - Desired insert
- VMR - Vector molar ratio
- VM - Vector mass (g)
- RIV - Ratio of insert to vector lengths

Once assembled the reaction was incubated at 50°C for 1hr. Then 10µl of the reaction mix was transformed into *E. coli* DH10βcells.

2.1.4 Polymerase Chain Reaction (PCR)

All PCR reactions were carried out using Phusion DNA polymerase (NEB) according to the manufacturer's instructions using a thermocycler T-100 (Bio-Rad) with certain modifications to the annealing and extension temperatures as required for the amplified product. Each PCR reaction had a total volume of 50µl and was assembled within PCR tubes (Appleton Woods). A table of all the primers used for each amplicon can be found in (Appendix 4.1). PCR reactions

were then stopped using 6X gel loading dye (NEB).

2.1.5 Plasmid Extraction

Plasmids were purified from either a 5ml culture, for minipreps, Qiaprep (Qiagen) or a 200ml culture for maxipreps, GenElute (Merk) according to the manufacturer's instructions. Bacterial cultures for each type of preparation were grown overnight at 37°C shaking at 220RPM from either a single colony or a glycerol stock. The cell pellet was then obtained through centrifugation of the culture for 15min at 1500RCF at 4°C.

2.1.6 Restriction Digests

Vector backbones used for cloning in Gibson Assembly reactions were digested using restriction endonucleases (NEB). Each reaction was carried out as per the manufacturer's instructions. Each digestion reaction was assembled in a total of 50µl and supplemented with 1µl of the required restriction endonuclease and a total of 500ng of the chosen plasmid in a designated buffer. The reaction was then incubated at 37°C for 20min after which 1µl of quick CIP (NEB) was added and the reaction allowed to further incubate for up to 1hr. Reaction digests were then stopped using 6X gel loading dye (NEB).

2.1.7 Transformations

Chemical competent *E. coli* DH10β(NEB) and BL21 Lys^Y (NEB) cells were transformed as follows: A 50µl aliquot of cells was thawed on ice for 5min after which plasmid DNA was added. Both the plasmid and bacterial cells were then incubated on ice for 1hr. A heat shock step was performed where the aliquot of cells and DNA were incubated at 42°C for 30sec followed by an incubation on ice for 2min. Then 300µl of super optimal broth with catabolite repressor (SOC) (Invitrogen) was added and the aliquot of cells allowed to incubate at 37°C

for 1hr. After which the total cell suspension was spread onto an Luria Bertani (LB) agar plate (Merck) containing a selection antibiotic of either carbenicillin (Merck) at 100µg/ml or kanamycin at 50µg/ml (Merck). The agar plate was then incubated overnight at 37°C.

2.1.8 Bacterial Cell Culture

Bacterial growths were performed in either 5ml total volumes using 50ml polypropylene tubes or 200ml cultures in 1.5L erlenmeyer flasks. All 5ml cultures were grown in LB (Merk) whereas all 200ml cultures were grown in Terrific Broth (Fisher Scientific). A flask or tube containing broth was inoculated with either material from a glycerol stock or a colony from an agar plate. The cultures unless otherwise indicated were allowed to grow overnight at 37°C shaking at 220RPM. The following day bacterial cells were pelleted by centrifugation at 1500RCF at 4°C. Each culture contained an antibiotic selection depending on the plasmid; for pET28b this was 100µg/ml of kanamycin (Merck) or for the pHLH, pIX and pSLI series this was 100µg/ml of carbenicillin (Merck).

2.2 Cell Culture

2.2.1 Human Embryonic 293F (HEK 293F)

A vial of HEK 293F cells (Gibco) was thawed according to the manufacturer's instructions, in brief a vial containing approximately $1x10^7$ cells was used to initiate a culture. The cells were thawed at 37°C and immediately transferred to a 125ml polycarbonate Erlenmeyer flask with a vented cap containing 30ml of FreeStyle 293 expression medium (Gibco). The flask was then placed in an incubator with a humidified atmosphere of 8% CO_2 at 37°C and shaking at 125RPM . Cell viability was determined using Trypan Blue stain (Gibco) and assessed for viability and density. Cultures with a viability of <90% one day post thaw were discarded.

The cells were subcultured as the cell density reached $3x10^6$ cells/ml. Expansion of the cultures was carried out after the sixth passage initially to a volume of 50ml in a 250ml Erlenmeyer polycarbonate flask up to 100ml in a 500ml Erlenmeyer polycarbonate flask.

2.2.2 HEK 293F Culture Isolation - DualI-IVT

Half a litre of FreeStyle 293F HEK cells (Gibco) were grown in five 500ml Polycarbonate Erlenmeyer vented flasks (Corning) containing FreeStyle 293 Expression medium (Gibco) as detailed in section 2.2.1. Upon reaching a density of approximately 3 x 10^6cells/ml the cells were centrifuged at 1000 RCF for 10min at 4°C. The media was discarded and the pellet was washed twice in ice-cold RBC lysis buffer. The cell pellet was finally resuspended 1:1 in RBC lysis buffer without saponin and supplemented with 20U of human placental RNase inhibitor (Merck) and Complete® EDTA-free inhibitor cocktail (Roche).

2.2.3 HEK 293F Culture Isolation - CFPS

Between 0.5 - 0.8L FreeStyle 293F HEK cells (Gibco) were grown as detailed in section 2.2.1, upon cells reaching a density of 3 x 10^6cells/ml the cells were centrifuged at 1000 RCF for 10min at 4°C. The media was discarded and the cell pellets pooled and washed twice in cell lysis buffer (30mM HEPES-KOH (Merck) pH 7.6, 100mM Sodium Acetate (Merck) and 4mM DTT (Merck)). Finally, the cell pellet was resuspended in half the pellet volume of cell lysis buffer.

2.2.4 *P. falciparum* 3D7

P. falciparum 3D7 asexual parasites were grown and maintained in 75cm^3 flasks (Corning) containing 30ml of complete media (RPMI - 1640 medium (Merck), 50µg/ml hypoxanthine (Merck), 25µg/L gentamycin (Merck), l-glutamine 0.3mg/ml (Merck) and 0.5% (w/v) Albumax

II (Life Technologies). Each flask contained 4% haematocrit blood (NHS UK Blood Transfusion Service) and gassed with 'Malaria gas' (3% (vol/vol), O2 / 5% CO2 / 92% N2 (BOC)) and incubated at 37°C. Parasitemia within a flask was determined by counting 300 RBCs using a thin Gimza (Merck) smear. Parasite stocks were continuously maintained by dilution and media changes with parasitemia in stock cultures not exceeding 10-12%. Media changes were performed until the culture reached 10 – 20% parasitaemia. To produce highly synchronised parasites, a *P. falciparum* (3D7) culture of 30ml containing complete media maintained at 4% haematocrit was synchronised with 5% sorbitol three times per week.

2.2.5 *P. falciparum* 3D7 - Large Scale

Highly synchronised P. falciparum 3D7 asexual parasites were grown in 225cm3 flasks (Corning) containing 300ml of complete media (RPMI - 1640 medium (Sigma-Aldrich), 50µg/ml hypoxanthine (Sigma-Aldrich), 25µg/L gentamycin (Sigma-Aldrich), l-glutamine 0.3mg/ml (Sigma-Aldrich) and 0.5% (w/v) Albumax II (Life Technologies). Each flask contained 2% haematocrit blood (NHS UK blood Transfusion Service), gassed with 'Malaria gas' (3% (vol/vol), O2 / 5% CO2 / 92% N2 (BOC)) and incubated at 37^{o}C. Daily media changes were performed until the culture reached a late trophozoite stage at 10 – 20% parasitaemia.

2.2.6 *Plasmodium falciparum* Parasite Culture Isolation

Infected RBCs containing parasites at the late trophozoite stage were isolated by centrifugation for 5min 800 RCF (Eppendorf) at room temperature (RTP). The RBCs were then lysed in cell lysis buffer (45mM HEPES-KOH pH 7.45 (Merck), 100mM Potassium Acetate (Merck), 2.5mM Magnesium Acetate (Merck), 2mM DTT (Merck), 250mM Sucrose (Merck) and 0.075% (w/v) Saponin (Merck)) for 10min at RTP then centrifuged for 10min at 2800 RCF at 4°C for 10min. The isolated parasite pellets were washed in ice-cold RBC lysis buffer that did not contain

saponin. The wash steps were repeated until the supernatant lost its red colour. The parasite pellet was finally resuspended 1:1 in RBC lysis buffer without saponin and supplemented with 20U of human placental RNase inhibitor (Merck) and Complete® EDTA-free inhibitor cocktail (Roche).

2.2.7 SYBR Green *P. falciparum* Growth Inhibition Assay

The SYBR Green asexual growth assay was undertaken approximately as published (Matthews et al., 2017). In brief 96-well black clear bottom plates (Corning) were pre-printed with a compound and normalised with DMSO (Merck) to 0.5% of a total assay volume of 100µl. Highly synchronised ring stage parasites (see section 2.2.4) and blood was added to each well so that the final parasitaemia was 2% and the haematocrit was 1%. The compound was incubated with parasites for 72hrs before being frozen at -20°C (to aid with cell lysis). The plate was thawed on ice and a lysis buffer (20mM Tris pH7.5 (Merck), 5mM EDTA (Merck), 0.008% w/vol saponin (Merck), 0.08% vol/vol triton-x100 (Merck) and SYBR-Green I (Thermo Fisher Scientific) at a final concentration of 0.02% vol/vol). The 96-well plate was incubated for 1hr at RTP before each well was assayed for fluorescence using GFP filters (Excitation 485 nm/Emission 535 nm) on a microplate reader (TECAN).

2.3 Cell Lysis

2.3.1 Nitrogen Cavitation

The resuspended cell pellets from sections 2.2.2, 2.2.3 and 2.2.6 were transferred to a nitrogen cavitation chamber (Parr Instrument Company) that had been pre-chilled on ice and had a stirrer bar placed inside before the chamber was sealed. The chamber was then pressurised to 1500 PSI and left for 45min on ice gently stirring. The chamber was slowly depressurised by

allowing a single drop of lysate exit per second from the chamber. Lysate was then centrifuged. For lysate collected from sections 2.2.2 and 2.2.6, underwent differential centrifugation, first, at 10,000 RCF for 15min and secondly at 30,000 RCF for 15min both at 4°C (Beckman-Coulter). For the cellular lysate produced from section 2.2.3 a single centrifugation was performed at 10,000 RCF for 12min at 4°C. The clarified lysate from sections 2.2.2 and 2.2.6 protein concentration was measured at 280nM using a NanoDrop 2000 (ThermoFisher) and the concentration adjusted to 12mg/ml before being flash frozen and stored at -80°C. Lysate produced from section 2.2.3 was then taken and added to a G-25 buffer exchange column (Cytiva) pre-equilibrated with lysis buffer from section 2.2.3 and the manufacturer's instructions followed. Fractions from the column were collected and measured for RNA concentration at 260nM. Fractions with an absorbance above 90 were pooled, 1mM of $CaCl_2$ was added to them before the addition of 10U/ml of micrococcal nuclease (ThermoFisher). This was then incubated at RTP for 2min to allow digestion of endogenous mRNA. The reaction was stopped through the addition of 6.7mM EGTA (Merck). The lysate was further supplemented with 100µg/ml of creatine kinase (Meck) and 50µg/ml tRNA from Bakers Yeast (Invitrogen). The lysate was then flash frozen and stored at -80°C.

2.4 Cell-Free Technologies

2.4.1 Dual-IVT

White polystyrene low bind 384-well plates (Corning) were pre-printed (Tecan) with compounds dissolved DMSO of 0.5% the total reaction volume. Each 10µl well contained the following reaction mixture; 5µl *P. falciparum* clarified lysate thawed on ice. Added to this was 4.5µl of the following; 20 amino acids at 200µM (Biotechrabbit), 45mM HEPES pH7.45 (Merck), 100mM Potassium Acetate (Merck), 1.5mM Magnesium Acetate (Merck), 2mM DTT (Merck), 20U

of human placental RNase inhibitor (Merck), 15µM Leupeptin (Merck), 1.5mM ATP (Merck), 0.15mM GTP (Merck), 40U/M Creatine Phosphokinase (Merck) and 4mM Creatine Phosphate (Fisher Scientific), 2% (w/w) PEG3000 (Merck), 1mM Spermidine (Merck), 0.5mM Folinic acid (Merck). Finally, 0.45µl at 1µg/µl of purified green click-beetle luciferase mRNA produced from the pHLH_HCBGH vector was added (see section 2.4.4). Each reaction condition assessed was assayed using three independently produced batches of human and malaria cellular lysates (see section 2.2).

Once assembled the plate was incubated at 32°C for 1hr and 40min. On completion 10µl of Luciferin mix was added to each well; 45mM HEPES pH 7.45 (Merck), 1 mM Magnesium Chloride (Merck), 1mM ATP (Merck), 5mM DTT (Merck), 1% (v/v) Triton-X (Merck), 10 mg/ml BSA (Merck), 1 x Luciferase Reaction Enhancer (Thermo Fisher Scientific), 1 mg/ml D-Luciferin in Sodium Bicarbonate (Thermo Fisher Scientific), 0.5mM cycloheximide (Merck). Luminescence for each well was measured using a microplate reader (Tecan M200 Pro) set to 37°C. For compound validation using human cell lysate (HEK 293F) the assay was repeated like-for-like however, instead of mRNA from the pHLH_HCBGH being added, purified mRNA made from the pT7CFE_CBG (containing the EMCV IRES KF836387.1) vector was added to the same concentration.

For Dual-IVT assay development using *P. falciparum* lysate and testing a further vector using the pHLH series containing the firefly luciferase gene fused to a 3XHA tag (pHLH_HLucH_HA) was used for luminescence detection and western blot analysis (see section 2.5.2).

The luminescence data obtained was converted into the percentage translation for each compound assayed for single dose experiments (see below). The Z-factor (Z), a measure of the reproducibility of the Dual-IVT assay was also calculated:

$$\%Inhibition = \left(\frac{X - \bar{X}C}{D - \bar{X}C}\right)$$

$$\%Translation = \left(\frac{X - \bar{X}C}{D - \bar{X}C}\right) x100$$

$$Z = 1 - \left(3x\frac{(\sigma D + \sigma C)}{(\bar{X}D - \bar{X}C)}\right)$$

- X - Compound assayed luminescence (Au)
- C - Luminescence, positive control
- D - Luminescence, negative control

A compound of interest were subjected to a dose response assay, here percentage inhibition was calculated for compounds descending in concentration. The results were then analysed in Prism 9. Initially a dose response set for a compound of interest was transformed in the following way:

$$X = Log(X)$$

The transformed data was subjected to a nonlinear fit using the 'log(inhibitor) vs. response - Variable slope (four parameters)' function in Prism 9 with the error reported as mean with standard deviation. This allowed the IC_{50} values of compounds assayed to be reported for the Dual-IVT assay.

2.4.2 Continuous Cell-Free Protein Synthesis - Human

Reactions were assembled in Slide-A-Lyzer MINI Dialysis Devices (ThermoFisher) with a molecular weight (mw) cut off 10kDa. The reaction mixture was assembled inside the dialysis cup. This consisted of 40% reaction lysate from section 2.3.1, 5µl of 10X solution A (0.3M HEPES-KOH (Merck) pH 7.6, 2M Potassium Acetate (Merck), 0.23M Magnesium Acetate (Merck) and 2.5mM Spermidine (Merck)), 10µl of 5X solution B (0.1M Creatine Phosphate (Fisher Scientific), 1.5mM dUTP (ThermoFisher), 1.5mM dGTP (ThermoFisher), 1.5mM dCTP (ThermoFisher) and 8.75mM dATP (ThermoFisher), Plasmid DNA (900ng/µl) and 3 Units of T7

RNA Polymerase (ThermoFisher). The dialysis device containing the reaction mix was then placed in a 1.5ml polypropylene tube containing 1ml of feeding mixture. This consisted of 100µl of 10X solution A containing 39mM Magnesium Acetate (Merck), 200µl of 5X solution B, 50µl of a 2mM amino acid solution (Biotechrabbit), 2.5µl 1M DTT (Merck) and 20µl 20% Sodium Azide solution (Fisher Scientific). Once assembled the reaction was placed at 30°C for 24-48hrs shaking at 600RPM using a heat block (Eppendorf). This method was adapted from Thoring et al., 2017.

2.4.3 Cell-Free Protein Synthesis - *Plasmodium*

The reaction setups from section 2.4.1 for *P. falciparum* using a batch format were used as described for the Dual-IVT, in a linked or TX-TL format. CFPS reactions were modified in a transcription-translation (TX-TL) format instead of a linked setup to use plasmid DNA. To accomplish this the ATP concentration was increased from 1.5mM to 8.75mM and dUTP, dCTP were all added to a final concentration of 1.5mM (ThermoFisher). In addition the concentration of Spermidine (Merck) was doubled to 2mM. The reaction was then setup in a similar configuration as section 2.4.2. 50% *P. falciparum* prepared lysate was added to the reaction mixture (25µl), 2.5µg Creatine phosphokinase (Merck) and 20mM Creatine Phosphate (Merck). When assembling continuous CFPS reactions the modified TX-TL reaction setup, as detailed here, was setup in a similar way to human CFPS in section 2.4.2; however, creatine phosphokinase was omitted from the feeder reaction. Plasmid DNA was added to the reaction at 120ng/µl.

2.4.4 Production of mRNA

The pHLH_HCBGH and the pT7CFE_CBG vectors (Baumann et al., 2018), using click-beetle green luciferase (CBG99) derived from *Photinus pyralis* (Wood et al., 1989) and pHLH_HLucH_HA

containing firefly luciferase were used for the production of mRNA. These vectors, (see Appendix 5 .1) were used in the following to produce large quantities of mRNA for all the Dual-IVT assay (see section 2.4.1). A single reaction was assembled (40mM HEPES-KOH pH 7.4 (Merck), 18mM Magnesium acetate (Merck), 5mM each of rNTPs (GE Healthcare), 2mM spermidine (Merck), 40mM DTT (Merck), 0.0025U/µl inorganic pyrophosphatase (ThermoFisher), cDNA 60ng/µl, 3.0U RNAse inhibitor (Merck) and 50U T7 RNA polymerase (ThermoFisher). The reaction was allowed to proceed at 37°C for 1hr and 20min before 0.5µl of DNaseI (ThermoFisher) was added and the reaction was further incubated for another 20min at 37°C. The reaction was then diluted with RNase-free water and the mRNA precipitated with 50µl 8M LiCl (Merck) and incubated on ice for another 30min before being centrifuged for 20min at 17,000 RCF. The RNA pellet was dissolved in 270µl of RNase-free water followed by the addition of 30µl of 3M Ammonium Acetate (Merck) and 750µl of absolute ethanol (VWR). This was incubated at -80°C for 1hr before being centrifuged for 20min at 17,000 RCF. The pellet was then washed once with 70% ethanol and allowed to dry overnight. It was then resuspended in 100µl of RNase-free water and allowed to fully dissolve. The dissolved pellet was measured using a Nanodrop 2000 (ThermoFisher).

2.5 Protein Analysis

2.5.1 SDS-PAGE

Samples to be analysed had 4X Laemmli buffer (250mM Tris-HCl pH 6.8 (Merck), 40% glycerol (v/v) (Merck), 0.4% (w/v) bromophenol blue (Bio-Rad), 10% 2- mercaptoethanol (Merck), 8% SDS (SDS)) added to them and the resulting samples were heated at 95°C for 5min. This was then loaded onto a 4-12% pre-cast polyacrylamide gel (ThermoFisher) together with Precision Plus Protein Ladder (Bio-Rad). The gel was run at 200V for 38min at RTP. Once the run

was complete the gel was either transferred to a nitrocellulose membrane (see section 2.5.2) or stained using bromophenol blue to visualise protein banding.

2.5.2 Western blot

On completion of SDS-PAGE gels were transferred to a nitrocellulose membrane using an iblot 2 (ThermoFisher) system as per the manufacture's instructions. The membrane was blocked in 10% milk powder PBS-T for 1hr. This was then discarded and the membrane incubated in 2% milk powder PBS-T for 1hr with the primary antibody (either: anti-rabbit ADF-1 used at 1:2500, anti-mouse CSP (2a10) used at 1:2500), anti-mouse FLAG F3166 used at 1:1000 (Merck), anti-rabbit 3xHA 12CA5 (Roche) used at 1:2500, anti-rabbit GFP (Stratech) used at 1:10000, anti-mouse pentahistidine (Qiagen) used at 1:2500, anti-POLR1C (Merck) used at 1:2500 or human serum from post-infected COVID-19 adults from the Disease Research Group Tissue Bank used at 1:1000). Following this the membrane was washed with PBS-T (three times for 5min each). A secondary antibody conjugated to HRP was then added at a concentration of 2 in 5000 with affinity to either rabbit, mouse or human primary antibodies. This was incubated at RTP for 1hr after which this was then discarded and the was membrane washed four times in PBS-T for 5 min each. ELC western blot detection reagent was added (GE Healthcare) as per the manufacturer's instructions, the blot was visualised by either CL-Xposure film (ThermoFisher) or Gel Doc XR+ (Bio-Rad).

2.6 Gene Editing

2.6.1 Production of Selection-Linked Integration (SLI) Plasmids

Genomic DNA extracted using PureLinkTM Genomic DNA Mini Kit (Invitrogen) as per the manufacturer's instructions using 200µl of RBCs infected with *P. falciparum* 3D7 parasites.

The genes RPAC1 (PF3D71143300), RPABC2 (PF3D70303300) and RPB3 (PF3D70923000) were amplified by PCR with primers (see Table 2.1) that gave the genes homology to the 5' and 3' ends of pSLI-2×FKBP-GFP (Birnbaum et al., 2017) that had been linearised with SalI and NotI had 2xFKB-GFP removed and a 3XFLAG tag inserted so that all *P. falciparum* genes which were subsequently inserted had a C-terminal 3' FLAG tag. The PCR products were purified and inserted into the pSLI-2×FKBP-GFP vector using Gibson Assembly® (see section 2.1.3), transformed into *E. coli* DH10β cells; isolated plasmids were purified and confirmed by Sanger Sequencing (Source Bioscience).

2.6.2 *P. falciparum* 3D7 Transfections

A 5ml culture containing 5% early rings stage *P. falciparum* parasites at 4% haematocrit was centrifuged at 800 RCF at RTP for 5min. The 0.25ml blood pellet was isolated and suspended in 350µl of cytomix (120mM KCl (Merck), 0.15mM $CaCl_2$ (Merck), 2mM EGTA (Merck), 5mM $MgCl_2$ (Merck), 10mM $KHPO_4$/$KH2PO_4$ pH7.6 (Merck)) and 50µl of DNA (2µg/µl in sterile TE (10mM Tris-HCl pH8 (Merck), 1mM EDTA (Merck)). The mixtures were transferred to a 2mm cuvette (Bio-Rad) and electroporated using the following conditions, 950µF, 310V, 4ms pulse length. Immediately after this the blood pellet was transferred into a 25 cm^2 culture flask containing 10ml of complete media at 4% haematocrit. After transfection, WR99210 was added at a final concentration of 4nM to select for episomal expression. In general, healthy parasites were observed after two weeks. The parental culture was then diluted to 1-4% parasitaemia in a new 25cm^2 flask containing 10ml of media at 5% haematocrit and supplemented with G418 at 400µg/ml (final concentration) to select for integrants. The media was changed daily for ten days and then every other day for 14 days.

2.6.3 Genotyping

Transfectants were confirmed using genotyping. Isolated genomic material from *P. falciparum* 3D7 parasites transfected with pSLI and grown to 5% parasitaemia at 4% haematocrit were used for the characterisation of an integrated gene fused to a C-terminal 3X FLAG tag by PCR. Primers were designed (see Appendix 5.1) so that transfected plasmid and integration populations could be detected using PCR amplification. After genomic DNA isolation of *P. falciparum* 3D7 parasites transfected with SLI plasmids containing the RPAC1, RPABC2 and RPB3 (see Appendix 5.1). PCR reactions were setup and compared to control *P. falciparum* 3D7 genomic DNA. The following is the generalised protocol used, Phusion High-fidelity DNA polymerase (NEB) was added as per the manufacturer's instructions with the following thermocycling protocol: An Initial denaturation step 95°C for 30sec, this was followed by 35 cycles of: denaturation 95°C for 10sec, annealing 60°C for 20sec and extension 68°C for 2min 30 sec. Lastly, a final extension at 68°C was carried out for 10min. Agarose gel electrophoresis was used to visualise the results from the PCR reactions.

Table 2.1: Genotyping Primer Pairs

Gene	Stage	**Primer Pair No.**	**Sequence**
RPAC1	Wild Type	2 & 3	**F**:AGCTTGGAGAAGAGGGTCCA **R**:AATCATACCTTAGTGGACAGGTAAT
RPAC1	Plasmid	M13 & 1	**F**:CAGGAAACAGCTATGAC **R**:AATCCATCTTGTTCAATCATTGGT
RPAC1	Integrant	2 & 1	**F**:AGCTTGGAGAAGAGGGTCCA **R**:AATCCATCTTGTTCAATCATTGGT
RPABC2	Wild Type	2 & 3	**F**CTTTTGTACAAGTTTATATTTCCATCTTATATAGAAAC **R**:CATTTTATGATTGCACAATGGCTC
RPABC2RPABC2	Plasmid	M13 & 1	**F**:CAGGAAACAGCTATGAC **R**:AATCCATCTTGTTCAATCATTGGT
RPABC2RPABC2	Integrant	2 & 1	**F**CTTTTGTACAAGTTTATATTTCCATCTTATATAGAAAC **R**:AATCCATCTTGTTCAATCATTGGT
RPABC2RPB3	Wild Type	2 & 3	**F**ATGACTACTTATAATGATAATACAAACAAACATC **R**:ATATAAGAACATGAATCCTTTATGTTCCC
RPABC2RPB3	Plasmid	M13 & 1	**F**:CAGGAAACAGCTATGAC **R**:AATCCATCTTGTTCAATCATTGGT
RPABC2RPB3	Integrant	2 & 1	**F**ATGACTACTTATAATGATAATACAAACAAACATC **R**:AATCCATCTTGTTCAATCATTGGT

2.6.4 Parasite Preparation for Western Blot Analysis

P. falciparum 3D7 parasites were grown to 5% parasitaemia, trophozoite stage at 4% haematocrit. The parasite culture was taken and frozen at -80°C. The isolated culture was then allowed to thaw which caused the lysis of RBCs and centrifuged at 3000 RCF for 10 min at 4°C. The lysed RBC supernatant was discarded and the parasite pellet washed in ice-cold PBS (Fisher Scientific) until the supernatant lost its red stain. The parasite pellet was then resuspended in 250-300µl of parasite lysis buffer (4% SDS (Merck), 0.5% triton x-100 (Merck) and 0.5% PBS (Fisher Scientific). This was then incubated at room temperature for 10min then centrifuged at 17,000 RCF for 5min at 4°C. The supernatant was isolated and added to a 4x laemmli sample buffer. The samples were treated as described in section 2.5.2.

2.6.5 Purification of *P. falciparum* RNA Polymerase Complexes

Transfected *P. falciparum* 3D7 parasites with the modified pSLI plasmids (see section 2.6.1), confirmed by western blot (see section 2.5.2) were grown to sufficient quantities (see section 2.2.5) that produced a 3-4ml parasite pellet which was resuspended in cell lysis buffer (45mM HEPES-NaOH pH 7.45 (Merck), 150mM Ammonium Acetate, 10mM Magnesium Chloride (Merck), 10µM Zinc Chloride (Merck), 5mM DTT (Merck) and 20% (v/v) Glycerol (Merck)) and lysed by nitrogen cavitation (see section 2.3.1). The lysate was collected and centrifuged at 15,000 RCF for 10min at 4°C to remove cellular debris. The supernatant was then transferred to 200µl of anti-FLAG M2 affinity resin (Merck), pre-equilibrated in lysis buffer and incubated at 4°C, turning for 1-2hrs. The affinity resin was then washed with lysis buffer before being eluted in elution buffer (45mM HEPES-NaOH pH 7.45 (Merck), 150mM Ammonium Acetate, 10mM Magnesium Chloride (Merck), 10µM Zinc Chloride (Merck), 5mM DTT (Merck), 20% (v/v) Glycerol (Merck) and 100 µg/ml FLAG peptide (Merck) for 5-10min.

2.7 Recombinant Protein Expression

2.7.1 *P. falciparum* CSP

The pHLH_HCBRH plasmid used as a vector for the luciferase gene required for mRNA production in the Dual-IVT (see section 2.4.1) was modified for CFPS and CSP insertion. The pHLH_HCBRH vector was digested with BssHII and BlpI (see section 2.1.6), a DNA cassette containing a T7 RNA polymerase promotor site followed by a CrPV (NC - 003924.1) IGR-IRES (6025-6216), a 3X Hemagglutinin (HA) tag and a 30 residue long poly(A) tail was inserted using Gibson Assembly®. This resulting vector was further digested using an EcoRI and CSP (PF3D7 - 0304600) containing a WT signal sequence (1-384) or a melittin signal sequence (from honey bee) - fused to CSP (20-384). Both resulting vectors, pHLH_met_CSP_HA and pHLH_CSP_HA (see Appendix) were used in *Plasmodium* specific CFPS (see section 2.4.3) to detect the presence of recombinantly produced CSP by western blot analysis (see section 2.5.2).

2.7.2 Superfolder GFP (sfGFP)

The sfGFP gene (ASL68970) codon optimised for *H. sapiens* (Invitrogen) was inserted into the pHLH vector modified with a CrPV IGR-IRES and a poly(A) tail as in section 2.7.1. However, CSP was replaced for the sfGFP gene and contained a C-terminal twin strepII tag or 3XHA tag. Four versions of this construct were created, pHLH_sfGFP_SII, pHLH_sfGFP_HA, pHLH_met_sfGFP_SII and pHLH_met_sfGFP_HA (see Appendix 5.1) This created two types of plasmid backbone, one containing the IRES followed by the sfGFP gene and the other with the IRES followed by a melittin signal sequence (from honey bee) that was then followed by sfGFP. The two plasmids were used to produce sfGFP using CFPS in the human and malaria systems (see sections 2.4.2 & 2.4.3). In addition sfGFP was fused to the CSP signal sequence (1-20) creating the pHLH_CSPSP_sfGFP_HA (see Appendix 5.1). The expressed sfGFP was

then detected by SDS-PAGE (see section 2.5.1), western blot (see section 2.5.2) or by detecting sfGFP fluorescence (ClarioStar). Here, for each reaction condition 5µl of the reaction mix was loaded in triplicate onto a well of a 96-well black plate (Corning) that had 15µl of PBS (Fisher Scientific) pre-dispensed. The sfGFP was excited at 485nm and an emission was detected at 510nm. The data was analysed and reported using Prism 9 with the error for each data point reported as the mean with standard deviation. Both sfGFP proteins were also purified using StrepTactin sepharose resin (Cytiva) pre-equilibrated in PBS (Fisher Scientific) and loaded into a 0.5ml spin cup containing an acetate filter (ThermoScientific). The reaction mix from CFPS was incubated with the sepharose resin for 1hr at RTP. The flow-through was collected through centrifugation at 1000 RCF for 1min at 4°C and added to 4X laemmli sample buffer. The sepharose was then washed three times in PBS (Fisher Scientific) and the nucleocapsid protein eluted using 2.5mM D-Desthiobiotin (Merck) in PBS (Fisher Scientific) and incubated for 10min at RTP. The sepharose was next centrifuged as before and the elution fraction collected was placed into 4X laemmeli sample for further analysis as described earlier.

2.7.3 Firefly Luciferase

The firefly luciferase gene codon optimised for *P. falciparum* was synthesised (Invitrogen) and cloned into the pHLH vector modified with a CrPV IGR-IRES and a poly(A) tail as in section 2.7.1. The resulting vector pHLH_Luc_HA (see Appendix 4.1) was used in both human (see section 2.4.2) and *P. falciparum* (see section 2.4.3) CFPS reactions. The luciferase protein produced in a reaction was either detected using d-luciferin (Thermo Fisher) and measuring luminescence (see section 2.4.1), or via western blot analysis through detection of the 3XHA affinity tag (see section 2.5.2).

2.7.4 SARS-CoV-2 Nucleocapsid

The nucleocapsid protein (MT079845.1) was codon optimised and synthesised (Invitrogen), this was then inserted into the pHLH vector containing the CrPV IGR IRES using Gibson Assembly® (see section 2.1.3) either as a fusion protein with sfGFP containing a twin strepII tag or as a singular gene insertion with a C-terminal 6X poly-histidine tag. Two resulting vectors, pHLH_Nuc_sfGFP_SII and pHLH_Nuc_His were created (see Appendix). These were then used in human CFPS reactions (see section 2.4.2). The nucleocapsid proteins produced were either detected by western blot (see section 2.5.2) using anti-mouse pentahistidine antibody (Qiagen), an anti-rabbit GFP (Stratech) antibody, COVID-19 recovered patient serum, SDS-PAGE stained with coomassie or GFP fluorescence (see section 2.7.2). Nucleocapsid protein produced from the pHLH_Nuc_sfGFP_SII plasmid was synthesised over 48hrs, purified using the twin strepII tag and analysed (see section 2.7.2).

2.7.5 SARS-CoV-2 Receptor Binding Domain (RBD)

The RBD (318-517) of the spike protein was codon optimised and synthesised (Invitrogen), this was then inserted into the pHLH vector containing the CrPV IGR IRES using Gibson Assembly® (see section 2.1.3) either as a fusion protein with sfGFP containing a twin strepII tag or as a singular gene insertion with a C-terminal 6X poly-histidine tag. Two resulting vectors, pHLH_RBD_His and pHLH_RBD_sGFP SII were created (see Appendix 4.1). These were both then used as in section 2.7.4. To purify synthesised proteins from microsomes, the reaction mixture was first centrifuged at 16,000 RCF for 15min at 4°C. The supernatant was then isolated and the microsomal pellet washed three times in ice-cold 1X PBS (Fisher Scientific). The pellet was then resuspended in 3X its original volume in 1X PBS containing 0.1% triton x-100 and incubated at RTP for 30min with gentle agitation. The sample was then centrifuged once more and the supernatant loaded onto a StrepTactin column.

Chapter 3

Results

3.1 A Screen for Malaria Specific Translation Inhibitors Using an *in vitro* Translation Assay

There has been significant progress in reducing the incidence of malaria infection since the new millennium however, this progress has stalled (World Health Organization, 2019) (see Figure 1.1). In the absence of a broadly effective vaccine, current global control efforts have focused on dissemination of insecticide-treated bed nets, indoor mosquito spraying, and for treatment, ACTs(Bhatt et al., 2015). Worryingly, parasite resistance to ACTs and mosquito resistance to insecticides are both on the rise, threatening future control efforts (Protopopoff et al., 2018). There is a need to find new chemotherapeutics that are more resistance-proof with new MoAs(Rabinovich et al., 2017).

Several compounds have emerged from recent cell-based screens that potently target the *P. falciparum* translation machinery. Two of these, DDD107498 (Baragana., 2015) and cladosporin (Hoepfner et al., 2012) are malaria specific inhibitors of protein synthesis, with half-effective inhibitory concentrations (EC_{50}) in the nanomolar range (see Figure 1.5 and 1.6). Their MoA determination by WGS is time-consuming, since it necessitates that resistance to an inhibitor be possible via mutation and as such is a key discovery 'bottleneck' for new antimalarial compound discovery(Cowell & Winzeler, 2018). However, a targeted based approach to drug discovery offers an alternative HTP methodology.

Several groups have sought to develop *in vitro* translation platforms that have the capacity to screen for antimalarial compounds from drug libraries (Baumann et al., 2018; Sheridan et al., 2018). However, their versatility and movement to HTP screening, including capacity for parallel human translation screening has not been met. Here, building on prior methods, a versatile dual *in vitro* translation (Dual-IVT) assay using translationally active lysates from *P. falciparum* and Human Embryonic Kidney 293F cells was developed. By monitoring luminescence

from a click-beetle luciferase reporter, the assay developed can be used to screen for malaria specific translation inhibitors and validate some translation-specific MoAs. This enabled the screening of the Pathogen Box, a library of 400 active compounds targeting neglected diseases. From the 400 compounds screened, five showed specific activity against *P. falciparum*. Reassuringly, of these five compounds two were quinoline 4-carboxamides, analogues of DDD1077498 known to target eEF2 in *Plasmodim*(Calit et al., 2018) and one previously identified as a small molecule kinase inhibitor(Duffy et al., 2017).

3.1.1 Producing Translationally Active *P. falciparum* and Human Cell Lysate

The production of translationally active lysate requires the isolation and lysis of *P. falciparum* and human cells in a way that preserves their respective translation machinery. Therefore, we considered appropriate lysis methods including: sonication, homogenisation or nitrogen cavitation depending on the cell type and downstream necessity, noting that the medium in which the cell is lysed requires specific optimisation based on the downstream requirement or the cell type being used. Malaria presented a significant challenge since the parasite has a stage-specific life cycle (see Figure 1.2), split in the case of *P. falciparum* between a human host and a mosquito vector. To produce the quantities of lysate required for library scale compound screening, large quantities of malaria cellular lysate were required to make the assay viable. *P. falciparum* 3D7 parasites are a well-established culture adapted strain of malaria that can be propagated *in vitro*. During the asexual stage of infection, the parasite replicates within a host and cycles between rings, trophozoites, schizonts and eventually bursts out of infected RBCs as merozoites to further invade more RBCs (see Introduction 1.2). The late-trophozoite, early schizont stage was chosen as the point at which *P. falciparum* parasites should be isolated. During, the trophozoite stage a malaria parasite will undergo massive amounts of

protein synthesis as it transitions stages (Roch et al., 2004).

P. falciparum 3D7 asexual blood stage parasites grow in static cultures with a defined concentration of RBCs, with parasitemia roughly increasing by a factor of eight every time a schizont bursts releasing merozoites for reinfection (see Introduction 1.2). This makes large scale parasite growth problematic compared to cell types adapted for culturing in suspension, such as HEK 293F cells when factoring in growth media requirments. Therefore, to achieve suitable quantities of translationally active *P. falciparum* 3D7 lysate required for HTP compound library screening, an optimised culturing strategy was developed. Here, highly synchronised parasites were cultured at 2% hematocrit and allowed to reach a parasitemia of 15-20% at late trophozoite, early schizont stage of development (see Material & Methods 2.2.5). The resulting parasite pellet, once isolated from the RBCs could then be lysed to produce the quantities of translationally active lysate required for the *Pf*IVT assay. To meet the requirements of the human component of the IVT assay the HEK 293F cell line was selected based on the cell types fast doubling time, ease of culturing requirements and use of synthetic serum for increased reproducibility (see Figure 3.1 (A)).

Once both the human and malaria cell types were isolated, they were lysed using nitrogen cavitation. There are many popular non-detergent methods used to rupture cells such as Dounce homogenisation, disruption through a fine gauge needle, ball bearing, bead-beating, sonication and nitrogen cavitation. In nitrogen cavitation, cellular material is subjected to intense pressure using nitrogen gas that results in the gas being dissolved within the cytoplasm of the cell. On releasing the pressure within a vessel back to atmospheric pressure, the dissolved nitrogen gas expands, ripping open the cell causing cellular lysis (Hunter & Commerford, 1961; Simpson, 2010). The advantages of this setup are three-fold: firstly, decompression of a pressurised chamber results in cooling of the chamber and sample, naturally preventing protein degradation; secondly, it provides a uniform distribution of pressure throughout the chamber resulting in a

uniform destructive force that increases reproducibility between the lysis of different batches of cellular material; and thirdly, a cell will only experience a disruptive force a single time, rather than repeated exposures that can result in protein and membrane degradation (Magun et al., 1988).

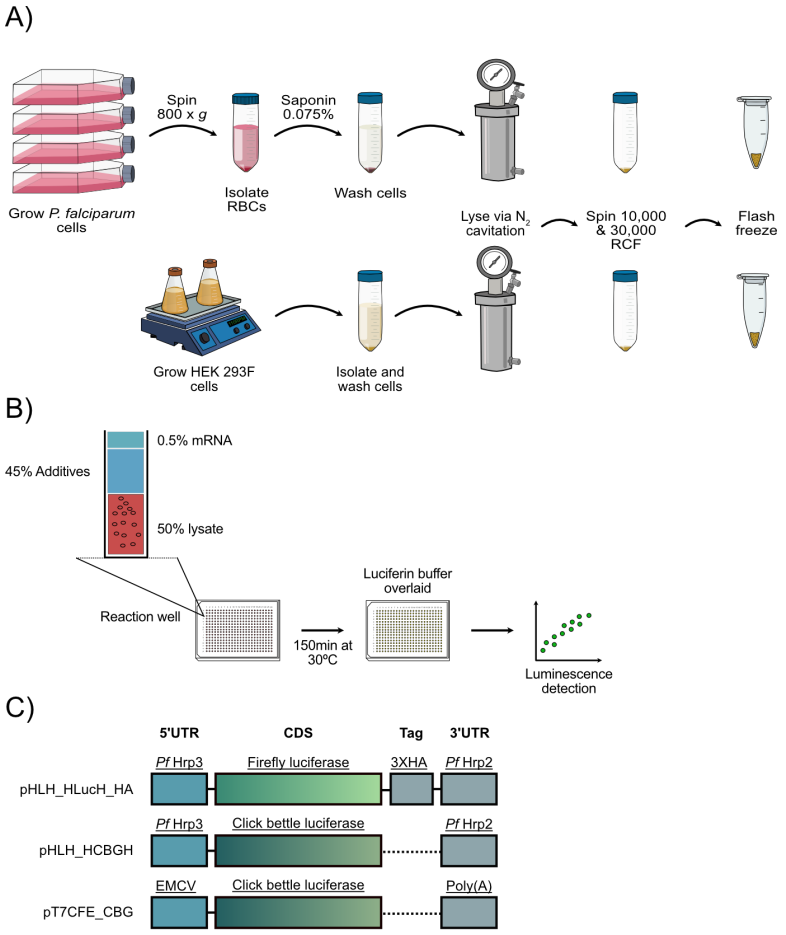

Figure 3.1: The Dual-IVT Assay Workflow

A) The workflow for the production of translationally active lysate from human and malaria sources using nitrogen cavitation. The cellular pellets from both malaria and human cell types are lysed and then processed in the same manner (see Material & Methods 2.2). **B**) A reaction well within a 384-well plate is magnified, the total reaction is comprised of up to 50% lysate (red), 45% additives (blue) such as energy regeneration, amino acid components and 0.5% mRNA containing the luciferase gene for expression (green). The 384-well plate is incubated for 2-hr and 30min at 32°C after which a buffer containing d-luciferin for luminescence detection and cycloheximide to stop further protein translation. **C**) The three mRNA species produced from the corresponding plasmid used for optimisation and library screening in the Dual-IVT assay. The plasmids pHLH_HLucH_HA and pHLH_HCBGH are used in the *Pf*IVT assay as these both contain UTRs from the *P. falciparum* histidine rich protein-3 (Hrp3) and 2 (Hrp2) proteins. Whereas the plasmid, pT7CFE_CBG contains an IRES from the EMCV virus that makes up the 5'UTR and a poly(A) tail comprising 30 adenine repeats used to initiate translation in the human IVT assay.

3.1.2 A High-Throughput Dual-IVT Assay

To robustly report reconstituted *in vitro* translation in both human and malaria cell lysates, two 5'UTR regions were inserted upstream of a green click-beetle (*CBG99*) and firefly luciferase gene. This has been previously shown to initiate *in vitro* translation and give a strong luminescence signal under experimental conditions (Baumann et al., 2018). To initiate translation in malaria, the native 5'UTR from the *P. falciparum* histidine rich protein-3 (*Pf*Hrp3) was inserted upstream of the luciferase gene. A 3'UTR from the *P. falciparum* histidine rich protein-2 (Hrp2) was inserted downstream of the luciferase gene. To initiate translation in human cellular lysate, the 5'UTR used for malaria was replaced with an IRES from the encephalomyocarditis virus (EMCV) (E. T. Wong et al., 2002) and the 3'UTR replaced with a poly(A) tail (Gallie, 1991).

Each translation reaction was then reconstituted in a 10µl total volume, 50% of which was made up of lysate from either of the cell types within a 384-well plate (see Material & Methods 2.4.1). The remaining reaction volume comprised of four solutions (an accessory, helper, amino acids and energy regeneration) making up 45% of the total reaction volume. Translation of luciferase was initiated by the addition of mRNA to each reaction well, making up the final 5% of the reaction volume. Reactions were incubated for 150min at 32°C before being assayed for luciferase activity (see Figure 3.1 (B)).

To investigate which conditions within the IVT assay give the best signal to noise ratio, firefly luciferase was fused to a C-terminal 3XHA tag. This enabled the correlation of luciferase activity with protein production. The following four parameters were then tested; the mRNA concentration within a reaction, lysate protein concentration, reaction duration and reaction temperature. The best parameters discovered through the assay optimisation strategy were as follows; assay time was adjusted to 2hrs 30min, temperature was fixed to 32°C, an mRNA concentration of 93.6ng/µl and finally a lysate protein concentration of 8-10mg/ml. Although

these were optimised with *P. falciparum* lysate, the reaction conditions were applied like-for-like for human cell lysate IVT reactions (see Figure 3.3).

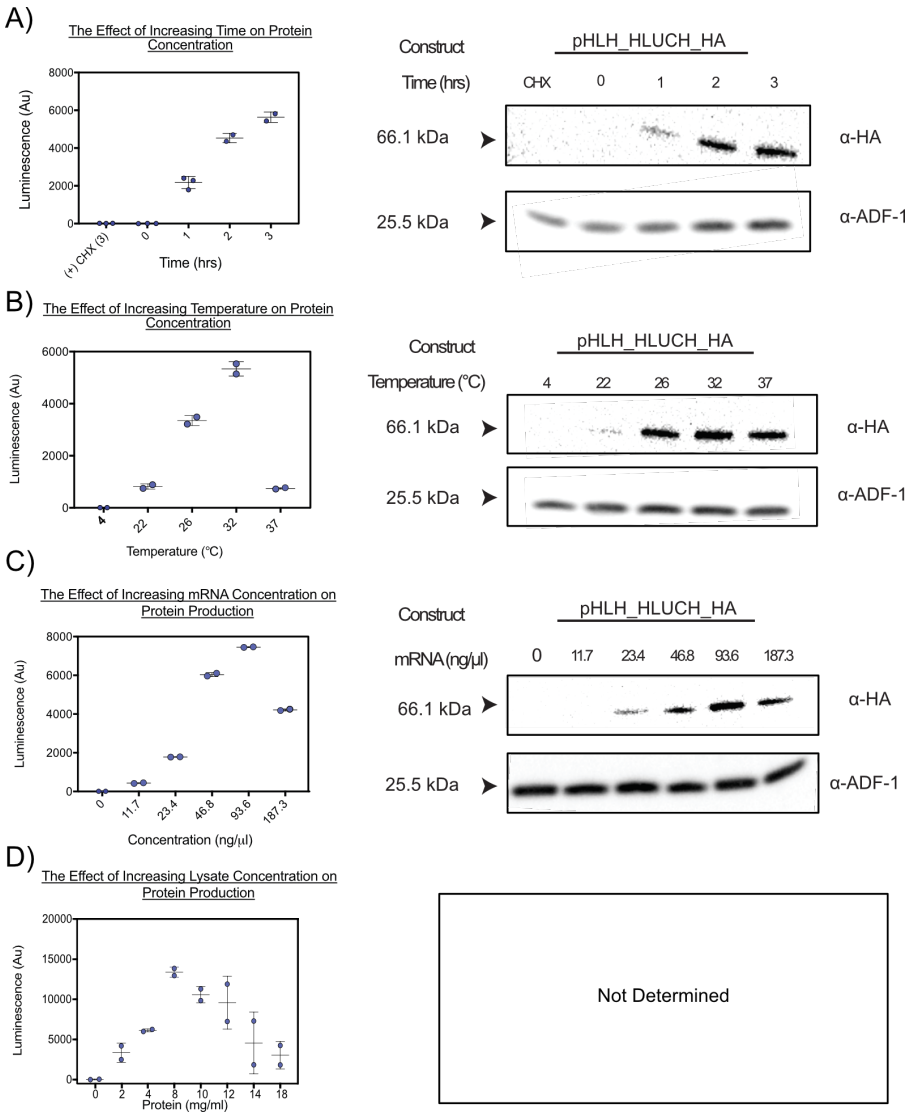

Figure 3.2: Dual-IVT Optimisation Parameters

Each optimisation step was tested in the order shown, with the initial reaction conditions set at an endpoint of 3hrs, a temperature of 37°C, an mRNA concentration of 187.3ng/µl and a lysate protein concentration of 18mg/ml. After each optimisation step the reaction was adjusted accordingly. Each point on the graph represents a single biological replicate of the average of three technical replicates. The error bars indicate the mean with standard deviation (SD). **A**) As the time of the reaction proceeds from 0 to 3hrs the production of firefly luciferase increases compared to a 3hr cycloheximide control (CHX) reaction. The firefly luciferase protein is also detected by western blot at the predicted size. **B**) Protein production steadily increased from 0 and peaked at 32°C before rapidly decreasing on reaching 37°C, again this was confirmed by western blot with a strong HA signal observed at 26°C and above. **C**) Protein production increased with the concentration of mRNA added, peaking 93.6ng/µl before decreasing. This was also confirmed by western blot detection. **D**) The protein concentration of the isolated *P. falciparum* lysate was most efficient at protein production when adjusted to 8-10 mg/ml.

Two reporters of translation were then tested for luminescence signal after a translation reaction, the firefly luciferase gene (as detailed previously) and a click beetle green luciferase gene *CBG99*, reported to have increased stability (Hall et al., 2018). The production of CBG99 resulted in > two-fold increase in luminescence over that from firefly luciferase (see Figure 3.3 (A)). The ability to screen libraries using a single batch of lysate is advantageous due not having to deal with batch to batch lysate variations. As such the reaction volume in the Dual-IVT was lowered from an initial 10µl to 5µl halving the quantity of lysate needed. Although there was an almost 50% decrease in luminescence signal it was still substantially higher than background noise(see Figure 3.3 (B)). To conclude the assay optimisation strategy the modifications made for malaria derived translation were applied to reactions using human lysate (see Figure 3.3 (C)). A luminescence signal was detected above background noise above that produced using malaria lysate. This was expected due to the incorporation of the EMCV IRES element.

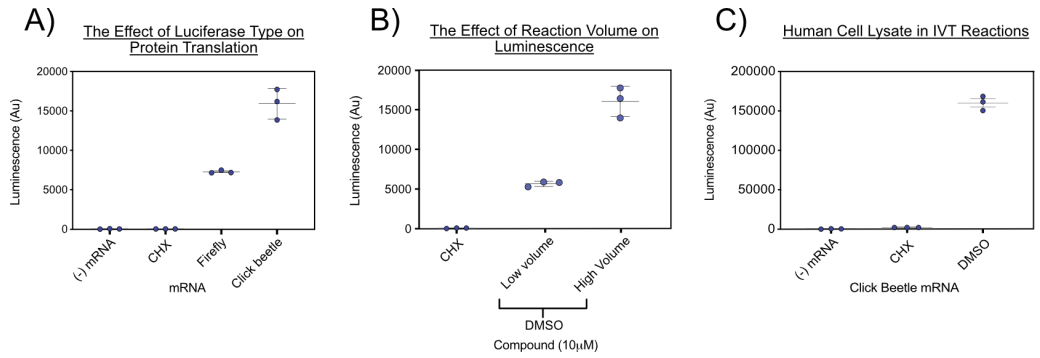

Figure 3.3: Increasing Luminescence - Click Beetle Luciferase
The reaction conditions used here are as follows; an endpoint of 2hrs 30min, a temperature of 32°C, an mRNA concentration of 93.6ng/µl and a lysate protein concentration of 8-10mg/ml. Each point on the graph represents a single biological replicate of the average of three technical replicates. The error bars indicate the mean with SD. The error bars indicate the mean with SD. **A**) In a standard 10µl reaction volume the addition of firefly luciferase (from pHLH_HLucH_HA) versus click beetle luciferase (from pHLH_HCBGH) was tested against a control in which mRNA was omitted ((-)mRNA) and a cycloheximide control was added (CHX). **B**) The reduction of whole reaction volume per well from 10µl to 5µl was explored using malaria derived lysate. This resulted in >50% reduction of luminescence but was above a cycloheximide (CHX) control. **C**) Human cellular lysate was tested for the production of luciferase against a no mRNA ((-)mRNA), a cycloheximide (CHX) and a DMSO control. The DMSO (0.5%) control produced a robust luminescence signal over the two negative controls used.

3.1.3 Production of a Robust Dual-IVT Assay

To interrogate the Dual-IVT assay a panel of compounds with different but known MoA's, specific for cytoplasmic protein translation were selected. The five compounds target different complexes within the parasite and human translation mileu (see Figure 1.5); These included, cycloheximide, cladosporin, DDD107498, emetine and halofuginone. As expected, each of the five compounds were fully effective at inhibiting *P. falciparum* parasite translation with cycloheximide, DDD107498, emetine and halofuginone all showing 100% inhibition at a concentration of 10µM. However, cladosporin required a concentration of 100µM to achieve full inhibition inhibition (Figure 3.4 (A)).

Consistent with known specificity, DDD107498 and cladosporin were both shown to have little effect at inhibiting human translation(Figure 3.4 (B)). Dose response curves for each of the five inhibitor compounds enabled their respective EC_{50} values to be calculated. In parallel, for the parasite-active compounds, a *P. falciparum* 72-hr growth inhibition assay (GIA) was used to calculate EC_{50} values for parasites in culture. Reassuringly the GIA gave comparable EC_{50} values to those from the published literature (Table 3.1) ((Baragaña et al., 2015; Delves et al., 2012; Jain et al., 2015; Panwar et al., 2020; T. Yang et al., 2021)). Comparison of the EC_{50} values between cell-based GIA and Dual-IVT showed that the cell-based EC_{50} was in most cases lower than that obtained via IVT. This could be explained by a number of factors: Firstly, the intra-cellular dynamics within the parasite will be different to that in the *in vitro* reconstituted assay; secondly, the regulation of translation within a cell is dynamic and controlled by internal but also external factors which will not be representative of the drug pressure applied in the assay; and thirdly, the concentrations of amino acids and ATP within the IVT will be different to that in the cell, some inhibitors assayed like cladosporin bind the lysyl-aaRS synergistically with ATP (Fang et al., 2015). Therefore, a change in ATP concentration from that found in a parasite cell could account for the substantial differences in EC_{50} values for calculated for

Dual-IVT and GIA assays.

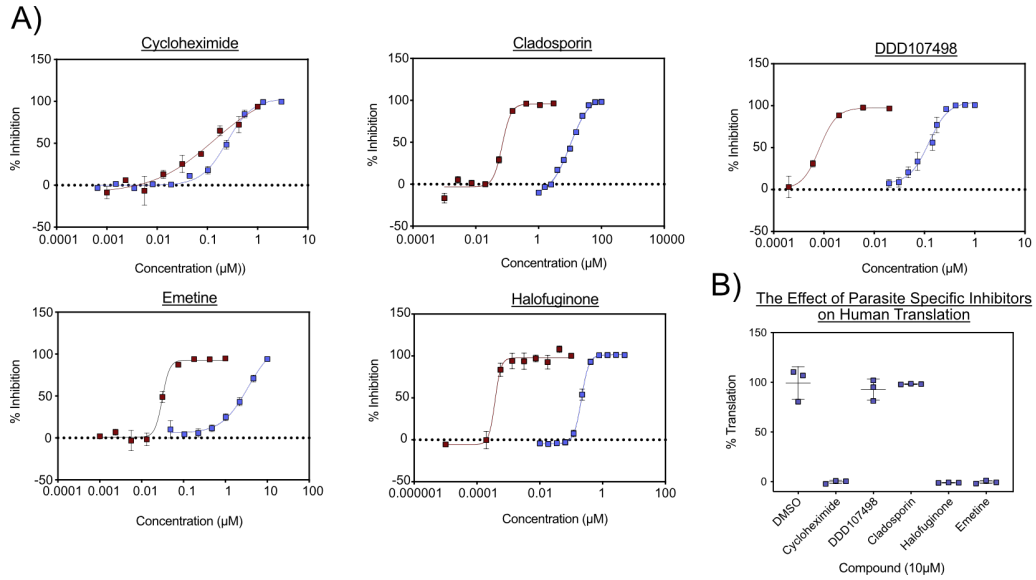

Figure 3.4: Testing a Panel of Known Translation Inhibitors

The reaction conditions used here are as follows; an endpoint of 2hrs 30min, a temperature of 32°C, an mRNA concentration of 93.6ng/µl, a lysate protein concentration of 8-10mg/ml and an assay volume of 5µl. Each point on the graph represents a single biological replicate of the average of three technical replicates. The error bars indicate the mean with SD. **A**) A panel of five translation inhibitors; cycloheximide, cladosporin, DDD107498, emetine and halofuginone were tested using both the Dual-IVT assay (purple squares), using malaria derived lysate and the GIA (red squares). The EC_{50} values for each inhibitor using both types of assay were calculated from the dose response curves and reported in Table 3.1. **B**) The two malaria specific translation inhibitors, cladosporin and DDD107498 were used together with a pan-translation inhibitor, cycloheximide to test for translation inhibition of human cellular lysate using the IVT assay. Each compound was used at a concentration of 10µM apart from cladosporin which was used at 100µM.

Table 3.1: Dual-IVT Compound Validation

Compound	*Pf*GIA EC_{50}(µM)	Reported *Pf*GIA EC_{50}(µM)	*Pf*IVT EC_{50} (µM)	HumanIVT EC_{50}(µM)
Cycloheximide	0.1190	0.2000	0.2450	0.2020
Cladosporin	0.0690	0.0730	10.100	n/a
DDD107498	0.0008	0.0010	0.1223	n/a
Emetine	0.0310	0.0470	0.3460	1.3830
Halofuginone	0.0004	0.0003	0.2110	1.6660

3.1.4 Ribosome Target Validation: Cycloheximide, Emetine & Mefloquine

Within a cell the ribosome acts as the central nexus point for translation that is critical for cell survival (D. N. Wilson & Doudna Cate, 2012). To ensure transitionally active lysate

isolated from *P. falciparum* contained the main cytoplasmic translationally active 80S ribosome and not those from the apicoplast, the drugs doxycycline and clindamycin, both reported to target protein solely within the apicoplast were used as controls (Dahl & Rosenthal, 2007). These two drugs were found not to have any effect on translation within malaria derived lysate. Indicating that translation was being initiated by the 80S, cytosolic ribosome (see Figure 3.5 (A)).

Cycloheximide is a small molecule that inhibits translation elongation by binding to the ribosome E-site and subsequently interfering with eEF2 mediated translocation (Schneider-Poetsch et al., 2010). Cyclohexamide was found to have comparable EC_{50} values in the nano-molar range as calculated in the Dual-IVT assay for both HEK293F and *P. falciparum* and the growth inhibition assay (GIA). The EC_{50} calculated from the GIA for *P. falciparum* was 119nM and similarly reflects that calculated using similar methods for Dd2 strain of *P. falciparum* with an EC_{50} of 200nM (Rottmann et al., 2010) (see Table 3.1).

Emetine is an anti-protozoan drug that inhibits protein translation however, prolonged periods of taking this drug also result in toxic effects on humans as the compound has been shown to target human translation machinery (Dempsey & Salem, 1966). Emetine binds near the E-site of the 40S ribosomal subunit blocking mRNA translocation across the ribosome(Wong et al., 2014). Although the *P. falciparum* GIA conducted showed a comparable EC_{50} to that previously published for *P. falciparum* K1 strain (47nM) (Matthews et al., 2013) the EC_{50} values obtained in the Dual-IVT were significantly higher (see Table 3.1). This could possibly be explained by the intra-cellular dynamics at play within a cell compared to those found in an *in vitro* reaction (see Introduction 1.8.1). Interestingly, the EC_{50} obtained from the Dual-IVT showed emetine is >3-times more effective at inhibiting *P. falciparum* translation compared to human HEK 293 translation (see Table 3.1). This is consistent with emetine's use as a therapeutic(Matthews et al., 2017).

Similar to emetine, the cryo-EM structure of mefloquine bound to the 80S ribosome of the *P. falciparum* has also been resolved. Mefloquine is produced as a racemic mix of the +RS and -RS enantiomers. It has been previously shown that +RS enantiomer of mefloquine binds to the ribosome GTPase associated centre of the 60S large ribosomal subunit. This in turn inhibits mRNA translocation. Authors of this study conducted site directed mutagenesis of mefloquine binding residues resulting in an increase of resistance to the drug as determined by S-35 methionine incorporation(W. Wong et al., 2017). The racemic mix of mefloquine as well as the +RS enantiomer (reported to directly inhibit translation *in vitro*), failed to inhibit protein translation even at concentrations of 100µM when assessed by the *Pf*IVT assay (see Figure 3.5 (B)). This adds weight to the claim that mefloquine may not be a direct, potent inhibitor of the 80S ribosome, instead having an alternate MoA (Sheridan et al., 2018).

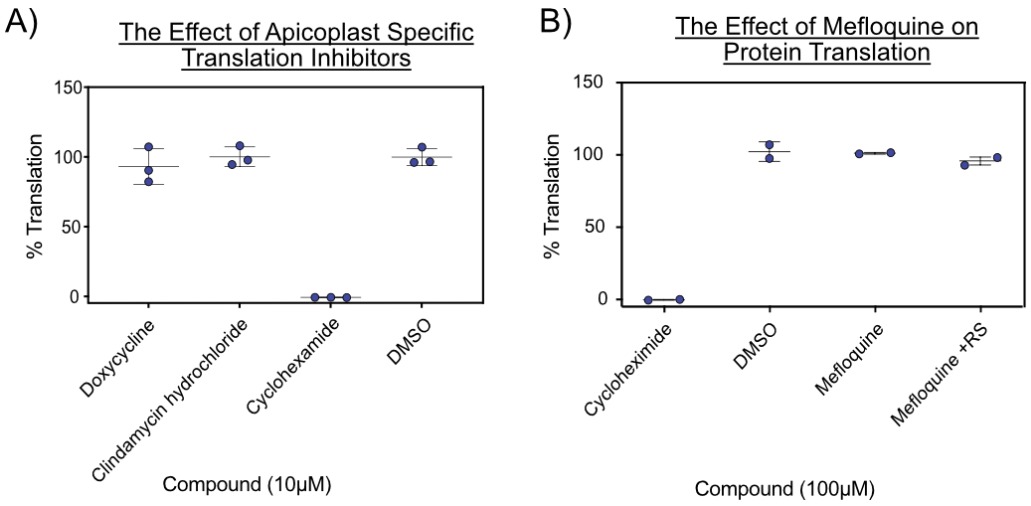

Figure 3.5: Target Validation - 80S Ribosome

The reaction conditions used here are as follows; an endpoint of 2hrs 30min, a temperature of 32°C, an mRNA concentration of 93.6ng/µl, a lysate protein concentration of 8-10mg/ml and an assay volume of 5µl. Each point on the graph represents a single biological replicate of the average of three technical replicates. The error bars indicate the mean with SD. **A**) The two drugs, doxycycline and clindamycin specific for targeting apicoplast translation were tested against a known inhibitor of the cytoplasmic 80S ribosome, cycloheximide at a concentration of 10µM. **B**) The antimalarial mefloquine, was tested along with the +RS enantiomer at 100µM and compared to a 10µM cycloheximide control.

3.1.5 Lysyl-tRNA Synthetase Drug Development: Cladosporin

Cladosporin is a fungal secondary metabolite made of a THP ring (2,6-disubstituted tetrahydropyran) linked to an isocoumarin group (see Introduction 1.5.7). It can be isolated from fungal *spp* including Cladosporium, Aspergillus and Eurotium and has been reported to be >100-fold more potent at inhibiting protein translation in malaria compared to humans. Cladospodrin inhibits the cytosolic KRS of *Plasmodium spp* by preferentially binding to two residues (Val328 and Ser344) within the enzyme's ATP binding pocket, giving the compound anti-parasitic activity in both the blood and liver stage of *P. falciparum* infection(Baragaña et al., 2019). This would make cladosporin an ideal chemotherapeutic however, its low oral bioavailability has been well reported rendering it unsuitable as an antimalarial.

Cladosporin and two of its derivatives (DDD13060706 and DDD1306076) were screened using the GIA and the Dual-IVT assay for activity in *P. falciparum* and human cellular lysates (see Figures 3.4 & 3.6). Using the GIA, cladosporin was found to have an EC_{50} of 69nM which is in line with other reports, highlighting its potency at killing blood stage parasites (see Table 3.1); whilst cladosporin was found to have an EC_{50} of 10µM as determined by the Dual-IVT assay using *P. falciparum* cellular lysate. There was a large disparity when comparing the EC_{50} values obtained from the GIA and the IVT assay for *P. falciparum* for this compound. This may be due to the mechanism by which cladosporin inhibits the KRS and concentration of supplemented ATP and L-proline required for translation in the IVT. Reassuringly though, cladosporin did not affect human translation (see Figure 3.5 (A)), highlighting its affinity for binding the KRS from malaria over its human counterpart.

Derivatisation of cladosporin is required due to its instability and consequently its low oral bioavailability. The compounds DDD13060706 and DDD1306076, synthesised by The Drug Discovery Group at the University of Dundee are an attempt at achieving oral availability. These two compounds were tested for potency using the *Pf*IVT assay with DDD13060706

calculated to have an EC_{50} of 0.12µM by the GIA. This is a marked reduction in its potency compared to that of its parent compound. This was then reflected when the compound was tested in the *Pf*IVT assay. Peak inhibition for DDD1306077 could not be achieved at 100µM. DDD1306077 was also found to have a potent parasite killing effect as detected by the GIA with a calculated EC_{50} of 0.03µM. This is more in line with that calculated and reported for cladosporin(see table 3.1). DDD1306077 was screened using the Dual-IVT assay against *P. falciparum* cellular lysate. Again maximum inhibition could not be achieved. An EC_{50} of approximately 70.63µM could be predicted though with a low degree of confidence.

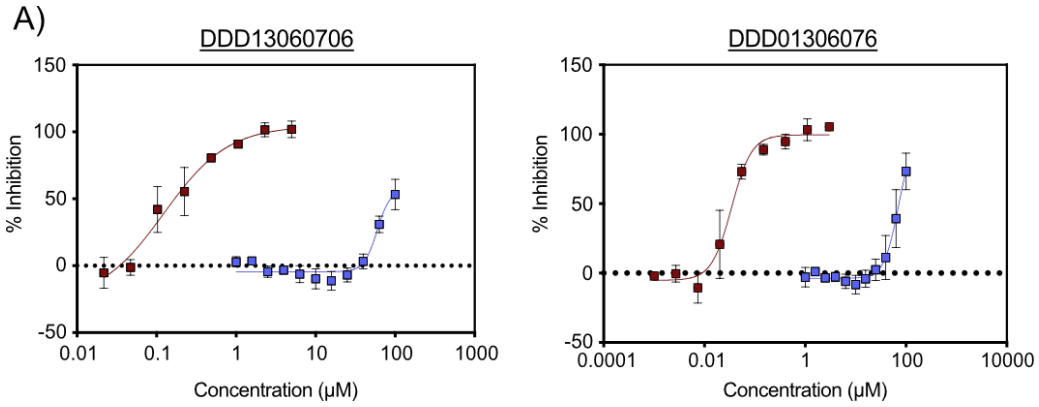

Figure 3.6: Cladosporin Derivatization
The reaction conditions used here are as follows; an endpoint of 2hrs 30min, a temperature of 32°C, an mRNA concentration of 93.6ng/µl, a lysate protein concentration of 8-10mg/ml and an assay volume of 5µl. Each point on the graph represents a single biological replicate of the average of three technical replicates. The error bars indicate the mean with SD. **A**) Two cladosporin derivatives, DDD13060706 and DDD01306076 were both tested by GIA and Dual-IVT assay for activity in *P. falciparum*. Three separate batches of *P. falciparum* lysate and parasites were used, each assayed for luminescence in the case of the Dual-IVT assay or fluorescence using the GIA assay in triplicate and the values averaged to obtain three biological replicates. The red squares show data points for the GIA assay whereas purple squares indicate data points for the Dual-IVT assay.

3.1.6 Prolyl-tRNA Synthetase Target Validation: Halofuginone

The *Pf*IVT assay was used to explore the MoA of the well-characterised, PRS inhibitor halofuginone(Jain et al., 2014, 2015). Halofuginone is a quinazolinone ring fused to hydroxypiperidine, the two chemical groups mimic tRNA and L-proline structures inhibiting protein translation

by interacting with their binding sites within the pro-aaRS. Previously, it has been shown that increasing the concentration of L-proline within the culture medium containing *P. falciparum* 3D7 parasites can outcompete the inhibitory effect of halofuginone addition(Jain et al., 2014). The supplementation of L-proline was attempted, using *P. falciparum* cellular lysate. Each IVT reaction is normally initiated with a cocktail containing each of the 20 essential amino acids at a final concentration of 25µM. An initial *Pf*IVT assay was used to determine the EC_{50} for halofugione as a baseline for probing its MoA. By titrating L-proline in each *Plasmodium* specific reaction from 25µM to 200µM, the progressive shift in the EC_{50} of halofuginone from its initial calculation of 0.2µM to 0.9µM was then observed (see Figure 3.7). The EC_{50} values calculated were then compared to a control using the amino acid L-alanine because it does not interact with the PRS. A linear relationship between the calculated EC_{50} values for halofuginone and the concentration of L-proline supplemented into a reaction was found. This confirms the specificity of L-proline and halofuginone for the PRS. Halofuginone binds the PRS occupying the L-proline binding site. By outcompeting halofuginone inhibition of translation can be relieved, reducing the potency of halofuginone in the reaction. By exploiting similar processes this strategy could be used to identify other inhibitors of aaRS's that have MoAs that mimic amino acid binding.

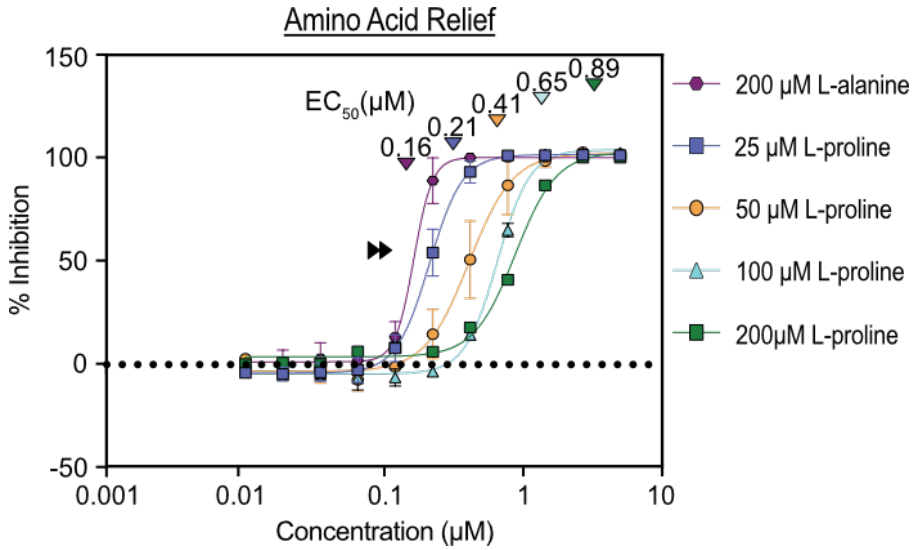

Figure 3.7: Amino Acid Relief Validation

The reaction conditions used here are as follows; an endpoint of 2hrs 30min, a temperature of 32°C, an mRNA concentration of 93.6ng/µl, a lysate protein concentration of 8-10mg/ml and an assay volume of 5µl. Each point on the graph represents a single biological replicate of the average of three technical replicates. The error bars indicate the mean with SD. The *Pf*IVT was used to test the MoA of halofuginone *P. falciparum* cellular lysate. A halofuginone concentration gradient from 5-0.01µM was used to generate four dose response curves in the presence of four increasing concentrations of L-proline from 25 to 200µM, with 200µM L-alanine used as a control. The data points for each amino acid concentration indicated with the EC_{50} generated for each curve shown. The dose response curves are progressively shifted to the right of the graph (purple to green) indicating an increase in the EC_{50} of halofuginone for each of the progressively higher concentrations of L-proline.

3.1.7 High-Throughput Screening of the MMV Pathogen Box

We next sought to test whether the Dual-IVT assay could be applied to aid in the screening of large libraries of compounds through the use of translationally active *P. falciparum* 3D7 and HEK 293F cell lysates, in parallel towards detecting parasite specific inhibitors. To maximise the efficiency and cost-effectiveness of the assay, the total lysate volume was further reduced from 5µl to 2.5µl per plate well. The low reaction volumes used for the Dual-IVT assay enabled the efficient screening of the entire compound library: The MMV Pathogen box (MMV, n.d.). This Pathogen Box is a library of 400 compounds active against neglected diseases.

Each compound from the pathogen box was tested in triplicate at a single dose of 30µM using cycloheximide and DMSO as positive and negative controls. The *Pf*IVT revealed 11 'hit' compounds that caused a 50% reduction or greater in protein translation in *P. falciparum* (see Figure 3.8 (B)). From the 11 inhibitors identified, four were parasite specific and included MMV667494, MMV634140, MMV010576 and MMV007625. A simple literature search of each of the hit compounds revealed studies that identified a proposed mechanism of action for four out of the eleven compounds. Reassuringly MMV667494 and MMV634140 (a crossover compound) have been reported to inhibit *P. falciparum* eukaryotic elongation factor-2 (eEF2) (Calit et al., 2018). MMV010576 is a 3,5-diaryl-2-aminopyridine *Plasmodium* specific small molecule kinase inhibitor shown not to be toxic to human cells (Duffy et al., 2017). This demonstrates the power of the Dual-IVT assay for HTP library screening and *P. falciparum* specific translation inhibitor discovery.

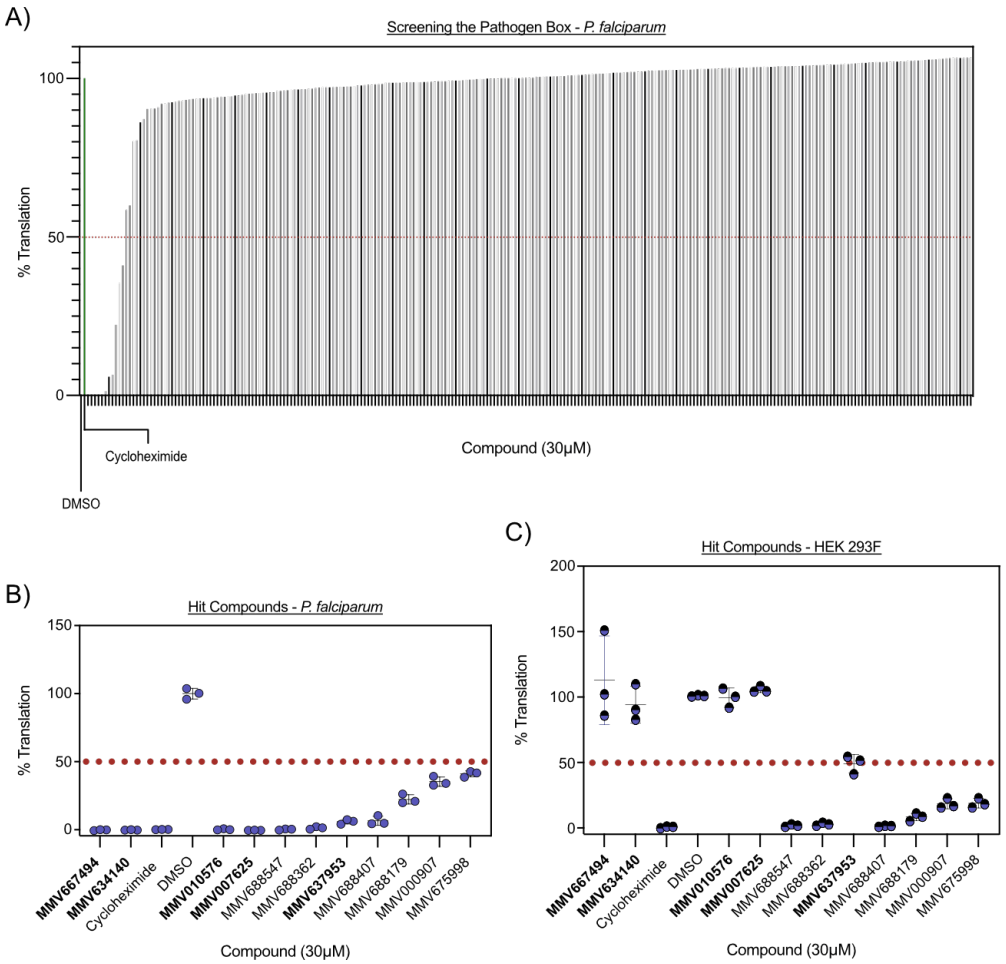

Figure 3.8: Screening the MMV Pathogen Box

The reaction conditions used here are as follows; an endpoint of 2hrs 30min, a temperature of 32°C, an mRNA concentration of 93.6ng/µl, a lysate protein concentration of 8-10mg/ml and an assay volume of 5µl. Each point on the graph represents a single technical replicate using a single batch of lystae. The MMV Pathogen Box consisting of 400 compounds was screened using the Dual-IVT assay developed using human and *Plasmodium* translationally active cellular lysates. The compound library was screened using a single batch of lysate from each cell type with each compound assayed in triplicate. The potent translation inhibitor, cycloheximide was used as a positive control and 0.5% DMSO as a negative control for the screen. **A**) The Dual-IVT using *P. falciparum* lysate was used to accumulate the percentage translation for each of the 400 compounds within the library. The DMSO and cycloheximide control are highlighted as is the 50% cut-off (red dashed line) used to progress compounds that may be of interest. **B**) There were 11 'hit' compounds that inhibited *P. falciparum* translation which are shown from most to least potent. Those that were shown not to inhibit human translation are highlighted in bold text. **C**) The translation data accumulated for the 11 'hit' compounds from human cellular lysate is shown. (Highlighted in bold text are those compounds showing minimal translation inhibition in human cellular lysate).

3.1.8 Summary

Protein translation is critical for parasite survival yet until recently there were no compounds in clinical development targeting this process (see Introduction 1.5.1) in malaria, conversely this in one of the most common MoAs for antibiotics that target pathogenic bacteria. Here,

unlike *Plasmodium* chemotherapeutic interventions can take advantage of the 70S ribosome and prokaryotic translation apparatus, inhibiting processes such as ribosome assembly and processing (M. Walsh et al., 2003). Antibiotic development can therefore take advantage of the divergence of the prokaryotic and eukaryotic translation machinery. Targeting the malaria parasite over its human host on the other hand relies on the discovery of nuances of differences between human and *P. falciparum* translation machinery. The translation inhibitor DDD107498 (M5717) developed in 2015 from a phenotypic compound screen of the DDU kinase scaffold library has been shown to be active against multiple stages of the parasite life cycle in *P. falciparum*. This includes the blocking of transmission as well as alleviating clinical symptoms associated with malaria infection through inhibition of *Pf*eEF2 (see Introduction 1.5.4). DD107498 also satisfies many of the factors within the malaria drug development sector by preventing transmission, being effective after a single dose whilst having a long half life, is chemically tractable and targets a single process (J. Burrows et al., 2017). The discovery and development of this compound now incentivises others to develop and discover other potent antimalarials targeting translation within *P. falciparum*.

Although there is great interest in identifying single molecular targets, phenotypic screens whilst slow often reveal a diverse range of compound types with a variety of MoAs. The discovery of DDD107498 and many other potential and active antimalarials occurs in discrete steps. Firstly, a molecular target is defined such as a kinase. Next, a library of potential inhibitors is screened for activity, typically in a phenotypic based assay. Then the precise MoA is elucidated through induction of a compound resistant line, using genomic analysis allowing the precise mutation to be pinpointed to a specific protein within the parasite. This molecular interaction is then recreated *in vitro* and the compound of interest added to precipitate inhibition (see Introduction 1.4.2). Translation within the malaria parasite is highly choreographed, encompassing many protein complexes that could not all be reconstituted individually *in vitro* to

screen for potential inhibitors, especially when screening large compound libraries. To aid the discovery of antimalarials and to specifically reduce the time of compound discovery to MoA determination, a Dual-IVT assay, derived from translationally active human and *P. falciparum* cellular lysates was developed.

The use of cellular lysates from both *spp*, termed 'Dual' enabled the determination of parasite specific inhibitors of cytosolic translation. This was critical as for the first time it enabled the simultaneous screening of a library of 400 bioactive compounds from the MMV Pathogen Box, crucially allowing the progression of four active compounds against *P. falciparum*. Reassuringly two of these compounds, MMV667494 and MMV634140 are quinoline 4-carboxamides and known analogues of the DDD107498, a compound that targets malaria specific eEF2 preventing mRNA translocation across the ribosome (Calit et al., 2018). Excitingly the next compound identified, MMV010576 (2-amino-3,5-diaryl pyridine) is a small molecule kinase inhibitor that has been previously identified to have malaria parasite specific activity (Duffy et al., 2017)which may target phosphatidylinositol 4-kinase (PI4K), based on its derivative MMV390048 (Ghidelli-Disse et al., 2014). However, PI4K is a known kinase that phosphorylates lipids to regulate intracellular trafficking and signalling (McNamara et al., 2013). Therefore, further investigation of MMV010576 and MMV007625 is now required to elucidate their precise MoAs in the context of translation, initially through a phenotypic based screen to asses potency when applied directly to asexual parasites. If this reveals either or both to be a potent antimalarial with an EC_{50} in the nano molar range further MoA investigation could be pursued as detailed earlier.

The robustness of the assay was confirmed using compounds that target translation in human and *P. falciparum* with known MoAs. This gave expected results of inhibition whilst, with respect to *P. falciparum* cellular lysate confirming the presence of the cytosolic 80S ribosome. This was important as typically compounds targeting translation in the parasites cytosolic com-

partment have been shown to be fast acting, stage transcending and more in line with current guidelines for the development of effective antimalarials (Wells et al., 2015). This process also included the testing of the antimalarial mefloquine which, has been previously shown to bind to the GTPase associated centre of the 80S ribosome inhibiting the movement of the tRNA-mRNA complex and in turn reducing cytosolic protein synthesis in *P. falciparum*. Mefloquin was also shown to inhibit parasite protein synthesis *in vitro* with mutagenesis conducted around the binding site resulting in a decrease in the drugs EC_{50} (see Introduction 1.3.2). Mefloquine was therefore tested in the IVT assay using *Plasmodium* cellular lysates, however no inhibition even at concentrations of 100µM was observed. This has also confirmed previous observations by Sheridan et al who also point to the inaccuracy in S-35 label incorporation as predictors of translation inhibitors, one of the methods used to characterise the translation inhibition associated with mefloquine. For example, the compounds lumefantrine and quinine are not designated translation inhibitors yet they both show translation inhibition when assessed using S-35 label incorporation. Taken together this may point to a target for mefloquine within complexes regulating translation that in turn cause translation repression (Y. Chen et al., 2018) and association with the ribosome being a secondary effect. The Dual-IVT assay whilst shown to be robust does not account for other dynamic intracellular processes that may concentrate or activate mefloquine in ways that do not occur with the isolated lysate *in vitro*.

Recently there has been an increase in interest of aaRS's and the ability to specifically target these in the malaria parasite over the human host. Compounds targeting aaRS's have also gained attention in antibacterial and anti-fungal drug discovery, for example mupirocin has been shown to target the IRS (isoleucyl-aaRS) (J. Hughes et al., 1980). Whilst the compound AN2690 has been shown to target LRS (leucyl-aaRS) in yeast (F.L Rock et al., 2007) indicating an evolutionary divergence between these pathogens and human aaRS's that make them amenable to targeting. Indeed when cladosporin and two of its derivatives, DDD13060706

and DDD01306076 were tested in the Dual-IVT assay malaria specific translation inhibition could be observed. To further probe malaria specific aaRS's the *Pf*IVT assay was able to then interrogate the MoA of the PRS (see Figure 3.7), for the first time recreating previous amino acid relief studies that had only been accomplished with malaria in culture using an IVT assay (Jain et al., 2014, 2015).

The creation of the Dual-IVT assay therefore represents an important milestone to aid in the antimalarial discovery pipeline with respect to translation inhibitors. In addition to HTP drug discovery, the assay developed here could further enable aaRS inhibitor development, derivatization and MoA elucidation.

3.2 Towards the Structural Resolution of *P. falciparum* RNAPI-III

The use of cryo-EM has revolutionised the generation of atomic resolution structures of macromolecular complexes from the malaria parasite that would otherwise not have been possible or taken years to achieve using alternative methods, for example crystollography(Wong et al., 2017; C.M. Ho et al., 2018). This is due to the difficulty in the expression of *P. falciparum* complex proteins using standard heterologous systems and the challenge of growing parasites to sufficient quantities (see Introduction 1.6.5). The isolation of a native protein complex and low sample volumes now required for structural resolution using cryo-EM could facilitate structural aided drug design or compound derivatization.

The malaria parasite uses three nuclear RNA polymerases, without which the parasite cannot survive: RNAP I is required for the transcription of rRNA (Sentenac, 1985); RNAP II is required for the production of mRNA and consequently protein within the cell(Myer & Young, 1998); and finally RNAP III, is used for the transcription of small RNA molecules such as tRNA (Callebaut et al., 2005). In general, these large protein complexes are formed of 8-14 small subunits and two larger subunits which are essential for enzymatic activity(Kornberg, 2014). As important as these three protein complexes are little to no structural data currently exists, hampering drug discovery.

To aid in this area, the three nuclear RNAP complexes (I-III) from *P. falciparum* 3D7 parasites were selected for structural resolution by cryo-EM through their purification directly from the parasite. The selection of three polymerase subunits (RPAC1, RPABC2 and RPB3) spread across all three RNAP complexes were genetically modified by selection-linked integration (SLI) (see Material & Methods 2.6.1). The fusion of a 3X FLAG tag to the C-terminus of each of these three polymerase subunits allowed the purification of the native RNAP complex from asexual blood stage parasites, facilitating the determination of a low resolution cryo-EM structure for

RNAP II. The methodology developed and structural data obtained lays the ground-work for future atomic resolution and structural determination of all three RNAP complexes from *P. falciparum* 3D7 parasites.

3.2.1 Bioinformatic Analysis of *P. falciparum* RPAC1, RPABC2 & RPB3

To enable the purification of all three of the nuclear RNAP complexes within *P. falciparum* 3D7 parasites, the three polymerase subunits; RPAC1, RPABC2 and RPB3 were selected for affinity tagging using a C-terminal 3XFLAG tag based on previously tagged subunits that enabled the atomic resolution of RNAP structures in yeast. These three subunits were, in the case of *S. cerevisiae*, amenable to the introduction of an affinity tag to the aforementioned subunits that did not detrimentally affect the growth of the organism (see Figure 3.9 (A)). However, as no structural data has been made available for the *P. falciparum* RNAP complexes and their respective subunits, the similarity of these three subunits compared to homologues in *S. cerevisiae* had to be predicted. This was carried out to try and determine whether the fusion of a 3X FLAG tag would be accessible for purification or drastically affect the growth of the modified parasites. Protein sequence data for each of the three subunits was obtained from PlasmoDB. Phyre^2 (Kelley et al., 2016) was used to generate structural models, each of the subunits were fitted to the homologues yeast structures, with 80% of each of the malaria specific subunits modelled to $>$ 80% confidence. The structures generated for each of the subunits were overlaid onto the resolved *S. cerevisiae* structures with much of the core secondary structure aligning. The predicted structure for RPABC2 appeared to contain a large disordered region compared to the *S. cerevisea* structure, probably due to the inaccuracy in the structural prediction (see Figure 3.9 (B)). In addition to the structural modelling, the three putative subunit sequences *P. falciparum* RPAC1, RPABC2 and RPB3 were aligned to those from *Drosophila*, human, mouse, *Toxoplasma* and yeast using the Muscle alignment

tool (Edgar, 2004). The conservation varied within the sequences depending on the aligned subunits. Possibly the most striking difference in sequences is that of the RPABC2 subunit where *T. gondii* contains a long stretch of 140 residues that are not present in RPB3 from any other of the *spp* (see Figure 3.10 (C)).

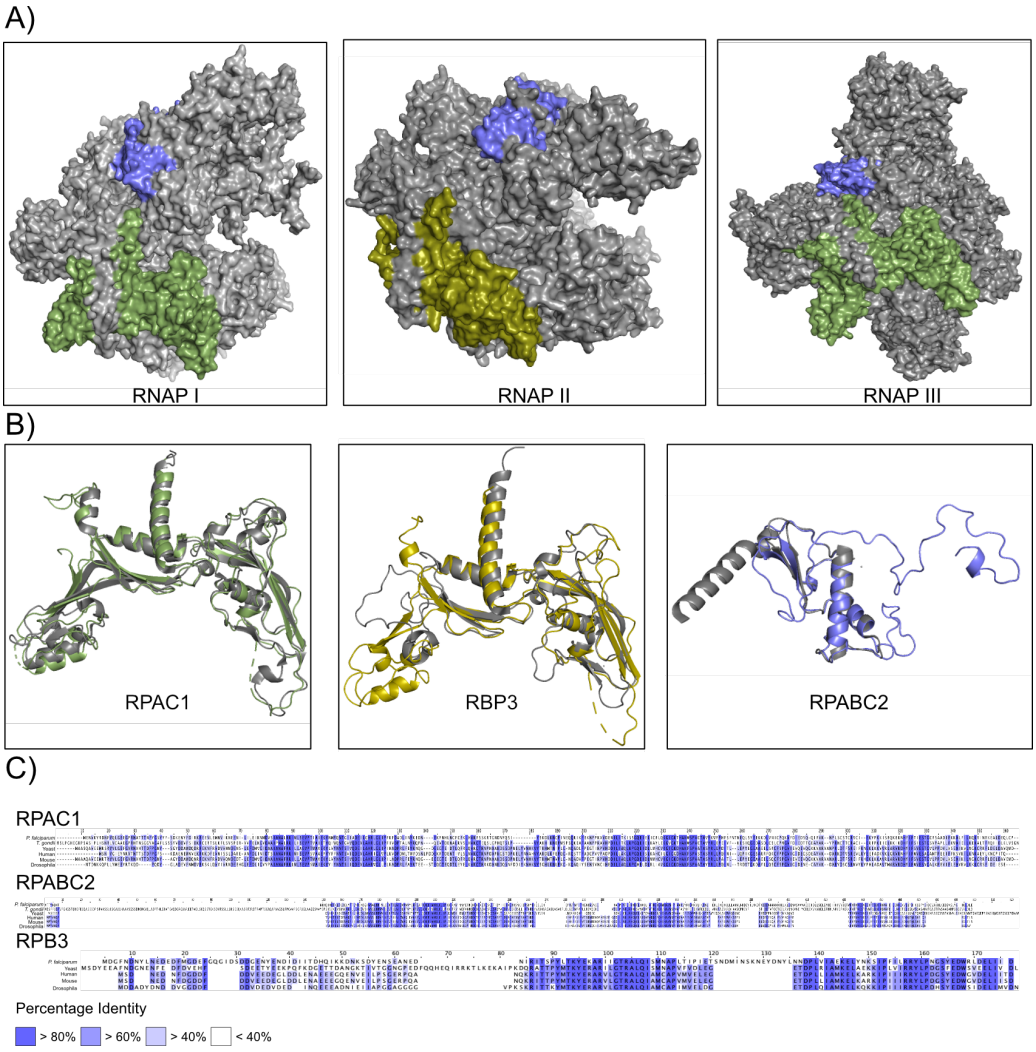

Figure 3.9: The Structural Comparison of RNAPI-III

A) The atomic structures of the three nuclear RNA Polymerases from *S. cerevisiae* (4c3j, Fernandez-Tornero., et al 2013; 1k83, Bushnell., et al 2002; 5fj8, Hoffmann., et al 2015). Each structure was generated to show the molecular surface of each polymerase in grey(The PyMOL Molecular Graphics System, Version 2.0 Schrödinger, LLC), the subunits RPAC1 (dark-green), RPABC2 (purple) and RPB3 (dark-yellow). **B**) The atomic structure of RPAC1(dark-green), RPB3 (dark-yellow) and RPABC2 (purple) were generated using Phyre^2(Kelley et al., 2016). These were overlaid onto their respective homologous from the *S. cerevisiae* structures above (grey). **C**) The predicted protein sequence for *P. falciparum* RPAC1, RPABC2 and RPB3 were taken from PlasmoDB (Bahl et al., 2003) and aligned using the Muscle alignment tool(Edgar, 2004) to homologous sequences from *T. gondii*, yeast, human, mouse and *Drosophila spp* taken from Uniprot (Bateman et al., 2021). These alignments are shown for each of the three subunits, the greater the conservation for a residue at a specific position, the darker the highlighted blue using Jalview (Waterhouse et al., 2009). This is meant as a visual representation to appreciate the sequence conservation among these six *spp*.

3.2.2 Genetic Modification of *P. falciparum* RNAPI-III

Three RNAP subunits present in the three nuclear RNAPs of *P. falciparum* 3D7 parasites were selected: RPAC1 is present in RNAPI and III; RPB3 is present in RNAPII; and RPABC2 is present in all three polymerases. These three subunits were modified at their C-terminus using SLI to introduce a cassette containing a 3XFLAG(Munro & Pelham, 1984), a T2A skip peptide(Liu et al., 2017) and a neomycin resistance gene (see Figure 3.10 (A)). The use of SLI allows the modification of a gene locus at the 3' end of a gene using homologous recombination, allowing integration of a chosen coding sequence of interest to the 3' end of a gene (Birnbaum et al., 2017). The modified plasmids pSLIRPAC1, pSLIPABC2 and pSLIRPB3 were created and contained at least 800bp of the 3'end of the gene being modified as efficiency has been shown to be directly related to the size of the homologous repair template. All three of the plasmids transfected into parasites were confirmed by genomic PCR amplification of the integrated 3XFLAG tag, T2A skip peptide (see Figure 3.10 (B)) and western blot analysis (see Figure 3.10 (C)), compared to wild type *P. falciparum* 3D7 parasites. The subunits RPAC1 and RPB3 have a predicted molecular weight that includes the 3XFLAG tag of 44.1kDa and 43.5kDa. Each of these two proteins were detected close to their respective sizes by western blot. RPABC2 detection was more confusing, its predicted molecular weight is reported to be 24.2kDa but when detected by western blot it is observed migrating with the larger RPAC1 and RPB3 proteins, which requires further investigation (see Table 3.1).

Table 3.2: Molecular Weights for Modified RNAP Subunits

Modified Gene	Predicted Size (kDa)	Detected Size (kDa)
RPAC1	44.1	46
RPABC2	24.2	46
RPB3	43.5	46

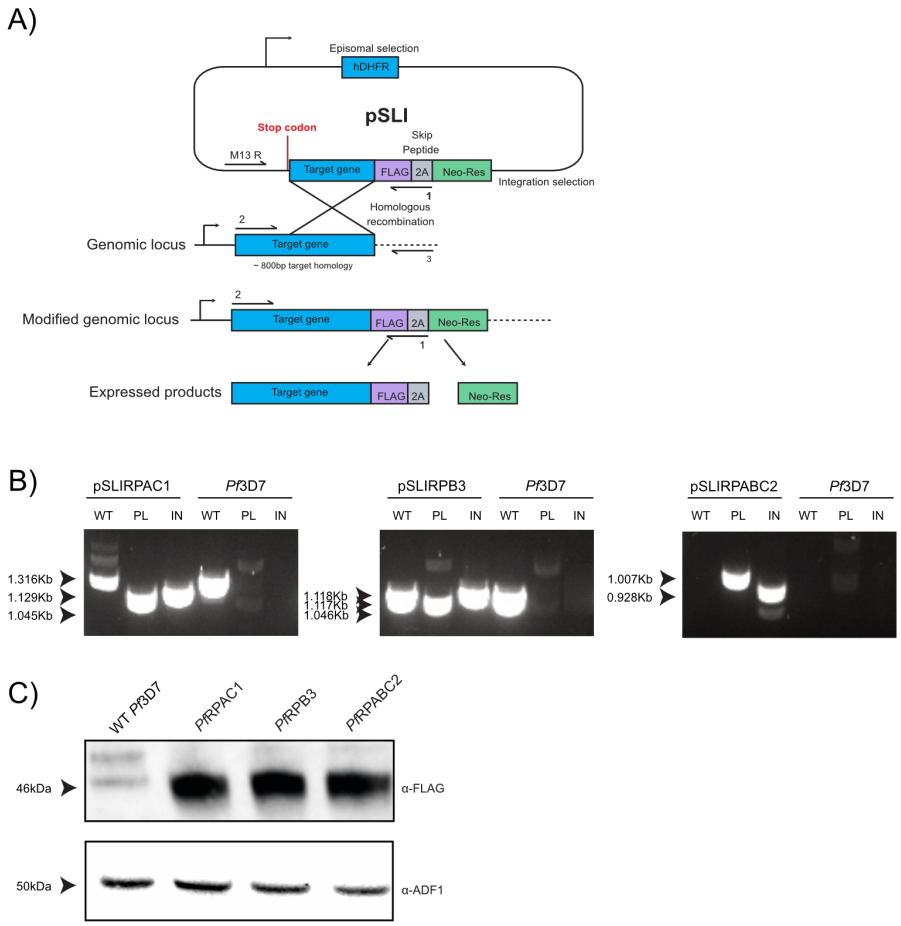

Figure 3.10: Genetic Modification of RNAPI-III

A) A schematic of the SLI plasmid containing a hDHFR (human dihydrofolate reductase gene conferring resistance to WR99210 that can be used as a selection marker for successful transfection with a plasmid. A target gene (blue) sequence to be used in homologous recombination, a 3XFLAG tag (purple), the T2A skip peptide (grey) and the neomycin resistance gene (green). Prior to recombination the gene cassette contained within the plasmid cannot be expressed due to the presence of a stop codon (red). When integration occurs the cassette is used as a repair template for the target gene and inserted. This creates a fusion protein with the 3XFLAG tag and the skip peptide (T2A). When the ribosome encounters the T2A signal it causes it to stall releasing a subunit from the resistance gene. This allows selection of parasites that have integrated the 3XFLAG tag through the application of the antibiotic G418. The detection of WT subunit DNA, the presence of the SLI plasmid or successful integration of the 3XFLAG tag PCR through isolation of genomic DNA can be used. The schematic highlights this using half arrows and shows the primer pairs that can be used for detection. **B**) The isolation of genomic DNA from the three *P. falciparum* 3D7 parasite lines selected for integration using G418 confirmed for the insertion of the 3XFLAG tag using PCR. Primers specific for either the WT, presence of the transfected plasmid (PL) and integration of the cassette including the 3XFLAG tag (IN) were detected using specific primers designed to amplify the stated section of DNA. For RPAC1 a PCR product can be seen at 1.316Kb for WT, 1.129Kb for integrated and 1.045Kb for PL DNA. For RPB3 a PCR product can be seen at 1.117Kb for WT, 1.118Kb for integrated and 1.046Kb for plasmid DNA. Finally for RPABC2 a PCR product can be seen at 0.928Kb for integrated and 1.007Kb for plasmid DNA, however no PCR bands were detected for WT DNA. **C**) A western blot showing the presence of the integrated 3XFLAG in all three transfected lines, ADF-1 was used as a loading control.

3.2.3 Towards the Purification of *P. falciparum* RNAP I & III

The two nuclear eukaryotic RNAPs I and III are responsible for the transcription of genetic information encoding rRNA and small molecule RNA (5s rRNA and tRNA) respectively (Sentenac, 1985; Willis, 1994). In yeast RNAP I is formed of 14-subunits of varying sizes with a total mass of 589kDa(Fernández-Tornero et al., 2013). RNAP III consists of 17-subunits with a total molecular mass of 700kDa, making it the largest of all three RNAPs (Vannini et al., 2010).

The *P. falciparum* RPAC1-subunit was genetically modified to introduce a 3XFLAG tag at the protein's C-terminus which resulted in a modified subunit that is shared between RNAPI and III (Fernandez-Tornero., et al 2013; Bushnell., et al 2002). This allowed the purification of both RNAP complexes using a single transfected parasite line. A protocol that allowed the culturing of high volumes of *P. falciparum* 3D7 parasites, initially developed for the Dual-IVT assay (see Results 3.1) was also used here. The purification of RPAC1 was confirmed by western blot and coomassie stained SDS-PAGE (see Figure 3.11 (A & B)). Cellular lysate was generated for the RPAC1-3XFLAG tagged line and sent to our collaborators, once there they developed a suitable purification based on similar work they had previously conducted in yeast (Tornero Lab - CISC, Madrid) (Fernandez-Tornero., et al 2013). Mass spectrometry was also used to confirm the presence of RPAC1, RPC3 and RPABC1 (data not shown here). Negative stain EM grids were then generated from purified RNAP I and III complexes with observable particles detected at the correct size. Whilst this was positive, progression to a higher resolution using cryo-EM grids was not possible. This was due to the low amount of homogenous protein spread on the grids sufficient for 2D classification. Therefore, further work is currently underway to increase protein yields and improve the purification strategy (see Figure 3.11 (C)).

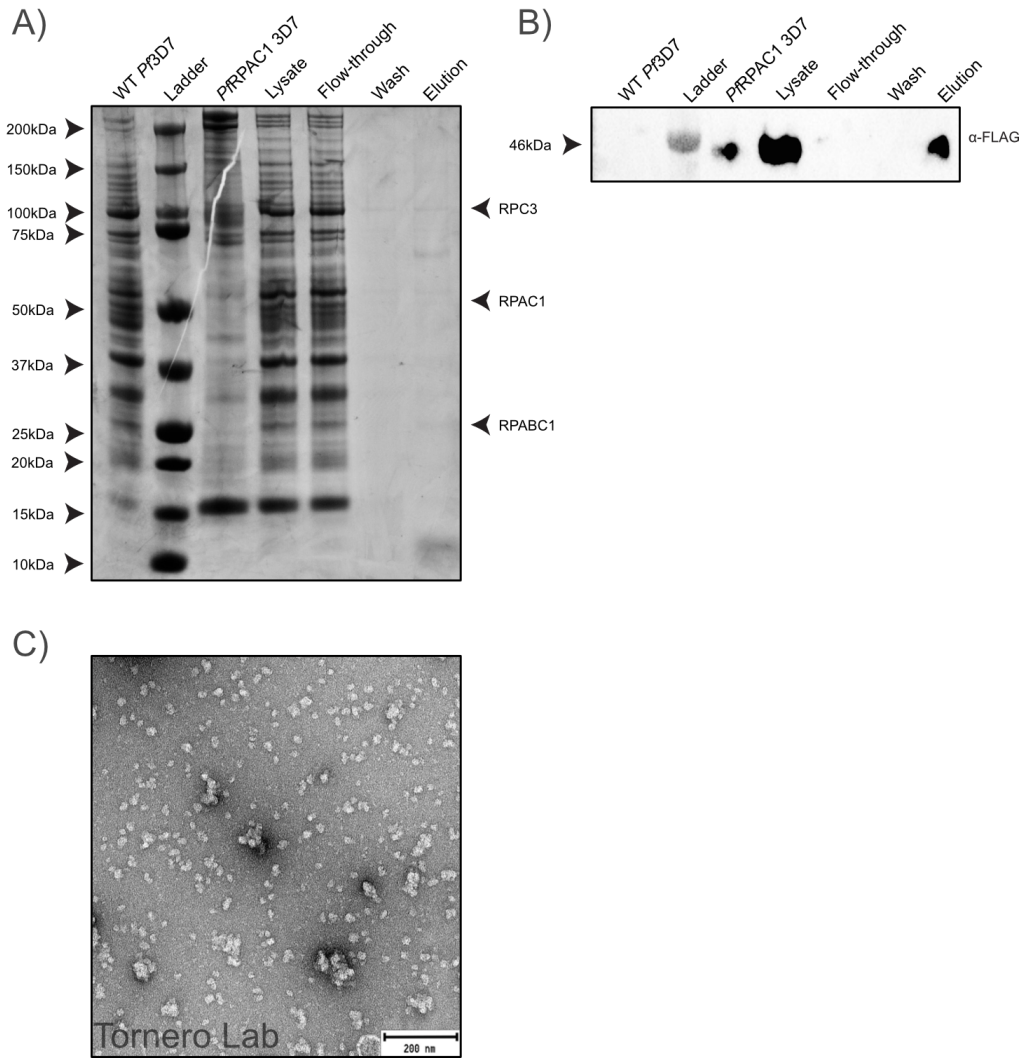

Figure 3.11: The Purification of RNAP I & III

A) An SDS-PAGE gel stained with coomassie blue stain showing the purification of RNAP I and III using the RPAC1 3XFLAG fusion tag from pSLIRPAC1 transfected *P. falciparum* 3D7 parasites (see section 3.2.3). The lanes of the gel contain wild type *P. falciparum* 3D7 parasites as a control (WT). A 'ladder' (All Standards, Bio-Rad) and parasites from the pSLIRPAC1 transfected line (*Pf*RPAC1 3D7). Lysate from the isolated parasite pellet was disrupted using nitrogen cavitation. The 'flow-through' that passed through the FLAG affinity resin containing unbound protein material. A 'wash' step where the FLAG affinity resin was subjected to lysis buffer to wash any unbound proteins. Finally the 'elution' step whereby the two bound RNAP complexes I and III was eluted using the FLAG peptide. **B**) A western blot further confirms the presence of the RPAC1-3XFLAG fusion protein in the lysate and elution fractions. *C*) A cryo-EM grid provided by the Tornero Lab (CISC, Madrid) showing the presence of RNAP I and III at a size of approximately 11nm).

3.2.4 Towards the Purification & Structural Resolution of *P. falciparum* RNAP II

The nuclear RNAPII is the most researched complex out of the three RNA polymerases in part, due to its function in the transcription of mRNA that will go onto produce the majority of

protein within the cell, directing the cells function over time. The eukaryotic RNAP II complex contains 12-subunits, with a molecular weight around 550kDa (Hahn, 2004; Young, 1991). The 12-subunit complex can expand with up to 35-subunits during transcription initiation binding various gene regulatory elements that forms the initiation complex at a promotor region allowing the initiation of transcription of a gene. There is currently no structural data for the *P. falciparum* RNAP II complex. Therefore, to provide greater structural insights the purification of RNAP II and efforts towards its structural resolution were attempted. As was the case for RNAP I and III, a 3XFLAG tag was used to purify RNAP II. Here, a 3XFLAG tag was fused to the C-terminus of the RPB3-subunit(see section 3.2.3). Cellular material from the RPB3-3XFLAG tagged line was generated, the lysate produced was sent to our collaborators as before for purification and eventual structural characterisation. Negative stain EM grids generated from the purification of RNAP II yielded a heterogenous mixture of particles with a size and shape analogous to RNAP II in *S. cerevisiae*. The classification of each of these particles allowed the Tornero Lab to construct a volumetric model at a resolution of 18Å for *P. falciparum* RNAP II(see Figure 3.13 (C)). However, for precise characterisation increased resolution is required. There is now ongoing work to refine this purification strategy and optimise protein yields to progress to higher resolutions using cryo-EM (see Figure 3.13 (C)).

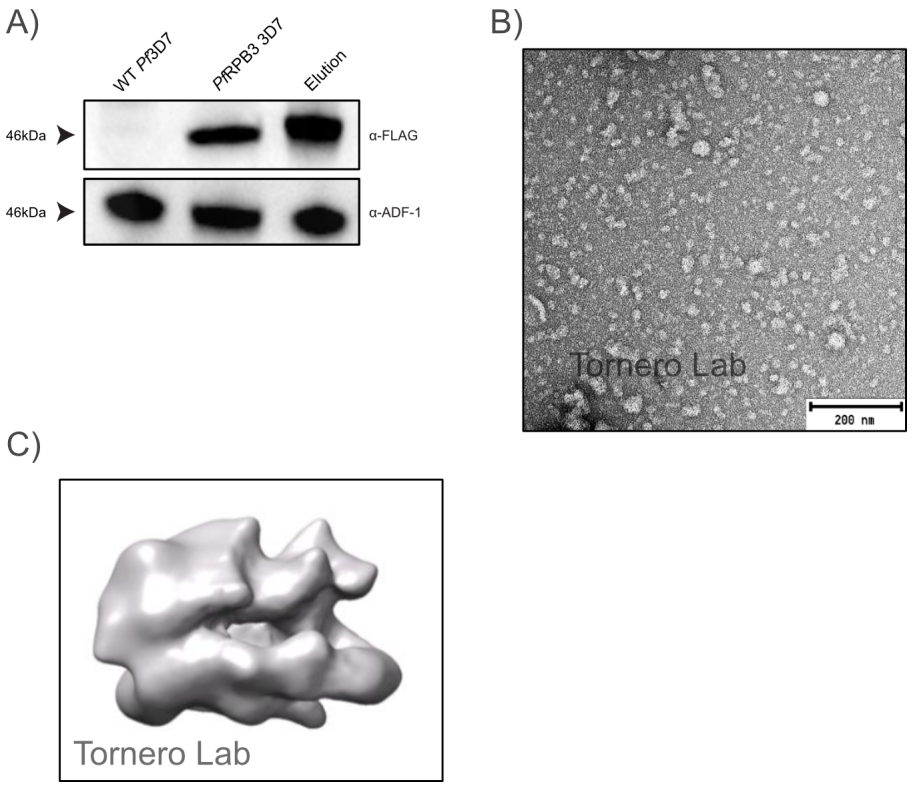

Figure 3.12: Towards the Structural Resolution of RNAP II

A) The purification of RNAP II from *P. falciparum* 3D7 parasites transfected with the pSLIRPB3 plasmid that created a 3XFLAG tag fusion protein. Western blot analysis (see Material & Methods 2.5.2) of the protein compared to wild type parasites (WT *Pf*3D7), cellular lysate from pSLIRPB3 transfected parasites lysed by nitrogen cavitation (*Pf*RPB3 3D7) and an 'elution' sample from the purification of RPB3 using anti-FLAG affinity resin. The *P. falciparum* protein ADF-1 was used as a loading control. **B**) A negative stain EM grid of purified RPB3 containing the RNAP II particles stained with 5% Uranyl Acetate provided by the Tornero Lab (CISC, Madrid). **C** A proposed low resolution model based of detected RNAP II averaged particles, that shares similarity with the RNAP structure from *S. cerevisiae*.

3.2.5 Summary

Transcription within the nucleus is carried out by three nuclear DNA-directed RNA polymerases, I-III in *P. falciparum* that have remained uncharacterised. Given their importance at transcribing the parasite genome, their structures have also remained elusive and hampered any drug development associated in targeting them. RNAP complexes are multi-subunit structures each defined by their sensitivity to α-amanitin (Seifart & Sekeris, 1969). Each polymerase is responsible for the synthesis of a particular type of RNA, with RNAP I transcribing rRNA precursors, RNAP II transcribing mRNA and RNAP III transcribing short untranslated RNA (Anthony Weil et al., 1979; Bikoff et al., 1975; Manley et al., 1980). The emergence of drug

resistant *P. falciparum* has made finding new drug targets a priority but little is known with respect to the structures and subunit makeup of each of the three RNAPs and associated factors. The three polymerases contain between 14-17 subunits that expand in number on formation of the initiation complex just prior to transcription (Ruan et al., 2011). Thanks to the increase in tools for the genetic manipulation of *Plasmodium* parasites, SLI was successfully employed in the modification of the 3' end of three subunits (RPAC1, RPABC2 and RPB3) present in the RNAP complexes (see Figure 3.11). These modified subunits contained a C-terminal 3XFLAG fusion protein, providing a means to purify the polymerase complexes from the parasite. This, coupled with a successful method to grow *P. falciparum* on a litre-scale, enabled the purification and detection of RNAP I and RNAP II for the first time (see Figure 3.12).

The ability to purify these complexes from the parasite milieu enabled collaborators in the Tornero Lab (CSIC, Madrid) to identify these complexes by EM particle classification and produce a low resolution model based on data obtained from negative stain EM data for RNAP II (see Figure 3.12). The *P. falciparum* RNAP II complex observed here is believed to share an overall structural similarity with RNAP II from yeast due to the highly conserved nature of eukaryotic RNAPs (Grohmann & Werner, 2011).

Interestingly though, this structure indicates the presence of a smaller stalk region on the polymerase. The stalk region of RNAP II is made of a heterodimer of RPB4 and RPB7 subunits in yeast, humans and putatively in *P. falciparum*, located near the RNA exit channel. These, unlike the majority of the other subunits in RNAP, do not share a high degree of sequence similarity which, may be due to the their roles in coordinating gene expression. Association of RPB7 in yeast requires association with the core RPB6 and RPB1 subunits and some association with RPB4. In yeast the RPB4 and RPB7 also have the capacity to dissociate form the RNAP II complex to perform other nuclear functions (Armache et al., 2005). The dissociation of RB4 and RPB7 in yeast may also explain the smaller stalk region observed negative stain

EM image of RNAP II presented here. Alternatively, the putative RPB4 sequence in *P. falciparum* is missing much of the amino acid sequence present in its yeast homologue which could account for the smaller stalk region. Without a structure at higher resolution this cannot be fully resolved. Therefore, further work is now underway to optimise the purification strategy for both the RPAC1 and RPB3 tagged lines to increase protein yields and purity.

Resolving each of these three RNAP structures would enhance our understanding of the fundamental mechanisms by which *Plasmodium* control transcription and overall replication. The production of mRNA via RNAP II in eukaryotes requires the recruitment of the pre-initiation complex (PIC) to the transcription start site. The PIC is generally composed of the TATA-binding proteins, TBP-associated factors, transcription factors TFII and RNAPII itself (Callebaut et al., 2005). Despite *Plasmodium* predicted to contain many of these subunits some have not been identified which could suggest a different mechanism of transcription regulation and processing. The three RNAP structures could also reveal potential targetable areas on the complex that could guide drug discovery in this area through the exploitation of any divergence between transcription of human and parasite for example differences within the stalk region of RNAP II. The stalk region is required for efficient capping, polyadenylation and splicing of pre-mRNA, inhibiting this recruitment could severely hamper downstream translation (Cho, 2007). The purification of each of these complexes would also allow their use in transcription based assays for the purposes of drug discovery, allowing small libraries of potential RNAP inhibitors to be tested against *P. falciparum*.

Thanks to new developments in gene targeting and modification the work carried out here has for the first time provided a glimpse at the structure of RNAP II in the most virulent malaria parasite, *P. falciparum*. The further exploration of different affininty tags and other taggable subunits within RNAP II or the two other complexes could enhance the efficiency of purifications allowing higher yield preparations of greater purity that would enhance structural

resolution through progression to cryo-EM.

3.3 Malaria Cell-Free Protein Synthesis

Vaccines are a vital tool and another avenue of control and eradication of malaria in endemic areas(Challenger et al., 2021). However, the production of malaria surface antigens as a potential vaccine has been severely hampered by the difficulty of producing parasite proteins using widely available heterologous expression systems. The expression of parasite surface antigens in these systems, in particular those from *P. falciparum*, often result in misfolded or aggregated proteins (Mudeppa & Rathod, 2013; Morita et al., 2017). More complex heterologous insect cell technologies, such as the baculovirus system have been used but only to limited success in the production of malaria surface proteins (Iyori et al., 2013; Hjerrild et al., 2016).

The most advanced malaria vaccine to date is R21, this uses the repeat region and C-terminal domain of *P. falciparum* CSP fused to the HBsAg which self-assemble into VLPs in yeast (see Introduction 1.7.7). Although recent clinical trials have shown a high efficacy in those vaccinated, multiple booster doses are required to sustain protection that wanes over time. This is by no means ideal especially considering the impoverished parts of the world where the vaccine would need to be deployed (Mahmoudi & Keshavarz, 2017). Vaccinations with attenuated sporozoites have yielded success, in part due to the array of antigens presented on the parasite surface to the immune system. This has resulted in protection that is strain transcending and effective at preventing malaria infection in children(Burns, 2018). However purification of whole sporozoites is laborious and expensive, with their distribution requiring ultra-cold storage, making the deployment of a vaccine of this nature to malaria endemic areas troublesome. The full repertoire of proteins on the sporozoite surface have remained largely uncharacterised instead much focus has been placed on the dominant surface antigen CSP (Hoo et al., 2019; Real et al., 2020). Vaccinations involving CSP whilst partially effective have resulted in only modest protection; therefore the exploration of other less dominant but essential antigens on the sporozoite's surface is vital.

Investigating the immunological potential of novel antigens relies on recombinant production of large libraries of proteins that are correctly folded to produce a structure recognisable by antibodies present within a previously infected individual's serum (Aguiar et al., 2015; Kamuyu et al., 2018). This includes recognition of post-translational modifications however, the challenge in producing these proteins in their native form is significant (see Introduction 1.7.6).

CFPS can offer a novel avenue to recombinant protein production (see Introduction 1.8), unencumbered by the usual constraints of an intact cell-based expression system and with a proven ability in the production of difficult to express proteins (Thoring et al., 2017). *P. falciaprum* proteins contain unique folds, requiring specific chaperones and glycosylation patterns not present in other CFPS systems derived from mammalian, bacterial or wheatgerm cellular extracts (Birkholtz et al., 2008; Bookwalter et al., 2017; Lopaticki et al., 2017). This often results in truncated proteins which may be less immunogenic(Kapoor et al., 2018). There is currently no proven overexpression system derived from *P. falciparum*. This is due to challenges in finding a suitable promotor system, problems attributed to the parasite life cycle and the complexities of removing a protein from inside the RBC.

A CFPS derived from malaria lysate short-circuits many of these obstacles and challenges. Given the success of the *Pf*IVT as a base for which to generate proteins, the expression of *P. falciparum* CSP, an O-linked fucosylated protein (Lopaticki et al., 2017), was chosen as a control candidate because of its widespread use in RTS,S and R21 (see Figure 1.8). A continuous, TX-TL CFPS system was developed using cellular lysate derived from *P. falciparum* 3D7 parasites. The CrPV IRES was able to initiate translation in *P. falciparum* 3D7 lysates. CSP was successfully produced in the system and compared to that on the surface of *P. falciparum* sporozoites. This laid the foundations for further CSP characterisation as well as the potential production of other malaria antigens of interest.

3.3.1 Translation Initiation Using the CrPV IRES in Malaria

Eukaryotes have a complex choreographed system for the initiation of translation, usually requiring 5' capped mRNA that binds to elF-4a and the poly(A)-binding protein to recruit the 43S ribosomal subunit. This binds to other initiation factors and the Met-tRNAi initiator (see Introduction 1.8.11). Translation in eukaryotes, including *P. falciparum* can be controlled and regulated through phosphorylation of certain initiation factors to downregulate translation for example the eIF4E-eIF4G complex (Jackson et al., 2010). IRES elements allow viruses infecting eukaryotic cells to bypass the usual translation initiation process (see Figure 1.11). The CrPV-IGR IRES has been shown to initiate translation in a manner that is *spp* independent (Kerr et al., 2016). This has led to the CrPV-IGR IRES being reported to initiate translation in mammalian, yeast and insect cellular lysates in CFPS reactions (Brödel et al., 2013).

During the development of the Dual-IVT assay a native 5'UTR from *P. falciparum* was used to initiate translation in malaria lysate for the purposes of drug screening (Baumann et al., 2018). Translation initiation in this context became a rate-limiting step for protein synthesis. The 5'UTR from the CrPV-IGR IRES (containing the GCU start codon) and an EMCV IRES was used to initiate translation of a firefly luciferase fused to a C-terminal 3XHA tag. Translation could be detected where the CrPV-IGR IRES was used but not where the EMCV IRES had been used. This is consistent with the mechanism by which the CrPV-IGR IRES has been reported to initiate translation (see Figure 3.13 (A)). A titration of mRNA into the reaction was used to assess the point at which translation became saturated. Due to volume constraints this was tested up to 8µg/µl however, translation was seen to begin peaking at this concentration (see Figure 3.13 (B)). This demonstrates for the first time that initiation of translation with the CrPV-IRES is possible in *P. falciparum*.

The production of large quantities of mRNA are laborious resulting in the purification of unstable mRNA. This can be eliminated by using the TX-TL setup. Here, transcription and

translation occur in the same reaction, eliminating the need for the *in vitro* production and purification of mRNA. DNA is more stable allowing easier storage and handling. Through slight modification of the reaction mixture, including the incorporation of a T7 RNAP, firefly luciferase could be detected after a 24-hr incubation period (see Figure 3.13 (C)). This shows for the first time the ability to transcribe and translate in the same reaction using *P. facliparum*, opening up the possibility of HTP protein production or the investigation of protein pathways within the parasite.

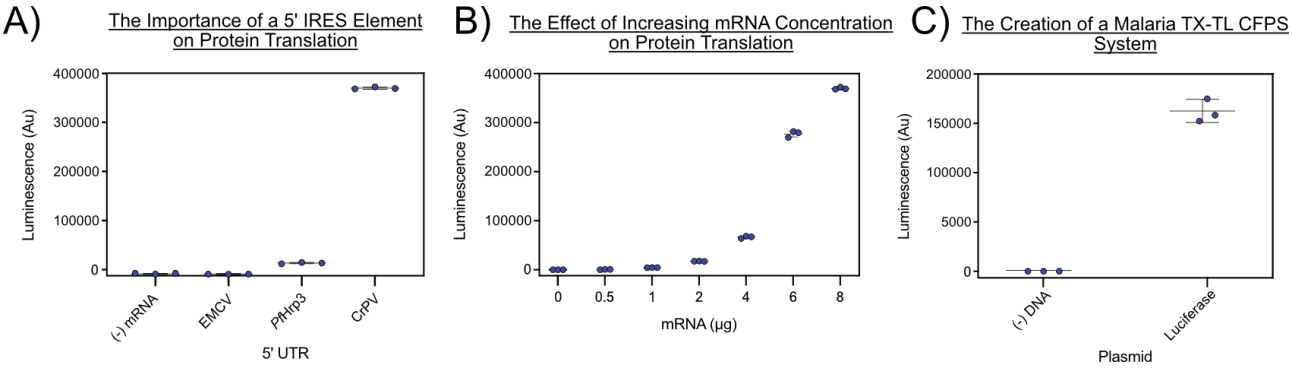

Figure 3.13: Translation Initiation in Malaria

The reactions conditions used here are detailed in Material & Methods 2.4.3. Each was setup in a batch format and incubated for 3-hrs using the final reaction conditions as detailed in figure 3.2. Each point on the graph represents a single biological replicate of the average of three technical replicates. **A**) The use of the CrPV-IGR IRES element was able to initiate the translation of firefly luciferase mRNA added to a reaction, on completion the reaction was taken and assayed for luminescence. In the case of mRNA containing either the EMCV IRES or the *Pf*Hrp3 5'UTR a final concentration of 93.6ng/µl was used as this has been previously shown produce the most optimal luciferase translation. In the case of mRNA containing the CrPV-IGR IRES a concentration of 8µ/µl was used. **B**) The addition of increasing concentrations of mRNA increased the translation of firefly luciferase. Each reaction was setup in a batch format and incubated for 3hrs, on completion the reaction was taken and assayed for luminescence. **C**) The production of firefly luciferase in a TX-TL batch system, incubated over a 3hr period using 120ng/µl of plasmid DNA containing the CrPV-IGR IRES, the firefly luciferase gene and a poly(A) tail.

3.3.2 A Continuous Malaria CFPS System

The development of a continuous exchange cell-free (CEFC) setup over the batch style setup has been reported to drastically increase protein production by sustaining translation for longer (Kigawa & Yokoyama, 1991; Sawasaki et al., 2002). This segregates the reaction mixture con-

taining the cellular lysate and other enzymatic components via a semipermeable membrane. A reservoir then 'feeds' the reaction mixture with energy containing solutions, buffering components, amino acids and salts. In batch-style TX-TL setups, reactions occur in the same environment with no segregation of reaction mixture resulting in earlier translation termination. This is due to the depletion of the energy components and a buildup of free ions that can inhibit protein synthesis (Gan & Jewett, 2014). To evade this problem and increase protein production, the malaria CFPS system was adapted to a CEFC system (see Figure 3.14 (A))). Although firefly luciferase was used to monitor reactions, prolonged protein translation appeared to result in C-terminal firefly luciferase degradation after a 24-hr incubation (see Figure 3.14 (B)). To avoid this issue firefly luciferase was exchanged for super-folder GFP (sfGFP) which did not show any C-terminal degradation over a 24-hr period and could also be detected by western blot (see Figure 3.14 (C)).

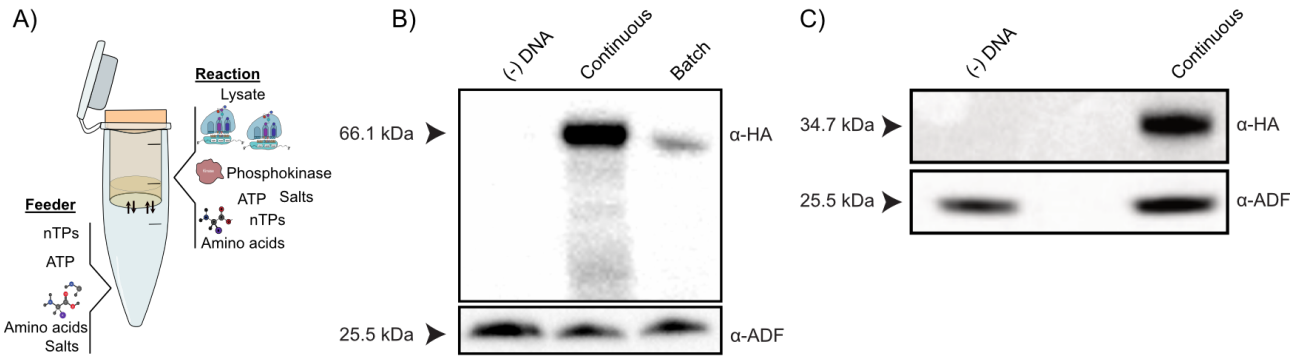

Figure 3.14: Malaria - Continuous CFPS

A) A schematic representation of a CECF protein synthesis system. The reaction mixture is segregated by a 10kDa cut-off dialysis membrane. The dialysis device containing the membrane is placed inside a 1.5ml tube filled with 1ml of a 'feeder' solution containing a reservoir of buffer, ATP, amino acids, nTPs and salts. The feeder solution and small ion reaction byproducts can freely flow between compartments (black arrows). Each standard reaction is incubated at 32°C over 24hrs. **B**) The TX-TL of 3XHA-tagged firefly luciferase in a batch and CECF protein synthesis setup using 120ng/µl of plasmid DNA. Firefly luciferase was detected by western blot probing for its C-terminal 3XHA tag. **C**) The production of 3XHA-tagged sfGFP using the CECF TX-TL protein synthesis, incubated for 24hrs and detected by western blot using 120ng/µl of plasmid DNA.

3.3.3 Towards the Production of CSP

The production of complex surface-bound *P. falciparum* antigens for vaccine and immunological research has been hampered by the difficulty in their manufacture using standard heterologous systems (Mudeppa & Rathod, 2013). Recombinant expression systems require large culturing facilities and do not lend themselves to HTP protein production. The architecture of CFPS systems lends themselves towards the production of large libraries of antigens. The popularity of antigens-on-a-chip, where a group of target surface proteins are immobilised onto glass slides that enable the rapid detection of antibodies within infected patient serum, have the ability to transform malaria vaccinology, potentially revealing potent immunogens of malaria infection unknown to current vaccine pipelines (Kamuyu et al., 2018). The most advanced malaria vaccines are the product of fusion proteins consisting of the CSP NANP repeat region and TSR domain linked to the Hepatitis B surface antigen (see Figure 1.8). CSP contains a number of post-translational modifications at its C-terminus including two disulphide bonds(Patra et al., 2017), a single fucosylation site within the TSR domain (Lopaticki et al., 2017) and finally a GPI anchor that fixes it to the sporozoite surface (Reymond et al., 1995), all of which were absent from these vaccines. In CFPS systems, post-translational modifications that would usually occur within the ER can also be encouraged in the presence of endogenous microsomes within the lysate or the addition of exogenous microsomes (Dondapati, Lübberding, et al., 2019).

To test for translocation into endogenous microsomes within *P. falciparum* cellular lysate, sfGFP was fused to an N-terminal, CSP signal peptide. The production of sfGFP with and without a fused signal sequence was then used to determine whether translocation had occurred. The protein ADF-1 is an abundant *P. falciparum* cytosolic soluble protein (W. Wong, Webb, et al., 2014). Its detection by western blot was used to indicate the presence of the reaction mixture. The microsomes within a CFPS reaction were then isolated as indicated previously

(Thoring et al., 2017).

When synthesised without a signal peptide sfGFP could be detected in the reaction mixture but not in isolated microsomal pellets (Figure 3.16 ((A)(i)). The *P. falciparum* CSP signal peptide (see Appendix 4.3.1) was then fused to sfGFP. Surprisingly a decrease in protein production was seen in the reaction mixture and sfGFP could not be detected in isolated microsomal pellet fractions (Figure 3.16 ((A)(ii)). Due to the low quantity of sfGFP observed here other signal sequences reported to efficiently translocate protein into microsomes in CFPS were attempted. The melittin signal peptide is used extensively in baculoviral recombinant protein expression systems(Soejima et al., 2013). However, more recently it has also been shown to translocate protein into microsomes present within CFPS systems derived from CHO lysates(Thoring et al., 2017). To test this using *P. falciparum* lysate the CSP signal peptide was replaced with the melittin (UniProt_P01501) signal peptide. Expression of sfGFP in this instance could be detected both in the reaction mixture and the isolated microsomal pellet (Figure 3.16 ((A)(iii)).

The production of truncated *P. falciparum* CSP (20-384) without the GPI signal sequence (J. Zhao et al., 2016) was attempted using the methodology as previously described for the translocation of sfGFP into microsomes. The melittin signal sequence was fused to CSP and expressed using the CFPS system. The CSP protein fused to a C-terminal 3XHA-tag has a predicted molecular weight of 44.3kDa based on its amino acid sequence. After a 24hr incubation period, CSP could be detected by western blot at approximately the 70kDa mark. Reassuringly, this is also where native CSP was detected on the surface of *P. falciparum* NF54 sporozoites are detected (see Appendix 4.3.2). The synthesised CSP was also detected in the microsomal fraction, again ADF-1 was not detected within this fraction. As the synthesised CSP contains a 3XHA affinity tag, its purification from microsomes was also attempted and could be detected by western blot in the elution fraction.

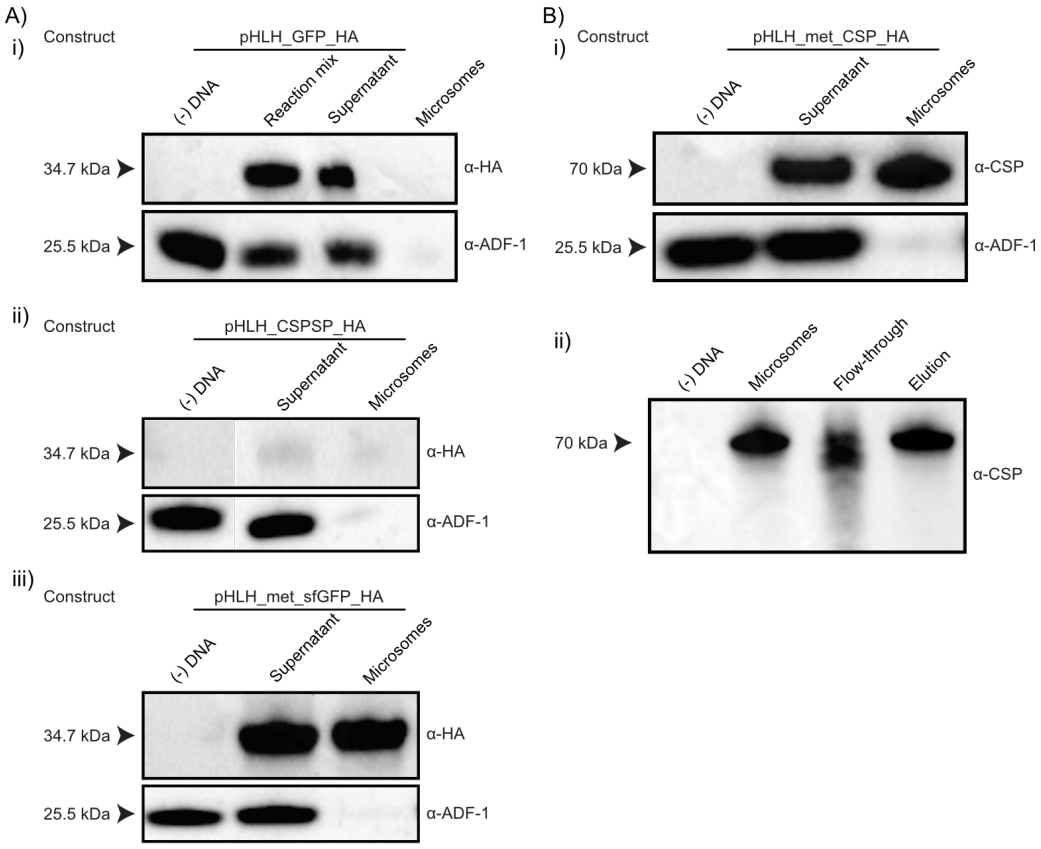

Figure 3.15: Towards the Production of CSP

Each reaction was setup as detailed in Figure 3.14. **A**) (i) The production of sfGFP without a signal peptide resulted in no detectable translocation. (ii) The production of sfGFP fused to the *P. falciparum* 3D7 CSP signal peptide resulted in severely reduced CSP production with none detected in the microsomal fraction. (iii) The production of sfGFP fused to the melittin singal peptide from honey bee produced a strong detectable sfGFP signal in both the supernatant and microsomal fractions. **B**) *P. falciparum* CSP fused to the melittin signal peptide was expressed using the continuous exchange CFPS TX-TL system over 24hrs. The CSP produced was directly detected by western blot using an anti-CSP antibody. (i) CSP was detected in both supernatant and microsomal fractions after a CFPS reaction. (ii) CSP produced after a CFPS was purified using a 3XHA-tag fused to its C-terminus. The isolated microsomal fraction was disrupted releasing CSP and purified using anti-HA affinity resin.

3.3.4 Summary

Vaccine development is seen by many as a critical component of malaria eradication (see Introduction 1.7). However, its development has been hampered by the difficulty in expressing surface antigens of *P. falciparum* using standard heterologous expression systems. These are known to struggle with the production of soluble, correctly folded and post-translationally modified malaria proteins (see Introduction 1.7.6).

The most advanced malaria vaccine, RTS,S has evolved over time but still only produces a modest efficacy requiring multiple booster doses with protection that wanes (see Introduction

1.7.5). CFPS offers a different approach to the recombinant production of protein, unencumbered by the usual cellular processes and culturing considerations. Malaria proteins, produced in CFPS system could enable the HTP production of libraries of malaria surface antigens that could be used to reveal vaccine candidates through exposure to semi-immune serum from those in malaria endemic areas (see Introduction 1.8.1). This has been some what attempted using the well-characterised WGCF system however, this system currently lacks the capacity to produce post-translational modifications associated with protein translocation to the ER without the need for microsome supplementation. Therefore malaria proteins in WGCF systems are often truncated and have their glycosylation sites removed (see Introduction 1.8.7).

Here, the development of a continuous exchange CFPS, TX-TL system has been shown to be successful for the first time using translationally active cellular lysate derived from *P. falciparum*. A key driver of any cell-free system is the means in which translation initiation occurs. In eukaryotes this normally requires mRNA containing a 5' cap, for initiation and a 3'UTR region that stabilises the mRNA through polyadenylation. The importance of the 5'UTR at initiating translation in a *Plasmodium* derived IVT system has already been shown here (see Figure 3.13) and by others (H. Baumann et al., 2018). The 5' cap-dependent mechanism for translation initiation is widely regarded to be a rate limiting step in CFPS, with *P. falciparum* also shown to initiate translation in this manner (R. Tuteja et al., 2009). To explore the full potential of a malaria derived CFPS two mechanisms of translation initiation were pursued; Firstly an EMCV IRES, widely used for human cell derived CFPS systems uses a subset of eukaryotic translation initiation factors (eIF4G, eIF4A, eIF2 and eIF3) to assemble the 48S initiation complex (see Introduction 1.8.12). The most complex of which is elF3 that facilitates the association with the 40S ribosomal subunit (Gomes-Duarte et al., 2018). The elF3 complex has been identified in the nuclear genome of *P. falciparum* as have the other three eIF's, yet when the EMCV IRES is used here it failed to initiate translation. This

suggests a sequence divergence between malaria and human factors that prevents ribosome recruitment by the EMCV IRES. The discovery of a type IV IRES that initiates translation through direct interaction with the 40S ribosomal subunit from the IGR-region of the CrPV has been recently employed in mammalian CFPS systems (see Introduction 1.8.13). Devoid of the need to recruit any initiation factors this type of translation initiation mechanism can also by-pass eIF2α mediated translation repression. This IRES was tested for the first time in a CFPS system derived from *P. facliparum* cellular lysate and successfully used to enhance the translation efficiency of the system compared to a native 5'UTR. Testing other classes of IRES elements in the context of a malaria derived CFPS system for their ability to initiate translation would enable the interrogation of the essential eIF's thought to be present in *P. falciparum*.

Successful translation initiation then allowed the validation of protein translocation into endogenous microsomes present within the lysate. Here, the creation of a CECF system containing cellular lysate produced using nitrogen cavitation, a method known to allow the formation of microsomes during cell lysis was used (Svardal & Pryme, 1978; Trigg et al., 1970). Microsomes are ER remnants formed from the gentle lysis of a number of cell types including mammalian and insect cells. The ER architecture in *P. falciparum* has not been extensively investigated, instead it has been characterised by a small number of EM studies. Importantly the ER in *P. falciparum* has been reported in all stages of the parasite life cycle, in the late trophozoite stage the ER has been shown to create a complex mesh network that branches through the cytosol (Van Dooren et al., 2005). In addition, microsomal pellets have been previously collected from a number of stages of the *P. falciparum* life cycle including gametocyte, merozoite and trophozoite stages (Venkataramaiah & Gajanana, 1987). Microsomal structures have been shown to contain many of the enzymes and protein structures in the ER (see Introduction 1.8.10). Through the use of an endogenous and exogenous signal peptide fused to sfGFP translocation into mi-

crosomes present in the *P. falciparum* lysate was shown to be successful. Interestingly, these signal peptides resulted in drastically differing levels of of protein translocation and synthesis when fused to sfGFP. Signal peptides in *P. falciparum* differ from those of other eukaryotes *spp* due to the high A/T richness of its genome. It has therefore been proposed that these native malaria signal peptides could be targeted as therapeutics for new antimalarials (Harbut et al., 2012; Tonkin et al., 2008). The novel CFPS created here may therefore offer a means to easily enhance therapeutic discovery in this field. For example mycolactone, an exotoxin produced by *Mycobacterium ulcerans* has been shown to inhibit the Sec61 co-translational translocation of proteins through the cytosol to the ER. Testing this compound and potentially others with respect to translocation in *P. falciparum* could reveal novel antimalarials that would otherwise have not been considered (Ogbechi et al., 2018). However, to fully validate the presence of microsomal structures in the lysate the detection of an integral membrane protein spanning the microsomal structure would be required.

The use of these discovered elements allowed for the first time the production of *P. falciparum* CSP in a CFPS system derived from *P. falciparum*, its translocation into microsomes and its small-scale purification (see Figure 3.16). The ability to produce correctly folded protein in a native manner could enable the detection of unknown malaria antigens that produce an immune response within infected individuals in endemic areas (Kamuyu et al., 2018). This is because current methods that produce large libraries of antigens for detection with infected patient serum use heterologous expression systems that may not produce proteins in the correct configuration resulting in poor detection when serum is applied (Karlsson et al., 2012). A malaria-derived CFPS has the ability to transform this process. The production and characterisation of CSP in this system, compared to CSP produced in more standardised systems, could lay the foundations for HTP antigen discovery. However, further biological characterisation would be necessary for full validation. To confirm the presence of glycosylation on the

CSP produced would also give further support of the presence of functional microsomes within the lysate. This could be accomplished through simple deglycosylation assays to test for its presence or via mass spectrometry analysis to confirm fucosylation. To further confirm correct folding native gel SDS-PAGE and analytical gel filtration could be used for sizing precluding the presence of aggregated protein.

A novel CFPS system derived from the lysate of the most virulent malaria parasite *P. falciparum* has been successfully created and used for the production of the sporozoite surface protein CSP. The ability to express malaria proteins using the parasites own translation machinery may alleviate the bottleneck for the production and characterisation of malaria surface antigens or enzymatic complexes of interest that standard heterologous systems struggle to produce. In addition this system opens up the ability to explore translation and translocation pathways within the malaria parasite that have otherwise been difficult to characterise.

3.4 Development and Refinement of a Human CFPS System

CFPS systems offer an alternative method for recombinant protein expression. Devoid of the usual cellular boundaries, survival, translation and regulatory factors, they enable the expression difficult-to-express proteins (see Introduction 1.8.1). These may include: membrane proteins (Sachse et al., 2013), toxins (Ramm et al., 2020), ion channels (Berrier et al., 2004) and VLPs(K. G. Patel & Swartz, 2011). They enable the rapid expression of proteins in a miniaturised format using a variety of translationally active lysate from prokaryotic and eukaryotic sources. However, mammalian and some insect based CFPS technologies have been reported to contain endogenous microsomes that enable the production of proteins containing post-translational modifications (Stech et al., 2017). These include disulphide bond formation, glycosylation and membrane attachment (see Introduction 1.8.1).

HEK 293 cells have been used for decades for the heterologous expression of proteins due to their ability to rapidly divide, produce human protein post-translational modifications and they are easily transfected (Thomas & Smart, 2005). The HEK 293 genome has also been elucidated allowing the potential future genetic modification and optimisation of a CFPS platform derived from its lysate (Y. C. Lin et al., 2014). One of the most common post-translational modifications glycosylation, has important roles in protein folding, stability and function. Significant differences exist in glycosylation patterns and structures between yeast, mammalian, insect and malaria cell types. Although mammalian cells share much of the same glycosylation machinery there can be significantly different glycosylation patterns observed between them (Böhm et al., 2015; Croset et al., 2012). As such HEK 293 cells have been intensively used to examine viral surface proteins (Bayati et al., 2021; Le Ru et al., 2010).

Coronaviruses (CoVs) are zoonotic viruses, able to infect both human and animal cells

causing a variety of diseases that range in their degree of severity (Howley, Peter M.; Knipe, David M.; Whelan, 2020). CoVs can be divided into four genera which include alpha, beta, gamma and delta coronaviruses (F. Li, 2012). Beta-coronaviruses have accounted for all the major CoV outbreaks (see Figure 3.16 (A)) including those producing severe acute respiratory syndrome coronavirus (SARS-CoV) and Middle East respiratory syndrome coronavirus (MERS-CoV) (Petrosillo et al., 2020). The novel coronavirus SARS-CoV-2 isolated originally in China in 2019, was found in patients experiencing symptoms of severe pneumonia and has accounted for at the time of writing, almost 3M worldwide deaths(WHO, 2021). The sequencing of the SARS-CoV-2 genome revealed a high degree of conservation with SARS-CoV RaTG13, originally isolated from a cave containing high numbers of bats, pointing to a potential reservoir for the SARS-CoV-2 outbreak(Huang et al., 2020). SARS-CoV-2 and future viral outbreaks of as yet unknown origin represent a serious ongoing health challenge for governments going forwards in the 20th century. The SARS-CoV-2 virus contains four structural proteins; an envelope protein (E), membrane protein (M), nucleocapsid protein (N) and the spike protein (S) (Astuti & Ysrafil, 2020). High antibody titres directed against the N and S protein have been reported in patients who have recovered from SARS-CoV-2 infection (Burbelo et al., 2020; Ravichandran et al., 2020).

The N protein is critical for the binding of viral RNA and packaging of the SARS-CoV-2 genome. However, large parts of the N protein are intrinsically disordered making its structural characterisation difficult (Cubuk et al., 2021). The N protein is split into five domains that include: the N-terminal domain (NTD), an RNA binding domain (RBD), a linker region, a dimerisation domain (DD) and a C-terminal domain (CTD) (see Figure 3.16 (E)) (Zeng et al., 2020). However, the majority of vaccine technologies currently deployed for country-wide immunisation programs against SARS-CoV-2 rely on the S protein to elicit an immune response. These platforms include, the Oxford-AstraZeneca adenoviral vector vaccine, AZD1222, the

Pfizer-BioNTech mRNA encapsulated vaccine BNT162 and the Novavax subunit vaccine NVX-CoV2373. Viral entry into host cells is via the interaction of the S-protein, receptor-binding domain (RBD) with the angiotensin-converting enzyme 2 (ACE2) (see Figure 3.17 (B)) (Cuervo & Grandvaux, 2020). Antibodies blocking this molecular interaction prevent viral invasion of cells and consequently establishment of disease (Yu et al., 2020). Whilst these vaccines have so far proved highly effective at reducing deaths associated with SARS-CoV-2, increasing viral surveillance has identified a number of SARS-CoV-2 emerging variants (see Figure 3.17 (C)) that have the potential to reduce vaccine effectiveness due to mutations within the S-protein(Karim, 2021).

The ability to rapidly produce viral structural proteins can aid in ongoing pandemic preparedness and is crucial in assessing continual antibody reactiveness. CFPS therefore, has the ability to aid in the immune surveillance of current and emerging zoonotic viruses, through HTP antigen production and serum testing. The recent emergence of COVID-19 enabled the development, optimisation and ultimate expansion of the human element of the Dual-IVT assay, beyond what was originally intended. This system was converted into a CECF protein synthesis, in a TX-TL format, to explore scaled production of SARS-CoV-2 proteins. The development and optimisation of the human CFPS system was required to increase translation efficiency. The translocation of protein into endogenous microsomes was confirmed using sfGFP fused to an N-terminal signal peptide and later adapted for the production of the RBD from the S-protein. Both the SARS-CoV-2 N-protein and the RBD domain from the S-protein of SARS-CoV-2 (NCBI NC_045512.2) were then used to evaluate the developed CFPS system. The resulting technology could enable the production and purification of viral proteins applied to other proteins of interest.

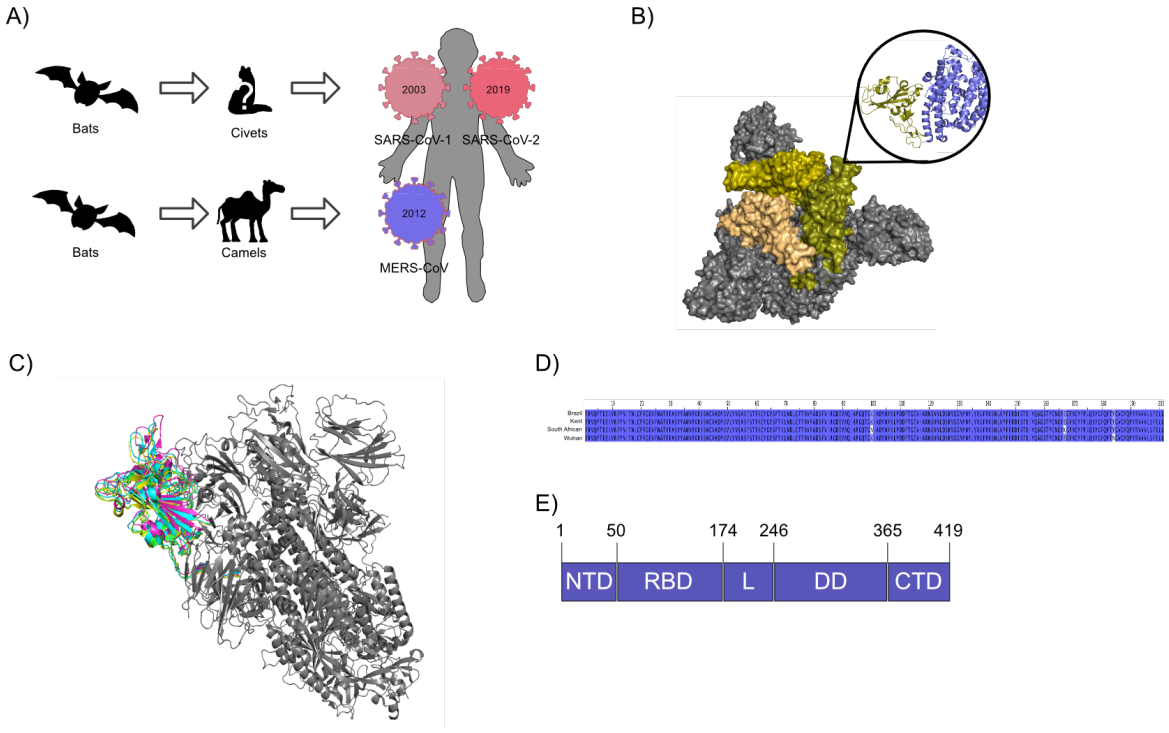

Figure 3.16: Coronaviruses

A) Bats are currently theorised to be reservoirs of three betacoronaviruses that cause serious disease in humans. These include SARS-CoV, SARS-CoV-2 and MERS. With respect to SARS-CoV (2003) horseshoe bats were identified as the viral reservoir together with civets present in live markets as the direct source of human infection (L.-F. Wang & Eaton, 2007). Although there is a high degree of evidence pointing to bats as the reservoir for the emergence of SARS-CoV-2 (2019), currently the animal with direct human contact is unknown (Wacharapluesadee et al., 2021). MERS (2012) is known to have also originated in bats with camels acting as the direct source of human infection(Omrani et al., 2015). **B**) The molecular surface of the S-protein of SARS-CoV-2 forms a trimeric structure (Grey), containing three RBD-domains (dark-yellow, yellow and green-yellow) at the top of the protein(PDB 7bnm). The RBD interacts with the ACE2 receptor to gain entry into cells, this interaction is shown for one RBD (dark-yellow) of the S-protein in a magnified circle with the ACE2 receptor (purple) (PDB 6vw1) (The PyMOL Molecular Graphics System, Version 2.0 Schrödinger, LLC). **C**) The RBD of the SARS-CoV-2 S-protein share high-degrees of structural similarity between varients(see Table 4.3). The molecular structure of the SARS-CoV-2 S-protein (Grey) (PDB 6x2a) with the secondary structure of the RBD of four SARS-CoV-2 RBD variants aligned to the 'Wuhan' reference strain Genbank_MN908947 (PDB_6X2A) (green) (PDB 6x2a), the 'Brazil' variant B.1.1.28 (pink) (PDB_97lww), the 'Kent' variant B.1.1.7 (PDB_7lwv) (cyan) and the 'South African' variant B.1.351 (PDB_7lyp) (yellow) (The PyMOL Molecular Graphics System, Version 2.0 Schrödinger, LLC). **D**) The S-protein RBD variants were aligned using the Muscle alignment tool (Edgar, 2004) and show small single or double residue mutations compared to that of the 'Wuhan' variant (NCBI YP_009724390.1). The 'Brazil' (NCBI 33758838), 'Kent' (NCBI 33758838/1-201) and 'South African' (SA) (NCBI 33758838/1-201) variants all contain an N184Y mutation. In addition the 'South African' variant contains additional E167K and K100N mutations. **E**) The five domains of the nucleocapsid from SARS-CoV-2; N-terminal domain (NTD), RNA binding domain (RBD), linker region (L), disordered domain (DD) and C-terminal domain (CTD) are indicated including their respective residue boundaries.

3.4.1 Transition From Batch to Continuous, TX-TL

The development of mammalian-based CFPS systems derived from translationally active lysate has evolved considerably since the use of rabbit reticulocyte lysate over 50 years ago(A. M. Jackson, 2004). This has enabled the production of therapeutics (M. Stech et al., 2017), investigation of gene circuits (Contreras-Llano et al., 2020), production of VLPS (Spice et al., 2020)and serology based studies(França et al., 2017). The use of a variety of translationally active lysates for CFPS systems derived from CHO (Dondapati, Pietruschka, et al., 2019; Hunt et al., 2020; Thoring et al., 2017; Tran et al., 2018) and HeLa (Bergamini et al., 2000; Mikami et al., 2006) cells have been well defined. Yet those produced from HEK 293 cells have not received nearly as much attention. However, their extensive use in protein production, ease of genetic manipulation and rapid growth in suspension makes them a good alternative to HeLa and CHO-based CFPS systems. The HEK 293F line was chosen for the production of lysate due to its rapid growth in suspension and ease of culture(Portolano et al., 2014). The CrPV-IGR IRES was used to drive the expression of sfGFP that could be detected after a 24-hr incubation in the reaction mixture (see Figure 3.17 (B)).

3.4.2 Optimisation of mRNA Synthesis

The efficiency at which genes are transcribed can have a significant impact on expression yields, often driven by strong, and in some cases, inducible promotor systems (Briand et al., 2016). CFPS environments unlike cellular environments can be uniquely modified to attenuate gene expression. Although, ultimately this will be a balance between considerations for transcription and translation (Introduction 1.8.1). Therefore four factors were chosen based on their perceived impact on mRNA synthesis: plasmid concentration, magnesium concentration, T7 RNAP concentration and the T7 bacteriophage RNAP promotor sequence (see Figure 3.18).

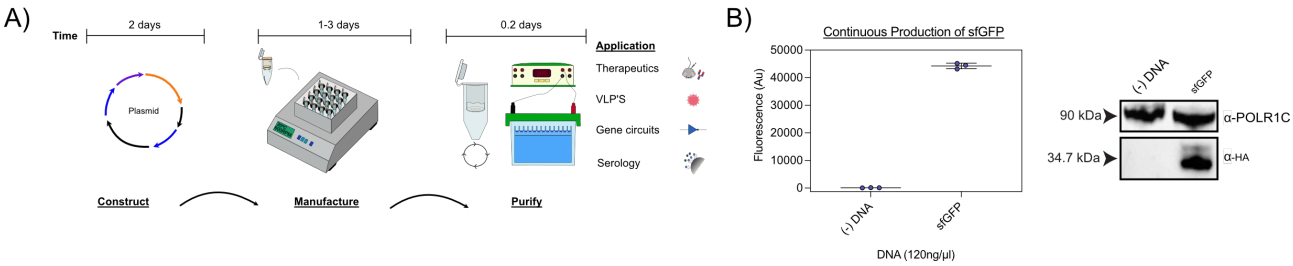

Figure 3.17: Production of a Human, Continuous Exchange CFPS System

Each optimisation step was tested in the order shown with initial reaction conditions set at endpoint of 24hrs, a temperature of 30°C in a continous TX-TL format. After each optimisation step the reaction was adjusted accordingly. Each data point on the graph is a single biological replicate containing an average of three technical repeats. **A**) Continuous exchange CFPS systems can be adapted to a HTP setup to enable the rapid purification of complex proteins for a variety of indicated functions. Timescales are approximate based on heterologous cell-based mammalian recombinant technologies and purification strategies. **B**) The production of sfGFP in a continuous exchange CFPS TX-TL system using human cellular lysate derived from HEK293F cells was compared to a CFPS reaction where plasmid was omitted from the reaction. The sfGFP protein was detected directly by fluorescence and by western blot using POLR1C as a loading control. Here the reaction was setup as detailed in Material and Methods 2.4.2 however the magnesium concentration in the reaction compartment was set at 3.9mM. Each point on the graph indicates one biological repeat that is an average of three technical replicates.

Plasmid DNA containing the sfGFP gene was added to a reaction instead of mRNA due to the stability of DNA over RNA. This allowed a continual supply of mRNA for translation until transcription could not be sustained. Whilst 2µg/µl of plasmid DNA produced the highest sfGFP output, achieving these high concentrations of DNA becomes impractical. Therefore a concentration of 0.9µg/µl was decided upon for future reactions. A T7 RNAP promotor sequence upstream of the IRES was inserted to efficiently drive transcription through the addition of T7 RNAP. The concentration of polymerase and magnesium within the reaction chamber was optimised using similar methodologies described by others (Thoring et al., 2017). T7 RNA polymerase has been shown to bind a single magnesium ion that is essential for its function (Lykke-Andersen & Christiansen, 1998) however, although magnesium is required for mRNA stabilisation at high magnesium concentrations, this can destabilise translation. The concentrations of both T7 RNAP and magnesium in the reaction chamber were found to be 2U/µl and 24mM respectively. Finally, the sequence directly after the T7 bacteriophage RNAP promotor was modified based on recently discovered sequence regions directly after the promotor

that has been shown to enhance transcription efficiency (Conrad et al., 2020). This modified eight base 'spacer' region between the promotor and the start of the IRES sequence increased sfGFP output by over two-fold and led to the creation of the pHLH2.0 vector series, used in all subsequent reactions.

The final reactions conditions from this optimisation strategy resulted resulted in a modified protocol as detailed in Material & Methods 2.4.2. In brief this meant the use of the pHLH2.0 plasmid containing the CrPV-IGR IRES followed by a coding sequence and a poly(A) tail. A final plasmid concentration within the reaction chamber of 900ng/µl, a T7 RNAP final concentration of 2U/µl and a final magnesium concentration within the reaction chamber of 24mM.

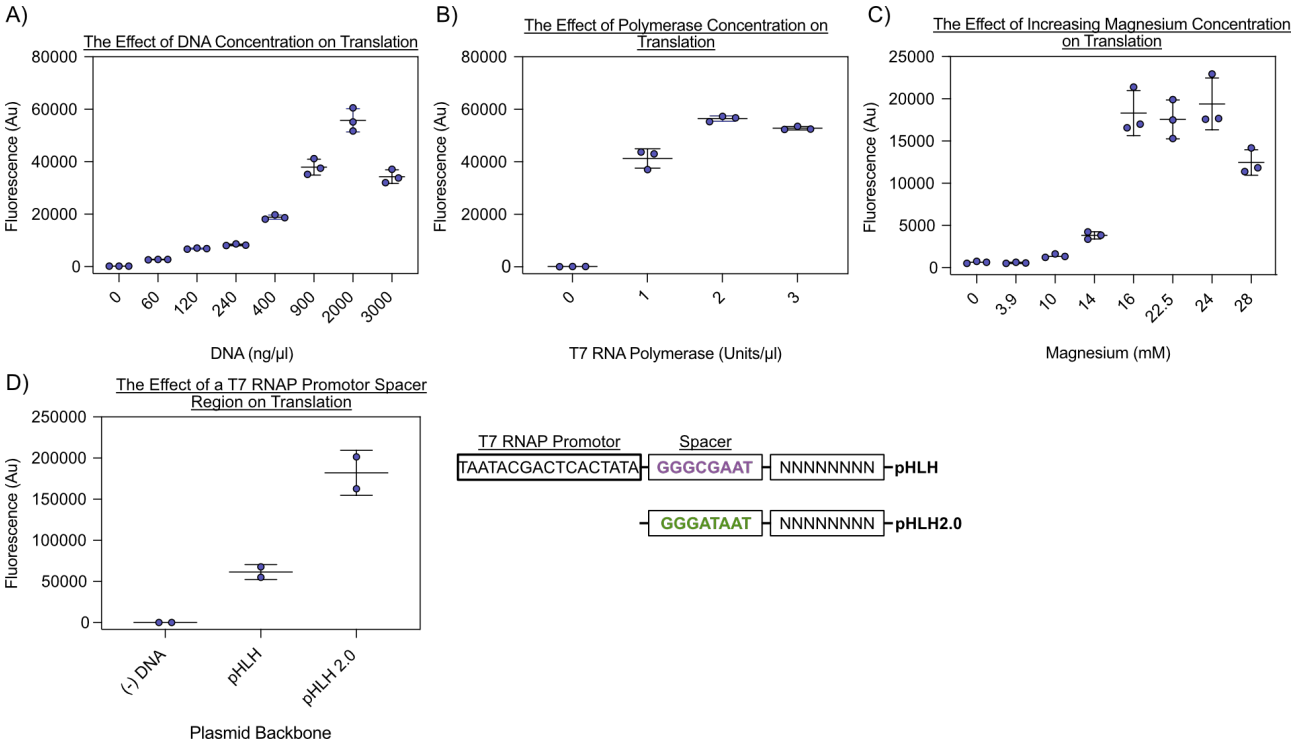

Figure 3.18: Modification of Factors Influencing mRNA Synthesis

A) An increase in plasmid concentration then increases sfGFP synthesis up to 2000ng/µl. **B**) The addition of T7 RNAP enables the production of sfGFP mRNA. This peaks with the addition of 2U/µl of polymerase. **C**) Increasing the concentration of magnesium within the reaction chamber between 16-24mM increases sfGFP yields. **D**) The modification of the eight base spacer region between the T7 RNAP and the start of the IRES increases sfGFP production > two-fold (Conrad et al., 2020).

3.4.3 Optimisation of Protein Synthesis

Approximately 30% of the eukaryotic proteasome requires translocation to the ER(Keenan et al., 2001); regulation of the state of protein folding within this space is controlled by a complex signal transduction pathway known as the unfolded protein response (UPR). Three membrane bound sensors spanning the ER membrane; activating transcription factor 6 (AFT6), inositol-requiring enzyme 1 (IRE1) and protein kinase RNA-like endoplasmic reticulum kinase (PERK) regulate the cell's response to ER stress that will result in the down-regulation of protein synthesis. During cellular stress each of the three sensors change their oligomerisation state, which causes autophosphorylation of their cytoplasmic domains as a result of the dissociation of BiP (Hetz et al., 2020).

During the isolation of cellular lysate and the overexpression of protein in CFPS reactions translation repression may occur due to the presence of stress factors (Malm et al., 2020). Caspase inhibitors have been shown to enhance translation efficiency in in CFPS reactions using CHO lysate (Thoring et al., 2017). Caspases are an evolutionary conserved family of aspartate-specific cysteine proteases involved in apoptosis. Here they cleave eukaryotic translation initiation factor 4 G (elF4G) and eukaryotic initiation factor 2 elF2α. The caspase-3, 6, 8 and 10 have been reported to down-regulate protein synthesis (Marissen et al., 2000).

To examine this in the context of a HEK based CFPS system, inhibitors of enzymes involved within the UPR cascade were assessed as to their ability to enhance translation efficiency. Ceapin-A7 has been reported to be a highly specific inhibitor of ATF6α(Torres et al., 2019). When the compound was titrated from 0µM to 30µM in CFPS reactions, there was a >50% increase in protein synthesis at 1µM. Next, two irreversibly binding caspase inhibitors were added to CFPS reactions, caspase-3 specific inhibitor Z-DEVD-FMK and the pan-caspase inhibitor Z-VAD-FMK. When used singularly, the addition of each caspase inhibitor resulted in a doubling of sfGFP synthesis however, when combined this resulted in a 2.3-fold increase

in sfGFP synthesis. Lastly, the PERK specific inhibitor GSK606414(Ganz et al., 2020) was tested in the same way. Its addition resulted in no significant difference in sfGFP yields that was detected at an inhibitor concentration of 10µM. This lead to the use of ceapin A-7 at a concentration of 1µM and the caspase inhibitors Z-VAD-FMK and Z-DEVD-FMK at 30µM in all subsequent reactions.

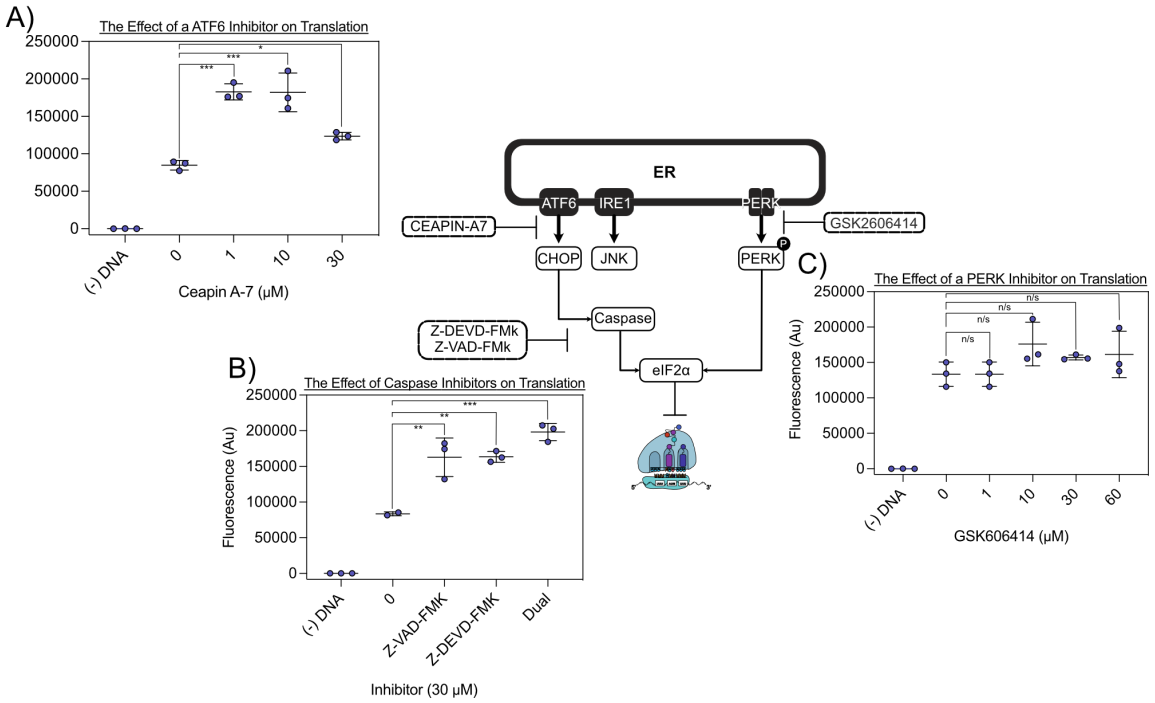

Figure 3.19: Inhibiting the UPR

The three UPR sensors, ATF6, IRE1 and PERK span the membrane of the ER. Each point on the graphs indicates a biological repeat, which is an average of three technical replicates. For each data set a one-way Anova statistical test was performed to ascertain significance compared to the control condition and indicated, where there is no indication there is no significant difference. (The P-values are indicated: ≤0.05 *, ≤0.01 **, ≤0.001 *** and ≤0.0001 ****). **A**) The autophosphorylation of ATF6 causes it too translocate to the Golgi where it is processed releasing its cytoplasmic domain. This further translocates to the nucleus and initiates transcription of proteins involved in the UPR e.g. C/EBP homologous protein (CHOP). Addition of ceapin-A7 resulted in an increase of sfGFP yields at a concentration of between 1-10µM. **B**) The up-regulation of CHOP expression leads to an increase in Tribbles homolog 3 (TRB3), activating caspases 3, 8 and 9. The caspases 3, 6, and 10 have all been reported to inhibit elF2αand elF4G. Addition of the caspase-3 inhibitors: (Z-DEVD-FMK) and pan-caspase inhbitor (Z-VAD-FMK) caused an increase in sfGFP synthesis. However, when combined (Dual) both inhibitors resulted in a 2.3-fold increase in sfGFP synthesis. **C**) During the accumulation of misfolded protein within the ER, BiP dissociates from PERK due to its higher affinity for unfolded proteins. This causes autophosphorylation of the cytoplasmic PERK domain and leads to the phosphorylation of elF2α, reducing cellular translation. Application of the PERK specific inhibitor, GSK606414 (Ganz et al., 2020) had no effect on sfGFP synthesis.

3.4.4 Protein Translocation into Microsomes

The gentle lysis of certain types of mammalian or insect cell sources, results in the disruption of cellular ER forming microsomes within the lysate. These microsomes have been shown to contain much of the post-translational machinery required for the formation of disulphide bonds, glycosylation and membrane attachment (see Introduction 1.8.19). Endogenous microsomes or substituted microsomes in CFPS reactions have been shown to translocate protein inside when fused to an N-terminal signal peptide. The melittin signal peptide, as reported by others was assessed for its ability to translocate sfGFP into endogenous HEK 293F microsomes which were then separated from the CFPS reaction supernatant (Dondapati, Lübberding, et al., 2019; Hunt et al., 2020; M. Stech et al., 2017; Thoring et al., 2016). To separate microsomes the reaction mixture was isolated and centrifuged at 16,000 RCF for 15min and the supernatant was removed. The pellet was washed and resuspended back to the original reaction volume (see Figure 3.20 (A)). The isolated supernatants and pellet fractions were then assessed in three ways; firstly a visual inspection by a blue light (470nm) (see Figure 3.20 (B)), by fluorescence detection (see Figure 3.20 (C)) and finally by western blot (see Figure 3.20 (D)). The fusion of the melittin signal peptide to the N-terminal of sfGFP resulted in its translocation into isolated microsomal pellet fractions. This was then compared to sfGFP that did not contain a signal peptide, in this case sfGFP was not detected in the isolated microsomal pellet fractions.

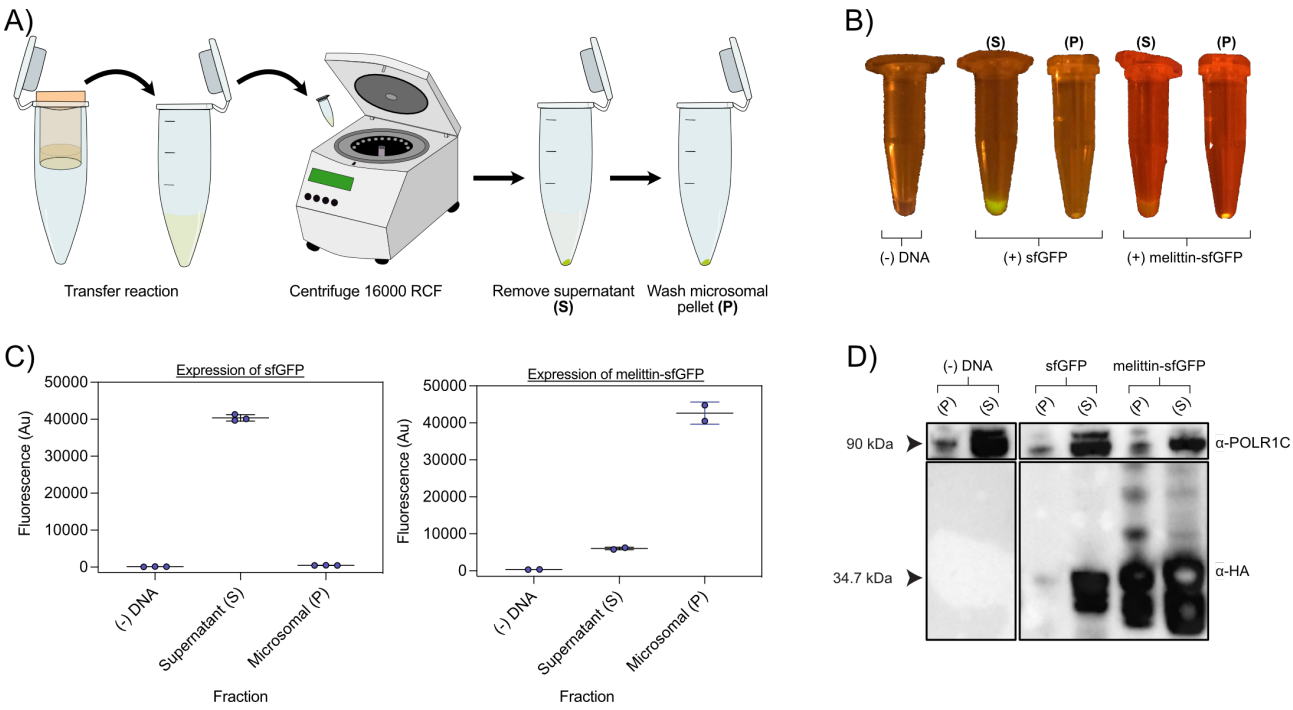

Figure 3.20: Translocation into Microsomes

The reaction conditions used here lead on from those established in Figure 3.19. Each point on the graphs indicates a biological repeat, which is an average of three technical replicates. **A**) A generalised procedure for the isolation of microsomes at the end of a CFPS reaction. **B**) The use of a blue light transilluminator allowed visual inspection of the isolated supernatant (S) and microsomal pellet (P) fractions in the presence and absence of a signal peptide. **C**) The sFGFP isolated as described in (A) was detected for each fraction using fluorescence as a measure of GFP for a reaction with and without the melitting signal peptide. **D**) The detection of sfGFP in the presence and absence of a melittin signal peptide, fractionated as described in (A) and detected using an anti-HA antibody.

3.4.5 Standardising the Purification of Proteins from CFPS Reactions

The purification of proteins away from the milieu of the lysate, protein rich environment is advantageous for the purposes: enzymatic characterisation (Berg JM, Tymoczko JL, 2002), structural biology (McPherson & Gavira, 2014) and vaccinology (M. Wang et al., 2016). There are a wide variety of fusion tags used for affinity purification. These allow a target protein to be isolated from a containing rich protein mixture (Costa et al., 2014; C. L. Young et al., 2012). The twin StrepII tag has been reported to allow efficient, one-step purification strategies from small volumes. Therefore, this was C-terminally fused to sfGFP to assess this tag's purification efficiency (Ivanov et al., 2014).

The purification of sfGFP, expressed in 50µl reactions for 24-48-hrs was assessed for purity

and relative yields. Almost completely pure protein was isolated from the purification of sfGFP at each point. However, more noticeable was the dramatic increase in protein yields that resulted in a 3.2-fold increase in sfGFP when expressed over 48hrs (see Figure 3.22 (A)). Next, sfGFP fused to an N-terminal melittin signal peptide was expressed over 48hrs. On completion, microsomes were removed from the the reaction mixture and sfGFP liberated through chemical lysis. Elution of sfGFP bound to StrepTactin resin required the presence of 0.1% Triton x-100 to allow maximum recovery. When analysed the elution fraction contained a single major protein band corresponding to the size of sfGFP.

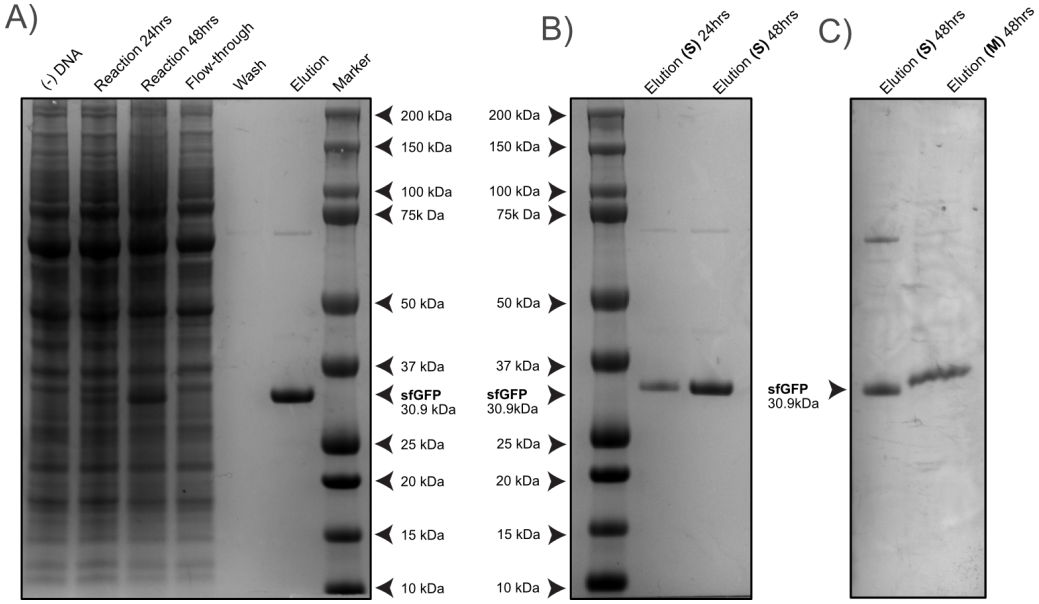

Figure 3.21: The Purification of sfGFP Within CFPS Reactions
A) The expression of sfGFP (containing no signal peptide) over 24-48hrs. The flow-through, wash and elution fractions are only shown here for the purification of sfGFP from a 48hr reaction in this coomassie stained gel. **B**) A comparison of the two elution fractions from the purification of sfGFP from a 24hr and 48hr CFPS reaction. **C**) The purification of sfGFP fused to the melittin signal peptide from either supernatant (S) or microsomes (M) from a CFPS reaction incubated over 48hrs. The band for the (M) fraction is distorted due to the presence of Triton x-100 in the elution fraction.

3.4.6 The Production of the N and RBD of SARS-CoV-2

The production of the nucleocapsid and RBD from the spike protein of SARS-CoV-2 was used for testing and development of the optimised human CFPS system. These two proteins were selected based on their respective complexities. The spike protein of SARS-CoV-2 has been

shown to contain a high quantity of glycosylation (Walls et al., 2020); viruses often use these glycan structures for immune evasion through shielding from antibodies (Helle et al., 2011; Marth & Grewal, 2008). Through antigenic drift these glycoyslation patterns may alter over time reducing antibody binding efficacy (Hütter et al., 2013). Analysis of the spike protein has shown that the RBD contains two N-linked glycosylation sites at positions N331 and N343. Both of which have been reported to contain fucosylated glycans at their respective positions (Watanabe et al., 2020). The RBD also forms three disulphide bonds at positions C336-C361, C391-C525, C379-C432 that stabilise its β-sheet core and a fifth at C480-C488 (Lan et al., 2020). The production of the RBD in cell-free reactions requires the presence of microsomes for for these protein modifications to occur. Conversely the nucleocapsid is reported to not contain any disulphide bonds or glycosylation and is easily produced in *E. coli* heterologous expression systems (Pei et al., 2005). Therefore the production of this protein does not require the presence of microsomes in the lysate.

To monitor the expression levels of the nucleocapsid and RBD, sfGFP was fused to the C-terminus of both proteins. The proteins were then produced in 50µl reactions over 48-hrs. The yields of each SARS-CoV-2 protein were compared to sfGFP production(see Figure 3.23 (A)). Whilst the nucleocapsid and sfGFP proteins were expressed at similar levels, the RBD, possibly due to its increased complexity, did not express as well(see Figure 3.22 (A)). The purification of each protein was attempted using the twin StrepII tag, in combination with a developed HTP purification strategy. Each of the three expressed proteins could then be detected at their respective sizes by western blot (see Figure 3.22 (B)). In addition both the purified sfGFP and nucleocapsid proteins were visible on a coomassie stained gel at 30.9kDa and 76.8kDa respectively. However, the presence of the RBD on this gel is less clear with a faint band observed just above the 50kDa mark that could be indicative of the RBD based on its predicted molecular weight of 53kDa (see Figure 3.23 (B)). Finally, patient serum collected from

individuals known to have recovered from COVID-19 was used to detect both the nucleocapsid and RBD proteins. Surprisingly only the nucleocapsid could be detected by western blot using patient-111 serum (see Figure 3.23 (C)). Whilst this shows the successful production of two COVID-19 proteins, there is still a question as to whether the RBD is folded correctly and all the post-translational modifications that have been reported for it have been achieved here.

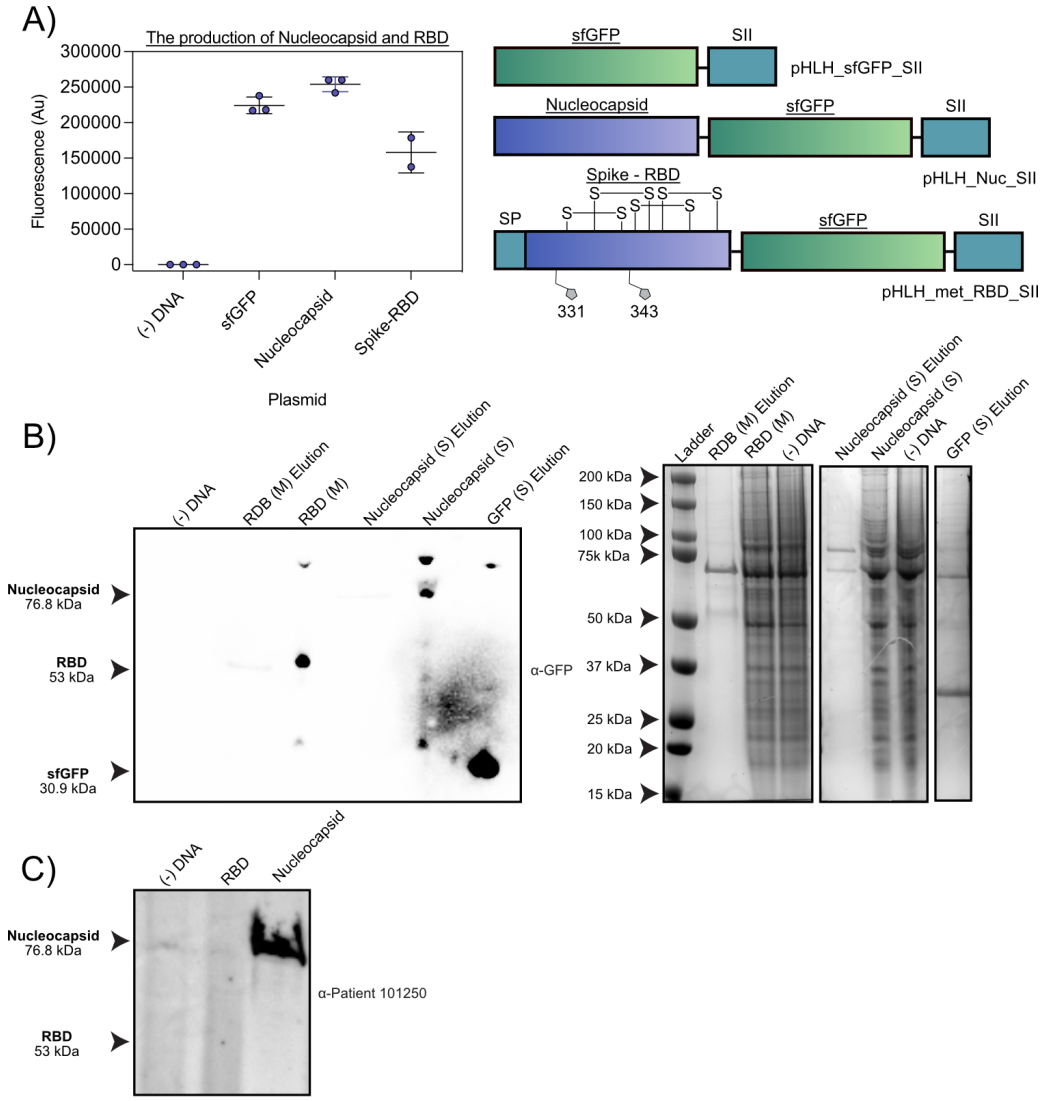

Figure 3.22: The Production of SARS-CoV-2 Structural Proteins

A) The detection of the SARS-CoV-2 nucleocapsid and RBD proteins fused to sfGFP and compared to sfGFP. The schematic shows each expression cassette. In the case of the RBD, glycosylation sites are indicated by grey pentagons, disulphide bonds shown by S-S and the (SP) indicates the presence of the melittin signal peptide. Each point on the graphs indicates a biological repeat, which is an average of three technical replicates. **B**) On the left a western blot indicating the presence of the respective proteins as described above, each protein is shown with its predicted molecular weight. The (M) indicates the presence of a microsomal fraction whereas (S) indicates the presence of supernatant taken from a reaction that has been fractionated to isolate microsomes. On the right the corresponding coomassie stained gel. **C**) Serum from an adult (101250) known to have recovered from COVID-19 was used for the detection of the purified nucleocapsid and RBD sfGFP fusion proteins in a western blot.

3.4.7 Summary

The emergence of COVID-19 provided an opportunity to adapt and develop the human component of the Dual-IVT assay, initially produced for the purposes of antimalarial drug counter-screening. CFPS offers the ability to rapidly produce proteins devoid of the usual cellular constraints in a miniaturised setup using a HTP workflow. Therefore, these systems have been particularly useful in the synthesis of large libraries of potentially cytotoxic proteins for characterisation based studies (Perez et al., 2016). Although there are a wide variety of cell types that can be used to produce translationally active lysate, mammalian based systems are of interest due the lysates ability at producing post translational modifications such as disulphide bonds but in particular glycosylation (see Introduction 1.8.10). Production of proteins is particularly prominent in the biopharmaceutical industry as protein based therapeutics or targets, like membrane proteins are often difficult to express using standard heterologous systems (Khambhati et al., 2019). The production of SARS-CoV-2 structural proteins as well as many other viral proteins for the purposes of research and development centre around the use HEK 293 cells. As viral structural proteins are often highly glycosylated, expressing them in other mammalian-based systems may produce unintended glycan patterns. Therefore, a novel semi-HTP CFPS system was created derived from translationally active HEK 293F lysate, a cell type that has not been used in the context of cell-free systems. The purification of proteins away from the highly concentrated protein environment within CFPS systems has not been fully explored with mammalian based systems therefore, a standardised workflow was attempted for the purification of both of these proteins that could be applied to the purification of others produced in this context. To achieve a HTP CFPS system capable of producing proteins at 'scale' sfGFP was used as a reporter of translation, this allowed the development and optimisation of the system in a variety of areas to increase the overall translation efficiency. This included testing a recent development in synthetic T7 RNAP promotor efficiency.

In TX-TL CFPS systems a T7 RNAP promotor sequence is used to initiate transcription through the binding of T7 RNAP to the promotor sequence. Through the modification of the immediate downstream sequence the efficiency of this interaction can be modified. Although this has been explored in a cellular context (Conrad et al., 2020), this was the first time this was looked at for the purposes of CFPS. The exploration of which significantly increased translation output through increased production of mRNA. Transcription is then terminated using a T7 RNAP terminator sequence that forms a hairpin structure in the mRNA (Hartvig & Christiansen, 1996). However, T7 RNAP is prone to read through resulting in longer transcripts almost 20% of the time Revised transcription map of the late region of bacteriophage T7 DNA. This may interfere with the efficiency at which these mRNA transcripts are translated, thereby effecting overall protein yields within a system. Mairhofer et al were able to increase the efficiency at which T7 RNAP terminates transcription through the incorporation of different termination sequences fused together resulting in a 99% termination efficiency (Mairhofer et al., 2014). As this has not been explored in the context of CFPS it would be interesting to see if this could boost translation efficiency. Exploration of transcription initiation and termination highlights the versatility of CFPS as a tool in synthetic biology for rapidly testing genetic elements without the need for cell based studies.

The production of many complex surface proteins, including viral proteins requires the presence of endogenous microsomes that provide a contained environment for post-translational modifications to occur. To examine this, an N-terminal melittin signal peptide was validated for its effectiveness at translocating sfGFP into microsomes within the HEK 293F lysate, further confirming the conservation of the co-translational pathway between eukaryotes. This also reaffirmed previous work using CHO cellular lysate (Thoring et al., 2017) but also more recently its use in conjunction with *P. falciparum* lysate (see Figure 3.1.5). When unfolded protein accumulates within the lumen of the ER the three branches of the UPR sensory path-

way activate to reduce cellular translation and increase the expression of chaperones to assist folding. Translation repression subsequently occurs, predominantly though the phosphorylation of eIF2α through the PERK pathway, however the use of the CrPV IRES circumvents this initiation factor by directly recruiting the ribosome by-passing this mechanism of regulation (see Introduction 1.8.13). Indeed when the PERK specific inhibitor, GSK 606414 was used no significant difference in translation could be seen in line with what was expected.

Further attenuation of the CFPS environment through the addition of well characterised inhibitors of caspase proteins were trialled for their effectiveness at increasing overall translation efficiency. Whilst, caspases-3, 8 and 9 have all been reported to inhibit elF2α they also have the potential to degrade any protein synthesised, being cysteine-aspartic acid proteases (Brentnall et al., 2013). However, through their inhibition the levels of protein synthesis in a reaction could be increased within the CFPS environment. The ability to target these caspases within the HEK lysate environment may allow a similar workflow using *P. falciparum* lysate. Here, caspase homologues, termed meta-caspases have remained poorly understood but using this setup it may be possible to probe the malaria lysate environment for crossover inhibitors (Kumar et al., 2019). This would not only confirm their presence but potentially open a further avenue for antimalarial drug discovery. Finally and perhaps the most interesting observation here was the ability to attenuate the levels of translation within the CFPS environment using ceapin-A7, a specific inhibitor of ATF6. During ER stress ATF6 is activated, translocates to the Golgi where it is cleaved releasing a cytosolic transcription factor that induces the expression of chaperones that leads to ER expansion increasing the folding capacity within it (Hetz, 2012). However, ATF6 has now been shown to reduce translation within the cell when overexpressed, this was attributed to an increase in phosphorylation again of elF2α (Spaan et al., 2019). During the isolation of the HEK cell lysate and its use in the artificially created environment of a CFPS reaction it is exposed to temperature shock, introduction of reactive oxygen species,

the destructive forces of cell lysis and a massive up-regulation of protein synthesis (Islam et al., 2017). This resulting stress can activate sensors of the UPR such as ATF6 reducing protein synthesis. Through the use of a specific inhibitor of ATF6 within the lysate this inhibition of protein synthesis can be alleviated. It still remains to be seen the exact mechanism by which this is accomplished in the context of CrPV-IGR IRES induced protein expression as this by-passes the normal elF2α mode of translation initiation.

These modifications in conjunction with general translation optimisation and validation steps allowed the creation of a novel HEK cell derived CFPS system that was applied to the production of the SARS-CoV-2 nucleocapsid protein and the RBD from the spike protein, each selected for its relative complexity. The two proteins were successfully produced and the nucleocapsid validated against the serum of an adult previously infected with SARS-CoV-2. The rapid, direct production of useful and potentially hard to express proteins have the ability to allow point of expression protein synthesis to areas where large culturing facilities may not be available. Indeed it has been possible to lyophilise bacterial cellular lysate, rehydrate it with water and use it in the context of CFPS (Smith et al., 2014). It therefore remains to be seen if this would be possible with more complex mammalian cell lysate in addition to preserving the functionality of the microsomes within it. Initially CFPS was to probe cellular circuits and fundamental mechanisms of protein synthesis (Nirenberg, 1964), here to we have been able to probe cellular circuits advancing our understanding of the mechanism of translocation into the ER and the regulation of cellular translation by the ER in the form of the UPR pathway.

Chapter 4

Conclusions & Future Work

4.1 The Dual-IVT, its Significance & Beyond...

The development of resistance to frontline antimalarials by *P. falciparum* represents an increasing challenge for those living in malaria endemic areas. There is a necessity to rapidly increase the discovery and development of new compounds with novel MoAs to ensure treatment efficacy. Translation is a fundamental process within all stages of the parasite's complex life cycle, the targeting of which by a compound may not only alleviate the clinical symptoms of malaria but also block its transmission. The introduction of HTP assays capable of dissecting translation in malaria mostly centre around recreating a single enzymatic pathway *in vitro* that can be probed for inhibition through the use of available compound libraries(Fang et al., 2015). If a compound is thought to inhibit translation, it is often assessed in culture using S-35 radio labelling however, whilst being time consuming this method has been reported to give false positives(Sheridan et al., 2018; W. Wong et al., 2017). An alternative approach that can equally be adapted to a HTP format uses the translationally active lysate from *P. falciparum* to screen libraries of inhibitors for activity. The recreation of parasite translation in isolation from all the other cellular processes has the potential to increase the speed of drug development.

4.1.1 What Does This Mean for Malaria Drug Screening?

The isolation of translationally active lysate from the most virulent malaria parasite, *P. falciparum*, containing the 80S ribosome was successfully reconstituted into an *in vitro* translation assay (see Results 3.1). This assay was validated through the detection of known, well-characterised broad spectrum translation inhibitors as well as malaria-specific inhibitors. Malaria parasites have two main sites of protein translation, the cytoplasm and apicoplast. The addition of two specific inhibitors of the apicoplast ribosome were shown not to effect translation in the assay, indicating the presence of translationally active lysate from the cy-

tosol of the parasite. The assay was developed so that malaria lysate could be switched out for translationally active human lysate allowing prioritisation of malaria specific inhibitors (see Results 3.1.2). The sensitivity of the assay was such that dose response curves could be calculated accurately for any compound assayed provided maximum inhibition could be achieved. This sensitivity and high accuracy of reporting meant that the MoA for halofuginone could be probed. By using amino acid increasing concentrations of the amino acid L-proline, the EC_{50} of halofuginone was progressively shifted, reducing the compound's potency (see Results 3.1.6). This process could be used to search for other aaRS inhibitors providing they can be outcompeted by their constituent amino acid. Most crucially the creation of a Dual-IVT assay and the development of a HTP workflow, culminated in the screening of the Pathogen box, a library of over 400 bioactive compounds (see Results 3.1.7). Although there have been a small number of malaria IVT assays that have been reported, this is the first that combines this level of sensitivity and the ability to counter-screen using human lysate. This could therefore allow the rapid selection and progression of compounds that solely inhibit parasite translation over its human host. Deciphering the molecular targets of current and next generation antimalarial compounds is crucial for drug development. The Dual-IVT assay shows that it is possible to detect compounds that target the malaria translation apparatus over that of humans.

4.1.2 The Pursuit of Malaria Translation inhibitors

There are currently no malaria specific translation inhibitors used as frontline antimalarials other than mefloquine (see Introduction 1.3.3). However, recently there has been a resurgence in the discovery of potent malaria selective translation inhibitors that could result in a new generation of antimalarials. The discovery of the DDD107498, a malaria specific eEF2 translation inhibitor that targets all stages of the human part of the malaria life cycle highlights the importance of pursuing translation inhibitors as next generation antimalarials (see Introduction

1.5.5). The DDD107498 compound is a highly potent antimalarial with efficacy in the nano molar range as determined by the GIA. The Dual-IVT assay was able to effectively identify this compound as a potent malaria specific translation inhibitor with an efficacy comparable to cycloheximide. Eukaryotes share much of the same translation machinery, the divergence of malaria eEF2 from humans makes it amenable to inhibition even though they share just over 67% sequence identity. However, whilst being divergent enough from human eEF2, 1685 genome sequences from *P. falciparum* field isolates reveal a high degree of eEF2 conservation between malaria strains(Baragaña et al., 2015). In fact the core translation machinery of *P. falciparum* strains in terms of ribosome components, tRNAs and aaRSs show little divergence making translation a good target for drug development. By comparing the sequence alignments of eEF2 from both human and *P. falciparum* a relatively high degree of sequence conservation is seen. Yet, *P. falciparum* contains three distinct areas of extra sequence not present in the human eEF2 sequence (see Figure 5.2). This divergence in key aspects of the translation components means HTP translation based assays, such as the Dual-IVT, could offer a real benefit to antimalarial drug screening reducing the need for laborious S-35 radio labelling experiments.

Another compound receiving attention because of its ability to target the malaria specific lysyl-aaRS is cladosporin (see Introduction 1.5.7). Due to its bioavailability, cladosporin cannot be used in its native form and as such requires derivatization to make it more stable. The Dual-IVT assay was able to identify cladosporin as a malaria specific translation inhibitor as well as two of its derivatives (see Results 3.1.5). The identification of cladosporin opens the possibility of targeting other aaRSs encoded by *P. falciparum*. As although the human and *P. falciparum* lysyl-aaRS enzymes share almost 55% sequence identity, this divergence is enough to translate into compound selectivity. Cladosporin competes for the ATP binding pocket in the lysyl-aaRS through interaction with two residues, V328 and S344 in *P. falciparum*. On

the other hand in the human lysyl-aaRS the equivalent ATP binding positions are changed for glutamine and threonine providing larger side chains that are thought to reduce cladosporin binding(Guiguemde & Guy, 2012).

4.1.3 Mefloquine

Since its initial use decades ago mefloquine's specific MoA has remained elusive. However, the atomic structure of the +RS enantiomer of mefloquine bound to the GTPase centre of the 80S ribosome of *P. falciparum* combined with radio labelled S35 methionine incorporation enabled conformation and elucidation of the MoA for mefloquine. To assess the primary binding site the authors then carried out a series of mutations within the mefloquine binding pocket. Mefloquine was assessed by the Dual-IVT assay using a racemic drug mixture and the +RS enantiomer (see Figure 3.6 (B)). At a drug concentration of 100µM there was no inhibition of translation indicating mefloquine may not be a translation specific inhibitor. This suggests that the MoA may be more complicated than previously thought, possibly indicating a mechanism of indirectly inhibiting protein synthesis. For example, thapsigargin, a plant-derived sesquiterpene lactone selectively inhibits the sarco endoplasmic reticulum Ca^{2+} ATPase (SERCA) present on the endoplasmic reticulum of eukaryotes. It causes an increase of Ca^{2+} in the cytosol serving as an efficacious inhibitor of amino acid incorporation(Lytton et al., 1991). Mefloquine may target a number of components including the ribosome, to suppress translation. Further investigation of mefloquine is now required given the weight of evidence suggesting the drug does not inhibit translation.

4.1.4 Pathogen Box

The Dual-IVT enabled the screening of a library of 400 compounds for translation inhibition in both malaria and human cellular lysates (see Results 3.1.7). The screen was adapted to a

384-well format but could equally be applied to a 1536-well format based on the small volumes used. This miniaturisation can enable the screening of large libraries of compounds using a single batch of cellular lysate eliminating batch to batch variations that can affect other *in vitro* translation assays. Although the screen identified 11 potential translation inhibitors, the human component of the Dual-IVT reduced this to four selective malaria specific inhibitors. The compounds MMV667494 and MMV634140 are quinoline-4-carboxamides, related to the DDD107498 compound(Baragana et al., 2016). This may mean they have a similar MoA and continue to be selective for malaria as opposed to human eEF2. Interestingly, the small molecule kinase inhibitor MMV010576 was identified by the Dual-IVT as a malaria specific potential translation inhibitor; however, its precise MoA is yet to be confirmed in the context of malaria inhibition. To further investigate the potency of each of these five compounds, EC_{50} values will need to be determined. These values can then be compared to inhibitor compounds used to standardised the Dual-IVT assay.

4.1.5 Potential Problems Associated with the Dual-IVT

The Dual-IVT was developed using human and malaria lysates that contain a mixture of concentrated cytosolic contents as well as components that have been liberated from organelles within the lysed cellular material. Compounds tested by the Dual-IVT assay are therefore free to interact with proteins that in a native context, they may never interact with and as such may be metabolised differently. In addition the assay requires the substitution of certain compounds to facilitate translation such as an energy regeneration mixture and amino acids. This could impact the testing of certain compounds in a positive or negative way due to a changes in a compounds pharmacokinetics and dynamic properties that cannot be predicted in advance. The use of control compounds with known MoAs were used to probe both human and malaria lysates to fully test the validity of the Dual-IVT as a tool for detecting malaria specific

translation inhibitors. The pharmacokinetics and dynamics of a drug used in the assay will also be different when compared to *in vitro* culture causing differences in EC_{50}. Taking the example of a parasite in culture, drugs added would have to first cross the RBC membrane before crossing the parasitophorous vacuole and then cross into the target cell. Therefore, results indicated by this assay are seen to guide the user on a generalised MoA when screening a large compound library, findings should always be tested in a phenotypic screen for conformation of a result. This can be seen when comparing EC_{50} values obtained from the Dual-IVT versus that of the GIA with some compounds like cycloheximide giving $EC50_{50}$ values within a similar range. In contrast compounds like halofuginone and cladosporin show large differences differences (see Table 3.1).

In addition, the enzymatic conversion of luciferin to oxyluciferin through the production of luciferase as a marker of translation could predispose the assay to false positives. This could be due to an unknown compound inhibiting luciferase or partially inhibiting luciferase in a reaction. The five 'hit' compounds selected from the pathogen box screen provided little or no inhibition in human cellular lysates, eliminating the possibility of luciferase inhibition. However, it could be beneficial to test compounds using recombinant luciferase in a counter-screen to eliminate any possible error.

4.2 Dissecting the *Plasmodium* RNAP Complexes

Transcription is a fundamental process for growth and development in malaria but currently the structures of the nuclear RNAPI-III in *P. falciparum* do not exist (see Introduction 1.6). There are also no current drugs deployed in the field or in pipelines that are known to target any of these complexes in malaria. The structural resolution of the 80S ribosome within *P. falciparum* (see Introduction 1.5.3) combined with the invasion complex of *P. vivax* (PDB_6bpe) has shown the power of cryo-EM as a technique that allows the resolution of macromolecular complexes

purified from the target organism (see Introduction 1.6.5). To aid in the understanding of the fundamental mechanisms of transcription in *P. falciparum*, the three nuclear RNAP complexes were modified with an affinity tag to enable their purification. This then led to the purification of RNAPII, responsible for the production of mRNA and its partial resolution using negative stain EM (see Results 3.23-3.24).

Whilst this lays the foundation for future structural refinements, the purification of RNAPII has remained challenging often resulting in contaminated products. This has subsequently hampered structural resolution due to the low heterogeneity of polymerase like particles within the prepared sample, reducing the ability to accumulate enough 2D images in enough conformations to build a reliable model. Further attempts may involve switching the 3XFLAG tag for a TAP tag which has enabled the purification and structural resolution of RNAP III in yeast (Han et al., 2018). This methodology could also be combined with the purification of nuclei away from cellular material in tagged parasite lines (Oehring et al., 2012), potentially reducing the number of contaminant proteins after purification steps.

Whilst the three polymerase complexes share a degree of conservation with other eukaryotic nuclear RNAP complexes, like the structures of the *P. falciparum* ribosome have shown, there may be inherent differences that could be exploited for the purposes of drug development. Although only a partial structure for RNAP II has been elucidated (see Results 3.24), phylogenetic trees could give an indication of the divergence from mammalian nuclear RNA polymerases. Maximum likelihood phylogenetic trees can be used as an evolutionary model to explain the differences observed in amino acid sequences of related proteins by computing the evolutionary difference between the groups of proteins from multiple sequence alignments (Sievers & Higgins, 2018). Phylogenetic trees were constructed for the five *P. falciparum* RNAP subunits shared between the three nuclear polymerases (RPB5, RPB6, RPB8, RPB10 and RPB12). The trees that were constructed show distinct clustering of the five Plasmodium *spp* that infect humans

indicating a high degree of conservation. However, human and mouse variants clustered in clads far from the *P. falciparum*. In fact the *P. falciparum* RPB8 subunit only shares 25% sequence identity with its human homologue (see Figure 5.1). Taken together this may indicate an evolutionary divergence by *P. falciparum* RNAPs that could make them amiable to inhibition over human complexes.

4.3 Malaria CFPS

The majority of deaths attributed to malaria infection are caused by *P. falciparum* and to date, a fully protective, licensed vaccine with an efficacy as set by the WHO of at least 75% has remained elusive. New antimalarial combination therapies have sought to alleviate the burden of malaria but their efficacy is under constant attack from an ever-mutating parasite (see Introduction 1.3). If global eradication is ever going to be achieved, an efficacious vaccine will need to be deployed to malaria endemic regions. Although vaccine candidates centred on the blood-stage essential parasite antigens such as MSP-1 and Rh5 are being pursued they do not induce immunity against the sexual stage of parasite development (see Introduction 1.7.8). Instead pre-erythrocytic vaccines aim to halt the establishment of malaria infection within the human host by inhibiting sporozoite invasion of liver cells. These types of vaccine mainly focus on the dominant sporozoite antigen CSP however, vaccine trials using CSP chimeras have resulted in limited efficacy requiring multiple doses with protection that wanes over time (see Introduction 1.7.5). Whole sporozoite based vaccines contain the full protein repertoire of the parasite and have resulted in strain transcending protection from malaria (see Introduction 1.7.4). These types of vaccines are impractical for large-scale deployment in remote areas. The characterisation of other sporozoite surface antigens is crucial for not only understanding fundamental parasite invasion biology but also discovering antigens that offer better protection.

The production and characterisation of sporozoite surface antigens has been problematic, in

part due to the unique type of O-linked fucosylation and unusual protein structures adopted by *P. falciparum*. The sequencing of the parasite genome and now the publication of transcriptomic data can assist in the identification of proteins present on the surface of the sporozoite when injected into the human host. The HTP production of these antigens in standard heterologous systems is time-consuming and could result in the production of improperly folded protein. Identifying the full repertoire of surface antigens of the sporozoite that produce an immune response by producing these proteins using the parasite itself would be of benefit as it may reveal more reactive protein targets. A CFPS system derived from malaria lysate now makes this a real possibility, using *P. falciparum* CSP as a model protein for future malaria antigen production. This is because the production of full-length CSP using heterologous systems has been problematic. The design and production of the malaria part of the Dual-IVT assay had to be upscaled and adapted for the purposes of antigen production.

The translation of mRNA containing the usual 5'UTR progresses through the eukaryotic 5'cap dependent initiation pathway resulting in less efficient translation than mRNA containing a 5'IRES element like those used in CFPS reactions (see Introduction 1.8.11). Yet, the function of an IRES is for the most part *spp* dependent. An IRES element directs the translation of viral mRNA through the recruitment of ribosomes via a 5' cap independent pathway. There are currently no viruses known to infect *P. falciparum*, therefore an IRES had to be selected that initiated translation in a *spp* independent manner through the recruitment of the ribosome itself. The IGR-CrPV IRES was found to initiate translation in a malaria derived CFPS system for the first time. Translation efficiency was assessed by measuring luciferase production with efficiency in the presence of the IRES element far exceeding that containing the Hrp3 5' UTR used in the Dual-IVT system (see Results 3.3.1).

The development of a malaria specific continuous exchange TX-TL CFPS system was then attempted initially using sfGFP to test for translocation into endogenous microsomes present

within the *P. falciparum* lysate (see Results 3.3.2). Whilst a native CSP signal peptide was tested, the use of a melittin signal peptide resulted in more efficient translocation of sfGFP into microsomes (see Figure 3.16). However, although translocation was confirmed using the presence and absence of a cytosolic marker, an antibody to an integral ER-resident protein specific for malaria is required to fully confirm the presence of microsomes within an isolated pellet fraction. Eukaryotic signal peptides contain a diverse amino acid sequence but usually contain a tripartite structure of 20-30 residues containing a basic N-terminal, a hydrophobic core and a polar C-terminal domain. This may suggest a mechanism for controlling the quantity of secretion of a particular protein. Whilst CSP is an abundant sporozoite surface protein, it has no function during asexual blood stage parasite growth and as such is not expressed at any appreciable quantity. It is unknown whether the level of CSP secretion using lysate from sporozoite stage parasites would result in considerably more efficient microsomal translocation.

The production of *P. falciparum* CSP was attempted using a malaria derived CFPS system and detected using a CSP specific antibody (see Results 3.3.3). Although CSP with its tag cassette was predicted to have a molecular weight of 41.8kDa, when CSP was detected by western blot on sporozoite material it can be seen migrating at approximately 70kDa. The CSP produced from CFPS reactions was also detected using western blot analysis in a similar way and it too can also be observed migrating at a similar molecular weight to CSP from sporozoite material at 70kDa. This is the first time a complex malaria surface protein has been produced using malaria lysate in a CFPS reaction.

Although the production and detection of CSP was possible using this setup the preparation of the lysate must be refined to increase the level of protein production. Lysate RNA and protein concentration can have a drastic effect on the levels of recombinant protein made in CFPS systems (see Figure 5.6 (F)). This malaria CFPS was adapted from the Dual-IVT assay and as such uses *P. falciparum* lysate not optimised for a CECF protein synthesis system.

Increasing the quantity of ribosomal material within the lysate could increase yields of CSP. At this stage it is unknown if this would be possible due to the logistics in preparing parasite material to sufficient levels. In addition increasing the concentration of the parasite lysate will also result in an increase in the concentration of hemozoin liberated from the parasite. Hemozoin is a crystalline byproduct formed from the digestion of haemoglobin by the parasite and stored in the food vacuole, due to the toxicity of circulating free heme (Fong & Wright, 2013). It is currently unknown how high concentrations of heme present in the lysate may interfere with translation in CFPS.

P. falciparum exports almost 8% of its genome into the host erythrocyte during infection, these proteins require secretion through the ER (Marti et al., 2004). The levels of protein folding and protein statues within the ER is managed the UPR. Once triggered the UPR aims to reduce protein synthesis and up-regulate protein folding pathways. Generally this is managed by ER-resident proteins ATF6, IRE1 and PERK. However, little is known with respect to the UPR pathways in malaria, with a number of studies pointing toward the absence of a canonical UPR pathway that results in parasite stress when a drug is applied (Gosline et al., 2011). There is some evidence to suggest the presence of a UPR centred on PERK in *T. gondii* but PERK appears absent from other protozoans such as *T. brucei*(Narasimhan et al., 2008). *Plasmodium* can attenuate translation through phosphorylation of eIF2 by four elF2 kinases: elK1, elK2 and PK4. Interestingly, PK4 has been shown to be localised to the parasite ER and like PERK is activated by oligomerization and autophosphorylation. The PERK specific inhibitor GSK2606414 was able to specifically inhibit the *Plasmodium* homologue PK4 and not elK1 and elK2(Zhang et al., 2017). Once optimised a testing strategy based on the human CFPS system could be applied to the malaria CFPS system. Only the PERK pathway has been identified in *P. falciparum*. As such inhibitors of the UPR pathway found to increase translation in human CFPS can be applied to malaria CFPS. This may or may not result in an increase in detectable

translation with *Plasmodium* lysate provdining that the inhibitors are cross reactive.

4.4 Human CFPS

The rapid HTP production of antigens present on disease causing organisms can be advantageous for the purposes of serum screening and vaccinology. The development of the Dual-IVT assay required the use of a human *in vitro* translation assay component to act as a counter-screen allowing the identification of malaria specific translation inhibitors. The establishment of SARS-CoV-2 as a pandemic presented an opportunity to pivot this towards viral antigen production using a human-derived system. The system was moved from a short batch style setup to a CECF system. This has been shown to increase the levels of protein production due to the continuous supply of energy components and the removal of inhibitory components generated from translation in CFPS systems. Whilst the EMCV IRES remains the most popular in mammalian CFPS systems, the IGR-CrPV IRES was used instead. This type of IRES allows the direct recruitment of the ribosome without the presence of initiation factors thereby reducing overall energy consumption associated with translation initiation.

4.4.1 Optimising mRNA Synthesis

Once an overriding CECF setup was established, an optimisation strategy was employed to tailor the translation environment towards maximum protein production using sfGFP. Although translation efficiency is likely to be protein dependent, some overriding processes in a reaction are likely to be universal, such as transcription efficiency. A balance of conditions that are optimal for both transcription and translation was needed which in the context of a normal HEK 293F cell are segregated. To optimise transcription the optimal quantity of magnesium in the reaction compartment was increased from 0-28mM, whilst that contained within the 'feeding' solution was fixed at 3.9mM. There was a distinct increase in translation when the reaction

magnesium concentration was between 16-24mM before dropping down. The T7 RNAP binds a single magnesium ion which is required for its function, as such magnesium plays a critical role in the transcription of mRNA.

The ability to continuously and efficiently supply mRNA in a reaction using T7 RNAP is beneficial due to RNA degradation over time. DNA, supplied in the form of a plasmid is known to be more stable and as such can provide a template for the T7 RNAP to continuously transcribe from. This requires the presence of a T7 RNAP promotor sequence upstream of the 5' IRES used to initiate translation. The sequence down stream of the T7 promotor can influence transcription efficiency. The nature of the bases at sequence positions +4 and +8 after the transcription initiation start site have been found to affect overall transcription efficiency (Conrad et al., 2020). To test this phenomenon in the context of CFPS reactions, the promotor initiation sites at positions +4 and +5 were modified which, resulted in > two-fold increase of sfGFP translation attributed to an increase in transcription efficiency.

4.4.2 Inhibiting Cell Signal Cascades to Upregulate CFPS

The production of cellular HEK 293F lysate and its use in CFPS reactions is likely to initiate cascades that may result in a universal decrease of translation due to perceived cellular stress. Caspases are aspartate-specific cysteine proteases that can reduce cellular protein synthesis through the cleavage of elF4G and elF2α. The use of caspases for the purposes of increasing protein production in insect and CHO cellular lysates has already been documented. To optimise HEK 293F CFPS two caspase inhibitors were chosen, a pan-caspase inhibitor (Z-VAD-FMK) and a caspase-3 inhibitor (Z-DEVD-FMK). These were then used singularly or in combination and whilst each inhibitor produced an increase in protein synthesis, it was when these two were combined that resulted in the highest levels of protein synthesis. Thus highlighting the influence that these caspases have on the protein synthesis machinery within the

lysate.

The ER within a cell contains a key sensory network that monitors the build-up of miss-formed protein accumulating within the cell. These sensors are connected to a global cellular network that will down-regulate translation and induce cascades designed to promote the expression of genes to assist in protein folding. However, when levels of aggregated protein reach a critical level, apoptosis may be triggered. During the lysis of certain cell types the ER can reform into microsomal structures which contain the machinery of the ER. The inhibitor ceapin-A7 is a highly specific inhibitor of ATF6, its use at a concentration of between 1-10µM was shown to increase the levels of protein synthesis within a CFPS reaction. Although ATF6 plays a key role in gene expression, it can have an indirect effect on caspase activity due to the induced cleavage of elF2 that in turn reduces protein synthesis. Another sensor of the ER that plays a key role in the UPR is PERK. The autophosphorylation of PERK due to the accumulation of aggregated protein within the ER leads to the inhibition of protein synthesis through the increased phosphorylation of eLF2. This reduces binding of the Met-tRNAi initiator to the ribosome in a GTP dependent manner. The use of the PERK specific inhibitor GSK606414 resulted in a very modest increase in protein synthesis. This may be because the IGR-CrPV IRES does not require the Met-tRNAi initiator to initiate translation.

4.4.3 Microsome Translocation

The presence of endogenous microsomes within the prepared HEK 293F lysate was confirmed using a signal peptide fused to sfGFP. By allowing sfGFP to translocate during a CFPS reaction, its presence in either a cytosolic or a pelleted microsomal fraction could be inspected visually or by fluorescence measurements. This could then be compared to sfGFP lacking a signal peptide isolated from microsomal fractions after a CFPS reaction. A comparison of sfGFP with and without a signal peptide revealed significantly higher sfGFP levels in pelleted fractions

that contained an N-terminal signal peptide. Translocation into microsomes is required for a number of post-translational modifications such as disulphide bond formation and glycosylation as they may contain enzymes such as disulphide isomareases and glycosyltransferases. The direct conformation of translocation through the detection of an ER specific integral membrane protein would have been beneficial for a definitive conformation of ER remnants, the detection of sfGFP in an isolated microsomal pellet provided enough evidence at the time to proceed with.

4.4.4 The Production and Purification of Proteins

The purification of recombinantly, over expressed proteins from heterologous systems has become standard practice and is required for many downstream applications. Although mammalian based CFPS systems have advanced considerably, there is often little evidence provided on how a protein is separated from the highly concentrated lysate it's produced in. To address this, sfGFP was used to optimise a generalised purification strategy after a CFPS reaction. The twin StrepII tag was C-terminally fused to sfGFP with and without an N-terminal signal peptide. This allowed a strategy to be developed for a translocated protein destined for microsomes and a non-translocated protein. The purification of sfGFP was successfully attempted for both translocated and non-translocated proteins resulting in sfGFP that contained little contaminated protein. Whilst the purification of non-translocated sfGFP away from the lysate was simplistic that contained within a microsome fraction was less so. The elution of the protein from the StrepTactin resin required the presence of detergent, if this was omitted elution yields of sfGFP were significantly reduced. This may be due to precipitation of the protein on the column however, because sfGFP that was not purified from microsomes did not exhibit this effect, the exact reason is unknown. Membrane proteins may precipitate on a column when detergent is removed in the wash steps requiring the presence of detergent throughout

the purification process. As sfGFP is not a membrane protein this would seem unlikely unless some form of membrane attachment is occurring either within the microsome itself or on lysis for sfGFP isolation.

Even though it is likely that different complex proteins may require modifications of this generalised purification protocol, it did provide a starting point for the production and purification of both the nucleocapsid and RBD domain of the spike protein. Both of the two viral proteins were fused to sfGFP as a method to monitor their production and journey through the purification process. The two proteins were detected after a 48-hr CFPS reaction with the nucleocapsid showing the highest degree of expression when compared to sfGFP on its own.

The two SARS-CoV-2 proteins were then purified along-side sfGFP as a control. The nucleocapsid and RBD fusion proteins were both successfully detected using a sfGFP recognising antibody. Probing each of the purified proteins with patient serum enabled the detection of the nucleocapsid protein but surprisingly not the RBD protein. Further investigation is currently underway to ascertain why this is the case. This will include the use of a variety of serum collected from other COVID-19 patients, upscaling the production of the RBD to account for any losses during the purification process and removal of detergent used during the purification process. Conclusion of this investigation will then allow the full quantification of each of the two COVID-19 proteins and sfGFP to ascertain the efficiency of this HEK 293F derived CFPS system.

4.5 Final Thoughts

Malaria remains a serious global threat to those living in endemic areas, in particular those where the most virulent malaria parasite *P. falciparum* is prevalent. The parasite's complex life cycle, large genome and predominantly intracellular life style within the human host complicates development of both effective drugs and a still elusive malaria vaccine. Antimalarial drugs

have been relied upon heavily for malaria treatment and prevention over many decades, which have been effective at reducing annual malaria deaths and increasing progress towards eradication. This progress however, has now stalled. Resistance continues to emerge to all frontline antimalarial drugs and there is, as such, an increased drive to find novel replacements targeting essential processes in *P. falciparum*. The work presented in this thesis set out to address the challenge of novel technology to renew progress towards malaria eradication by attempting to shed light on malaria parasite transcription, translation and methods that can exploit the parasite protein synthesis machinery for the purposes of drug and vaccine characterisation.

Transcription and translation are two fundamental, linked processes that the parasite cannot function without, but have not been extensively used for the development of inhibitory compounds. Mefloquine is the only antimalarial in current circulation reported, though not without controversy, to target translation within the parasite. With transcription, structural characterisation of the *Plasmodium* ribosome has previously been a powerful route to shed light on this important macromolecular complex (and helped elucidate mefloquine's potential MoA). With translation, in contrast, little is known regarding the structure of the three nuclear RNAPs in *P. falciparum*, hampering our understanding of and potential to target transcription. To address this gap in our knowledge of translation, the three nuclear DNA directed RNAPs of *P.falciparum* were affinity tagged and purification of each was attempted. In conjunction with collaborators in Madrid, this thesis presents the first glimpse of the structure of RNAP II. Although this is only an initial step towards atomic resolution, it provides a framework that can be applied to the two other polymerases. In addition, further work is underway to increase yields and purities of RNAP II during the purification process, which should enable progression of its structure to atomic resolution using cryo-EM.

A number of compounds have been reported to target the process of translation in *P. falciparum*, which, unlike many other drugs in current use, have been reported to be effective

at multiple stages during the parasite life cycle. Novel translation inhibitors would therefore not only eliminate the clinical symptoms associated with infection but could also inhibit transmission and help move towards malaria eradication. Discovery of these types of inhibitors has, however, traditionally been slow and laborious. To speed up the discovery of antimalarial compounds that target translation, we sought to develop an assay termed the Dual-IVT that could enable the detection of a parasite inhibitor and concomitantly point towards its MoA. This thesis presents the successful reconstitution of the cytosolic translation machinery of *P. falciparum* translation *in vitro*, verified translation inhibitor screening using known inhibitors specific to malaria. This thesis then presents a HTP screen of 400 bioactive compounds, quickly identifying five parasite specific inhibitors of translation. On analysis two of these compounds contained structural elements of a known parasite specific translation inhibitor currently in clinical trials (validating the discovery approach). Another compound was found to be a small kinase inhibitor that had previously been identified during a phenotypic screen of the same 400 compounds. *P. falciparum* are reported to contain between 60-90 kinases encoded by their genome and given that phosphorylation of translation initiation factors is a key mechanism by which eukaryotes regulate cellular protein synthesis, points to a potential route by which a drug might inhibit translation via kinase activity. Further work is now underway to fully characterise these five 'hit' compounds through characterisation of their respective EC_{50} values both in the assay and in culture which may yet yield new drugs with potential for full development.

The creation of an IVT assay for the purposes of drug screening required reconstitution of *P. falciparum* translation *in vitro*. Having successfully developed this system, it then became possible to push *in vitro* translation towards Cell Free Protein Synthesis (CFPS). There are currently no methods that can easily overexpress all proteins from *Plasmodium spp*, hampering the characterisation of the *P. falciparum* proteome. This is because standard heterologous expression systems often struggle to produce complex proteins from malaria (given their often

repetitive structure, complex novel folds and post-translational modifications). Difficulty in the expression of these types of proteins by extension may also be a key factor impeding malaria vaccine production, yielding proteins that incompletely elicit an immunological response that would be seen if a native *Plasmodium* surface antigen was presented. For example, the circumsporozoite protein, CSP, has been used extensively in current leading malaria vaccine designs, yet it contains a single O-linked fucosylation, two predicted disulphide bonds and a GPI anchor – secondary structural elements that will be incompletely achieved by heterologous systems. Vaccines such as R21 use truncated portions of CSP and are produced in yeast without these modifications. To fully characterise CSP we attempted its production using translationally active lysate produced from *P. falciparum*. This thesis presents a series of innovations towards native CFPS. For the first time, translation initiation was achieved using the CrPV IGR IRES, which led to an increase in translation efficiency over the native 5'UTR used in our IVT assay. Combined with other efficiencies, this thesis presents the successful expression, detection and purification of CSP that behaves biochemically in a comparable way to CSP found on the surface of the sporozoite. This represents the first steps at producing a *Plasmodium* surface antigen using the parasite itself. Further work is now underway to increase protein yields through an improved method for the isolation of parasite lysate.

Finally, to meet the demands of the emergence of SARS-CoV-2 and subsequent COVID-19 pandemic, this thesis attempted to repurpose the human IVT assay into a CFPS platform capable of expressing viral proteins that might also serve as a technology for the expression of other human viral proteins. Adaptation of the system gave us vital insights into how we might also go about further optimising the malaria CFPS system. The use of translationally active lysate from human HEK 293F cells combined with the CrPV-IGR IRES allowed us to create a generalised protein production and purification workflow for HTP production of protein libraries. This served as a starting point for the expression of both the nucleocapsid and RBD from

SARS-CoV-2. Patient serum was then used to probe both the purified SARS-CoV-2 proteins, with inconclusive results for the spike protein RBD, but definitive expression of immunologically identifiable nucleocapsid protein. Future work to further optimise protein production at scale should yield a system capable of large scale production of micro-to-milligrams of protein, as an enabler for immunological screening – something with potential relevance to variant screening in the future.

In summary, the technologies developed here represent key milestones towards HTP screening of malaria translation inhibitors, characterisation of the malaria parasite transcription machinery and production of native malaria parasite proteins at scales that will facilitate immunological screening and potentially future vaccinology development (as well as potential application for viral protein production).

Bibliography

Aguiar, J. C., Bolton, J., Wanga, J., Sacci, J. B., Iriko, H., Mazeika, J. K., Han, E. T., Limbach, K., Patterso, N. B., Sedegah, M., Cruz, A. M., Tsuboi, T., Hoffman, S. L., Carucci, D., Hollingdale, M. R., Villasante, E. D., & Richie, T. L. (2015). Discovery of novel plasmodium falciparum pre-erythrocytic antigens for vaccine development. PLoS ONE, 10(8), 1–24.https://doi.org/10.1371/journal.pone.0136109

Alout, H., Roche, B., Dabiré, R. K., & Cohuet, A. (2017). Consequences of insecticide resistance on malaria transmission Malaria burden and control The threat of insecticide resistance. 3–7.

Anderson, M. J., Stark, J. C., Hodgman, C. E., & Jewett, M. C. (2015). Energizing eukaryotic cell-free protein synthesis with glucose metabolism. FEBS Letters, 589(15), 1723–1727. https://doi.org/10.1016/j.febslet.2015.05.045

Andréll, J., & Tate, C. G. (2013). Overexpression of membrane proteins in mammalian cells for structural studies. Molecular Membrane Biology, 30(1), 52–63. https://doi.org/10.3109/09687688.2012.703703

Anthony Weil, P., Luse, D. S., Segall, J., & Roeder, R. G. (1979). Selective and accurate initiation of transcription at the ad2 major late promotor in a soluble system dependent on purified RNA polymerase ii and DNA. Cell, 18(2), 469–484. https://doi.org/10.1016/0092-8674(79)90065-5

Apweiler, R. (1999). On the frequency of protein glycosylation, as deduced from analysis of the SWISS-PROT database. Biochimica et Biophysica Acta (BBA) - General Subjects, 1473(1), 4–8. https://doi.org/10.1016/S0304-4165(99)00165-8

Armache, K. J., Mitterweger, S., Meinhart, A., & Cramer, P. (2005). Structures of complete RNA polymerase II and its subcomplex, Rpb4/7. Journal of Biological Chemistry, 280(8), 7131–7134. https://doi.org/10.1074/jbc.M413038200

Astuti, I., & Ysrafil. (2020). Severe Acute Respiratory Syndrome Coronavirus 2 (SARS-CoV-2): An overview of viral structure and host response. Diabetes & Metabolic Syndrome: Clinical Research & Reviews, 14(4), 407–412. https://doi.org/10.1016/j.dsx.2020.04.020

Bahl, A., Brunk, B., Crabtree, J., Fraunholz, M. J., Gajria, B., Grant, G. R., Ginsburg, H., Gupta, D., Kissinger, J. C., Labo, P., Li, L., Mailman, M. D., Milgram, A. J., Pearson, D. S., Roos, D. S., Schug, J., Stoeckert, C. J., & Whetzel, P. (2003). PlasmoDB: The Plasmodium genome resource. A database integrating experimental and computational data. Nucleic Acids

Research, 31(1), 212–215. https://doi.org/10.1093/nar/gkg081

Bai, X. chen, McMullan, G., & Scheres, S. H. W. (2015). How cryo-EM is revolutionizing structural biology. Trends in Biochemical Sciences, 40(1), 49–57. https://doi.org/10.1016/j.tibs.2014.10.005

Baldwin, J., Michnoff, C. H., Malmquist, N. A., White, J., Roth, M. G., Rathod, P. K., & Phillips, M. A. (2005). High-throughput screening for potent and selective inhibitors of Plasmodium falciparum dihydroorotate dehydrogenase. Journal of Biological Chemistry, 280(23), 21847–21853. https://doi.org/10.1074/jbc.M501100200

Baniecki, M. L., Wirth, D. F., & Clardy, J. (2007). High-throughput Plasmodium falciparum growth assay for malaria drug discovery. Antimicrobial Agents and Chemotherapy, 51(2), 716–723. https://doi.org/10.1128/AAC.01144-06

Bankamp, B., Hickman, C., Icenogle, J. P., & Rota, P. A. (2019). Successes and challenges for preventing measles, mumps and rubella by vaccination. Current Opinion in Virology, 34(Figure 1), 110–116. https://doi.org/10.1016/j.coviro.2019.01.002

Baragaña, B., Forte, B., Choi, R., Hewitt, S. N., Bueren-Calabuig, J. A., Pisco, J. P., Peet, C., Dranow, D. M., Robinson, D. A., Jansen, C., Norcross, N. R., Vinayak, S., Anderson, M., Brooks, C. F., Cooper, C. A., Damerow, S., Delves, M., Dowers, K., Duffy, J., … Gilbert, I. H. (2019). Lysyl-tRNA synthetase as a drug target in malaria and cryptosporidiosis. Proceedings of the National Academy of Sciences of the United States of America, 116(14), 7015–7020. https://doi.org/10.1073/pnas.1814685116

Baragaña, B., Hallyburton, I., Lee, M. C. S., Norcross, N. R., Grimaldi, R., Otto, T. D., Proto, W. R., Blagborough, A. M., Meister, S., Wirjanata, G., Ruecker, A., Upton, L. M., Abraham, T. S., Almeida, M. J., Pradhan, A., Porzelle, A., Martínez, M. S., Bolscher, J. M., Woodland, A., … Gilbert, I. H. (2015). A novel multiple-stage antimalarial agent that inhibits protein synthesis. Nature, 522(7556), 315–320. https://doi.org/10.1038/nature14451

Baragana, B., Norcross, N. R., Wilson, C., Porzelle, A., Hallyburton, I., Grimaldi, R., Osuna-Cabello, M., Norval, S., Riley, J., Stojanovski, L., Simeons, F. R. C., Wyatt, P. G., Delves, M. J., Meister, S., Duffy, S., Avery, V. M., Winzeler, E. A., Sinden, R. E., Wittlin, S., … Gilbert, I. H. (2016). Discovery of a Quinoline-4-carboxamide Derivative with a Novel Mechanism of Action, Multistage Antimalarial Activity, and Potent in Vivo Efficacy. Journal of Medicinal Chemistry, 59(21), 9672–9685. https://doi.org/10.1021/acs.jmedchem.6b00723

Barr, P. J., Green, K. M., Gibson, H. L., Bathurst, I. C., Quakyi, I. A., & Kaslow, D. C. (1991). Recombinant pfs25 protein of plasmocdium falciparum elicits malaria transmission-blocking immunity in experimental animals. Journal of Experimental Medicine, 174(5), 1203–1208. https://doi.org/10.1084/jem.174.5.1203

Basco, L. K., de Pécoulas, P. E., Wilson, C. M., Le Bras, J., & Mazabraud, A. (1995). Point mutations in the dihydrofolate reductase-thymidylate synthase gene and pyrimethamine and cycloguanil resistance in Plasmodium falciparum. Molecular and Biochemical Parasitology, 69(1), 135–138. https://doi.org/10.1016/0166-6851(94)00207-4

Bateman, A., Martin, M.-J., Orchard, S., Magrane, M., Agivetova, R., Ahmad, S., Alpi,

E., Bowler-Barnett, E. H., Britto, R., Bursteinas, B., Bye-A-Jee, H., Coetzee, R., Cukura, A., Da Silva, A., Denny, P., Dogan, T., Ebenezer, T., Fan, J., Castro, L. G., ... Teodoro, D. (2021). UniProt: the universal protein knowledgebase in 2021. Nucleic Acids Research, 49(D1), D480–D489. https://doi.org/10.1093/nar/gkaa1100

Baumann, H., Matthews, H., Li, M., Hu, J. J., Willison, K. R., & Baum, J. (2018). A high-throughput in vitro translation screen towards discovery of novel antimalarial protein translation inhibitors. BioRxiv, 44(0), 248740. https://doi.org/10.1101/248740

Bayati, A., Kumar, R., Francis, V., & McPherson, P. S. (2021). SARS-CoV-2 infects cells after viral entry via clathrin-mediated endocytosis. Journal of Biological Chemistry, 296, 100306. https://doi.org/10.1016/j.jbc.2021.100306

Belyi, Y., Tartakovskaya, D., Tais, A., Fitzke, E., Tzivelekidis, T., Jank, T., Rospert, S., & Aktories, K. (2012). Elongation factor 1A is the target of growth inhibition in yeast caused by Legionella pneumophila glucosyltransferase Lgt. Journal of Biological Chemistry, 287(31), 26029–26037. https://doi.org/10.1074/jbc.M112.372672

Benz, B. A., Nandadasa, S., Takeuchi, M., Grady, R. C., Takeuchi, H., LoPilato, R. K., Kakuda, S., Somerville, R. P. T., Apte, S. S., Haltiwanger, R. S., & Holdener, B. C. (2016). Genetic and biochemical evidence that gastrulation defects in Pofut2 mutants result from defects in ADAMTS9 secretion. Developmental Biology, 416(1), 111–122. https://doi.org/10.1016/j.ydbio.2016.05.038

Berg JM, Tymoczko JL, S. L. (2002). The Purification of Proteins Is an Essential First Step in Understanding Their Function. Biochemistry (5th edition). ISBN: 0-7167-3051-0
Bergamini, G., Preiss, T., & Hentze, M. W. (2000). Picornavirus IRESes and the poly(A) tail jointly promote cap-independent translation in a mammalian cell-free system. Rna, 6(12), 1781–1790. https://doi.org/10.1017/S1355838200001679

Berrier, C., Park, K. H., Abes, S., Bibonne, A., Betton, J. M., & Ghazi, A. (2004). Cell-free synthesis of a functional ion channel in the absence of a membrane and in the presence of detergent. Biochemistry, 43(39), 12585–12591. https://doi.org/10.1021/bi049049y

Bettencourt, P. (2020). Current Challenges in the Identification of Pre-Erythrocytic Malaria Vaccine Candidate Antigens. Frontiers in Immunology, 11(February), 1–15. https://doi.org/10.3389/fimmu.2020.00190

Bhatt, S., Weiss, D. J., Cameron, E., Bisanzio, D., Mappin, B., Dalrymple, U., Battle, K. E., Moyes, C. L., Henry, A., Eckhoff, P. A., Wenger, E. A., Briët, O., Penny, M. A., Smith, T. A., Bennett, A., Yukich, J., Eisele, T. P., Griffin, J. T., Fergus, C. A., ... Gething, P. W. (2015). The effect of malaria control on Plasmodium falciparum in Africa between 2000 and 2015. Nature, 526(7572), 207–211. https://doi.org/10.1038/nature15535

Bhattarai, A., Ali, A. S., Kachur, S. P., Mårtensson, A., Abbas, A. K., Khatib, R., Al-mafazy, A. W., Ramsan, M., Rotllant, G., Gerstenmaier, J. F., Molteni, F., Abdulla, S., Montgomery, S. M., Kaneko, A., & Björkman, A. (2007). Impact of artemisinin-based combination therapy and insecticide-treated nets on malaria burden in Zanzibar. PLoS Medicine, 4(11), 1784–1790. https://doi.org/10.1371/journal.pmed.0040309

Bikoff, E. K., LaRue, B. F., & Gefter, M. L. (1975). In vitro synthesis of transfer RNA. II. Identification of required enzymatic activities. The Journal of Biological Chemistry, 250(16), 6248–6255. http://www.ncbi.nlm.nih.gov/pubmed/1099090

Birkholtz, L. M., Blatch, G., Coetzer, T. L., Hoppe, H. C., Human, E., Morris, E. J., Ngcete, Z., Oldfield, L., Roth, R., Shonhai, A., Stephens, L., & Louw, A. I. (2008). Heterologous expression of plasmodial proteins for structural studies and functional annotation. Malaria Journal, 7, 1–20. https://doi.org/10.1186/1475-2875-7-197

Birnbaum, J., Flemming, S., Reichard, N., Soares, A. B., Mesén-Ramírez, P., Jonscher, E., Bergmann, B., & Spielmann, T. (2017). A genetic system to study Plasmodium falciparum protein function. Nature Methods, 14(4), 450–456. https://doi.org/10.1038/nmeth.4223

Blank, A., Fürle, K., Jäschke, A., Mikus, G., Lehmann, M., Hüsing, J., Heiss, K., Giese, T., Carter, D., Böhnlein, E., Lanzer, M., Haefeli, W. E., & Bujard, H. (2020). Immunization with full-length Plasmodium falciparum merozoite surface protein 1 is safe and elicits functional cytophilic antibodies in a randomized first-in-human trial. Npj Vaccines, 5(1). https://doi.org/10.1038/s41541-020-0160-2.

Blume, S. (2000). A Brief History of Polio Vaccines. Science, 288(5471), 1593–1594. https://doi.org/10.1126/science.288.5471.1593.

Böhm, E., Seyfried, B. K., Dockal, M., Graninger, M., Hasslacher, M., Neurath, M., Konetschny, C., Matthiessen, P., Mitterer, A., & Scheiflinger, F. (2015). Differences in N-glycosylation of recombinant human coagulation factor VII derived from BHK, CHO, and HEK293 cells. BMC Biotechnology, 15(1), 1–15. https://doi.org/10.1186/s12896-015-0205-1

Bookwalter, C. S., Tay, C. L., McCrorie, R., Previs, M. J., Lu, H., Krementsova, E. B., Fagnant, P. M., Baum, J., & Trybus, K. M. (2017). Reconstitution of the core of the malaria parasite glideosome with recombinant Plasmodium class XIV myosin A and Plasmodium actin. Journal of Biological Chemistry, 292(47), 19290–19303. https://doi.org/10.1074/jbc.M117.813972

Boudreau, E., Webster, H. K., Pavanand, K., & Thosingha, L. (1982). Type II Mefloquine Resistance in Thailand. The Lancet, 320(8311), 1335. https://doi.org/10.1016/S0140-6736(82)91532-X

Bray, R. S., & Garnham, P. C. C. (1982). The Life-Cycle of Primate Malaria Parasites. British Medical Bulletin, 38(2), 117–122. https://doi.org/10.1093/oxfordjournals.bmb.a071746

Briand, L., Marcion, G., Kriznik, A., Heydel, J. M., Artur, Y., Garrido, C., Seigneuric, R., & Neiers, F. (2016). A self-inducible heterologous protein expression system in *Escherichia coli*. Scientific Reports, 6(September), 1–11. https://doi.org/10.1038/srep33037

Brentnall, M., Rodriguez-Menocal, L., De Guevara, R., Cepero, E., & Boise, L. H. (2013). Caspase-9, caspase-3 and caspase-7 have distinct roles during intrinsic apoptosis. BMC Cell Biology, 14(1), 32. https://doi.org/10.1186/1471-2121-14-32

Brödel, A. K., Sonnabend, A., Roberts, L. O., Stech, M., Wüstenhagen, D. A., & Kubick, S. (2013). IRES-mediated translation of membrane proteins and glycoproteins in eukaryotic cell-free systems. PLoS ONE, 8(12). https://doi.org/10.1371/journal.pone.0082234

Browning, D. F., & Busby, S. J. W. (2016). Local and global regulation of transcription initiation in bacteria. Nature Reviews Microbiology, 14(10), 638–650. https://doi.org/10.1038/nrmicro.2016.103

Bulaj, G. (2005). Formation of disulfide bonds in proteins and peptides. Biotechnology Advances, 23(1), 87–92. https://doi.org/10.1016/j.biotechadv.2004.09.002

Burbelo, P. D., Riedo, F. X., Morishima, C., Rawlings, S., Smith, D., Das, S., Strich, J. R., Chertow, D. S., Davey, R. T., & Cohen, J. I. (2020). Sensitivity in detection of antibodies to nucleocapsid and spike proteins of severe acute respiratory syndrome coronavirus 2 in patients with coronavirus disease 2019. Journal of Infectious Diseases, 222, 206–213. https://doi.org/10.1093/infdis/jiaa273

Burrows, J. N., Duparc, S., Gutteridge, W. E., Hooft Van Huijsduijnen, R., Kaszubska, W., Macintyre, F., Mazzuri, S., Möhrle, J. J., & Wells, T. N. C. (2017). New developments in anti-malarial target candidate and product profiles. Malaria Journal, 16(1), 1–29. https://doi.org/10.1186/s12936-016-1675-x

Burns, J. M. (2018). A step forward for an attenuated blood-stage malaria vaccine. BMC Medicine, 16(1), 14–16. https://doi.org/10.1186/s12916-018-1197-1

Calhoun, K. A., & Swartz, J. R. (2007). Energy Systems for ATP Regeneration in Cell-Free Protein Synthesis Reactions. In In Vitro Transcription and Translation Protocols (Vol. 235, pp. 3–17). Humana Press. https://doi.org/10.1007/978-1-59745-388-2_1

Callebaut, I., Prat, K., Meurice, E., Mornon, J. P., & Tomavo, S. (2005). Prediction of the general transcription factors associated with RNA polymerase II in *Plasmodium falciparum*: Conserved features and differences relative to other eukaryotes. BMC Genomics, 6, 1–20. https://doi.org/10.1186/1471-2164-6-100

Carter, R., & Mendis, K. N. (2002). Evolutionary and historical aspects of the burden of malaria. Clinical Microbiology Reviews, 15(4), 564–594. https://doi.org/10.1128/CMR.15.4.564-594.2002

Carter, A. D., Morris, C. E., & McAllister, W. T. (1981). Revised transcription map of the late region of bacteriophage T7 DNA. Journal of Virology, 37(2), 636–642. https://doi.org/10.1128/jvi.37.2.636-642.1981

Casteleijn, M. G., Urtti, A., & Sarkhel, S. (2013). Expression without boundaries: Cell-free protein synthesis in pharmaceutical research. International Journal of Pharmaceutics, 440(1), 39–47. https://doi.org/10.1016/j.ijpharm.2012.04.005

Cazenave, C., Frank, P., & Busen, W. (1993). Characterization of ribonuclease H activities present in two cell-free protein synthesizing systems, the wheat germ extract and the rabbit reticulocyte lysate. Biochimie, 75(1–2), 113–122. https://doi.org/10.1016/0300-9084(93)90032-N

Ceska, T., Chung, C., Cooke, R., Phillips, C., & Williams, P. A. (2019). Cryo-EM in drug discovery. 0(December 2018), 281–293.

Challenger, J. D., Olivera Mesa, D., Da, D. F., Yerbanga, R. S., Lefèvre, T., Cohuet, A., & Churcher, T. S. (2021). Predicting the public health impact of a malaria transmission-blocking vaccine. Nature Communications, 12(1), 1–12. https://doi.org/10.1038/s41467-021-21775-3

Chapman, R. D., Heidemann, M., Hintermair, C., & Eick, D. (2008). Molecular evolution of the RNA polymerase II CTD. Trends in Genetics, 24(6), 289–296. https://doi.org/10.1016/j.tig.2008.03.010

Chen, R. (2012). Bacterial expression systems for recombinant protein production: *E. coli* and beyond. Biotechnology Advances, 30(5), 1102–1107. https://doi.org/10.1016/j.biotechadv.2011.09.013

Cheng, Y. (2015). Single-particle Cryo-EM at crystallographic resolution. Cell, 161(3), 450–457. https://doi.org/10.1016/j.cell.2015.03.049

Chhibber-Goel, J., Joshi, S., & Sharma, A. (2019). Aminoacyl tRNA synthetases as potential drug targets of the Panthera pathogen Babesia. Parasites and Vectors, 12(1), 1–15. https://doi.org/10.1186/s13071-019-3717-z

Chin, T., & Welsby, P. D. (2004). Malaria in the UK: Past, present, and future. Postgraduate Medical Journal, 80(949), 663–666. https://doi.org/10.1136/pgmj.2004.021857

Ciach, M., Zong, K., Kain, K. C., & Crandall, I. (2003). Reversal of mefloquine and quinine resistance in Plasmodium falciparum with NP30. Antimicrobial Agents and Chemotherapy, 47(8), 2393–2396. https://doi.org/10.1128/AAC.47.8.2393-2396.2003

Cho, E. J. (2007). RNA polymerase II carboxy-terminal domain with multiple connections. Experimental and Molecular Medicine, 39(3), 247–254. https://doi.org/10.1038/emm.2007.28
Conrad, T., Plumbom, I., Alcobendas, M., Vidal, R., & Sauer, S. (2020). Maximizing transcription of nucleic acids with efficient T7 promoters. Communications Biology, 3(1), 1–8. https://doi.org/10.1038/s42003-020-01167-x

Contreras-Llano, L. E., Meyer, C., Liu, Y., Sarker, M., Lim, S., Longo, M. L., & Tan, C. (2020). Holistic engineering of cell-free systems through proteome-reprogramming synthetic circuits. Nature Communications, 11(1). https://doi.org/10.1038/s41467-020-16900-7

Coppée, R., Sabbagh, A., & Clain, J. (2020). Structural and evolutionary analyses of the Plasmodium falciparum chloroquine resistance transporter. Scientific Reports, 10(1), 1–15. https://doi.org/10.1038/s41598-020-61181-1

Correia, B. E., Bates, J. T., Loomis, R. J., Baneyx, G., Carrico, C., Jardine, J. G., Rupert, P., Correnti, C., Kalyuzhniy, O., Vittal, V., Connell, M. J., Stevens, E., Schroeter, A., Chen, M., MacPherson, S., Serra, A. M., Adachi, Y., Holmes, M. A., Li, Y., … Schief, W. R. (2014). Proof of principle for epitope-focused vaccine design. Nature, 507(7491), 201–206. https://doi.org/10.1038/nature12966

Costa, S., Almeida, A., Castro, A., & Domingues, L. (2014). Fusion tags for protein solubility, purification, and immunogenicity in *Escherichia coli*: The novel Fh8 system. Frontiers in Microbiology, 5(FEB), 1–20. https://doi.org/10.3389/fmicb.2014.00063

Cowell, A., & Winzeler, E. (2018). Exploration of the Plasmodium falciparum Resistome and Druggable Genome Reveals New Mechanisms of Drug Resistance and Antimalarial Targets . Microbiology Insights, 11, 117863611880852. https://doi.org/10.1177/1178636118808529

Cowman, A. F., Berry, D., & Baum, J. (2012). The cellular and molecular basis for malaria parasite invasion of the human red blood cell. Journal of Cell Biology, 198(6), 961–971. https://doi.org/10.1083/jcb.201206112

Cranmer, S. L., Magowan, C., Liang, J., Coppel, R. L., & Cooke, B. M. (1997). An alternative to serum for cultivation of Plasmodium falciparum in vitro. Transactions of the Royal Society of Tropical Medicine and Hygiene, 91(3), 363–365. https://doi.org/10.1016/S0035-9203(97)90110-3

Cubuk, J., Alston, J. J., Incicco, J. J., Singh, S., Stuchell-Brereton, M. D., Ward, M. D., Zimmerman, M. I., Vithani, N., Griffith, D., Wagoner, J. A., Bowman, G. R., Hall, K. B., Soranno, A., & Holehouse, A. S. (2021). The SARS-CoV-2 nucleocapsid protein is dynamic, disordered, and phase separates with RNA. Nature Communications, 12(1), 1–17. https://doi.org/10.1038/s41467-021-21953-3

Croset, A., Delafosse, L., Gaudry, J. P., Arod, C., Glez, L., Losberger, C., Begue, D., Krstanovic, A., Robert, F., Vilbois, F., Chevalet, L., & Antonsson, B. (2012). Differences in the glycosylation of recombinant proteins expressed in HEK and CHO cells. Journal of Biotechnology, 161(3), 336–348. https://doi.org/10.1016/j.jbiotec.2012.06.038

Cuervo, N. Z., & Grandvaux, N. (2020). Ace2: Evidence of role as entry receptor for SARS-cov-2 and implications in comorbidities. ELife, 9, 1–25. https://doi.org/10.7554/eLife.61390

Cumming, D. A. (1991). Glycosylation of recombinant protein therapeutics: Control and functional implications. Glycobiology, 1(2), 115–130. https://doi.org/10.1093/glycob/1.2.115

Cusack, S. (1997). Aminoacyl-tRNA synthetases. Current Opinion in Structural Biology, 7(6), 881–889. https://doi.org/10.1016/S0959-440X(97)80161-3

Dahl, E. L., & Rosenthal, P. J. (2007). Multiple antibiotics exert delayed effects against the Plasmodium falciparum apicoplast. Antimicrobial Agents and Chemotherapy, 51(10), 3485–3490. https://doi.org/10.1128/AAC.00527-07

Das, P., Babbar, P., Malhotra, N., Sharma, M., Jachak, G. R., Gonnade, R. G., Shanmugam, D., Harlos, K., Yogavel, M., Sharma, A., & Reddy, D. S. (2018). Specific Stereoisomeric Conformations Determine the Drug Potency of Cladosporin Scaffold against Malarial Parasite. Journal of Medicinal Chemistry, 61(13), 5664–5678. https://doi.org/10.1021/acs.jmedchem.8b00565

Datoo, M. S., Natama, M. H., Somé, A., Traoré, O., Rouamba, T., Bellamy, D., Yameogo, P., Valia, D., Lopez, F. R., Flaxman, A., Cappuccini, F., Kailath, R., Elias, S., Mukhopadhyay, E., Noe, A., Cairns, M., Lawrie, A., Roberts, R., Valéa, I., … Tinto, H. (2021). Articles Efficacy of a low-dose candidate malaria vaccine , R21 in adjuvant Matrix-M , with seasonal administration to children in Burkina Faso: a randomised controlled trial. 6736(21), 1–10. https://doi.org/10.1016/S0140-6736(21)00943-0

Delarue, M. (1995). Aminoacyl-tRNA synthetases. Current Opinion in Structural Biology,

5(1), 48–55. https://doi.org/10.1016/0959-440X(95)80008-O

Delves, M., Plouffe, D., Scheurer, C., Meister, S., Wittlin, S., Winzeler, E. A., Sinden, R. E., & Leroy, D. (2012). The activities of current antimalarial drugs on the life cycle stages of plasmodium: A comparative study with human and rodent parasites. PLoS Medicine, 9(2). https://doi.org/10.1371/journal.pmed.1001169

Dempsey, J. J., & Salem, H. H. (1966). An enzymatic electrocardiographic study on toxicity of dehydroemetine. Heart, 28(4), 505–511. https://doi.org/10.1136/hrt.28.4.505

Dennis, A. S. M., Rosling, J. E. O., Lehane, A. M., & Kirk, K. (2018). Diverse antimalarials from whole-cell phenotypic screens disrupt malaria parasite ion and volume homeostasis. Scientific Reports, 8(1), 1–15. https://doi.org/10.1038/s41598-018-26819-1

Diagana, T. T. (2015). Supporting malaria elimination with 21st century antimalarial agent drug discovery. Drug Discovery Today, 20(10), 1265–1270. https://doi.org/10.1016/j.drudis.2015.06.009

Diakité, S. A. S., Traoré, K., Sanogo, I., Clark, T. G., Campino, S., Sangaré, M., Dabitao, D., Dara, A., Konaté, D. S., Doucouré, F., Cissé, A., Keita, B., Doumbouya, M., Guindo, M. A., Toure, M. B., Sogoba, N., Doumbia, S., Awandare, G. A., & Diakité, M. (2019). A comprehensive analysis of drug resistance molecular markers and Plasmodium falciparum genetic diversity in two malaria endemic sites in Mali. Malaria Journal, 18(1), 1–9. https://doi.org/10.1186/s12936-019-2986-5

Didgeon, J. A. (1963). Development of Smallpox Vaccine in England in the Eighteenth and Nineteenth Centuries. BMJ, 1(5342), 1367–1372. https://doi.org/10.1136/bmj.1.5342.1367

Djimdé, A., & Lefèvre, G. (2009). Understanding the pharmacokinetics of Coartem®. Malaria Journal, 8(SUPPL. 1), 1–8. https://doi.org/10.1186/1475-2875-8-S1-S4

Dobanõ, C., Ubillos, I., Jairoce, C., Gyan, B., Vidal, M., Jiménez, A., Santano, R., Dosoo, D., Nhabomba, A. J., Ayestaran, A., Aguilar, R., Williams, N. A., Diéz-Padrisa, N., Lanar, D., Chauhan, V., Chitnis, C., Dutta, S., Gaur, D., Angov, E., Moncunill, G. (2019). RTS,S/AS01E immunization increases antibody responses to vaccine-unrelated Plasmodium falciparum antigens associated with protection against clinical malaria in African children: A case-control study. BMC Medicine, 17(1), 1–19. https://doi.org/10.1186/s12916-019-1378-6

Domínguez, J. M., Kelly, V. A., Kinsman, O. S., Marriott, M. S., Gómez De Las Heras, F., & Martín, J. J. (1998). Sordarins: A new class of antifungals with selective inhibition of the protein synthesis elongation cycle in yeasts. Antimicrobial Agents and Chemotherapy, 42(9), 2274–2278. https://doi.org/10.1128/aac.42.9.2274

Dondapati, S. K., Lübberding, H., Zemella, A., Thoring, L., Wüstenhagen, D. A., & Kubick, S. (2019). Functional reconstitution of membrane proteins derived from eukaryotic cell-free systems. Frontiers in Pharmacology, 10(JULY), 1–9. https://doi.org/10.3389/fphar.2019.00917

Dondapati, S. K., Pietruschka, G., Thoring, L., Wüstenhagen, D. A., & Kubick, S. (2019). Cell-free synthesis of human toll-like receptor 9 (TLR9): Optimization of synthesis conditions and functional analysis. PLoS ONE, 14(4), 1–16. https://doi.org/10.1371/journal.pone.0215897

Drouin, G., & De Sa, M. M. (1995). The concerted evolution of 5S ribosomal genes linked to the repeat units of other multigene families. Molecular Biology and Evolution, 12(3), 481–493. https://doi.org/10.1093/oxfordjournals.molbev.a040223

Duffy, S., Sykes, M. L., Jones, A. J., Shelper, T. B., Simpson, M., Lang, R., Poulsen, S. A., Sleebs, B. E., & Avery, V. M. (2017). Screening the medicines for malaria venture pathogen box across multiple pathogens reclassifies starting points for open-source drug discovery. Antimicrobial Agents and Chemotherapy, 61(9), 1–22. https://doi.org/10.1128/AAC.00379-17

Duquesne, K., Prima, V., & Sturgis, J. N. (2016). Heterologous Expression of Membrane Proteins. In Methods in Molecular Biology (Vol. 1432). https://doi.org/10.1007/978-1-4939-3637-3

Durrand, V., Berry, A., Sem, R., Glaziou, P., Beaudou, J., & Fandeur, T. (2004). Variations in the sequence and expression of the Plasmodium falciparum chloroquine resistance transporter (Pfcrt) and their relationship to chloroquine resistance in vitro. Molecular and Biochemical Parasitology, 136(2), 273–285. https://doi.org/10.1016/j.molbiopara.2004.03.016

Edgar, R. C. (2004). MUSCLE: A multiple sequence alignment method with reduced time and space complexity. BMC Bioinformatics, 5, 1–19. https://doi.org/10.1186/1471-2105-5-113

Ellis, R. D., Martin, L. B., Shaffer, D., Long, C. A., Miura, K., Fay, M. P., Narum, D. L., Zhu, D., Mullen, G. E. D., Mahanty, S., Miller, L. H., & Durbin, A. P. (2010). Phase 1 trial of the Plasmodium falciparum blood stage vaccine MSP1 42-C1/alhydrogel with and without CPG 7909 in malaria naïve adults. PLoS ONE, 5(1), 1–9. https://doi.org/10.1371/journal.pone.0008787

Ellis, R. D., Sagara, I., Doumbo, O., & Wu, Y. (2010). Blood stage vaccines for Plasmodium falciparum: Current status and the way forward. Human Vaccines, 6(8), 627–634. https://doi.org/10.4161/hv.6.8.11446

Epstein, J. E., Tewari, K., Lyke, K. E., Sim, B. K. L., Billingsley, P. F., Laurens, M. B., Gunasekera, A., Chakravarty, S., James, E. R., Sedegah, M., Richman, A., Velmurugan, S., Reyes, S., Li, M., Tucker, K., Ahumada, A., Ruben, A. J., Li, T., Stafford, R., … Hoffman, S. L. (2011). Live Attenuated Malaria Vaccine Designed to Protect Through Hepatic CD8+ T Cell Immunity. Science, 334(6055), 475–480. https://doi.org/10.1126/science.1211548

Escalante, A. A., & Ayala, F. J. (1995). Evolutionary origin of Plasmodium and other Apicomplexa based on rRNA genes. Proceedings of the National Academy of Sciences of the United States of America, 92(13), 5793–5797. https://doi.org/10.1073/pnas.92.13.5793

Espinosa, D. A., Gutierrez, G. M., Rojas-Lopez, M., Noe, A. R., Shi, L., Tse, S. W., Sinnis, P., & Zavala, F. (2015). Proteolytic Cleavage of the Plasmodium falciparum Circumsporozoite Protein Is a Target of Protective Antibodies. Journal of Infectious Diseases, 212(7), 1111–1119. https://doi.org/10.1093/infdis/jiv154

Eugenin, E. A., Martiney, J. A., & Berman, J. W. (2019). The malaria toxin hemozoin induces apoptosis in human neurons and astrocytes: Potential role in the pathogenesis of cerebral malaria. Brain Research, 1720(July), 146317. https://doi.org/10.1016/j.brainres.2019.146317

Fan, Y. T., Wang, Y., Ju, C., Zhang, T., Xu, B., Hu, W., & Chen, J. H. (2013). Systematic analysis of natural antibody responses to P. falciparum merozoite antigens by protein arrays. Journal of Proteomics, 78, 148–158. https://doi.org/10.1016/j.jprot.2012.11.020

Fang, P., Han, H., Wang, J., Chen, K., Chen, X., & Guo, M. (2015). Structural Basis for Specific Inhibition of tRNA Synthetase by an ATP Competitive Inhibitor. Chemistry and Biology, 22(6), 734–744. https://doi.org/10.1016/j.chembiol.2015.05.007

Fenz, S. F., Sachse, R., Schmidt, T., & Kubick, S. (2014). Cell-free synthesis of membrane proteins: Tailored cell models out of microsomes. Biochimica et Biophysica Acta - Biomembranes, 1838(5), 1382–1388. https://doi.org/10.1016/j.bbamem.2013.12.009

Fernández-Tornero, C., Moreno-Morcillo, M., Rashid, U. J., Taylor, N. M. I., Ruiz, F. M., Gruene, T., Legrand, P., Steuerwald, U., & Müller, C. W. (2013). Crystal structure of the 14-subunit RNA polymerase i. Nature, 502(7473), 644–649. https://doi.org/10.1038/nature12636

Ferreira, M. U., da Silva Nunes, M., & Wunderlich, G. (2004). Antigenic Diversity and Immune Evasion by Malaria Parasites. Clinical Diagnostic Laboratory Immunology, 11(6), 987–995. https://doi.org/10.1128/CDLI.11.6.987-995.2004

Ferreira, M. U., & Hartl, D. L. (2007). Plasmodium falciparum: Worldwide sequence diversity and evolution of the malaria vaccine candidate merozoite surface protein-2 (MSP-2). Experimental Parasitology, 115(1), 32–40. https://doi.org/10.1016/j.exppara.2006.05.003

Fisher, N., Majid, R. A., Antoine, T., Al-Helal, M., Warman, A. J., Johnson, D. J., Lawrenson, A. S., Ranson, H., O'Neill, P. M., Ward, S. A., & Biagini, G. A. (2012). Cytochrome b mutation Y268S conferring atovaquone resistance phenotype in malaria parasite results in reduced parasite bc 1 catalytic turnover and protein expression. Journal of Biological Chemistry, 287(13), 9731–9741. https://doi.org/10.1074/jbc.M111.324319

Fong, K. Y., & Wright, D. W. (2013). Hemozoin and antimalarial drug discovery. Future Medicinal Chemistry, 5(12), 1437–1450. https://doi.org/10.4155/fmc.13.113

Forni, G., Mantovani, A., Forni, G., Mantovani, A., Moretta, L., Rappuoli, R., Rezza, G., Bagnasco, A., Barsacchi, G., Bussolati, G., Cacciari, M., Cappuccinelli, P., Cheli, E., Guarini, R., Bacci, M. L., Mancini, M., Marcuzzo, C., Morrone, M. C., Parisi, G., ... Vineis, P. (2021). COVID-19 vaccines: where we stand and challenges ahead. Cell Death and Differentiation, 28(2), 626–639. https://doi.org/10.1038/s41418-020-00720-9

Foth, B. J., Ralph, S. A., Tonkin, C. J., Struck, N. S., Fraunholz, M., Roos, D. S., Cowman, A. F., & McFadden, G. I. (2003). Dissecting apicoplast targeting in the malaria parasite Plasmodium falciparum. Science, 299(5607), 705–708. https://doi.org/10.1126/science.1078599

Fox, B. A., Li, W. B., Tanaka, M., Inselburg, J., & Bzik, D. J. (1993). Molecular characterization of the largest subunit of Plasmodium falciparum RNA polymerase I. Molecular and Biochemical Parasitology, 61(1), 37–48. https://doi.org/10.1016/0166-6851(93)90156-R

França, C. T., White, M. T., He, W. Q., Hostetler, J. B., Brewster, J., Frato, G., Malhotra, I., Gruszczyk, J., Huon, C., Lin, E., Kiniboro, B., Yadava, A., Siba, P., Galinski, M. R.,

Healer, J., Chitnis, C., Cowman, A. F., Takashima, E., Tsuboi, T., Mueller, I. (2017). Identification of Highly-Protective combinations of plasmodium vivax recombinant proteins for vaccine development. ELife, 6, 1–22. https://doi.org/10.7554/eLife.28673

Frank, J., Gao, H., Sengupta, J., Gao, N., & Taylor, D. J. (2007). The process of mRNA-tRNA translocation. In Proceedings of the National Academy of Sciences of the United States of America (Vol. 104, Issue 50, pp. 19671–19678). https://doi.org/10.1073/pnas.0708517104

Frosch, T., Schmitt, M., Bringmann, G., Kiefer, W., & Popp, J. (2007). Structural analysis of the anti-malaria active agent chloroquine under physiological conditions. Journal of Physical Chemistry B, 111(7), 1815–1822. https://doi.org/10.1021/jp065136j

Gallie, D. R. (1991). The cap and poly(A) tail function synergistically to regulate mRNA translational efficiency. Genes and Development, 5(11), 2108–2116. https://doi.org/10.1101/gad.5.11.2108

Gallwitz, D., & Mueller, G. C. (1969). Histone Synthesis in Vitro on HeLa Cell Microsomes. Journal of Biological Chemistry, 244(21), 5947–5952. https://doi.org/10.1016/s0021-9258(18)63564-1

Gamo, F. J., Sanz, L. M., Vidal, J., De Cozar, C., Alvarez, E., Lavandera, J. L., Vanderwall, D. E., Green, D. V. S., Kumar, V., Hasan, S., Brown, J. R., Peishoff, C. E., Cardon, L. R., & Garcia-Bustos, J. F. (2010). Thousands of chemical starting points for antimalarial lead identification. Nature, 465(7296), 305–310. https://doi.org/10.1038/nature09107

Gan, R., & Jewett, M. C. (2014). A combined cell-free transcription-translation system from Saccharomyces cerevisiae for rapid and robust protein synthesis. Biotechnology Journal, 9(5), 641–651. https://doi.org/10.1002/biot.201300545

Ganz, J., Shacham, T., Kramer, M., Shenkman, M., Eiger, H., Weinberg, N., Iancovici, O., Roy, S., Simhaev, L., Da'adoosh, B., Engel, H., Perets, N., Barhum, Y., Portnoy, M., Offen, D., & Lederkremer, G. Z. (2020). A novel specific PERK activator reduces toxicity and extends survival in Huntington's disease models. Scientific Reports, 10(1), 1–15. https://doi.org/10.1038/s41598-020-63899-4

Gardner, M. J., Hall, N., Fung, E., White, O., Berriman, M., Hyman, R. W., Carlton, J. M., Pain, A., Nelson, K. E., Bowman, S., Paulsen, I. T., James, K., Eisen, J. A., Rutherford, K., Salzberg, S. L., Craig, A., Kyes, S., Chan, M. S., Nene, V., ... Barrell, B. (2002). Genome sequence of the human malaria parasite Plasmodium falciparum. Nature, 419(6906), 498–511. https://doi.org/10.1038/nature01097

Gerardin, J., Bever, C. A., Hamainza, B., Miller, J. M., Eckhoff, P. A., & Wenger, E. A. (2016). Optimal Population-Level Infection Detection Strategies for Malaria Control and Elimination in a Spatial Model of Malaria Transmission. PLoS Computational Biology, 12(1), 1–19. https://doi.org/10.1371/journal.pcbi.1004707

Gerold, P., Schofield, L., Blackman, M. J., Holder, A. A., & Schwarz, R. T. (1996). Structural analysis of the glycosyl-phosphatidylinositol membrane anchor of the merozoite surface proteins-1 and -2 of Plasmodium falciparum. Molecular and Biochemical Parasitology, 75(2), 131–143. https://doi.org/10.1016/0166-6851(95)02518-9

Ghidelli-Disse, S., Lafuente-Monasterio, M. J., Waterson, D., Witty, M., Younis, Y., Paquet, T., Street, L. J., Chibale, K., Gamo-Benito, F. J., Bantscheff, M., & Drewes, G. (2014). Identification of Plasmodium PI4 kinase as target of MMV390048 by chemoproteomics. Malaria Journal, 13(S1), 2014. https://doi.org/10.1186/1475-2875-13-s1-p38

Gilson, P. R., Nebl, T., Vukcevic, D., Moritz, R. L., Sargeant, T., Speed, T. P., Schofield, L., & Crabb, B. S. (2006). Identification and stoichiometry of glycosylphosphatidylinositol-anchored membrane proteins of the human malaria parasite Plasmodium falciparum. Molecular and Cellular Proteomics, 5(7), 1286–1299. https://doi.org/10.1074/mcp.M600035-MCP200

Gomes, P. S., Bhardwaj, J., Rivera-Correa, J., Freire-De-Lima, C. G., & Morrot, A. (2016). Immune escape strategies of malaria parasites. Frontiers in Microbiology, 7(OCT). https://doi.org/10.3389/fmicb.2016.01617

Gomes-Duarte, A., Lacerda, R., Menezes, J., & Romão, L. (2018). eIF3: a factor for human health and disease. RNA Biology, 15(1), 26–34. https://doi.org/10.1080/15476286.2017.1391437
Good, M. F. (2001). Towards a blood-stage vaccine for malaria: Are we following all the leads? Nature Reviews Immunology, 1(2), 117–125. https://doi.org/10.1038/35100540

Gosline, S. J. C., Nascimento, M., McCall, L. I., Zilberstein, D., Thomas, D. Y., Matlashewski, G., & Hallett, M. (2011). Intracellular eukaryotic parasites have a distinct unfolded protein response. PLoS ONE, 6(4). https://doi.org/10.1371/journal.pone.0019118

Gualerzi, C. O., & Pon, C. L. (2015). Initiation of mRNA translation in bacteria: Structural and dynamic aspects. Cellular and Molecular Life Sciences, 72(22), 4341–4367. https://doi.org/10.1007/s00018-015-2010-3

Guiguemde, W. A., & Guy, R. K. (2012). An all-purpose antimalarial drug target. Cell Host and Microbe, 11(6), 555–557. https://doi.org/10.1016/j.chom.2012.05.008

Gupta, R. S., & Golding, G. B. (1996). The origin of the eukaryotic cell. Trends in Biochemical Sciences, 21(5), 166–171. https://doi.org/10.1016/S0968-0004(96)20013-1

Gupta, R. S., & Siminovitch, L. (1977). The molecular basis of emetine resistance in chinese hamster ovary cells: Alteration in the 40S ribosomal subunit. Cell, 10(1), 61–66. https://doi.org/10.1016/0092-8674(77)90140-4

Gurramkonda, C., Rao, A., Borhani, S., Pilli, M., Deldari, S., Ge, X., Pezeshk, N., Han, T. C., Tolosa, M., Kostov, Y., Tolosa, L., Wood, D. W., Vattem, K., Frey, D. D., & Rao, G. (2018). Improving the recombinant human erythropoietin glycosylation using microsome supplementation in CHO cell-free system. Biotechnology and Bioengineering, 115(5), 1253–1264. https://doi.org/10.1002/bit.26554

Hahn, S. (2004). Structure and mechanism of the RNA polymerase II transcription machinery. Nature Structural & Molecular Biology, 11(5), 394–403. https://doi.org/10.1038/nsmb763

Hall, M. P., Woodroofe, C. C., Wood, M. G., Que, I., Van'T Root, M., Ridwan, Y., Shi, C., Kirkland, T. A., Encell, L. P., Wood, K. V., Löwik, C., & Mezzanotte, L. (2018). Click beetle luciferase mutant and near infrared naphthyl-luciferins for improved bioluminescence

imaging. Nature Communications, 9(1). https://doi.org/10.1038/s41467-017-02542-9

Han, Y., Yan, C., Fishbain, S., Ivanov, I., & He, Y. (2018). Structural visualization of RNA polymerase III transcription machineries. Cell Discovery, 4(1). https://doi.org/10.1038/s41421-018-0044-z

Harbut, M. B., Patel, B. A., Yeung, B. K. S., McNamara, C. W., Bright, A. T., Ballard, J., Supek, F., Golde, T. E., Winzeler, E. A., Diagana, T. T., & Greenbaum, D. C. (2012). Targeting the ERAD pathway via inhibition of signal peptide peptidase for antiparasitic therapeutic design. Proceedings of the National Academy of Sciences of the United States of America, 109(52), 21486–21491. https://doi.org/10.1073/pnas.1216016110

Carter, A. D., Morris, C. E., & McAllister, W. T. (1981). Revised transcription map of the late region of bacteriophage T7 DNA. Journal of Virology, 37(2), 636–642. https://doi.org/10.1128/jvi.37.2.636-642.1981

Hauser, A. R., Mecsas, J., & Moir, D. T. (2016). Beyond antibiotics: New therapeutic approaches for bacterial infections. Clinical Infectious Diseases, 63(1), 89–95. https://doi.org/10.1093/cid/ciw200

Hay, S. I., Okiro, E. A., Gething, P. W., Patil, A. P., Tatem, A. J., Guerra, C. A., & Snow, R. W. (2010). Estimating the global clinical burden of plasmodium falciparum malaria in 2007. PLoS Medicine, 7(6). https://doi.org/10.1371/journal.pmed.1000290

Haynes D. J., Diggs C. L., Hines F. A., & Desjardins R. E. (1976). Culture of human malaria Plasmodium falciparum. Nature, 263(5580):, 767–769.

Heaton, J. H., Dlakic, W. M., Dlakic, M., & Gelehrter, T. D. (2001). Identification and cDNA Cloning of a Novel RNA-binding Protein that Interacts with the Cyclic Nucleotide-responsive Sequence in the Type-1 Plasminogen Activator Inhibitor mRNA. Journal of Biological Chemistry, 276(5), 3341–3347. https://doi.org/10
.1074/jbc.M006538200

Helle, F., Duverlie, G., & Dubuisson, J. (2011). The hepatitis C virus glycan shield and evasion of the humoral immune response. Viruses, 3(10), 1909–1932. https://doi.org/10.3390/v3101909

Herrera, R., Anderson, C., Kumar, K., Molina-Cruz, A., Nguyen, V., Burkhardt, M., Reiter, K., Shimp, R., Howard, R. F., Srinivasan, P., Nold, M. J., Ragheb, D., Shi, L., DeCotiis, M., Aebig, J., Lambert, L., Rausch, K. M., Muratova, O., Jin, A., ... Naruma, D. L. (2015). Reversible conformational change in the plasmodium falciparum circumsporozoite protein masks Its adhesion domains. Infection and Immunity, 83(10), 3771–3780. https://doi.org/10.1128/IAI.02676-14

Hertz, M. I., & Thompson, S. R. (2011). In vivo functional analysis of the Dicistroviridae intergenic region internal ribosome entry sites. Nucleic Acids Research, 39(16), 7276–7288. https://doi.org/10.1093/nar/gkr427

Hetz, C. (2012). The unfolded protein response: Controlling cell fate decisions under ER stress and beyond. Nature Reviews Molecular Cell Biology, 13(2), 89–102. https://doi.org/10.1038/nrm3270

Hetz, C., Zhang, K., & Kaufman, R. J. (2020). Mechanisms, regulation and functions of the unfolded protein response. Nature Reviews Molecular Cell Biology, 21(8), 421–438. https://doi.org/10.1038/s41580-020-0250-z

Hjerrild, K. A., Jin, J., Wright, K. E., Brown, R. E., Marshall, J. M., Labbé, G. M., Silk, S. E., Cherry, C. J., Clemmensen, S. B., Jørgensen, T., Illingworth, J. J., Alanine, D. G. W., Milne, K. H., Ashfield, R., De Jongh, W. A., Douglas, A. D., Higgins, M. K., & Draper, S. J. (2016). Production of full-length soluble Plasmodium falciparum RH5 protein vaccine using a Drosophila melanogaster Schneider 2 stable cell line system. Scientific Reports, 6(July), 1–15. https://doi.org/10.1038/srep30357

Ho, C.-M., Beck, J. R., Lai, M., Cui, Y., Goldberg, D. E., Egea, P. F., & Zhou, Z. H. (2018). Malaria parasite translocon structure and mechanism of effector export. Nature, 561(7721), 70–75. https://doi.org/10.1038/s41586-018-0469-4

Ho, K. K. Y., Murray, V. L., & Liu, A. P. (2015). Engineering artificial cells by combining HeLa-based cell-free expression and ultrathin double emulsion template (pp. 303–318). https://doi.org/10.1016/bs.mcb.2015.01.014

Hoepfner, D., McNamara, C. W., Lim, C. S., Studer, C., Riedl, R., Aust, T., McCormack, S. L., Plouffe, D. M., Meister, S., Schuierer, S., Plikat, U., Hartmann, N., Staedtler, F., Cotesta, S., Schmitt, E. K., Petersen, F., Supek, F., Glynne, R. J., Tallarico, J. A., ... Winzeler, E. A. (2012). Selective and specific inhibition of the plasmodium falciparum lysyl-tRNA synthetase by the fungal secondary metabolite cladosporin. Cell Host and Microbe, 11(6), 654–663. https://doi.org/10.1016/j.chom.2012.04.015

Hoo, R., Bruske, E., Dimonte, S., Zhu, L., Mordmüller, B., Sim, B. K. L., Kremsner, P. G., Hoffman, S. L., Bozdech, Z., Frank, M., & Preiser, P. R. (2019). Transcriptome profiling reveals functional variation in Plasmodium falciparum parasites from controlled human malaria infection studies. EBioMedicine, 48, 442–452. https://doi.org/10.1016/j.ebiom.2019.09.001

Hospital, J. R. (2004). Mechanisms of Disease Mefloquine resistance in Plasmodium falciparum and increased pfmdr1 gene copy number. 364.
Hossler, P., Khattak, S. F., & Li, Z. J. (2009). Optimal and consistent protein glycosylation in mammalian cell culture. Glycobiology, 19(9), 936–949. https://doi.org/10.1093/glycob/cwp079

Hovlid, M. L., & Winzeler, E. A. (2016). Phenotypic Screens in Antimalarial Drug Discovery. Trends in Parasitology, 32(9), 697–707. https://doi.org/10.1016/j.pt.2016.04.014

Howley, Peter M.; Knipe, David M.; Whelan, S. (2020). Fields Virology: Emerging Viruses. Lippincott Williams & Wilkins (LWW).

Huang, C., Wang, Y., Li, X., Ren, L., Zhao, J., Hu, Y., Zhang, L., Fan, G., Xu, J., Gu, X., Cheng, Z., Yu, T., Xia, J., Wei, Y., Wu, W., Xie, X., Yin, W., Li, H., Liu, M., ... Cao, B. (2020). Clinical features of patients infected with 2019 novel coronavirus in Wuhan, China. The Lancet, 395(10223), 497–506. https://doi.org/10.1016/S0140-6736(20)30183-5

Hughes, J., and Mellows, G. (1980). Interaction of pseudomonic acid A with Escherichia coli B isoleucyl-tRNA synthetase. Biochem. J. 191, 209–219. https://doi.org/10.1016/j.chom.2012.04.015

Hunt, J. P., Wilding, K. M., Barnett, R. J., Robinson, H., Soltani, M., Cho, J. E., & Bundy, B. C. (2020). Engineering Cell-Free Protein Synthesis for High-Yield Production and Human Serum Activity Assessment of Asparaginase: Toward On-Demand Treatment of Acute Lymphoblastic Leukemia. Biotechnology Journal, 15(4), 1–6. https://doi.org/10.1002/biot.201900294

Hunter, M. J., & Commerford, S. L. (1961). Pressure homogenization of mammalian tissues. Biochimica et Biophysica Acta, 47(3), 580–586. https://doi.org/10.1016/0006-3002(61)90553-4

Hütter, J., Rödig, J. V., Höper, D., Seeberger, P. H., Reichl, U., Rapp, E., & Lepenies, B. (2013). Toward Animal Cell Culture–Based Influenza Vaccine Design: Viral Hemagglutinin N- Glycosylation Markedly Impacts Immunogenicity. The Journal of Immunology, 190(1), 220–230. https://doi.org/10.4049/jimmunol.1201060

Imwong, M., Hien, T. T., Thuy-Nhien, N. T., Dondorp, A. M., & White, N. J. (2017). Spread of a single multidrug resistant malaria parasite lineage (PfPailin) to Vietnam. The Lancet Infectious Diseases, 17(10), 1022–1023. https://doi.org/10.1016/S1473-3099(17)30524-8

Imwong, M., Suwannasin, K., Kunasol, C., Sutawong, K., Mayxay, M., Rekol, H., Smithuis, F. M., Hlaing, T. M., Tun, K. M., van der Pluijm, R. W., Tripura, R., Miotto, O., Menard, D., Dhorda, M., Day, N. P. J., White, N. J., & Dondorp, A. M. (2017). The spread of artemisinin-resistant Plasmodium falciparum in the Greater Mekong subregion: a molecular epidemiology observational study. The Lancet Infectious Diseases, 17(5), 491–497. https://doi.org/10.1016/S1473-3099(17)30048-8

Islam, M. S., Aryasomayajula, A., & Selvaganapathy, P. R. (2017). A review on macroscale and microscale cell lysis methods. Micromachines, 8(3).

Istvan, E. S., Dharia, N. V., Bopp, S. E., Gluzman, I., Winzeler, E. A., & Goldberg, D. E. (2011). Validation of isoleucine utilization targets in Plasmodium falciparum. Proceedings of the National Academy of Sciences of the United States of America, 108(4), 1627–1632. https://doi.org/10.1073/pnas.1011560108

Ivanov, K. I., Bašić, M., Varjosalo, M., & Mäkinen, K. (2014). One-step purification of twin-strep-tagged proteins and their complexes on strep-tactin resin cross-linked with Bis(sulfosuccinimidyl) suberate (BS3). Journal of Visualized Experiments, 86. https://doi.org/10.3791/51536

Iyori, M., Nakaya, H., Inagaki, K., Pichyangkul, S., Yamamoto, D. S., Kawasaki, M., Kwak, K., Mizukoshi, M., Goto, Y., Matsuoka, H., Matsumoto, M., & Yoshida, S. (2013). Protective Efficacy of Baculovirus Dual Expression System Vaccine Expressing Plasmodium falciparum Circumsporozoite Protein. PLoS ONE, 8(8). https://doi.org/10.1371/journal.pone.0070819

Izumiyama, S., Omura, M., Takasaki, T., Ohmae, H., & Asahi, H. (2009). Plasmodium falciparum: Development and validation of a measure of intraerythrocytic growth using SYBR Green I in a flow cytometer. Experimental Parasitology, 121(2), 144–150. https://doi.org/10.1016/j.exppara.2008.10.008

Jackson, A. M. (2004). Cell-free protein synthesis for proteomics. Briefings in Functional Genomics and Proteomics, 2(4), 308–319. https://doi.org/10.1093/bfgp/2.4.308

Jackson, R. J., Hellen, C. U. T., & Pestova, T. V. (2010). The mechanism of eukaryotic

translation initiation and principles of its regulation. Nature Reviews Molecular Cell Biology, 11(2), 113–127. https://doi.org/10.1038/nrm2838

Jain, V., Kikuchi, H., Oshima, Y., Sharma, A., & Yogavel, M. (2014). Structural and functional analysis of the anti-malarial drug target prolyl-tRNA synthetase. Journal of Structural and Functional Genomics, 15(4), 181–190. https://doi.org/10.1007/s10969-014-9186-x

Jain, V., Yogavel, M., Oshima, Y., Kikuchi, H., Touquet, B., Hakimi, M. A., & Sharma, A. (2015). Structure of prolyl-tRNA synthetase-halofuginone complex provides basis for development of drugs against malaria and toxoplasmosis. Structure, 23(5), 819–829. https://doi.org/10.1016/j.str.2015.02.011

Jaroentomeechai, T., Stark, J. C., Natarajan, A., Glasscock, C. J., Yates, L. E., Hsu, K. J., Mrksich, M., Jewett, M. C., & Delisa, M. P. (2018). Single-pot glycoprotein biosynthesis using a cell-free transcription-translation system enriched with glycosylation machinery. Nature Communications, 9(1), 1–11. https://doi.org/10.1038/s41467-018-05110-x

Jeffares, D. C., Pain, A., Berry, A., Cox, A. V., Stalker, J., Ingle, C. E., Thomas, A., Quail, M. A., Siebenthall, K., Uhlemann, A. C., Kyes, S., Krishna, S., Newbold, C., Dermitzakis, E. T., & Berriman, M. (2007). Genome variation and evolution of the malaria parasite Plasmodium falciparum. Nature Genetics, 39(1), 120–125. https://doi.org/10.1038/ng1931

Jefferis, R. (2009). Glycosylation as a strategy to improve antibody-based therapeutics. Nature Reviews Drug Discovery, 8(3), 226–234. https://doi.org/10.1038/nrd2804

José Juan Almagro Armenteros, Konstantinos D. Tsirigos, Casper Kaae Sønderby, Thomas Nordahl Petersen, Ole Winther, Søren Brunak, G. von H. and H. N. (n.d.). SignalP 5.0: improved signal peptide predictions across the tree of life using deep neural networks. http://www.cbs.dtu.dk/services/SignalP-5.0/

Joseph, B. C., Pichaimuthu, S., & Srimeenakshi, S. (2015). An Overview of the Parameters for Recombinant Protein Expression in Escherichia coli. Journal of Cell Science & Therapy, 06(05). https://doi.org/10.4172/2157-7013.1000221

Josling, G. A., Williamson, K. C., & Llinás, M. (2018). Regulation of Sexual Commitment and Gametocytogenesis in Malaria Parasites. Annual Review of Microbiology, 72, 501–519. https://doi.org/10.1146/annurev-micro-090817-062712

Julien, J. P., & Wardemann, H. (2019). Antibodies against Plasmodium falciparum malaria at the molecular level. Nature Reviews Immunology, 19(12), 761–775. https://doi.org/10.1038/s41577-019-0209-5

Justice, M. C., Hsu, M. J., Tse, B., Ku, T., Balkovec, J., Schmatz, D., & Nielsen, J. (1998). Elongation factor 2 as a novel target for selective inhibition of fungal protein synthesis. Journal of Biological Chemistry, 273(6), 3148–3151. https://doi.org/10.1074/jbc.273.6.3148

Kamuyu, G., Tuju, J., Kimathi, R., Mwai, K., Mburu, J., Kibinge, N., Chong Kwan, M., Hawkings, S., Yaa, R., Chepsat, E., Njunge, J. M., Chege, T., Guleid, F., Rosenkranz, M., Kariuki, C. K., Frank, R., Kinyanjui, S. M., Murungi, L. M., Bejon, P., ... Osier, F. H. A. (2018). KILchip v1.0: A Novel Plasmodium falciparum Merozoite Protein Microarray to Facil-

itate Malaria Vaccine Candidate Prioritization. Frontiers in Immunology, 9(December), 2866. https://doi.org/10.3389/fimmu.2018.02866

Kapoor, N., Vanjak, I., Rozzelle, J., Berges, A., Chan, W., Yin, G., Tran, C., Sato, A. K., Steiner, A. R., Pham, T. P., Birkett, A. J., Long, C. A., Fairman, J., & Miura, K. (2018). Malaria Derived Glycosylphosphatidylinositol Anchor Enhances Anti-Pfs25 Functional Antibodies That Block Malaria Transmission. Biochemistry, 57(5), 516–519. https://doi.org/10.1021/acs.biochem.7b01099

Karim, S. S. A. (2021). Vaccines and SARS-CoV-2 variants: the urgent need for a correlate of protection. Lancet (London, England), 397(10281), 1263–1264. https://doi.org/10.1016/S0140-6736(21)00468-2

Karlsson, A. J., Lim, H. K., Xu, H., Rocco, M. A., Bratkowski, M. A., Ke, A., & Delisa, M. P. (2012). Engineering antibody fitness and function using membrane-anchored display of correctly folded proteins. Journal of Molecular Biology, 416(1), 94–107. https://doi.org/10.1016/j.jmb.2011.12.021

Kaslow, D. C., Quakyi, I. A., Syin, C., Raum, M. G., Keister, D. B., Coligan, J. E., McCutchan, T. F., & Miller, L. H. (1988). A vaccine candidate from the sexual stage of human malaria that contains EGF-like domains. Nature, 333(6168), 74–76. https://doi.org/10.1038/333074a0

Kawasaki, T., Gouda, M. D., Sawasaki, T., Takai, K., & Endo, Y. (2003). Efficient synthesis of a disulfide-containing protein through a batch cell-free system from wheat germ. European Journal of Biochemistry, 270(23), 4780–4786. https://doi.org/10.1046/j.1432-1033.2003.03880.x

Kaznacheyeva, E., Lupu, V. D., & Bezprozvanny, I. (1998). Single-Channel Properties of Inositol (1,4,5)-Trisphosphate Receptor Heterologously Expressed in HEK-293 Cells. Journal of General Physiology, 111(6), 847–856. https://doi.org/10.1085/jgp.111.6.847

Keenan, R. J., Freymann, D. M., Stroud, R. M., & Walter, P. (2001). The Signal Recognition Particle. Annual Review of Biochemistry, 70(1), 755–775. https://doi.org/10.1146/annurev.biochem.70.1.755

Keller, T. L., Zocco, D., Sundrud, M. S., Hendrick, M., Edenius, M., Yum, J., Kim, Y. J., Lee, H. K., Cortese, J. F., Wirth, D. F., Dignam, J. D., Rao, A., Yeo, C. Y., Mazitschek, R., & Whitman, M. (2012). Halofuginone and other febrifugine derivatives inhibit prolyl-tRNA synthetase. Nature Chemical Biology, 8(3), 311–317. https://doi.org/10.1038/nchembio.790

Kelley, L. A., Mezulis, S., Yates, C. M., Wass, M. N., & Sternberg, M. J. (2016). The Phyre2 web portal for protein modeling, prediction and analysis. Nature Protocols, 10(6), 845–858. https://doi.org/10.1038/nprot.2015-053

Kennedy, K., Cobbold, S. A., Hanssen, E., Birnbaum, J., Spillman, N. J., McHugh, E., Brown, H., Tilley, L., Spielmann, T., McConville, M. J., & Ralph, S. A. (2019). Delayed death in the malaria parasite Plasmodium falciparum is caused by disruption of prenylation-dependent intracellular trafficking. PLoS Biology, 17(7), 1–28. https://doi.org/10.1371/journal.pbio.3000376

Kerr, C. H., Ma, Z. W., Jang, C. J., Thompson, S. R., & Jan, E. (2016). Molecular analysis of the factorless internal ribosome entry site in Cricket Paralysis virus infection. Scientific

Reports, 6(October), 1–11. https://doi.org/10.1038/srep37319

Khambhati, K., Bhattacharjee, G., Gohil, N., Braddick, D., Kulkarni, V., & Singh, V. (2019). Exploring the Potential of Cell-Free Protein Synthesis for Extending the Abilities of Biological Systems. Frontiers in Bioengineering and Biotechnology, 7(October), 1–16. https://doi.org/10.3389/fbioe.2019.00248

Khan, S. (2016). Recent advances in the biology and drug targeting of malaria parasite aminoacyl-tRNA synthetases. Malaria Journal, 15(1), 1–10. https://doi.org/10.1186/s12936-016-1247-0

Kigawa, T., & Yokoyama, S. (1991). A Continuous Cell-Free Protein Synthesis System for Coupled Transcription-Translation. The Journal of Biochemistry, 110(2), 166–168. https://doi.org/10.1093/oxfordjournals.jbchem.a123551

Kim, D. M., & Swartz, J. R. (1999). Prolonging cell-free protein synthesis with a novel ATP regeneration system. Biotechnology and Bioengineering, 66(3), 180–188. https://doi.org/10.1002/(SICI)1097-0290(1999)

Kim, D. M., & Swartz, J. R. (2001). Regeneration of adenosine triphosphate from glycolytic intermediates for cell-free protein synthesis. Biotechnology and Bioengineering, 74(4), 309–316. https://doi.org/10.1002/bit.1121

Klayman, D. L., Lin, A. J., Acton, N., Scovill, J. P., Hoch, J. M., Milhous, W. K., Theoharides, A. D., & Dobek, A. S. (1984). Isolation of Artemisinin (Qinghaosu) from Artemisia Annua Growing in the United States. Journal of Natural Products, 47(4), 715–717. https://doi.org/10.1021/np50034a027

Kobayashi, T., Yukigai, J., Ueda, K., Machida, K., Masutani, M., Nishino, Y., Miyazawa, A., & Imataka, H. (2013). Purification and visualization of encephalomyocarditisvirus synthesized by an in vitro protein expression system derived from mammalian cell extract. Biotechnology Letters, 35(3), 309–314. https://doi.org/10.1007/s10529-012-1086-1

Koh, E. Y. C., Ho, S. C. L., Mariati, Song, Z., Bi, X., Bardor, M., & Yang, Y. (2013). An internal ribosome entry site (IRES) mutant library for tuning expression level of multiple genes in mammalian cells. PLoS ONE, 8(12). https://doi.org/10.1371/journal.pone.0082100

Koirala, D., Shao, Y., Koldobskaya, Y., Fuller, J. R., Watkins, A. M., Shelke, S. A., Pilipenko, E. V., Das, R., Rice, P. A., & Piccirilli, J. A. (2019). A conserved RNA structural motif for organizing topology within picornaviral internal ribosome entry sites. Nature Communications, 10(1), 1–13. https://doi.org/10.1038/s41467-019-11585-z

Kornberg, R. D. (2014). The molecular basis of eukaryotic transcription. Nobel Lectures: Chemistry: 2006 - 2010, 104(32), 14–33. https://doi.org/10.1142/9789814635660_0001

Krafts, K., Hempelmann, E., & Skórska-Stania, A. (2012). From methylene blue to chloroquine: A brief review of the development of an antimalarial therapy. Parasitology Research, 111(1), 1–6. https://doi.org/10.1007/s00436-012-2886-x

Kublin, J. G., Mikolajczak, S. A., Sack, B. K., Fishbaugher, M. E., Seilie, A., Shelton, L.,

VonGoedert, T., Firat, M., Magee, S., Fritzen, E., Betz, W., Kain, H. S., Dankwa, D. A., Steel, R. W. J., Vaughan, A. M., Sather, D. N., Murphy, S. C., & Kappe, S. H. I. (2017). Complete attenuation of genetically engineered Plasmodium falciparum sporozoites in human subjects. Science Translational Medicine, 9(371). https://doi.org/10.1126/scitranslmed.aad9099

Kufareva, I., & Abagyan, R. (2012). Methods of protein structure comparison. Methods in Molecular Biology, 857, 231–257. https://doi.org/10.1007/978-1-61779-588-6_10

Kumar, B., Verma, S., Kashif, M., Sharma, R., Atul, Dixit, R., Singh, A. P., Pande, V., Saxena, A. K., Abid, M., & Pandey, K. C. (2019). Metacaspase-3 of Plasmodium falciparum: An atypical trypsin-like serine protease. International Journal of Biological Macromolecules, 138, 309–320. https://doi.org/10.1016/j.ijbiomac.2019.07.067

Lan, J., Ge, J., Yu, J., Shan, S., Zhou, H., Fan, S., Zhang, Q., Shi, X., Wang, Q., Zhang, L., & Wang, X. (2020). Structure of the SARS-CoV-2 spike receptor-binding domain bound to the ACE2 receptor. Nature, 581(7807), 215–220. https://doi.org/10.1038/s41586-020-2180-5

Langlais, C., Guilleaume, B., Wermke, N., Scheuermann, T., Ebert, L., LaBaer, J., & Korn, B. (2007). A systematic approach for testing expression of human full-length proteins in cell-free expression systems. BMC Biotechnology, 7, 1–11. https://doi.org/10.1186/1472-6750-7-64

Laurens, M. B., Kouriba, B., Bergmann-Leitner, E., Angov, E., Coulibaly, D., Diarra, I., Daou, M., Niangaly, A., Blackwelder, W. C., Wu, Y., Cohen, J., Ballou, W. R., Vekemans, J., Lanar, D. E., Dutta, S., Diggs, C., Soisson, L., Heppner, D. G., Doumbo, O. K., ... Thera, M. A. (2017). Strain-specific Plasmodium falciparum growth inhibition among Malian children immunized with a blood-stage malaria vaccine. PLoS ONE, 12(3), 1–13. https://doi.org/10.1371/journal.pone.0173294

Lawson, A. (2015). G Protein-Coupled Receptors - Targets for Fragment-based Drug Discovery. In Current Topics in Medicinal Chemistry (Vol. 15, Issue 24). https://doi.org/10.2174/1568026615666150701113151

Le Ru, A., Jacob, D., Transfiguracion, J., Ansorge, S., Henry, O., & Kamen, A. A. (2010). Scalable production of influenza virus in HEK-293 cells for efficient vaccine manufacturing. Vaccine, 28(21), 3661–3671. https://doi.org/10.1016/j.vaccine.2010.03.029

Lee, S. M., Wu, C. K., Plieskatt, J., McAdams, D. H., Miura, K., Ockenhouse, C., & King, C. R. (2016). Assessment of Pfs25 expressed from multiple soluble expression platforms for use as transmission-blocking vaccine candidates. Malaria Journal, 15(1), 1–12. https://doi.org/10.1186/s12936-016-1464-6

LenioBio. (n.d.). ALiCE® Cell Free Protein Expression. https://www.leniobio.com/buy-alice/

Li, F. (2012). Evidence for a Common Evolutionary Origin of Coronavirus Spike Protein Receptor-Binding Subunits. Journal of Virology, 86(5), 2856–2858. https://doi.org/10.1128/JVI.06882-11

Li, J., Zhang, L., & Liu, W. (2018). Cell-free synthetic biology for in vitro biosynthesis of pharmaceutical natural products. Synthetic and Systems Biotechnology, 3(2), 83–89. https://doi.org

/10.1016/j.synbio.2018.02.002

Li, W. B., Bzik, D. J., Gu, H., Tanaka, M., Fox, B. A., & Inselburg, J. (1989). An enlarged largest subunit or Plasmodium falciparum RNA polymerase II defines conserved and variable RNA polymerase domains. Nucleic Acids Research, 17(23), 9621–9636. https://doi.org/10.1093/nar/17.23.9621

Li, W. B., Bzik, D. J., Tanaka, M., Gu, H., Fox, B. A., & Inselburg, J. (1991). Characterization of the gene encoding the largest subunit of Plasmodium falciparum RNA polymerase III. Molecular and Biochemical Parasitology, 46(2), 229–239. https://doi.org/10.1016/0166-6851(91)90047-A

Li, Y., Carroll, D. S., Gardner, S. N., Walsh, M. C., Vitalis, E. A., & Damon, I. K. (2007). On the origin of smallpox: Correlating variola phylogenics with historical smallpox records. Proceedings of the National Academy of Sciences of the United States of America, 104(40), 15787–15792. https://doi.org/10.1073/pnas.0609268104

Libicher, K., Hornberger, R., Heymann, M., & Mutschler, H. (2020). In vitro self-replication and multicistronic expression of large synthetic genomes. Nature Communications, 11(1), 1–8. https://doi.org/10.1038/s41467-020-14694-2

Lin, C. S., Uboldi, A. D., Epp, C., Bujard, H., Tsuboi, T., Czabotar, P. E., & Cowman, X. A. F. (2016). Multiple plasmodium falciparum merozoite surface protein 1 complexes mediate merozoite binding to human erythrocytes. Journal of Biological Chemistry, 291(14), 7703–7715. https://doi.org/10.1074/jbc.M115.698282

Lin, Y. C., Boone, M., Meuris, L., Lemmens, I., Van Roy, N., Soete, A., Reumers, J., Moisse, M., Plaisance, S., Drmanac, R., Chen, J., Speleman, F., Lambrechts, D., Van De Peer, Y., Tavernier, J., & Callewaert, N. (2014). Genome dynamics of the human embryonic kidney 293 lineage in response to cell biology manipulations. Nature Communications, 5(11). https://doi.org/10.1038/ncomms5767

Liu, Z., Chen, O., Wall, J. B. J., Zheng, M., Zhou, Y., Wang, L., Ruth Vaseghi, H., Qian, L., & Liu, J. (2017). Systematic comparison of 2A peptides for cloning multi-genes in a polycistronic vector. Scientific Reports, 7(1), 1–9. https://doi.org/10.1038/s41598-017-02460-2

Lobstein, J., Emrich, C. A., Jeans, C., Faulkner, M., Riggs, P., & Berkmen, M. (2016). SHuffle, a novel Escherichia coli protein expression strain capable of correctly folding disulfide bonded proteins in its cytoplasm. Microbial Cell Factories, 15(1), 124. https://doi.org/10.1186/s12934-016-0512-9

Lockard, R. E., & Lingrel, J. B. (1969). The synthesis of mouse hemoglobin chains in a rabbit reticulocyte cell-free system programmed with mouse reticulocyte 9S RNA. Biochemical and Biophysical Research Communications, 37(2), 204–212. https://doi.org/10.1016/0006-291X(69)90720-7

Longley, R. J., White, M. T., Takashima, E., Morita, M., Kanoi, B. N., Li Wai Suen, C. S. N., Betuela, I., Kuehn, A., Sripoorote, P., Franca, C. T., Siba, P., Robinson, L. J., Lacerda, M., Sattabongkot, J., Tsuboi, T., & Mueller, I. (2017). Naturally acquired antibody responses to more than 300 Plasmodium vivax proteins in three geographic regions. PLoS Neglected

Tropical Diseases, 11(9), 1–15. https://doi.org/10.1371/journal.pntd.0005888

Lopaticki, S., Yang, A. S. P., John, A., Scott, N. E., Lingford, J. P., O'Neill, M. T., Erickson, S. M., McKenzie, N. C., Jennison, C., Whitehead, L. W., Douglas, D. N., Kneteman, N. M., Goddard-Borger, E. D., & Boddey, J. A. (2017). Protein O-fucosylation in Plasmodium falciparum ensures efficient infection of mosquito and vertebrate hosts. Nature Communications, 8(1). https://doi.org/10.1038/s41467-017-00571-y

Loy, D. E., Liu, W., Li, Y., Learn, G. H., Plenderleith, L. J., Sundararaman, S. A., Sharp, P. M., & Hahn, B. H. (2017). Out of Africa: origins and evolution of the human malaria parasites Plasmodium falciparum and Plasmodium vivax. International Journal for Parasitology, 47(2–3), 87–97. https://doi.org/10.1016/j.ijpara.2016.05.008

Lozano, G., & Martínez-Salas, E. (2015). Structural insights into viral IRES-dependent translation mechanisms. Current Opinion in Virology, 12, 113–120. https://doi.org/10.1016/j.coviro.2015.04.008

Lu, C., Song, G., Beale, K., Yan, J., Garst, E., Feng, J., Lund, E., Catteruccia, F., & Springer, T. A. (2020). Design and assessment of TRAP-CSP fusion antigens as effective malaria vaccines. PLoS ONE, 15(1), 1–19. https://doi.org/10.1371/journal.pone.0216260

LU, F., HE, X.-L., Richard, C., & CAO, J. (2019). A brief history of artemisinin: Modes of action and mechanisms of resistance. Chinese Journal of Natural Medicines, 17(5), 331–336. https://doi.org/10.1016/S1875-5364(19)30038-X

Luttrell, B. M. (1994). Cellular actions of inositol phosphates and other natural calcium and magnesium chelators. Cellular Signalling, 6(4), 355–362. https://doi.org/10.1016/0898-6568(94)90084-1

Lykke-Andersen, J., & Christiansen, J. (1998). The C-terminal carboxy group of T7 RNA polymerase ensures efficient magnesium ion-dependent catalysis. Nucleic Acids Research, 26(24), 5630–5635. https://doi.org/10.1093/nar/26.24.5630

Lytton, J., Westlin, M., & Hanley, M. R. (1991). Thapsigargin inhibits the sarcoplasmic or endoplasmic reticulum Ca-ATPase family of calcium pumps. Journal of Biological Chemistry, 266(26), 17067–17071. https://doi.org/10.1016/s0021-9258(19)47340-7

Lyukmanova, E. N., Shenkarev, Z. O., Khabibullina, N. F., Kopeina, G. S., Shulepko, M. A., Paramonov, A. S., Mineev, K. S., Tikhonov, R. V., Shingarova, L. N., Petrovskaya, L. E., Dolgikh, D. A., Arseniev, A. S., & Kirpichnikov, M. P. (2012). Lipid-protein nanodiscs for cell-free production of integral membrane proteins in a soluble and folded state: Comparison with detergent micelles, bicelles and liposomes. Biochimica et Biophysica Acta - Biomembranes, 1818(3), 349–358. https://doi.org/10.1016/j.bbamem.2011.10.020

Ma, C., Yang, X., & Lewis, P. J. (2016). Bacterial Transcription as a Target for Antibacterial Drug Development. Microbiology and Molecular Biology Reviews, 80(1), 139–160. https://doi.org/10.1128/mmbr.00055-15

Mackinnon, M. J., & Read, A. F. (2004). Immunity promotes virulence evolution in a malaria model. PLoS Biology, 2(9). https://doi.org/10.1371/journal.pbio.0020230

Madin, K., Sawasaki, T., Ogasawara, T., & Endo, Y. (2000). A highly efficient and robust cell-free protein synthesis system prepared from wheat embryos: Plants apparently contain a suicide system directed at ribosomes. Proceedings of the National Academy of Sciences of the United States of America, 97(2), 559–564. https://doi.org/10.1073/pnas.97.2.559

Mahmoudi, S., & Keshavarz, H. (2017). Efficacy of phase 3 trial of RTS, S/AS01 malaria vaccine: The need for an alternative development plan. Human Vaccines and Immunotherapeutics, 13(9), 2098–2101. https://doi.org/10.1080/21645515.2017.1295906

McNamara, C. W., Lee, M. C. S., Lim, C. S., Lim, S. H., Roland, J., Nagle, A., Simon, O., Yeung, B. K. S., Chatterjee, A. K., McCormack, S. L., Manary, M. J., Zeeman, A. M., Dechering, K. J., Kumar, T. R. S., Henrich, P. P., Gagaring, K., Ibanez, M., Kato, N., Kuhen, K. L., . . . Winzeler, E. A. (2013). Targeting Plasmodium PI(4)K to eliminate malaria. Nature, 504(7479), 248–253. https://doi.org/10.1038/nature12782

Malm, M., Saghaleyni, R., Lundqvist, M., Giudici, M., Chotteau, V., Field, R., Varley, P. G., Hatton, D., Grassi, L., Svensson, T., Nielsen, J., & Rockberg, J. (2020). Evolution from adherent to suspension: systems biology of HEK293 cell line development. Scientific Reports, 10(1), 1–15. https://doi.org/10.1038/s41598-020-76137-8

Malpede, B. M., & Tolia, N. H. (2014). Malaria adhesins: Structure and function. Cellular Microbiology, 16(5), 621–631. https://doi.org/10.1111/cmi.12276

Manley, J. L., Fire, A., Cano, A., Sharp, P. A., & Gefter, M. L. (1980). DNA-dependent transcription of adenovirus genes in a soluble whole-cell extract. Proceedings of the National Academy of Sciences, 77(7), 3855–3859. https://doi.org/10.1073/pnas.77.7.3855

Mairhofer, J., Wittwer, A., Cserjan-puschmann, M., & Striedner, G. (2014). Synthetic Termination Signal Capable of Improving Bioprocess. ACS Synthetic Biology, May, web.

Marissen, W. E., Guo, Y., Thomas, A. A. M., Matts, R. L., & Lloyd, R. E. (2000). Identification of caspase 3-mediated cleavage and functional alteration of eukaryotic initiation factor 2α in apoptosis. Journal of Biological Chemistry, 275
(13), 9314–9323. https://doi.org/10.1074/jbc.275.13.9314

Marth, J. D., & Grewal, P. K. (2008). Mammalian glycosylation in immunity. Nature Reviews Immunology, 8(11), 874–887. https://doi.org/10.1038/nri2417

Marti, M., Good, R. T., Rug, M., Knuepfer, E., & Cowman, A. F. (2004). Targeting malaria virulence and remodeling proteins to the host erythrocyte. Science, 306(5703), 1930–1933. https://doi.org/10.1126/science.1102452

Martínez-Salas, E. (1999). Internal ribosome entry site biology and its use in expression vectors. Current Opinion in Biotechnology, 10(5), 458–464. https://doi.org/10.1016/S0958-1669(99)00010-5

Matos, C. F. R. O., Robinson, C., Alanen, H. I., Prus, P., Uchida, Y., Ruddock, L. W., Freedman, R. B., & Keshavarz-Moore, E. (2014). Efficient export of prefolded, disulfide-bonded recombinant proteins to the periplasm by the Tat pathway in Escherichia coli CyDisCo strains.

Biotechnology Progress, 30(2), 281–290. https://doi.org/10.1002/btpr.1858

Matsuda, T., Ito, T., Takemoto, C., Katsura, K., Ikeda, M., Wakiyama, M., Kukimoto-Niino, M., Yokoyama, S., Kurosawa, Y., & Shirouzu, M. (2018). Cell-free synthesis of functional antibody fragments to provide a structural basis for antibody–antigen interaction. PLoS ONE, 13(2), 1–19. https://doi.org/10.1371/journal.pone.0193158

Matsuda, T., Watanabe, S., & Kigawa, T. (2013). Cell-free synthesis system suitable for disulfide-containing proteins. Biochemical and Biophysical Research Communications, 431(2), 296–301. https://doi.org/10.1016/j.bbrc.2012.12.107

Matthews, H., Deakin, J., Rajab, M., Idris-Usman, M., & Nirmalan, N. J. (2017). Investigating antimalarial drug interactions of emetine dihydrochloride hydrate using CalcuSyn-based interactivity calculations. PLoS ONE, 12(3), 1–19. https://doi.org/10.1371/journal.pone.0173303

Matthews, H., Usman-Idris, M., Khan, F., Read, M., & Nirmalan, N. (2013). Drug repositioning as a route to anti-malarial drug discovery: Preliminary investigation of the in vitro antimalarial efficacy of emetine dihydrochloride hydrate. Malaria Journal, 12(1), 1–11. https://doi.org/10.1186/1475-2875-12-359

McCarthy, A. E., & Coyle, D. (2010). Determining utility values related to malaria and malaria chemoprophylaxis. Malaria Journal, 9(1), 1–5. https://doi.org/10.1186/1475-2875-9-92

McPherson, A., & Gavira, J. A. (2014). Introduction to protein crystallization. Acta Crystallographica Section F:Structural Biology Communications, 70(1), 2–20. https://doi.org/10.1107/S2053230X13033141

Mehlin, C., Boni, E., Buckner, F. S., Engel, L., Feist, T., Gelb, M. H., Haji, L., Kim, D., Liu, C., Mueller, N., Myler, P. J., Reddy, J. T., Sampson, J. N., Subramanian, E., Van Voorhis, W. C., Worthey, E., Zucker, F., & Hol, W. G. J. (2006). Heterologous expression of proteins from Plasmodium falciparum: Results from 1000 genes. Molecular and Biochemical Parasitology, 148(2), 144–160. https://doi.org/10.1016/j.molbiopara.2006.03.011

Mikami, S., Masutani, M., Sonenberg, N., Yokoyama, S., & Imataka, H. (2006). An efficient mammalian cell-free translation system supplemented with translation factors. Protein Expression and Purification, 46(2), 348–357. https://doi.org/10.1016/j.pep.2005.09.021

Mirando, A. C., Francklyn, C. S., & Lounsbury, K. M. (2014). Regulation of angiogenesis by aminoacyl-trna synthetases. International Journal of Molecular Sciences, 15(12), 23725–23748. https://doi.org/10.3390/ijms151223725

Mishra, M., Mishra, V. K., Kashaw, V., Iyer, A. K., & Kashaw, S. K. (2017). Comprehensive review on various strategies for antimalarial drug discovery. European Journal of Medicinal Chemistry, 125, 1300–1320. https://doi.org/10.1016/j.ejmech.2016.11.025
Missiakas, D., & Raina, S. (1997). Protein folding in the bacterial periplasm. Journal of Bacteriology, 179(8), 2465–2471. https://doi.org/10.1128/jb.179.8.2465-2471.1997

Miura, K., Tachibana, M., Takashima, E., Morita, M., Kanoi, B. N., Nagaoka, H., Baba, M., Torii, M., Ishino, T., & Tsuboi, T. (2019). Malaria transmission-blocking vaccines: wheat germ cell-free technology can accelerate vaccine development. Expert Review of Vaccines, 18(10),

1017–1027. https://doi.org/10.1080/14760584.2019.1674145

MMV. (n.d.). MMV - Pathogen Box. https://www.mmv.org/mmv-open/pathogen-box

Miura, K., Takashima, E., Deng, B., Tullo, G., Diouf, A., Moretz, S. E., Nikolaeva, D., Diakite, M., Fairhurst, R. M., Fay, M. P., Long, C. A., & Tsuboi, T. (2013). Functional comparison of plasmodium falciparum transmission-blocking vaccine candidates by the standard membrane-feeding assay. Infection and Immunity, 81(12), 4377–4382. https://doi.org/10.1128/IAI.01056-13

Moffat, J. G., Vincent, F., Lee, J. A., Eder, J., & Prunotto, M. (2017). Opportunities and challenges in phenotypic drug discovery: An industry perspective. Nature Reviews Drug Discovery, 16(8), 531–543. https://doi.org/10.1038/nrd.2017.111

Mokrejs, M., Vopálenský, V., Kolenaty, O., Masek, T., Feketová, Z., Sekyrová, P., Skaloudová, B., Kríz, V., & Pospísek, M. (2006). IRESite: the database of experimentally verified IRES structures (www.iresite.org). Nucleic Acids Research, 34, 125–130. https://doi.org/10.1093/nar/gkj081

Moldavel, K. (1985). Eukaryotic Protein Synthesis. Annual Reviews Biochemistry, 54:1109-49
Moore, A. J., Mangou, K., Diallo, F., Sene, S. D., Pouye, M. N., Sadio, B. D., Faye, O., Mbengue, A., & Bei, A. K. (2021). Assessing the functional impact of PfRh5 genetic diversity on ex vivo erythrocyte invasion inhibition. Scientific Reports, 11(1), 1–8. https://doi.org/10.1038/s41598-021-81711-9

Morita, M., Takashima, E., Ito, D., Miura, K., Thongkukiatkul, A., Diouf, A., Fairhurst, R. M., Diakite, M., Long, C. A., Torii, M., & Tsuboi, T. (2017). Immunoscreening of Plasmodium falciparum proteins expressed in a wheat germ cell-free system reveals a novel malaria vaccine candidate. Scientific Reports, 7(April), 1–8. https://doi.org/10.1038/srep46086

Morrison, T. G., & McQuain, C. (1977). Assembly of viral membranes. I. Association of vesicular stomatitis virus membrane proteins and membranes in a cell-free system. Journal of Virology, 21(2), 451–458. https://doi.org/10.1128/jvi.21.2.451-458.1977

Mudeppa, D. G., & Rathod, P. K. (2013). Expression of functional Plasmodium falciparum enzymes using a wheat germ cell-free system. Eukaryotic Cell, 12(12), 1653–1663. https://doi.org/10.1128/EC.00222-13

Müller, M. M. (2018). Post-Translational Modifications of Protein Backbones: Unique Functions, Mechanisms, and Challenges. Biochemistry, 57(2), 177–185. https://doi.org/10.1021/acs.biochem.7b00861

Munro, S., & Pelham, H. R. (1984). Use of peptide tagging to detect proteins expressed from cloned genes: deletion mapping functional domains of Drosophila hsp 70. The EMBO Journal, 3(13), 3087–3093. https://doi.org/10.1002/j.1460-2075.1984.tb02263.x

Murphy, S. C., & Breman, J. G. (2001). GAPS in the childhood malaria burden in Africa: Cerebral malaria, neurological sequelae, anemia, respiratory distress, hypoglycemia, and complications of pregnancy. American Journal of Tropical Medicine and Hygiene, 64(1-2 SUPPL.), 57–67. https://doi.org/10.4269/ajtmh.2001.64.57

Myer, V. E., & Young, R. A. (1998). RNA polymerase II holoenzymes and subcomplexes. Journal of Biological Chemistry, 273(43), 27757–27760. https://doi.org/10.1074/jbc.273.43.27757

Na-Bangchang, K., Ruengweerayut, R., Mahamad, P., Ruengweerayut, K., & Chaijaroenkul, W. (2010). Declining in efficacy of a three-day combination regimen of mefloquine-artesunate in a multi-drug resistance area along the Thai-Myanmar border. Malaria Journal, 9(1), 1–10. https://doi.org/10.1186/1475-2875-9-273

Naik, R. S., Branch, O. L. H., Woods, A. S., Vijaykumar, M., Perkins, D. J., Nahlen, B. L., Lal, A. A., Cotter, R. J., Costello, C. E., Ockenhouse, C. F., Davidson, E. A., & Gowda, D. C. (2000). Glycosylphosphatidylinositol anchors of Plasmodium falciparum: Molecular characterization and naturally elicited antibody response that may provide immunity to malaria pathogenesis. Journal of Experimental Medicine, 192(11), 1563–1575. https://doi.org/10.1084/jem.192.11.1563

Narasimhan, J., Joyce, B. R., Naguleswaran, A., Smith, A. T., Livingston, M. R., Dixon, S. E., Coppens, I., Wek, R. C., & Sullivan, W. J. (2008). Translation regulation by eukaryotic initiation factor-2 kinases in the development of latent cysts in Toxoplasma gondii. Journal of Biological Chemistry, 283(24), 16591–16601. https://doi.org/10.1074/jbc.M800681200

Nguyen, D., Stutz, R., Schorr, S., Lang, S., Pfeffer, S., Freeze, H. H., Förster, F., Helms, V., Dudek, J., & Zimmermann, R. (2018). Proteomics reveals signal peptide features determining the client specificity in human TRAP-dependent ER protein import. Nature Communications, 9(1). https://doi.org/10.1038/s41467-018-06188-z

Nie, A., Sun, B., Fu, Z., & Yu, D. (2019). Roles of aminoacyl-tRNA synthetases in immune regulation and immune diseases. Cell Death and Disease, 10(12). https://doi.org/10.1038/s41419-019-2145-5

Nielsen, H., Engelbrecht, J., von Heijne, G., & Brunak, S. (1996). Defining a similarity threshold for a functional protein sequence pattern: The signal peptide cleavage site. Proteins: Structure, Function, and Genetics, 24(2), 165–177. https://doi.org/10.1002/(SICI)1097-0134(199602)24:2¡165::AID-PROT4¿3.0.CO;2-I

Nirenberg, M. W. (1964). Cell-Free Protein Synthesis By Messenger RNA. Methods in Enzymology VI, 1588(1961), 17–23. https://doi.org/101584910X118

Njama-Meya, D., Kamya, M. R., & Dorsey, G. (2004). Asymptomatic parasitaemia as a risk factor for symptomatic malaria in a cohort of Ugandan children. Tropical Medicine and International Health, 9(8), 862–868. https://doi.org/10.1111/j.1365-3156.2004.01277.x

Noe, A. R., Espinosa, D., Li, X., Coelho-Dos-Reis, J. G. A., Funakoshi, R., Giardina, S., Jin, H., Retallack, D. M., Haverstock, R., Allen, J. R., Vedvick, T. S., Fox, C. B., Reed, S. G., Ayala, R., Roberts, B., Winram, S. B., Sacci, J., Tsuji, M., Zavala, F., & Gutierrez, G. M. (2014). A full-length Plasmodium falciparum recombinant circumsporozoite protein expressed by Pseudomonas fluorescens platform as a Malaria vaccine candidate. PLoS ONE, 9(9). https://doi.org/10.1371/journal.pone.0107764

Novikova, I. V., Sharma, N., Moser, T., Sontag, R., Liu, Y., Collazo, M. J., Cascio, D., Shokuh-

far, T., Hellmann, H., Knoblauch, M., & Evans, J. E. (2018). Protein structural biology using cell-free platform from wheat germ. Advanced Structural and Chemical Imaging, 4(1), 1–13. https://doi.org/10.1186/s40679-018-0062-9

Nyamai, D. W., & Tastan Bishop, Ö. (2019). Aminoacyl tRNA synthetases as malarial drug targets: A comparative bioinformatics study. Malaria Journal, 18(1), 1–27. https://doi.org/10.1186/s12936-019-2665-6

Nzila, A., & Mwai, L. (2009). In vitro selection of Plasmodium falciparum drug-resistant parasite lines. Journal of Antimicrobial Chemotherapy, 65(3), 390–398. https://doi.org/10.1093/jac/dkp449

Oehring, S. C., Woodcroft, B. J., Moes, S., Wetzel, J., Dietz, O., Pulfer, A., Dekiwadia, C., Maeser, P., Flueck, C., Witmer, K., Brancucci, N. M. B., Niederwieser, I., Jenoe, P., Ralph, S. A., & Voss, T. S. (2012). Organellar proteomics reveals hundreds of novel nuclear proteins in the malaria parasite Plasmodium falciparum. Genome Biology, 13(11). https://doi.org/10.1186/gb-2012-13-11-r108

Ogbechi, J., Hall, B. S., Sbarrato, T., Taunton, J., Willis, A. E., Wek, R. C., & Simmonds, R. E. (2018). Inhibition of Sec61-dependent translocation by mycolactone uncouples the integrated stress response from ER stress, driving cytotoxicity via translational activation of ATF4. Cell Death and Disease, 9(3). https://doi.org/10.1038/s41419-018-0427-y

Oka, O. B. V., & Bulleid, N. J. (2013). Forming disulfides in the endoplasmic reticulum. Biochimica et Biophysica Acta - Molecular Cell Research, 1833(11), 2425–2429. https://doi.org/10.1016/j.bbamcr.2013.02.007

Omrani, A. S., Al-Tawfiq, J. A., & Memish, Z. A. (2015). Middle east respiratory syndrome coronavirus (Mers-coV): Animal to human interaction. Pathogens and Global Health, 109(8), 354–362. https://doi.org/10.1080/20477724.2015.1122852

Ord, R. L., Rodriguez, M., & Lobo, C. A. (2015). Malaria invasion ligand RH5 and its prime candidacy in blood-stage malaria vaccine design. Human Vaccines and Immunotherapeutics, 11(6), 1465–1473. https://doi.org/10.1080/21645515.2015.1026496

Oyen, D., Torres, J. L., Aoto, P. C., Flores-Garcia, Y., Binter, Š., Pholcharee, T., Carroll, S., Reponen, S., Wash, R., Liang, Q., Lemiale, F., Locke, E., Bradley, A., Richter King, C., Emerling, D., Kellam, P., Zavala, F., Ward, A. B., & Wilson, I. A. (2020). Structure and mechanism of monoclonal antibody binding to the junctional epitope of Plasmodium falciparum circumsporozoite protein. PLoS Pathogens, 16(3), 1–22. https://doi.org/10.1371/journal.ppat.1008373

Oyen, D., Torres, J. L., Wille-Reece, U., Ockenhouse, C. F., Emerling, D., Glanville, J., Volkmuth, W., Flores-Garcia, Y., Zavala, F., Ward, A. B., Richter King, C., & Wilson, I. A. (2018). Structural basis for antibody recognition of the NANP repeats in Plasmodium falciparum circumsporozoite protein. Proceedings of the National Academy of Sciences, 115(25), E5838–E5839. https://doi.org/10.1073/pnas.1808460115

Painter, H. J., Chung, N. C., Sebastian, A., Albert, I., Storey, J. D., & Llinás, M. (2018). Genome-wide real-time in vivo transcriptional dynamics during Plasmodium falciparum blood-stage development. Nature Communications, 9(1), 1–12. https://doi.org/10.1038/s41467-018-

04966-3

Panwar, P., Burusco, K. K., Abubaker, M., Matthews, H., Gutnov, A., Fernández-Álvaro, E., Bryce, R. A., Wilkinson, J., & Nirmalan, N. (2020). Lead optimization of dehydroemetine for repositioned use in malaria. Antimicrobial Agents and Chemotherapy, 64(4). https://doi.org/10.1128/AAC.01444-19

Parks, G. D., Duke, G. M., & Palmenberg, A. C. (1986). Encephalomyocarditis virus 3C protease: efficient cell-free expression from clones which link viral 5' noncoding sequences to the P3 region. Journal of Virology, 60(2), 376–384. https://doi.org/10.1128/jvi.60.2.376-384.1986

Parra, M., Hui, G., Johnson, A. H., Berzofsky, J. A., Roberts, T., Quakyi, I. A., & Taylor, D. W. (2000). Characterization of conserved T- and B-cell epitopes in Plasmodium falciparum major merozoite surface protein 1. Infection and Immunity, 68(5), 2685–2691. https://doi.org/10.1128/IAI.68.5.2685-2691.2000

Patel, K. G., & Swartz, J. R. (2011). Surface functionalization of virus-like particles by direct conjugation using azide-alkyne click chemistry. Bioconjugate Chemistry, 22(3), 376–387. https://doi.org/10.1021/bc100367u

Patel, P. N., & Tolia, N. (2021). Structural vaccinology of malaria transmission-blocking vaccines. Expert Review of Vaccines, 00(00), 1–16. https://doi.org/10.1080/14760584.2021.1873135

Patra, A. P., Sharma, S., & Ainavarapu, S. R. K. (2017). Force spectroscopy of the Plasmodium falciparum vaccine candidate circumsporozoite protein suggests a mechanically pliable repeat region. Journal of Biological Chemistry, 292(6), 2110–2119. https://doi.org/10.1074/jbc.M116.754796

Paulick, M. G., & Bertozzi, C. R. (2008). The glycosylphosphatidylinositol anchor: A complex membrane-anchoring structure for proteins. Biochemistry, 47(27), 6991–7000. https://doi.org/10.1021/bi8006324

Payne, D. (1987). Spread of chloroquine resistance in Plasmodium falciparum. Parasitology Today, 3(8), 241–246. https://doi.org/10.1016/0169-4758(87)90147-5

Payne, R. O., Silk, S. E., Elias, S. C., Miura, K., Diouf, A., Galaway, F., De Graaf, H., Brendish, N. J., Poulton, I. D., Griffiths, O. J., Edwards, N. J., Jin, J., Labbé, G. M., Alanine, D. G. W., Siani, L., Marco, S. Di, Roberts, R., Green, N., Berrie, E., … Draper, S. J. (2017). Human vaccination against RH5 induces neutralizing antimalarial antibodies that inhibit RH5 invasion complex interactions. JCI Insight, 2(21), 1–19. https://doi.org/10.1172/jci.insight.96381

Pei, H., Liu, J., Cheng, Y., Sun, C., Wang, C., Lu, Y., Ding, J., Zhou, J., & Xiang, H. (2005). Expression of SARS-coronavirus nucleocapsid protein in Escherichia coli and Lactococcus lactis for serodiagnosis and mucosal vaccination. Applied Microbiology and Biotechnology, 68(2), 220–227. https://doi.org/10.1007/s00253-004-1869-y

Pennie, R. A., Koren, G., & Crevoisier, C. (1993). Steady state pharmacokinetics of mefloquine in long-term travellers. Transactions of the Royal Society of Tropical Medicine and Hygiene, 87(4), 459–462. https://doi.org/10.1016/0035-9203(93)90036-P

Perez, J. G., Stark, J. C., & Jewett, M. C. (2016). Cell-free synthetic biology: Engineering beyond the cell. Cold Spring Harbor Perspectives in Biology, 8(12), 1–25. https://doi.org/10.1101/cshperspec
Peterson, D. S., Gao, Y., Asokan, K., & Gaertig, J. (2002). The circumsporozoite protein of Plasmodium falciparum is expressed and localized to the cell surface in the free-living ciliate Tetrahymena thermophila. Molecular and Biochemical Parasitology, 122(2), 119–126. https://doi.org/10.1016/S0166-6851(02)00079-8

Petrosillo, N., Viceconte, G., Ergonul, O., Ippolito, G., & Petersen, E. (2020). Since January 2020 Elsevier has created a COVID-19 resource centre with free information in English and Mandarin on the novel coronavirus COVID- 19 . The COVID-19 resource centre is hosted on Elsevier Connect , the company ' s public news and information . January.

Phompradit, P., Muhamad, P., Wisedpanichkij, R., Chaijaroenkul, W., & Na-Bangchang, K. (2014). Four years' monitoring of in vitro sensitivity and candidate molecular markers of resistance of Plasmodium falciparum to artesunate-mefloquine combination in the Thai-Myanmar border. Malaria Journal, 13(1), 1–10. https://doi.org/10.1186/1475-2875-13-23

Pierleoni, A., Martelli, P., & Casadio, R. (2008). PredGPI: A GPI-anchor predictor. BMC Bioinformatics, 9, 1–11. https://doi.org/10.1186/1471-2105-9-392

Pines, M., & Nagler, A. (1998). Halofuginone: A novel antifibrotic therapy. General Pharmacology, 30(4), 445–450. https://doi.org/10.1016/S0306-3623(97)00307-8

Plassmeyer, M. L., Reiter, K., Shimp, R. L., Kotova, S., Smith, P. D., Hurt, D. E., House, B., Zou, X., Zhang, Y., Hickman, M., Uchime, O., Herrera, R., Nguyen, V., Glen, J., Lebowitz, J., Jin, A. J., Miller, L. H., MacDonald, N. J., Wu, Y., & Narum, D. L. (2009). Structure of the Plasmodium falciparum circumsporozoite protein, a leading malaria vaccine candidate. Journal of Biological Chemistry, 284(39), 26951–26963. https://doi.org/10.1074/jbc.M109.013706

Plouffe, D., Brinker, A., McNamara, C., Henson, K., Kato, N., Kuhen, K., Nagle, A., Adrián, F., Matzen, J. T., Anderson, P., Nam, T. G., Gray, N. S., Chatterjee, A., Janes, J., Yan, S. F., Trager, R., Caldwell, J. S., Schultz, P. G., Zhou, Y., & Winzeler, E. A. (2008). In silico activity profiling reveals the mechanism of action of antimalarials discovered in a high-throughput screen. Proceedings of the National Academy of Sciences of the United States of America, 105(26), 9059–9064. https://doi.org/10.1073/pnas.0802982105

Plowe, C. V. (2009). The evolution of drug-resistant malaria. Transactions of the Royal Society of Tropical Medicine and Hygiene, 103(1 SUPPL.), 11–16. https://doi.org/10.1016/j.trstmh.2008.11.002

Pontes, M. H., Sevostyanova, A., & Groisman, E. A. (2015). When Too Much ATP Is Bad for Protein Synthesis. Journal of Molecular Biology, 427(16), 2586–2594. https://doi.org/10.1016/j.jmb.2015.06.021

Portolano, N., Watson, P. J., Fairall, L., Millard, C. J., Milano, C. P., Song, Y., Cowley, S. M., & Schwabe, J. W. R. (2014). Recombinant protein expression for structural biology in HEK 293F suspension cells: A novel and accessible approach. Journal of Visualized Experiments, 1(92), 1–8. https://doi.org/10.3791/51897

Protopopoff, N., Mosha, J. F., Lukole, E., Charlwood, J. D., Wright, A., Mwalimu, C. D., Man-

jurano, A., Mosha, F. W., Kisinza, W., Kleinschmidt, I., & Rowland, M. (2018). Effectiveness of a long-lasting piperonyl butoxide-treated insecticidal net and indoor residual spray interventions, separately and together, against malaria transmitted by pyrethroid-resistant mosquitoes: a cluster, randomised controlled, two-by-two fact. The Lancet, 391(10130), 1577–1588. https://doi.org/10.1016/S0140-6736(18)30427-6

Quast, R. B., Claussnitzer, I., Merk, H., Kubick, S., & Gerrits, M. (2014). Synthesis and site-directed fluorescence labeling of azido proteins using eukaryotic cell-free orthogonal translation systems. Analytical Biochemistry, 451(1), 4–9. https://doi.org/10.1016/j.ab.2014.01.013

Rabinovich, R. N., Drakeley, C., Djimde, A. A., Hall, B. F., Hay, S. I., Hemingway, J., Kaslow, D. C., Noor, A., Okumu, F., Steketee, R., Tanner, M., Wells, T. N. C., Whittaker, M. A., Winzeler, E. A., Wirth, D. F., Whitfield, K., & Alonso, P. L. (2017). malERA: An updated research agenda for malaria elimination and eradication. PLoS Medicine, 14(11), 1–17. https://doi.org/10.1371/journal.pmed.1002456

Ragotte, R. J., Higgins, M. K., & Draper, S. J. (2020). The RH5-CyRPA-Ripr Complex as a Malaria Vaccine Target. Trends in Parasitology, 36(6), 545–559. https://doi.org/10.1016/j.pt.2020.04.003

Rapoport, T. A., Rolls, M. M., & Jungnickel, B. (1996). Approaching the mechanism of protein transport across the ER membrane. Current Opinion in Cell Biology, 8(4), 499–504. https://doi.org/10.1016/S0955-0674(96)80027-5

Ramm, F., Dondapati, S. K., Thoring, L., Zemella, A., Wüstenhagen, D. A., Frentzel, H., Stech, M., & Kubick, S. (2020). Mammalian cell-free protein expression promotes the functional characterization of the tripartite non-hemolytic enterotoxin from Bacillus cereus. Scientific Reports, 10(1), 1–12. https://doi.org/10.1038/s41598-020-59634-8

Rathore, D., Kumar, S., Lanar, D. E., & McCutchan, T. F. (2001). Disruption of disulfide linkages of the Plasmodium falciparum circumsporozoite protein: Effects on cytotoxic and antibody responses in mice. Molecular and Biochemical Parasitology, 118(1), 75–82. https://doi.org/10.1016/S0166-6851(01)00369-3

Ravichandran, S., Coyle, E. M., Klenow, L., Tang, J., Grubbs, G., Liu, S., Wang, T., Golding, H., & Khurana, S. (2020). Antibody signature induced by SARS-CoV-2 spike protein immunogens in rabbits. Science Translational Medicine, 12(550). https://doi.org/10.1101/2020.04.20.20071423

Real, E., Howick, V. M., Dahalan, F., Witmer, K., Cudini, J., Andradi-Brown, C., Blight, J., Davidson, M. S., Dogga, S. K., Reid, A. J., Baum, J., & Lawniczak, M. K. N. (2020). A single-cell atlas of Plasmodium falciparum transmission through the mosquito. BioRxiv. https://doi.org/10.1101/2020.10.11.333179

Reamtong, O., Srimuang, K., Saralamba, N., Sangvanich, P., Day, N. P. J., White, N. J., & Imwong, M. (2015). Protein profiling of mefloquine resistant Plasmodium falciparum using mass spectrometry-based proteomics. International Journal of Mass Spectrometry, 391, 82–92. https://doi.org/10.1016/j.ijms.2015.09.009

Regules, J. A., Cummings, J. F., & Ockenhouse, C. F. (2011). The RTS,S vaccine candidate

for malaria. Expert Review of Vaccines, 10(5), 589–599. https://doi.org/10.1586/erv.11.57

Renaud, J. P., Chari, A., Ciferri, C., Liu, W. T., Rémigy, H. W., Stark, H., & Wiesmann, C. (2018). Cryo-EM in drug discovery: Achievements, limitations and prospects. Nature Reviews Drug Discovery, 17(7), 471–492. https://doi.org/10.1038/nrd.2018.77

Reymond, C. D., Beghdadi-Rais, C., Roggero, M., Duarte, E. A., Desponds, C., Bernard, M., Groux, D., Matile, H., Bron, C., Corradin, G., & Fasel, N. J. (1995). Anchoring of an immunogenic Plasmodium falciparum circumsporozoite protein on the surface of Dictyostelium discoideum. Journal of Biological Chemistry, 270(21), 12941–12947. https://doi.org/10.1074/jbc.270.21.12941

Richards, J. S., Arumugam, T. U., Reiling, L., Healer, J., Hodder, A. N., Fowkes, F. J. I., Cross, N., Langer, C., Takeo, S., Uboldi, A. D., Thompson, J. K., Gilson, P. R., Coppel, R. L., Siba, P. M., King, C. L., Torii, M., Chitnis, C. E., Narum, D. L., Mueller, I., ... Beeson, J. G. (2013). Identification and Prioritization of Merozoite Antigens as Targets of Protective Human Immunity to Plasmodium falciparum Malaria for Vaccine and Biomarker Development. The Journal of Immunology, 191(2), 795–809. https://doi.org/10.4049/jimmunol.1300778

Riedel, S. (2005). Edward Jenner and the History of Smallpox and Vaccination. Baylor University Medical Center Proceedings, 18(1), 21–25. https://doi.org/10.1080/08998280.2005.11928028

Rivas, G., & Minton, A. P. (2018). Toward an understanding of biochemical equilibria within living cells. Biophysical Reviews, 10(2), 241–253. https://doi.org/10.1007/s12551-017-0347-6

Roch, K. G. Le, Johnson, J. R., Florens, L., Zhou, Y., Santrosyan, A., Grainger, M., Yan, S. F., Williamson, K. C., Holder, A. A., Carucci, D. J., Iii, J. R. Y., & Winzeler, E. A. (2004). Global analysis of transcript and protein levels across the. Genome Research, 2308–2318. https://doi.org/10.1101/gr.2523904.7

Rock, F.L., Mao, W., Yaremchuk, A., Tukalo, M., Crepin, T., Zhou, H., Zhang, Y.K., Hernandez, V., Akama, T., Baker, S.J., et al. (2007). An antifungal agent inhibits an aminoacyl-tRNA synthetase by trapping tRNA in the editing site. Science 316, 1759–1761

Rodisch, J. R., & Dudkin, G. N. (1983). Utilities' Perspective of Cogeneration. 19–27.

Roestenberg, M., Walk, J., Van Der Boor, S. C., Langenberg, M. C. C., Hoogerwerf, M. A., Janse, J. J., Manurung, M., Yap, X. Z., García, A. F., Koopman, J. P. R., Meij, P., Wessels, E., Teelen, K., Van Waardenburg, Y. M., Van De Vegte-Bolmer, M., Van Gemert, G. J., Visser, L. G., Van Der Ven, A. J. A. M., De Mast, Q., ... Sauerwein, R. W. (2020). A double-blind, placebo-controlled phase 1/2a trial of the genetically attenuated malaria vaccine PfSPZ-GA1. Science Translational Medicine, 12(544), 1–10. https://doi.org/10.1126/scitranslmed.aaz5629

Romisch, K., Webb, J., Herz, J., Prehn, S., Frank, R., Vingron, M., & Dobberstein, B. (1989). GYP-binding domains. 340(August), 478–482.

Rosenberg, R., Burge, R., & Schneider, I. (1990). An estimation of the number of malaria sporozoites ejected by a feeding mosquito. Transactions of the Royal Society of Tropical Medicine and Hygiene, 84(2), 209–212. https://doi.org/10.1016/0035-9203(90)90258-G

Rosengard, A. M., Liu, Y., Nie, Z., & Jimenez, R. (2002). Variola virus immune evasion design: Expression of a highly efficient inhibitor of human complement. Proceedings of the National Academy of Sciences of the United States of America, 99(13), 8808–8813. https://doi.org/10.1073/pnas.112220499

Rosenthal, P. J. (2020). Are three drugs for malaria better than two? The Lancet, 395(10233), 1316–1317. https://doi.org/10.1016/S0140-6736(20)30560-2

Ross, L. S., & Fidock, D. A. (2019). Elucidating Mechanisms of Drug-Resistant Plasmodium falciparum. Cell Host and Microbe, 26(1), 35–47. https://doi.org/10.1016/j.chom.2019.06.001

Rothe, K. E. K. and W. E. (1975). Biological Screening in the U. S. Army Antimalarial Drug Development Program. American Journal of Tropical Medicine and Hygiene, 24(2), 174–178. https://doi.org/10.4269/ajtmh.1975.24.174

Rottmann, M., Jonat, B., Gumpp, C., Dhingra, S. K., Giddins, M. J., Yin, X., Badolo, L., Greco, B., Fidock, D. A., Oeuvray, C., & Spangenberg, T. (2020). Preclinical antimalarial combination study of M5717, a Plasmodium falciparum elongation factor 2 inhibitor, and pyronaridine, a hemozoin formation inhibitor. Antimicrobial Agents and Chemotherapy, 64(4), 1–16. https://doi.org/10.1128/AAC.02181-19

Rottmann, M., McNamara, C., Yeung, B. K. S., Lee, M. C. S., Zou, B., Russell, B., Seitz, P., Plouffe, D. M., Dharia, N. V., Tan, J., Cohen, S. B., Spencer, K. R., González-Páez, G. E., Lakshminarayana, S. B., Goh, A., Suwanarusk, R., Jegla, T., Schmitt, E. K., Beck, H. P., … Diagana, T. T. (2010). Spiroindolones, a potent compound class for the treatment of malaria. Science, 329(5996), 1175–1180. https://doi.org/10.1126/science.1193225

Ruan, W., Lehmann, E., Thomm, M., Kostrewa, D., & Cramer, P. (2011). Evolution of Two Modes of Intrinsic RNA Polymerase Transcript Cleavage. Journal of Biological Chemistry, 286(21), 18701–18707. https://doi.org/10.1074/jbc.M111.222273

Rues, R.-B., Henrich, E., Boland, C., Caffrey, M., & Bernhard, F. (2016). Cell-Free Production of Membrane Proteins in Escherichia coli Lysates for Functional and Structural Studies. In Methods in molecular biology (Clifton, N.J.) (Vol. 601, pp. 1–21). https://doi.org/10.1007/978-1-4939-3637-3_1

Rui, E., Fernandez-Becerra, C., Takeo, S., Sanz, S., Lacerda, M. V., Tsuboi, T., & Del Portillo, H. A. (2011). Plasmodium vivax: Comparison of immunogenicity among proteins expressed in the cell-free systems of Escherichia coli and wheat germ by suspension array assays. Malaria Journal, 10, 1–8. https://doi.org/10.1186/1475-2875-10-192

Ryley, J. F., & Betts, M. J. (1973). Chemotherapy of Chicken Coccidiosis. Advances in Pharmacology, 11(C), 221–293. https://doi.org/10.1016/S1054-3589(08)60459-7

Sachs, J., & Malaney, P. (2002). The economic and social burden of malaria. Nature, 415(6872), 680–685. https://doi.org/10.1038/415680a

Sachse, R., Wüstenhagen, D., Šamalíková, M., Gerrits, M., Bier, F. F., & Kubick, S. (2013). Synthesis of membrane proteins in eukaryotic cell-free systems. Engineering in Life Sciences,

13(1), 39–48. https://doi.org/10.1002/elsc.201100235

Sawasaki, T., Hasegawa, Y., Tsuchimochi, M., Kamura, N., Ogasawara, T., Kuroita, T., & Endo, Y. (2002). A bilayer cell-free protein synthesis system for high-throughput screening of gene products. FEBS Letters, 514(1), 102–105. https://doi.org/10.1016/S0014-5793(02)02329-3

Scally, S. W., McLeod, B., Bosch, A., Miura, K., Liang, Q., Carroll, S., Reponen, S., Nguyen, N., Giladi, E., Rämisch, S., Yusibov, V., Bradley, A., Lemiale, F., Schief, W. R., Emerling, D., Kellam, P., King, C. R., & Julien, J. P. (2017). Molecular definition of multiple sites of antibody inhibition of malaria transmission-blocking vaccine antigen Pfs25. Nature Communications, 8(1). https://doi.org/10.1038/s41467-017-01924-3

Schena, M. (1989). The evolutionary conservation of eukaryotic gene transcription. Experientia, 45(10), 972–983. https://doi.org/10.1007/BF01953055

Schlitzer, M. (2007). Malaria chemotherapeutics part I: History of antimalarial drug development, currently used therapeutics, and drugs in clinical development. ChemMedChem, 2(7), 944–986. https://doi.org/10.1002/cmdc.200600240

Schneider-Poetsch, T., Ju, J., Eyler, D. E., Dang, Y., Bhat, S., Merrick, W. C., Green, R., Shen, B., & Liu, J. O. (2010). Inhibition of eukaryotic translation elongation by cycloheximide and lactimidomycin. Nature Chemical Biology, 6(3), 209–217. https://doi.org/10.1038/nchembio.304

Schofield, L., Vivas, L., Hackett, F., Gerold, P., Schwarz, R. T., & Tachado, S. (1993). Neutralising monoclonal antibodies to glycosylphosphatidylinositol, the dominant TNF alpha inducing toxin of Plasmodium falciparum: prospects for the immunotherapy of severe malaria. Annals of Tropical Medicine & Parasitology, 87(6), 617–626. https://doi.org/10.1080/00034983.1993.11812820

Schofield, Louis, Hewittt, M. C., Evans, K., Slomos, M. A., & Seeberger, P. H. (2002). Synthetic GPI as a candidate anti-toxic vaccine in a model of malaria. Nature, 418(6899), 785–789. https://doi.org/10.1038/nature00937

Schwarzer, T. S., Hermann, M., Krishnan, S., Simmel, F. C., & Castiglione, K. (2017). Preparative refolding of small monomeric outer membrane proteins. Protein Expression and Purification, 132, 171–181. https://doi.org/10.1016/j.pep.2017.01.012

Seifart, K. H., & Sekeris, C. E. (1969). α Amanitin, a specific inhibitor of transcription by mammalian RNA-polymerase. Zeitschrift Für Naturforschung B, 24(12), 1538–1544. https://doi.org/10.1515/znb-1969-1211

Selye, H. (1975). Homeostasis and Heterostasis BT - Trauma: Clinical and Biological Aspects (S. B. Day (ed.); pp. 25–29). Springer US. https://doi.org/10.1007/978-1-4684-2145-3_2

Sentenac, A. (1985). Eukaryotic RNA polymerase. Critical Reviews in Biochemistry and Molecular Biology, 18(1), 31–90. https://doi.org/10.3109/10409238509082539

Servín-Blanco, R., Zamora-Alvarado, R., Gevorkian, G., & Manoutcharian, K. (2016). Antigenic variability: Obstacles on the road to vaccines against traditionally difficult targets. Hu-

man Vaccines and Immunotherapeutics, 12(10), 2640–2648. https://doi.org/10.1080/21645515.2016.1191718

Sheridan, C. M., Garcia, V. E., Ahyong, V., & DeRisi, J. L. (2018). The Plasmodium falciparum cytoplasmic translation apparatus: a promising therapeutic target not yet exploited by clinically approved anti-malarials. Malaria Journal, 17(1), 1–13. https://doi.org/10.1186/s12936-018-2616-7

Shields, D., & Blobel, G. (1977). Cell free synthesis of fish preproinsulin, and processing by heterologous mammalian microsomal membranes. Proceedings of the National Academy of Sciences of the United States of America, 74(5), 2059–2063. https://doi.org/10.1073/pnas.74.5.2059

Shimizu, Y., & Ueda, T. (2010). PURE Technology (pp. 11–21). https://doi.org/10.1007/978-1-60327-331-2_2

Sievers, F., & Higgins, D. G. (2018). Clustal Omega for making accurate alignments of many protein sequences. Protein Science, 27(1), 135–145. https://doi.org/10.1002/pro.3290

Sievers, F., Wilm, A., Dineen, D., Gibson, T. J., Karplus, K., Li, W., Lopez, R., McWilliam, H., Remmert, M., Söding, J., Thompson, J. D., & Higgins, D. G. (2011). Fast, scalable generation of high-quality protein multiple sequence alignments using Clustal Omega. Molecular Systems Biology, 7(1), 539. https://doi.org/10.1038/msb.2011.75

Silvie, O., Franetich, J. F., Charrin, S., Mueller, M. S., Siau, A., Bodescot, M., Rubinstein, E., Hannoun, L., Charoenvit, Y., Kocken, C. H., Thomas, A. W., Van Gemert, G. J., Sauerwein, R. W., Blackman, M. J., Anders, R. F., Pluschke, G., & Mazier, D. (2004). A Role for Apical Membrane Antigen 1 during Invasion of Hepatocytes by Plasmodium falciparum Sporozoites. Journal of Biological Chemistry, 279(10), 9490–9496. https://doi.org/10.1074/jbc.M311331200

Simpson, R. J. (2010). Disruption of Cultured Cells by Nitrogen Cavitation. Cold Spring Harbor Protocols, 2010(11), pdb.prot5513-pdb.prot5513. https://doi.org/10.1101/pdb.prot5513

Smith, M. T. J., & Rubinstein, J. L. (2014). Beyond blob-ology. In Science (Vol. 345, Issue 6197, pp. 617–619). https://doi.org/10.1126/science.1256358

Smith, M. T., Berkheimer, S. D., Werner, C. J., & Bundy, B. C. (2014). Lyophilized Escherichia coli-based cell-free systems for robust, high-density, long-term storage. BioTechniques, 56(4), 186–193. https://doi.org/10.2144/000114158

Soejima, Y., Lee, J. M., Nagata, Y., Mon, H., Iiyama, K., Kitano, H., Matsuyama, M., & Kusakabe, T. (2013). Comparison of signal peptides for efficient protein secretion in the baculovirus-silkworm system. Central European Journal of Biology, 8(1), 1–7. https://doi.org/10.2478/s11535-012-0112-6

Sonenberg, N., & Hinnebusch, A. G. (2009). Regulation of Translation Initiation in Eukaryotes: Mechanisms and Biological Targets. Cell, 136(4), 731–745. https://doi.org/10.1016/j.cell.2009.01.042

Spaan, C. N., Smit, W. L., van Lidth de Jeude, J. F., Meijer, B. J., Muncan, V., van den Brink, G. R., & Heijmans, J. (2019). Expression of UPR effector proteins ATF6 and XBP1 reduce colorectal cancer cell proliferation and stemness by activating PERK signalling. Cell

Death and Disease, 10(7). https://doi.org/10.1038/s41419-019-1729-4

Spice, A. J., Aw, R., Bracewell, D. G., & Polizzi, K. M. (2020). Improving the reaction mix of a Pichia pastoris cell-free system using a design of experiments approach to minimise experimental effort. Synthetic and Systems Biotechnology, 5(3), 137–144. https://doi.org/10.1016/j.synbio.2020.06.003

Spirin, A., Baranov, V., Ryabova, L., Ovodov, S., & Alakhov, Y. (1988). A continuous cell-free translation system capable of producing polypeptides in high yield. Science, 242(4882), 1162–1164. https://doi.org/10.1126/science.3055301

Spirin, A. S. (2004). High-throughput cell-free systems for synthesis of functionally active proteins. Trends in Biotechnology, 22(10), 538–545. https://doi.org/10.1016/j.tibtech.2004.08.012

Stech, M., Nikolaeva, O., Thoring, L., Stöcklein, W. F. M., Wüstenhagen, D. A., Hust, M., Dübel, S., & Kubick, S. (2017). Cell-free synthesis of functional antibodies using a coupled in vitro transcription-Translation system based on CHO cell lysates. Scientific Reports, 7(1), 1–15. https://doi.org/10.1038/s41598-017-12364-w

Stech, Marlitt, Quast, R. B., Sachse, R., Schulze, C., & Wüstenhagen Stefan Kubick, D. A. (2014). A continuous-exchange cell-free protein synthesis system based on extracts from cultured insect cells. PLoS ONE, 9(5). https://doi.org/10.1371/journal.pone.0096635

Sun, M., Li, W., Blomqvist, K., Das, S., Hashem, Y., Dvorin, J. D., & Frank, J. (2015). Dynamical features of the Plasmodium falciparum ribosome during translation. Nucleic Acids Research, 43(21), 10515–10524. https://doi.org/10.1093/nar/gkv991

Svardal, A. M., & Pryme, I. F. (1978). The isolation of microsomal subfractions of mouse plasmacytoma cells: The effect of salt concentration during nitrogen cavitation. Analytical Biochemistry, 89(2), 332–336. https://doi.org/10.1016/0003-2697(78)90359-7
Swartz, J. R. (2001). Advances in Escherichia coli production of therapeutic proteins. Current Opinion in Biotechnology, 12(2), 195–201. https://doi.org/10.1016/S0958-1669(00)00199-3

Swinney, D. C. (2013). Phenotypic vs. Target-based drug discovery for first-in-class medicines. Clinical Pharmacology and Therapeutics, 93(4), 299–301. https://doi.org/10.1038/clpt.2012.236

Takahashi, M. K., Chappell, J., Hayes, C. A., Sun, Z. Z., Kim, J., Singhal, V., Spring, K. J., Al-Khabouri, S., Fall, C. P., Noireaux, V., Murray, R. M., & Lucks, J. B. (2015). Rapidly Characterizing the Fast Dynamics of RNA Genetic Circuitry with Cell-Free Transcription-Translation (TX-TL) Systems. ACS Synthetic Biology, 4(5), 503–515. https://doi.org/10.1021/sb400206c

Takai, K., Sawasaki, T., & Endo, Y. (2010). Practical cell-free protein synthesis system using purified wheat embryos. Nature Protocols, 5(2), 227–238. https://doi.org/10.1038/nprot.2009.207

Tate, J., Liljas, L., Scotti, P., Christian, P., Lin Tianwei, & Johnson, J. E. (1999). The crystal structure of cricket paralysis virus: The first view of a new virus family. Nature Structural Biology, 6(8), 765–774. https://doi.org/10.1038/11543

Terstappen, G. C., Schlüpen, C., Raggiaschi, R., & Gaviraghi, G. (2007). Target deconvolution

strategies in drug discovery. Nature Reviews Drug Discovery, 6(11), 891–903. https://doi.org/10.1038/nrd2410

Thomas, P., & Smart, T. G. (2005). HEK293 cell line: A vehicle for the expression of recombinant proteins. Journal of Pharmacological and Toxicological Methods, 51(3 SPEC. ISS.), 187–200. https://doi.org/10.1016/j.vascn.2004.08.014

Thompson, J., Van Spaendonk, R. M. L., Choudhuri, R., Sinden, R. E., Janse, C. J., & Waters, A. P. (1999). Heterogeneous ribosome populations are present in Plasmodium berghei during development in its vector. Molecular Microbiology, 31(1), 253–260. https://doi.org/10.1046/j.1365-2958.1999.01167.x

Thoring, L., Dondapati, S. K., Stech, M., Wüstenhagen, D. A., & Kubick, S. (2017). High-yield production of "difficult-to-express" proteins in a continuous exchange cell-free system based on CHO cell lysates. Scientific Reports, 7(1), 1–15. https://doi.org/10.1038/s41598-017-12188-8

Thoring, L., Wï¿½stenhagen, D. A., Borowiak, M., Stech, M., Sonnabend, A., & Kubick, S. (2016). Cell-free systems based on CHO cell lysates: Optimization strategies, synthesis of "difficult-to-express" proteins and future perspectives. PLoS ONE, 11(9), 1–21. https://doi.org/10.1371/journal.pone.0163670

Tilley, L., Straimer, J., Gnädig, N. F., Ralph, S. A., & Fidock, D. A. (2016). Artemisinin Action and Resistance in Plasmodium falciparum. Trends in Parasitology, 32(9), 682–696. https://doi.org/10.1016/j.pt.2016.05.010

Tolkunova, E., Park, H., Xia, J., King, M. P., & Davidson, E. (2000). The human lysyl-tRNA synthetase gene encodes both the cytoplasmic and mitochondrial enzymes by means of an unusual: Alternative splicing of the primary transcript. Journal of Biological Chemistry, 275(45), 35063–35069. https://doi.org/10.1074/jbc.M006265200

Tonkin, C. J., Kalanon, M., & McFadden, G. I. (2008). Protein targeting to the malaria parasite plastid. Traffic, 9(2), 166–175. https://doi.org/10.1111/j.1600-0854.2007.00660.x

Torres, S. E., Gallagher, C. M., Plate, L., Gupta, M., Liem, C. R., Guo, X., Tian, R., Stroud, R. M., Kampmann, M., Weissman, J. S., & Walter, P. (2019). Ceapins block the unfolded protein response sensor atf6α by inducing a neomorphic inter-organelle tether. ELife, 8, 1–19. https://doi.org/10.7554/eLife.46595

Tran, K., Gurramkonda, C., Cooper, M. A., Pilli, M., Taris, J. E., Selock, N., Han, T. C., Tolosa, M., Zuber, A., Peñalber-Johnstone, C., Dinkins, C., Pezeshk, N., Kostov, Y., Frey, D. D., Tolosa, L., Wood, D. W., & Rao, G. (2018). Cell-free production of a therapeutic protein: Expression, purification, and characterization of recombinant streptokinase using a CHO lysate. Biotechnology and Bioengineering, 115(1), 92–102. https://doi.org/10.1002/bit.26439

Trigg, P. I., Brown, I. N., Gutteridge, W. E., Hockley, D. J., & Williamson, J. (1970). The preparation of free malaria parasites by nitrogen cavitation. Transactions of the Royal Society of Tropical Medicine and Hygiene, 64(1), 2–3. http://www.ncbi.nlm.nih.gov/pubmed/4986063
Tsuboi, T., Takeo, S., Arumugam, T. U., Otsuki, H., & Torii, M. (2010). The wheat germ cell-free protein synthesis system: A key tool for novel malaria vaccine candidate discovery. Acta Tropica, 114(3), 171–176. https://doi.org/10.1016/j.actatropica.2009.10.024

Tsuboi, T., Takeo, S., Iriko, H., Jin, L., Tsuchimochi, M., Matsuda, S., Han, E. T., Otsuki, H., Kaneko, O., Sattabongkot, J., Udomsangpetch, R., Sawasaki, T., Torii, M., & Endo, Y. (2008). Wheat germ cell-free system-based production of malaria proteins for discovery of novel vaccine candidates. Infection and Immunity, 76(4), 1702–1708. https://doi.org/10.1128/IAI.01539-07

Tuteja, R. (2007). Malaria - An overview. FEBS Journal, 274(18), 4670–4679. https://doi.org/10.1111/j.1742-4658.2007.05997.x

Tuteja, R. (2009). Identification and bioinformatics characterization of translation initiation complex eIF4F components and poly(A)-binding protein from Plasmodium falciparum. Communicative and Integrative Biology, 2(3), 245–260. https://doi.org/10.4161/cib.2.3.8843

Tyedmers, J., Lerner, M., Wiedmann, M., Volkmer, J., & Zimmermann, R. (2003). Polypeptide-binding proteins mediate completion of co-translational protein translocation into the mammalian endoplasmic reticulum. EMBO Reports, 4(5), 505–510. https://doi.org/10.1038/sj.embor.embor826

Van Dooren, G. G., Marti, M., Tonkin, C. J., Stimmler, L. M., Cowman, A. F., & McFadden, G. I. (2005). Development of the endoplasmic reticulum, mitochondrion and apicoplast during the asexual life cycle of Plasmodium falciparum. Molecular Microbiology, 57(2), 405–419. https://doi.org/10.1111/j.1365-2958.2005.04699.x

Van Spaendonk, R. M. L., Ramesar, J., Van Wigcheren, A., Eling, W., Beetsma, A. L., Van Gemert, G. J., Hooghof, J., Janse, C. J., & Waters, A. P. (2001a). Journal of Biological Chemistry, 276(25), 22638–22647. https://doi.org/10.1074/jbc.M101234200

Van Spaendonk, R. M. L., Ramesar, J., Van Wigcheren, A., Eling, W., Beetsma, A. L., Van Gemert, G. J., Hooghof, J., Janse, C. J., & Waters, A. P. (2001b). Functional Equivalence of Structurally Distinct Ribosomes in the Malaria Parasite, Plasmodium berghei. Journal of Biological Chemistry, 276(25), 22638–22647. https://doi.org/10.1074/jbc.M101234200

Vannini, A., & Cramer, P. (2012). Conservation between the RNA Polymerase I, II, and III Transcription Initiation Machineries. Molecular Cell, 45(4), 439–446. https://doi.org/10.1016/j.molcel.2012.01.023

Vannini, A., Ringel, R., Kusser, A. G., Berninghausen, O., Kassavetis, G. A., & Cramer, P. (2010). Molecular basis of RNA polymerase III transcription repression by Maf1. Cell, 143(1), 59–70. https://doi.org/10.1016/j.cell.2010.09.002

Vembar, S. S., Droll, D., & Scherf, A. (2016). Translational regulation in blood stages of the malaria parasite Plasmodium spp.: systems-wide studies pave the way. Wiley Interdisciplinary Reviews: RNA, 7(6), 772–792. https://doi.org/10.1002/wrna.1365

Venkataramaiah, T., & Gajanana, A. (1987). Evaluation of Plasmodium falciparum-microsomal in vitro system for testing pro-drugs. The Indian Journal of Medical Research, 86, 579–581. http://www.ncbi.nlm.nih.gov/pubmed/3330544

Villa, M., Buysse, M., Berthomieu, A., & Rivero, A. (2021). The transmission-blocking effects of antimalarial drugs revisited: fitness costs and sporontocidal effects of artesunate and

sulfadoxine-pyrimethamine. International Journal for Parasitology, 51(4), 279–289. https://doi.org/10.1016/j.ijpara.2020.09.012

Vinayak, S., Jumani, R. S., Miller, P., Hasan, M. M., McLeod, B. I., Tandel, J., Stebbins, E. E., Teixeira, J. E., Borrel, J., Gonse, A., Zhang, M., Yu, X., Wernimont, A., Walpole, C., Eckley, S., Love, M. S., McNamara, C. W., Sharma, M., Sharma, A., ... Comer, E. (2020). Bicyclic azetidines kill the diarrheal pathogen Cryptosporidium in mice by inhibiting parasite phenylalanyl-tRNA synthetase. Science Translational Medicine, 12(563), 1–14. https://doi.org/10.1126/scitranslmed.aba8412

von Itzstein, M., Plebanski, M., Cooke, B. M., & Coppel, R. L. (2008). Hot, sweet and sticky: the glycobiology of Plasmodium falciparum. Trends in Parasitology, 24(5), 210–218. https://doi.org/10.1016/j.pt.2008.02.007

Wacharapluesadee, S., Tan, C. W., Maneeorn, P., Duengkae, P., Zhu, F., Joyjinda, Y., Kaewpom, T., Chia, W. N., Ampoot, W., Lim, B. L., Worachotsueptrakun, K., Chen, V. C. W., Sirichan, N., Ruchisrisarod, C., Rodpan, A., Noradechanon, K., Phaichana, T., Jantarat, N., Thongnumchaima, B., ... Wang, L. F. (2021). Evidence for SARS-CoV-2 related coronaviruses circulating in bats and pangolins in Southeast Asia. Nature Communications, 12(1). https://doi.org/10.1038/s41467-021-21240-1

Wahlgren, M., Goel, S., & Akhouri, R. R. (2017). Variant surface antigens of Plasmodium falciparum and their roles in severe malaria. Nature Reviews Microbiology, 15(8), 479–491. https://doi.org/10.1038/nrmicro.2017.47

Wakasugi, K., & Schimmel, P. (1999). Two distinct cytokines released from a human aminoacyl-tRNA synthetase. Science, 284(5411), 147–151. https://doi.org/10.1126/science.284.5411.147

Walls, A. C., Park, Y.-J., Tortorici, M. A., Wall, A., McGuire, A. T., & Veesler, D. (2020). Structure, Function, and Antigenicity of the SARS-CoV-2 Spike Glycoprotein. Cell, 1–12. https://doi.org/10.1016/j.cell.2020.02.058

Wang, L.-F., & Eaton, B. T. (2007). (pp. 325–344). https://doi.org/10.1007/978-3-540-70962-6_13

Wang, M., Jiang, S., & Wang, Y. (2016). Recent advances in the production of recombinant subunit vaccines in Pichia pastoris. Bioengineered, 7(3), 155–165. https://doi.org/10.1080/21655979.2016.1191707

Wang, Q., Fujioka, H., & Nussenzweig, V. (2005). Exit of plasmodium sporozoites from oocysts is an active process that involves the circumsporozoite protein. PLoS Pathogens, 1(1), 0072–0079. https://doi.org/10.1371/journal.ppat.0010009

Wang, X., Radwan, M. M., Taráwneh, A. H., Gao, J., Wedge, D. E., Rosa, L. H., Cutler, H. G., & Cutler, S. J. (2013). Antifungal activity against plant pathogens of metabolites from the endophytic fungus cladosporium cladosporioides. Journal of Agricultural and Food Chemistry, 61(19), 4551–4555. https://doi.org/10.1021/jf400212y

Watanabe, Y., Allen, J. D., Wrapp, D., McLellan, J. S. S. glycan analysis of the S.-C.-2 spike, & Crispin, M. (2020). Site-specific glycan analysis of the SARS-CoV-2 spike. Science,

369(6501), 330–333. https://doi.org/10.1126/science.abb9983

Waterhouse, A. M., Procter, J. B., Martin, D. M. A., Clamp, M., & Barton, G. J. (2009). Jalview Version 2–a multiple sequence alignment editor and analysis workbench. Bioinformatics, 25(9), 1189–1191. https://doi.org/10.1093/bioinformatics/btp033

Weber, L. A., Feman, E. R., & Baglioni, C. (1975). Cell free system from HeLa cells active in initiation of protein synthesis. Biochemistry, 14(24), 5315–5321. https://doi.org/10.1021/bi00695a015

Weerapana, E., & Imperiali, B. (2006). Asparagine-linked protein glycosylation: From eukaryotic to prokaryotic systems. Glycobiology, 16(6), 91–101. https://doi.org/10.1093/glycob/cwj099

Wei, Z., Xu, Z., Liu, X., Lo, W. S., Ye, F., Lau, C. F., Wang, F., Zhou, J. J., Nangle, L. A., Yang, X. L., Zhang, M., & Schimmel, P. (2016). Alternative splicing creates two new architectures for human tyrosyl-tRNA synthetase. Nucleic Acids Research, 44(3), 1247–1255. https://doi.org/10.1093/nar/gkw002

Wells, T. N. C., Van Huijsduijnen, R. H., & Van Voorhis, W. C. (2015). Malaria medicines: A glass half full? Nature Reviews Drug Discovery, 14(6), 424–442. https://doi.org/10.1038/nrd4573

White, N. J. (2013). Pharmacokinetic and pharmacodynamic considerations in antimalarial dose optimization. Antimicrobial Agents and Chemotherapy, 57(12), 5792–5807. https://doi.org/10.1128/AAC.00287-13

White, N. J. (2017). Malaria parasite clearance. Malaria Journal, 16(1), 1–14. https://doi.org/10.1186/s12936-017-1731-1

WHO. (2015). Global technical strategy for malaria 2016-2030. World Health Organization, 1–35. http://apps.who.int/iris/bitstream/10665/176712/1/9789241564991_eng.pdf?ua=1

WHO. (2021). WHO Coronavirus (COVID-19) Dashboard. https://covid19.who.int

Willis, I. M. (1994). RNA polymerase III. In EJB Reviews 1993 (pp. 29–39). Springer Berlin Heidelberg. https://doi.org/10.1007/978-3-642-78757-7_4

Wilson, D. N., & Doudna Cate, J. H. (2012). The Structure and Function of the Eukaryotic Ribosome. Cold Spring Harbor Perspectives in Biology, 4(5), a011536–a011536. https://doi.org/10.1101/cshperspect.a011536

Wilson, D. W., Crabb, B. S., & Beeson, J. G. (2010). Development of fluorescent Plasmodium falciparum for in vitro growth inhibition assays. Malaria Journal, 9(1), 1–12. https://doi.org/10.1186/1475-2875-9-152

Wilson, J. E., Powell, M. J., Hoover, S. E., & Sarnow, P. (2000). Naturally Occurring Dicistronic Cricket Paralysis Virus RNA Is Regulated by Two Internal Ribosome Entry Sites. Molecular and Cellular Biology, 20(14), 4990–4999. https://doi.org/10.1128/mcb.20.14.4990-4999.2000

Wilson, K. L., Flanagan, K. L., Prakash, M. D., & Plebanski, M. (2019). Malaria vaccines in the eradication era: current status and future perspectives. Expert Review of Vaccines, 18(2), 133–151. https://doi.org/10.1080/14760584.2019.1561289

Wong, E. T., Ngoi, S. M., & Lee, C. G. L. (2002). Improved co-expression of multiple genes in vectors containing internal ribosome entry sites (IRESes) from human genes. Gene Therapy, 9(5), 337–344. https://doi.org/10.1038/sj.gt.3301667

Wong, W., Bai, X. C., Brown, A., Fernandez, I. S., Hanssen, E., Condron, M., Tan, Y. H., Baum, J., & Scheres, S. H. W. (2014). Cryo-EM structure of the Plasmodium falciparum 80S ribosome bound to the anti-protozoan drug emetine. ELife, 2014(3), 1–20. https://doi.org/10.7554/eLife.03080

Wong, W., Bai, X. C., Sleebs, B. E., Triglia, T., Brown, A., Thompson, J. K., Jackson, K. E., Hanssen, E., Marapana, D. S., Fernandez, I. S., Ralph, S. A., Cowman, A. F., Scheres, S. H. W., & Baum, J. (2017). Mefloquine targets the Plasmodium falciparum 80S ribosome to inhibit protein synthesis. Nature Microbiology, 2(March). https://doi.org/10.1038/nmicrobiol.2017.31

Wong, W., Webb, A. I., Olshina, M. A., Infusini, G., Tan, Y. H., Hanssen, E., Catimel, B., Suarez, C., Condron, M., Angrisano, F., Nebl, T., Kovar, D. R., & Baum, J. (2014). A mechanism for actin filament severing by malaria parasite actin depolymerizing factor 1 via a low affinity binding interface. Journal of Biological Chemistry, 289(7), 4043–4054. https://doi.org/10.1074/jbc.M113.523365

Wood, K. V., Lam, Y. A., & McElroy, W. D. (1989). Introduction to beetle luciferases and their applications. Journal of Bioluminescence and Chemiluminescence, 4(1), 289–301. https://doi.org/10.1002/bio.1170040141

World Health Organization. (2015). Global Malaria Programme. Eliminating malaria. Geneva: World Health Organization. World Health Organization, 243. http://www.who.int/malaria/publications/world-malaria-report-2015/report/en/

World Health Organization. (2018). Artemisinin resistance and artemisinin-based combination therapy efficacy. Who, August, 10. https://www.who.int/malaria/publications/atoz/artemisinin-resistance-august2018/en/

World Health Organization. (2019). World Malaria Report 2019. Geneva. https://www.who.int/publications-detail/world-malaria-report-2019

Wright, K. E., Hjerrild, K. A., Bartlett, J., Douglas, A. D., Jin, J., Brown, R. E., Illingworth, J. J., Ashfield, R., Clemmensen, S. B., De Jongh, W. A., Draper, S. J., & Higgins, M. K. (2014). Structure of malaria invasion protein RH5 with erythrocyte basigin and blocking antibodies. Nature, 515(7527), 427–430. https://doi.org/10.1038/nature13715

Wu, Y., Sifri, C. D., Lei, H. H., Su, X. Z., & Wellems, T. E. (1995). Transfection of Plasmodium falciparum within human red blood cells. Proceedings of the National Academy of Sciences of the United States of America, 92(4), 973–977. https://doi.org/10.1073/pnas.92.4.973

Xie, S. C., Ralph, S. A., & Tilley, L. (2020). K13, the Cytostome, and Artemisinin Resistance. Trends in Parasitology, 36(6), 533–544. https://doi.org/10.1016/j.pt.2020.03.006

Xiong, X., Qu, K., Ciazynska, K. A., Hosmillo, M., Carter, A. P., Ebrahimi, S., Ke, Z., Scheres, S. H. W., Bergamaschi, L., Grice, G. L., Zhang, Y., Bradley, J., Lyons, P. A., Smith, K. G. C., Toshner, M., Elmer, A., Ribeiro, C., Kourampa, J., Jose, S., ... Briggs, J. A. G. (2020). A thermostable, closed SARS-CoV-2 spike protein trimer. Nature Structural and Molecular Biology, 27(10), 934–941. https://doi.org/10.1038/s41594-020-0478-5

Yadav, K., Shivahare, R., Shaham, S. H., Joshi, P., Sharma, A., & Tripathi, R. (2021). Repurposing of existing therapeutics to combat drug-resistant malaria. Biomedicine and Pharmacotherapy, 136(November 2020), 111275. https://doi.org/10.1016/j.biopha.2021.111275

Yadavalli, R., & Sam-Yellowe, T. (2015). HeLa Based Cell Free Expression Systems for Expression of Plasmodium Rhoptry Proteins. Journal of Visualized Experiments, 100. https://doi.org/10.3791/52772

Yahiya, S., Rueda-Zubiaurre, A., Delves, M. J., Fuchter, M. J., & Baum, J. (2019). The antimalarial screening landscape—looking beyond the asexual blood stage. Current Opinion in Chemical Biology, 50, 1–9. https://doi.org/10.1016/j.cbpa.2019.01.029

Yamauchi Lucy M., L. M., Coppi, A., Snounou, G., & Sinnis, P. (2007). Plasmodium sporozoites trickle out of the injection site. Cellular Microbiology, 9(5), 1215–1222. https://doi.org/10.1111/j.1462-5822.2006.00861.x

Yang, J., Kanter, G., Voloshin, A., Levy, R., & Swartz, J. R. (2004). Expression of active murine granulocyte-macrophage colony-stimulating factor in an Escherichia coli cell-free system. Biotechnology Progress, 20(6), 1689–1696. https://doi.org/10.1021/bp034350b

Yang, T., Ottilie, S., Istvan, E. S., Godinez-Macias, K. P., Lukens, A. K., Baragaña, B., Campo, B., Walpole, C., Niles, J. C., Chibale, K., Dechering, K. J., Llinás, M., Lee, M. C. S., Kato, N., Wyllie, S., McNamara, C. W., Gamo, F. J., Burrows, J., Fidock, D. A., ... Winzeler, E. A. (2021). MalDA, Accelerating Malaria Drug Discovery. Trends in Parasitology, xx(xx), 1–15. https://doi.org/10.1016/j.pt.2021.01.009

Yin, G., & Swartz, J. R. (2004). Enhancing Multiple Disulfide Bonded Protein Folding in a Cell-Free System. Biotechnology and Bioengineering, 86(2), 188–195. https://doi.org/10.1002/bit.10827

Yin, J., Li, G., Ren, X., & Herrler, G. (2007). Select what you need: A comparative evaluation of the advantages and limitations of frequently used expression systems for foreign genes. Journal of Biotechnology, 127(3), 335–347. https://doi.org/10.1016/j.jbiotec.2006.07.012

Young, C. L., Britton, Z. T., & Robinson, A. S. (2012). Recombinant protein expression and purification: A comprehensive review of affinity tags and microbial applications. Biotechnology Journal, 7(5), 620–634. https://doi.org/10.1002/biot.201100155

Young, R. A. (1991). RNA Polymerase II. Annual Review of Biochemistry, 60(1), 689–715. https://doi.org/10.1146/annurev.bi.60.070191.003353

Yu, F., Xiang, R., Deng, X., Wang, L., Yu, Z., Tian, S., Liang, R., Li, Y., Ying, T., & Jiang, S. (2020). Receptor-binding domain-specific human neutralizing monoclonal antibodies against SARS-CoV and SARS-CoV-2. Signal Transduction and Targeted Therapy, 5(1), 1–12.

https://doi.org/10.1038/s41392-020-00318-0

Zeng, W., Liu, G., Ma, H., Zhao, D., Yang, Y., Liu, M., Mohammed, A., Zhao, C., Yang, Y., Xie, J., Ding, C., Ma, X., Weng, J., Gao, Y., He, H., & Jin, T. (2020). Biochemical characterization of SARS-CoV-2 nucleocapsid protein. Biochemical and Biophysical Research Communications, 527(3), 618–623. https://doi.org/
10.1016/j.bbrc.2020.04.136

Zhang, M., Gallego-Delgado, J., Fernandez-Arias, C., Waters, N. C., Rodriguez, A., Tsuji, M., Wek, R. C., Nussenzweig, V., & Sullivan, W. J. (2017). Inhibiting the Plasmodium eIF2α Kinase PK4 Prevents Artemisinin-Induced Latency. Cell Host and Microbe, 22(6), 766-776.e4. https://doi.org/10.1016/j.chom.2017.11.005

Zhao, J., Bhanot, P., Hu, J., & Wang, Q. (2016). A comprehensive analysis of Plasmodium circumsporozoite protein binding to hepatocytes. PLoS ONE, 11(8), 1–13. https://doi.org/10.1371
/journal.pone.0161607

Zhao, L., Zhao, K. Q., Hurst, R., Slater, M. R., Acton, T. B., Swapna, G. V. T., Shastry, R., Kornhaber, G. J., & Montelione, G. T. (2010). Engineering of a wheat germ expression system to provide compatibility with a high throughput pET-based cloning platform. Journal of Structural and Functional Genomics, 11(3), 201–209. https://doi.org/10.1007/s10969-010-9093-8

Zhoua, Z., Danga, Y., Zhou, M., Li, L., Yu, C. H., Fu, J., Chen, S., & Liu, Y. (2016). Codon usage is an important determinant of gene expression levels largely through its effects on transcription. Proceedings of the National Academy of Sciences of the United States of America, 113(41), E6117–E6125. https://doi.org/10.1073/pnas.1606724113

Zhu, M. M., Mollet, M., Hubert, R. S., Kyung, Y. S., & Zhang, G. G. (2017). Handbook of Industrial Chemistry and Biotechnology. In Handbook of Industrial Chemistry and Biotechnology. https://doi.org/10.1007/978-3-319-52287-6

Zimmermann, R., Eyrisch, S., Ahmad, M., & Helms, V. (2011). Protein translocation across the ER membrane. Biochimica et Biophysica Acta - Biomembranes, 1808(3), 912–924. https://doi.org/10.1016/j.bbamem.2010.06.015

Chapter 5

Appendix

5.1 Cloning

The primer pairs used to amplify DNA giving the 5' and 3' ends homology for the construction of the plasmids used in the 'Results' section and made by Gibson Assembly® (see Material & Methods 2.1.3), showing the gene or CDS introduced as well as any affinity tags fused to the gene. The 'construct' designations are colour coded indicating their respective use. Those coloured purple indicate use in the Dual-IVT system, green indicates use in the malaria cell-free system, blue in the human cell-free system and finally violet indicating plasmids used for SLI.

Table 5.1: Plasmids

Construct	CDS	Affinity Tag	Cloning Primers
pHLH_HCBGH	Click-beetle Luciferase Green (1-542)	None	N.A
pHLH_met_CSP_HA	CSP (20-384)	3XHA	**F**:GAAAAACCTAAGAAATTTACCTGCTA TGAAATTCTTAGTCAACGTTGCCC **R**:TAATCAGGTACGTCATAAGGATAAT GCATATTTACGACATTAAACACACTGGAAC
pHLH_CSP_HA	CSP - (1-384)	3XHA	**F**:GAAAAACCTAAGAAATTTACCTGCTACAAT GATGAGAAAATTAGCTATTTTATCTGTTTC **R**:AATCAGGTACGTCATAAGGATAATGCA TTGAACTATTTACGACATTAAACACACTG
pHLH_GFP_HA	sfGFP (1-238)	3XHA	**F**:CTGAAAACCTTTACTTTCAGGGCAA GCTTATGCGTAAAGGCGAAGAGC **R**:TTTTTTTTTTTCAGTCAGATC TTAAATAAGTTAGGAGCCGGAGCC
pHLH_sfGFP_SII	sfGFP (1-238)	Twin StrepII	**F**:CCTAAGAAATTTACCTGC TATGCGTAAAGGCGAAGAGC **R**:GCCCTGAAAGTAAAGGTTTTCGAAT TTGTACAGTTCATCCATACCATGC
pHLH_CSPSP_sfGFP_HA	sfGFP (1-238)	3XHA	**F**:ATTAGGTAGTCGAAA AACCTAAGAAATTTACC **R**:TCAGGTACGTCATAAGGATAATGCATT TGTTTGTACAGTTCATCCATACCATGCG
pHLH_HLucH_HA	Firefly luciferase	3XHA (1-551)	**F**:CAACTGAAAACCTTTACTTTCAGG GCATGCATGAAGACGCCAA **R**:ATCTATTATTAAATAAGCTTT TACAATTTGGACTTTCCGCCC
pHLH_Luc_HA	Firefly luciferase (1-551)	3XHA	**F**:TTTACCTGCTACATTTCAAATGCAT TATCCTTATGACGTACCTGATTATGC **R**:AATATTTTTAATCTATTATTAAAT AAGCTTTTACAATTTGGACTTTCCGCCC
pHLH_met_sfGFP_SII	sfGFP (1-238)	Twin StrepII	**F**:CCTAAGAAATTTACCTGCTATG AAATTCTTAGTCAACGTTGCCC **R**:TAAAGGTTTTCGAATTTG TACAGTTCATCCATACCATGC
pHLH_Nuc_His	Nucleocapsid (1-418)	6X poly-histidine	**F**:GGTAGTCGAAAAACCTAAGAAATTTACC TGCTATGTCTGATAATGGACCCCAAAATC **R**:TGATGATGATGGCCGGTA CCGGCCTGAGTTGAGTCAGC

Construct	CDS	Affinity Tag	Cloning Primers
pHLH_Nuc_sfGFP_SII	Nucleocapsid (1-418) sfGFP fusion	Twin StrepII	**F_N**:GGTAGTCGAAAAACCTAAGAAATTTACC TGCTATGTCTGATAATGGACCCCAAAATC **R_N**:TGAACAGCTCTTCGCCTTTAC GCATGAAAGCCTGTGTAGAATCGGC **F_G**ATGCGTAAAGGCGAAGAGC **R_G**:CCCTGAAAGTAAAGGTTTTCGAATT TGTACAGTTCATCCATACCATGC
pHLH_RBD_His	Spike-RBD (318-517)	6X poly-histidine	**F**:ACATTTCTTACATCTATGC GATGAATATTACAAACTTGTGCC **R**:ATGCACCAGCAACTGT TTGTGGTACCGGCCATCAT
pHLH_RBD_sGFP_SII	Spike - RBD (318-517)	6X poly-histidine	**F_R**:ACATTTCTTACATCTATGC GATGAATATTACAAACTTGTGCC **R_R**: TGAACAGCTCTTCGCCTTTAC GCATGAAACAAACAGTTGCTGGTGC **F_G**:ATGCGTAAAGGCGAAGAGC **R_G**: See pHLH_Nuc_sfGFP_SII
pIX_sfGFP_SII	sfGFP(1-238)	Twin Strep II	**F**:ACCTAAGAAATTTACCTGC TATGCGTAAAGGCGAAGAGC **R**:CCCTGAAAGTAAAGGTTTTCAG ATTTGTACAGTTCATCCATACCATGC
pSLI_RPAC1_FLAG	RPAC1 (1637-2446)	3X FLAG	**F**:AGGTGACACTATAGAATACTCGCGGCC GCTAAATAAAGAATATGGATGTTTCGATAGCAA **R**:AGTCCTTATCGTCGTCATCCTTGTAATC GCCGGTACCAGGACATAATTGCTCGTCCAG
pSLI_RPACB2_FLAG	RPACB2 (334-1134)	3X FLAG	**F**:GAATACTCGCGGCCGCTAAAATAATATATTTATA ATGAGAAAAAAAAAAAAAAAAAAAAA **R**:GACTGGAGATTAGATGAACTTATAAT TGATGGTACCGGCGATTACAAGGATGA
pSLI_RPB3_FLAG	RPB3 (1-770)	3X FLAG	**F**:AGGTGACACTATAGAATACTCGCGGCCGCTAAGC TCATAGATTAGGTTTAATACCAATAG **R**:TTATCGTCGTCATCCTTGTAATCGCCG GTACCTTCCAAGTCTAGTTGTATACCGTATAAG
pT7CFE_CBG	Click-beetle Luciferase Green (1-542)	None	N.A

5.2 Dual-IVT

Figure 5.1: Sequence Similarity of eEF2

A) A sequence alignment of eEF2 produced using the Muscle tool(Edgar, 2004) in Jalview(Waterhouse et al., 2009) from human (P13639) and *P. falciparum* (Q8IKW5), sequences were taken from UniProt(Bateman et al., 2021). The blue shading shows the level of similarity at each amino acid position.

5.3 *P. falciparum RNAP*

The similarities of each of the predicted *P. falciparum* 3D7 RNAP subunit structures, FLAG-tagged using SLI (see Figure 3.10) were compared to the equivalent subunits from the deposited

structures, *S. cerevisiae*. The RMSD values for each comparison were generated using PyMOL (The PyMOL Molecular Graphics System, Version 2.0 Schrödinger, LLC) (see Table 5.2). The RMSD is a measure of the deviation between two corresponding atoms of two proteins, therefore the smaller the value the more similar the structures(Kufareva & Abagyan, 2012). However, this only is a measure of the equivalent residues or like for like atoms so any variations in the sequence cannot be calculated.

Table 5.2: A Comparison of RMSD Values Generated for Each RNAP Subunit Tagged

Putative *P. falciparum*	**Putative *S. cerevisiae***	**RMSD** (Å)
RPAC1	RPAC1 (PDB_4c3j)	0.95
RPABC2	RPABC2 (PDB_4c3j)	0.63
RPB3	RPB3 (PDB_1k83)	0.95

The RNAPI subunit sequences for each *spp* taken from UniProt(Bateman et al., 2021) (see Table 5.3).

Multiple sequence alignments were used to produce the phylogenetic tress that infer an evolutionary relationship between the eukaryotic nuclear RNAP subunits for each of the 11 organisms used. Proteins with similar sequences share a common ancestral protein with the quantity of genetic change seen as the average amino acid substitution per site.

The stalk of RNAP II is comprised of subunits RPB4 and RPB7 that interact to form a heterodimer. Multiple seqeunce allignments have been produced for each of the two subunits using the Muscle alignment tool(Edgar, 2004) and presented in Jalview(Waterhouse et al., 2009).

Table 5.3: RNAP Subunits

Organism/Strain	Protein Identification	Subunit
A. thaliana	O81098	RPB5
A. thaliana	Q9FJ98	RPB6
A. thaliana	Q9M1A8	RPB8
A. thaliana	Q9SYA6	RPB10
A. thaliana	Q8L5V0	RPB12
D. melanogaster	Q7JZF5	RPB5
D. melanogaster	Q24320	RPB6
D. melanogaster	Q9VNZ3	RPB8
D. melanogaster	Q9VC49	RPB10
D. melanogaster	Q6IGE3	RPB12
H. sapiens	P19388	RPB5
H. sapiens	P61218	RPB6
H. sapiens	P52434	RPB8
H. sapiens	P62875	RPB10
H. sapiens	P53803	RPB12
P. falciparum	Q8ID59	RPB5
P. falciparum	O77315	RPB6
P. falciparum	Q8I5R8	RPB8
P. falciparum	Q8IC08	RPB10
P. falciparum	Q8IDR2	RPB12
P. knowlesi	A0A1Y3DJU2	RPB5
P. knowlesi	A0A1Y3DLJ1	RPB6
P. knowlesi	A0A1Y3DNF5	RPB8
P. knowlesi	A0A1Y3DWB8	RPB10
P. knowlesi	A0A384LP29	RPB12
P. malariae	A0A1C3KZ66	RPB5
P. malariae	A0A1D3PAY5	RPB6
P. malariae	A0A1A8X795	RPB8
P. malariae	A0A1A8VPV7	RPB10
P. malariae	A0A1C3L0G7	RPB12
P. ovale	A0A1C3KTM1	RPB5
P. ovale	A0A1D3THH5	RPB6
P. ovale	A0A1C3L549	RPB8
P. ovale	A0A1C3KMD2	RPB10
P. ovale	A0A1D3TKA9	RPB12
S. cerevisiae	P20434	RPB5
S. cerevisiae	P20435	RPB6
S. cerevisiae	P20436	RPB8
S. cerevisiae	P22139	RPB10
S. cerevisiae	P40422	RPB12
T. gondii	A0A7J6K9U9	RPB5
T. gondii	A0A7J6K6F6	RPB6
T. gondii	A0A139Y5G2	RPB8
T. gondii	A0A7J6JW77	RPB10
T. gondii	A0A139XT14	RPB12

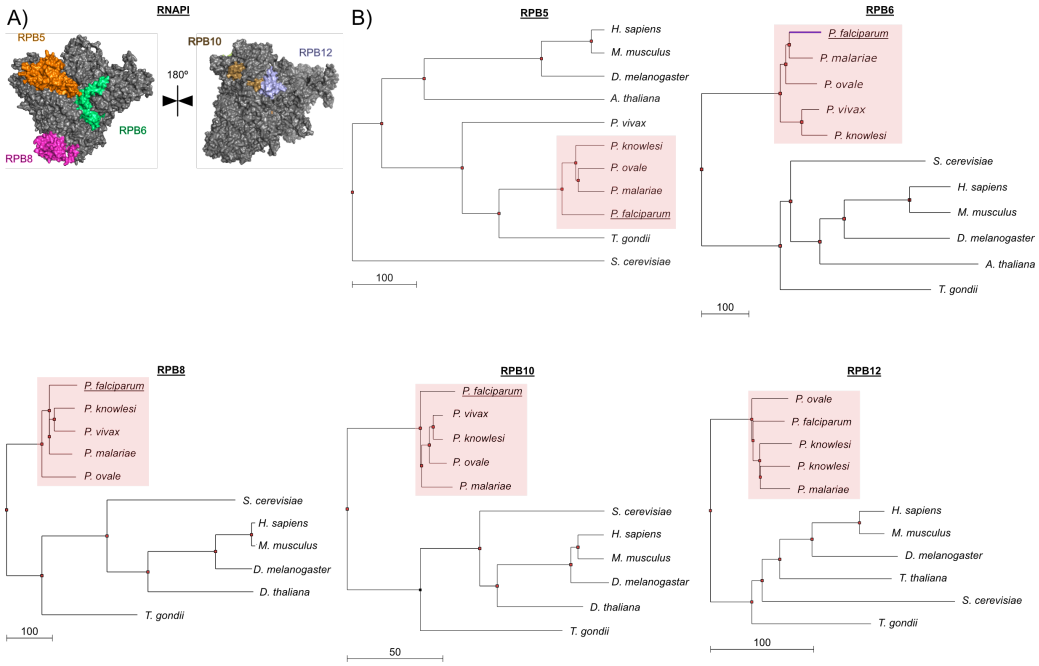

Figure 5.2: The Conservation of RNAP Subunits between *spp*

A) The RNAP subunits used to produce the sequence alignments are highlighted using the structure of *S. cerevisiae* (PDB_4c3j), the structure has been rotated horizontally by 180° to show all analysed subunits. **B** Maximum-likelihood phylogenetic trees produced from multiple sequence alignments using Clustal Omega(Sievers et al., 2011) and phylogenetic trees produced in Jalview(Waterhouse et al., 2009). Each of the analysed subunits was for each organism was obtained from Uniprot (see Table 5.3). A red box shows the clustering of the five malaria *spp* that infect humans.

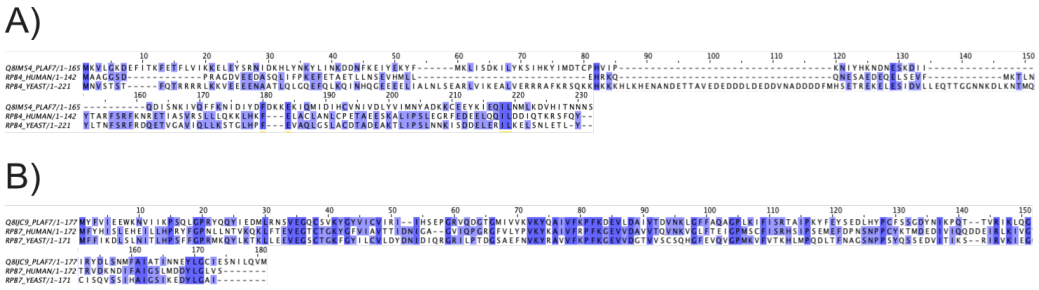

Figure 5.3: The Stalk of RNAP II

A) The amino acids from the RPB4 subunits from *P. falciparum* (UniProt_Q81M54), human (UniProt_O15514) and yeast (UniProt_P20433) have been aligned with the level of blue shading indicating the conservation at that position. **B**) The amino acids from the RPB7 subunits from *P. falciparum* (UniProt_Q8IJC9), human (UniProt_P62487) and yeast (UniProt_P34087) have been aligned with the level of blue shading indicating the conservation at that position.

5.4 Malaria CFPS

The additional optimisation steps for the creation of a CECF protein synthesis system using the translationally active lysate derived from *P. falciparum* (see Figure 4.1). Firefly luciferase (pHLH_Luc_HA) has been used as a reporter of translation. The IRES from the IGR of the CrPV was able to initiate translation of luciferase more efficiently than that of the native *P. falciparum* Hrp3 5'UTR. To further probe the ability of CrPV-IGR IRES to initiate translation in a *spp* independent manner, *P. falciparum* lysate was switched out for another *Apicomplexan, Toxoplasma gondii* (donated). The parasite material was then prepared and used in the same way as malaria lysate for the Dual-IVT assay (see Material & Methods 2.3.1 & 2.4.1). Translation of firefly luciferase was confirmed through the detection of luminescence (see Material & Methods 2.7.3).

5.4.1 *Pf*CSP Signal Peptide prediction

The production of *P. falciparum* CSP (PF3D7_0304600) using the malaria derived CFPS required the removal of the N-terminal signal peptide to compare the efficiency of translocation of protein into endogenous microsomes (see Figure 4.2).

5.4.2 *Pf*CSP Detection

The CSP present on the surface of *P. falciparum* NF54 parasites was detected by western blot and compared to *P. falciparum* 3D7 asexual stage schizonts (see Figure 4.3).

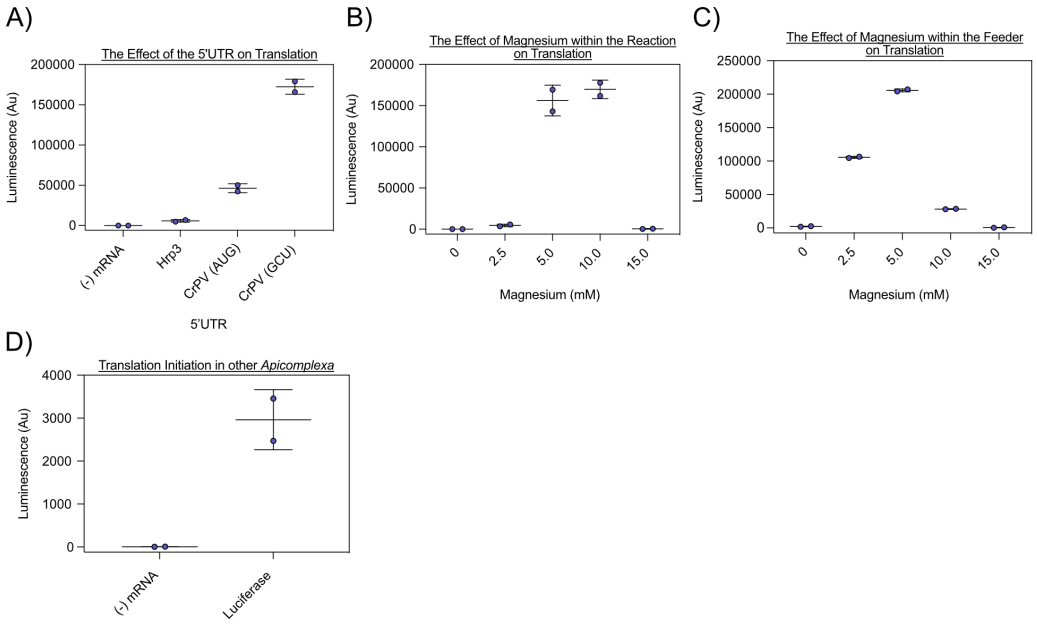

CSP was replaced for the sfGF

Figure 5.4: Further Optimisation & Characterisation of CFPS Using the CrPV-IGR IRES **A**) Three 5'UTR regions are compared for their efficiency at initiating the translation of firefly luciferase mRNA (17µg/µl) added in a batch reaction format and assessed through detection of luminescence (see Material & Methods 2.4.1). The introduction of the CrPV-IGR IRES containing a traditional 'AUG' start codon increased translation over the *Pf*Hrp3 5'UTR eight-fold. However, removing the traditional 'AUG' start codon and replacing it for 'GCU' further increased translation by 30-fold compared to the Hrp3 5'UTR. **B**) The optimal concentration of magnesium within the 'reaction' compartment during CECF protein-synthesis was found to be 10mM. This was determined using the expression of firefly luciferase and luminescence detection (see Material & Methods 2.4.3). **C**) The optimal concentration of magnesium within the 'feeder' compartment during CECF protein-synthesis was found to be 5mM. This was determined using the expression of firefly luciferase and luminescence detection (see Material & Methods 2.4.3). **D**) The ability of the CrPV-IGR IRES to initiate translation in other *spp* was probed. The other *Apicomplexan*, *Toxoplasma gondii* was used for the production on lysate and assessed for translation of firefly luciferase, showing a strong luminescence signal over the background.

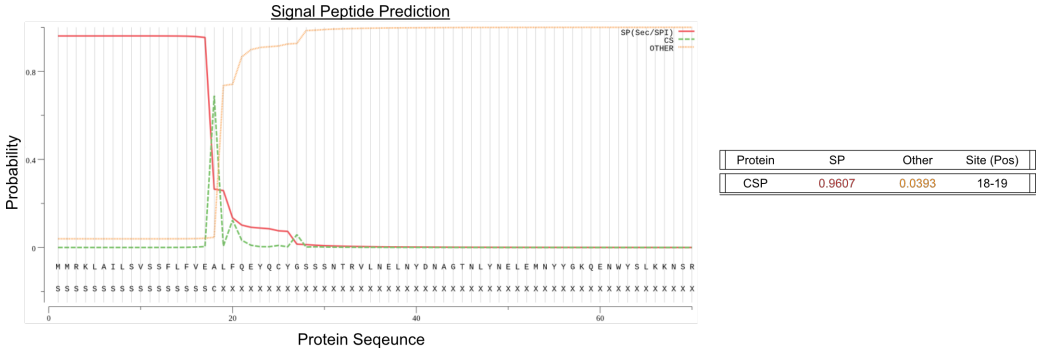

Figure 5.5: The Prediction of the Signal Peptide from *P. falciparum* 3D7 CSP The N-terminal signal peptide of PF3D7_0304600 CSP was predicted to be residues 0-19, with the cleavage site at residue A18 and 19L using the SignalP-5.0 tool (José Juan Almagro Armenteros et al., 1996 ; Nielsen et al., 1996)). The SP(Sec/SPI) predicts the likelihood of the signal peptide (SP) by analysing the first 70 residues of CSP, (CS) indicates the cleavage site and (Other) predicts the probability the sequence not containing a signal peptide.

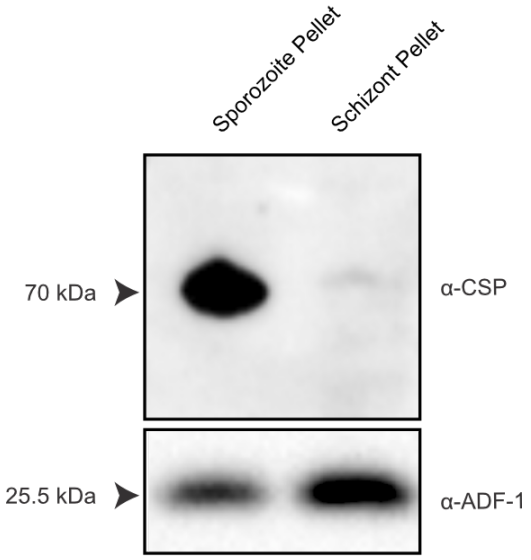

Figure 5.6: Detection of CSP in Sporozoites

The detection of CSP within asexual *P. falciparum* schizonts and sporozoites by western blot. Each of the samples was lysed and the protein concentration adjusted to match by measuring each sample at 280nm (see Material & Methods 2.5.2).

5.5 Human CFPS

The similarities of the spike protein structures were compared using RMSD values generated using PyMOL (The PyMOL Molecular Graphics System, Version 2.0 Schrödinger, LLC) by comparing their atomic structures deposited in the PDB. The data was used to compare the variants as indicated to the Wuhan reference SARS-CoV-2 strain (Genbank_MN908947). The RMSD is a measure of the deviation between two corresponding atoms of two proteins, therefore the smaller the value the more similar the structures(Kufareva & Abagyan, 2012). However, this only is a measure of the equivalent residues or like for like atoms so any variations in the sequence cannot be calculated.

Table 5.4: A Comparison of RMSD Values Generated for Each Spike Protein Variant

Variant 1	**Variant 2**	**RMSD** (Å)
B.1.351 SA (PDB_7lyp)	B.1.1.28 Brazil (PDB_97lww)	0.921
B.1.351 SA (PDB_7lyp)	B.1.1.7 Kent (PDB_7lwv)	0.808
(PDB_97lww)	B.1.1.7 Kent (PDB_7lwv)	0.921
Kent (PDB_7lwv)	Wuhan (PDB_6x2a)	0.943
(PDB_97lww)	Wuhan (PDB_6x2a)	1.097
B.1.351 SA (PDB_7lyp)	Wuhan (PDB_6x2a)	0.994

The optimisation of factors affecting the efficiency of recombinant protein expression within the HEK293F derived TX-TL CFPS system (see Material & Methods 2.4.2). Here the expression of sfGFP (pHLH_GFP_HA) in a 50µl reaction was used as a measure of expression efficiency through the detection of sfGFP fluorescence after a 48hr incubation (see Figure 4.3).

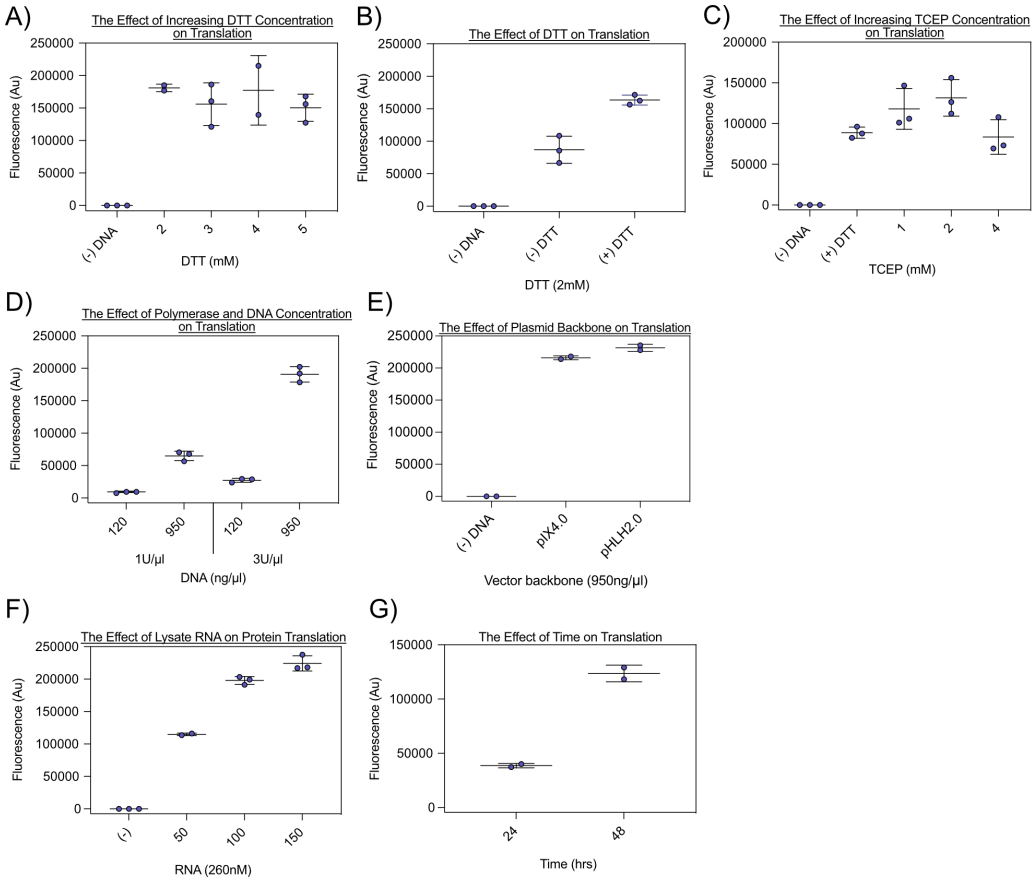

Figure 5.7: Further Optimisation of a Human Derived CFPS System

A) Increasing concentration of the reducing agent DTT into the 'feeder' solution had no significant impact on the synthesis of sfGP. **B**) The removal of DTT from the 'feeder' solution of a reaction decreased the production of sfGFP by approximately two-fold. **C**) The comparison of two reducing agents, DTT (2mM) and TCEP revealed that the inclusion of TCEP in a reaction increased translation efficiency by almost 1.5-fold. **D**) The joint effect of the T7 RNAP and DNA concentrations within a reaction. The final concentration of DNA within a reaction of 950ng/µl coupled with 3U/µl significantly increased the synthesis of sfGFP. **E**) The expression of sfGFP contained within the pIX4.0 and the modified pHLH2.0 vector backbone containing sfGFP were compared for sfGFP expression. The sfGFP contained within the modified pHLH vector gave a slightly higher output than sfGFP contained within the pIX4.0 vector. **F**) As the final RNA concentration of the isolated HEK293F lysate, measured at 260nm and used for CFPS increased so to did the levels of sfGFP translation. **G**) The production of sfGFP was monitored over 48hrs. There was 3.2-fold increase of sfGFP from 24 to 48hrs.